c-Myb maintains glucose metabolism and regulates differentiation across the pre-BCR checkpoint

Andrea Daamen
Greenville, South Carolina

B.S., University of South Carolina, 2012
M.S., University of Virginia, 2015

A Dissertation presented to the Graduate Faculty
of the University of Virginia in Candidacy for the
Degree of Doctor of Philosophy

Department of Microbiology, Immunology, and Cancer Biology

University of Virginia
December, 2019

Abstract

The transcription factor c-Myb is critical for normal adult hematopoiesis. However, analysis of c-Myb function is difficult due to the embryonic lethality of *Myb* null mutations. We previously utilized conditional inactivation at the *Myb* locus to demonstrate that c-Myb is absolutely required for the differentiation and survival of pro-B cells and that c-Myb coordinates the survival of pro-B cells with the expression of genes required for transition across the pre-BCR checkpoint to the large pre-B cell stage of differentiation. However, it is unclear what additional functions c-Myb and mediators of c-Myb activity have within the pro-B cell compartment and whether c-Myb is important for the proliferative expansion of large pre-B cells or subsequent differentiation into small pre-B cells. We demonstrate that c-Myb expression is critical to maintain glucose metabolism and fuel proliferation across the pre-BCR checkpoint at the pro-B and large pre-B cells stages of development. c-Myb-deficient pro-B and large pre-B cells exhibit decreased glucose uptake and Glut1 mRNA expression, decreased hexokinase activity and Hk1 mRNA expression, and are ultimately hypoproliferative and apoptotic. In pro-B cells, IL-7 signaling through the Plcγ/Pkcβ/mTORC1 signaling pathway promotes pro-B cell glucose metabolism and proliferation. Microarray differential gene expression analysis revealed that c-Myb regulates multiple components of the Plcγ/Pkcβ/mTORC1 signaling pathway as well as additional pathways dependent on glucose uptake and utilization, which are critical to maintain homeostatic metabolism in the pro-B cell compartment. In large pre-B cells, exit from the cell cycle and decreased metabolic activity accompany differentiation. We demonstrate that in addition to defects in proliferation and glucose utilization, c-Myb-deficient large pre-B cells exhibit premature expression of Ikaros and Aiolos, which act downstream of pre-BCR signaling and put into place a

gene expression program essential to drive the large to small pre-B cell transition. To assess c-Myb-dependent changes in gene expression in large pre-B cells, we performed RNA-seq and found a large proportion of c-Myb-dependent gene expression changes are Ikaros targets. However, c-Myb regulates glucose metabolism in an Ikaros-independent manner and due to loss of glucose-dependent survival and proliferation, c-Myb-deficient large pre-B cells fail to differentiate and undergo apoptotic cell death. Overall, this thesis demonstrates that c-Myb regulates glucose uptake and utilization in pro-B and large pre-B cells, which is critical to maintain proliferation and survival across the pre-BCR checkpoint.

Acknowledgements

The process of pursuing my doctoral degree at the University of Virginia has been a long, 7-year journey which has been both the hardest thing I have ever done and also the most fulfilling. I have grown immensely both mentally and emotionally as a scientist and as a human being. Overall, this would not have been possible without the teachers, advisors, colleagues, friends, and family who supported me along the way. I would like to thank my mentor and thesis advisor, Dr. Timothy Bender. While it took me a while to learn to seek out his expertise rather than fear his criticism, by the end of my time under his mentorship I feel we have become colleagues. Tim has taught me to think like a scientist, to see experimental failures as learning opportunities, and to see presentations as a chance to tell the story of my project. While many of these lessons are still sinking in, I believe he has left me well prepared to pursue the career of my choosing. This process has also been a trying time for me physically and emotionally and I can't thank Tim enough for believing in me and refusing to give up on me even when I was ready to give up on myself. I would also like to thank my thesis advisory committee, Drs. Loren Erickson, Ulrike Lorenz, Adam Goldfarb, and Mazhar Adli for their advice and expertise in guiding my project.

I would like to thank the other members of the Bender laboratory who have overlapped with my time in the lab, to Dr. Shawn Fahl, Dr. Jeff Bergen, and Rowena Crittenden. In particular, Shawn Fahl who was a graduate student finishing up his degree as I joined the lab and was the direct precursor to my project. Shawn was an amazing colleague and teacher who was always willing to train me in lab protocols and answer all of my questions. I would also like to thank Rowena Crittenden, our lab manager who has become a second mother to me. More than almost anyone else, Rowena is the reason I have been able to complete my doctoral degree. She has been an invaluable resource of knowledge about and assistance with scientific techniques as well as

emotional support where I always knew I could get a warm hug. I am profoundly grateful for all she has done for me over the years. There are a number of members of other laboratories and advisors who have generously offered their scientific expertise and, in particular, I would like to acknowledge the members of the Carter Immunology Center as well as the Kashatus laboratory and the Weber laboratory. I would also like to thank the administrative staff of the Carter Immunology Center and the Department of Microbiology, Immunology, and Cancer Biology for keeping me on track to receive my degree.

I would like to thank the friends and family who have helped support me in this process. To the fellow students who joined me in becoming the first official BIMS class affectionately referred to as “the guinea pigs”. We have since gone our separate ways but will be forever bonded by the hours, days, and weeks spent together in the core course. In particular, I would like to thank my hiking buddies Kathy Michels and Caitlin Hubbard. Thanks also to Greenberry’s Coffee and all the baristas I have come to know over the years who have kept me well-caffeinated. Finally, I would like to thank my parents who have always loved and supported me through all of the bumps in the road, my brother with whom I have grown closer the longer we have lived apart, and to my cat Mandy who is a better roommate than I could have ever asked for.

Table of Contents

List of Figures

List of Tables

List of Abbreviations

2-NBDG	2-deoxy-2-[(7-nitro-2,1,3-benzoxadiazol-4-yl) amino]-D-glucose
2-ME	β-mercaptoethanol
4-OHT	4-hydroxytamoxifen
7AAD	7-Aminoactinomycin D
ABL	Acute Basophilic Leukemia
ATP	Adenosine Triphosphate
ALP	All-Lymphoid Progenitor
AML	Acute Myeloid Leukemia
AMPK	AMP Activated Protein Kinase
AMV	Avian Myeloblastosis Virus
APC	Antigen Presenting Cell
Apaf-1	Apoptotic Protease Activating Factor 1
ATM	Ataxia Telangiectasia Mutated
B-ALL	B Cell Acute Lymphoblastic Leukemia
BCR	B Cell Receptor
BH	Bcl-2 Homology
BLP	B Cell-Biased Lymphoid Progenitor
Bregs	Regulatory B Cells
BSA	Bovine Serum Albumin
CA	Constitutively Active
CAD	Carbamoyl Phosphate Synthetase
cDNA	Complementary DNA

CDK	Cyclin Dependent Kinase
CHD3	Chromodomain-Helicase-DNA-Binding Protein 3
ChIP	Chromatin Immunoprecipitation
CKI	CDK Inhibitor
CLP	Common Lymphoid Progenitor
D	Diversity
DAPI	4',6-Diamidino-2-Phenylindole
DBD	DNA-Binding Domain
DMEM	Dulbecco's Modified Eagle Medium
DN	Dominant Negative
DNA	Deoxyribonucleic Acid
ECAR	Extracellular Acidification Rate
ES	Embryonic Stem
EVES	Glutamic Acid-Valine-Glutamic Acid-Serine
FACS	Fluorescence Activated Cell Sorting
FBS	Fetal Bovine Serum
FDR	False Discovery Rate
FLASH	FLICE-Associated Huge Protein
FNIP	Folliculin Interacting Protein
FO	Follicular
G6P	Glucose-6-Phosphate
GFP	Green Fluorescent Protein
Glut	Glucose Transporter

HIF1α	Hypoxia Inducible Factor 1 Subunit Alpha
Hk	Hexokinase
HLR	Heptad Leucine Repeat
HPRT	Hypoxanthine-Guanine Phosphoribosyltransferase
HSC	Hematopoietic Stem Cell
Ig	Immunoglobulin
IL-7Rα	IL-7 Receptor α
IMDM	Iscove's Modified Dulbecco's Medium
IRES	Interal Ribosome Entry Site
J	Joining
Jak	Janus Kinase
kb	Kilobase
kDA	Kilodalton
LMPP	Lymphoid-Primed Multipotential Progenitor
LZ	Leucine Zipper
M	Mitosis
MACS	Magnetic Activated Cell Sorting
MDG	c-Myb-Dependent Differentially Expressed Gene
MEL	Mouse Erythroleukemia
MEM	Minimum Essential Medium
MHC	Major Histocompatibility Complex
mIgM	Membrane Bound IgM
miRNA	microRNA

MOI	Multiplicity of Infection
MPP	Multipotential Progenitor
MRE	Myb Response Element
mRNA	Messenger RNA
MSigDb	Molecular Signatures Database
mtHk	Mitochondrial Hexokinase
mTORC	Mammalian Target of Rapamycin Complex
μHC	μ Heavy Chain
MuLV	Murine Leukemia Virus
MZ	Marginal Zone
N-CoR	Nuclear Receptor Co-Repressor
NRD	Negative Regulatory Domain
OCR	Oxygen Consumption Rate
PBS	Phosphate Buffered Saline
PCR	Polymerase Chain Reaction
Pkcβ	Protein Kinase Cβ
Plcγ	Phospholipase Cγ
PMF	Primary Myelofibrosis
PPP	Pentose Phosphate Pathway
R	Restriction Point
Rag	Recombinase Activating Gene
Raptor	Regulatory-Associated Protein of mTOR
RNA	Ribonucleic Acid

ROS	Reactive Oxygen Species
RPMI	Roswell Park Memorial Institute
RSS	Recombination Signal Sequence
SCF	Stem Cell Factor
Sgk	Serum/Glucocorticoid Regulated Kinase
SGLT	Sodium-Driven Sugar Co-Transporters
shRNA	small hairpin RNA
SLC	Surrogate Light Chain
SKP	S Phase Kinase-Associated Protein
SOCS	Suppressor of Cytokine Signaling
SREBP	Sterol Responsive Element Binding Protein
SYK	Spleen Tyrosine Kinase
TAD	Transactivation Domain
T-ALL	T Cell Acute Lymphoblastic Leukemia
TdT	Terminal Deoxynucleotidyl Transferase
TCR	T Cell Receptor
TdT	Terminal Deoxynucleotidyl Transferase
TIF1β	Transcriptional Intermediary Factor 1β
TNFR-1	Tumor Necrosis Factor Receptor 1
Txnip	Thioredoxin Interacting Protein
tNGFR	Truncated Nerve Growth Factor Receptor
TRAIL	TNF-Related Apoptosis-Inducing Ligand
UBC	ubiquitin C

UTR	Untranslated Region
V	Variable
YFP	Yellow Fluorescent Protein
γ_c	Common Gamma Chain

Chapter I. Introduction

1.1) The Immune System

The purpose of the immune system is to identify foreign pathogens and eliminate them through two main mechanisms: the innate immune system and the adaptive immune system. The innate immune system is shared by all organisms and is a generalized, non-specific response to conserved molecular patterns present on most pathogens (Brubaker et al., 2015). Thus, the innate immune response is activated early during infection and acts as a first line of defense to rapidly sense and eliminate pathogens. The adaptive immune system arose with the evolution of vertebrates and provides a targeted response to foreign antigens following recognition by antigen-specific receptors (Boehm and Swann, 2014). Thus, if the innate immune response fails to clear the infection, the adaptive immune system is activated, triggering the specific expansion of cells that recognize and respond to epitopes expressed by the invading pathogen. In addition, after the initial response, adaptive immunity creates immunological memory, which induces an enhanced response if that pathogen is encountered again and provides long-lasting protection against the pathogen, often for the lifetime of the host.

1.1.1) Antigen Receptors and V(D)J Recombination

Adaptive immunity is further divided into cellular immunity mediated by T lymphocytes and humoral or antibody-mediated immunity through B lymphocytes (Francisco A Bonilla MD and Hans C Oettgen MD, 2010). T and B lymphocytes are characterized by surface expression of antigen-specific receptors produced by somatic recombination of gene segments to generate a diverse repertoire of receptor specificities on mature, peripheral lymphocytes. T cells mediate cellular immunity through activation of their T cell receptors (TCRs) by antigenic peptides in complex with major histocompatibility complex (MHC) molecules displayed by antigen

presenting cells (APCs). B cell activation occurs upon interaction of B cell receptors (BCRs) or immunoglobulin (Ig) with antigen in a T cell dependent or independent manner. Then, activated clones proliferate and differentiate into effector cells, which secrete immunoglobulin as antibodies to mediate humoral immunity.

The B cell receptor is composed of two immunoglobulin heavy chains and two light chains formed by somatic recombination and fusion of variable (V), diversity (D), and joining (J) gene segments (Alt et al., 1984). Recombination first occurs at the *Igh* locus, which contains multiple V, D, and J segments, followed by recombination at the *Igl* loci, which contains multiple V and J segments. The process of V(D)J recombination is mediated by the V(D)J recombinase, a protein complex which includes the recombinase activating genes Rag1 and Rag2 (McBlane et al., 1995; Schatz et al., 1989). The V(D)J recombinase recognizes conserved DNA elements termed recombination signal sequences (RSSs) adjacent to each V, D, and J segment and cleaves the DNA to produce double-stranded breaks, which are then rejoined by the nonhomologous end-joining DNA repair pathway (Helmink and Sleckman, 2012). Antigen receptor diversity is generated by multiple mechanisms including the combinatorial diversity of different V, D, and J segments and junctional diversity generated at segment joining (Nishana and Raghavan, 2012). Expression of TdT further increases diversification by the addition of N-nucleotides to the segment junctions (Desiderio et al., 1984). Thus, the generation and maintenance of a diverse repertoire of antigen receptors is essential for generating a targeted immune response against any foreign antigen a host may encounter. Due to the relatively short life span of naïve peripheral B cells, this antigen receptor repertoire is maintained by constant renewal of B cells from the bone marrow, which occurs throughout the life of adult mammals.

1.2) B Lymphopoiesis

B lymphopoiesis is the process that gives rise to each type of B cell and is characterized by the sequential expression of cell surface markers and the ordered rearrangement of IgH and IgL chain gene segments. This process initiates in the fetal liver during embryonic development and shifts to the bone marrow, which remains the major source of B cells throughout adult life (Hardy et al., 1991). Early B cells are divided into stages denoted as progenitor (pro), precursor (pre), and immature based on surface marker expression, B-lineage-specific gene expression, and the status of antigen receptor formation. These early B cell developmental stages culminate in the production of immature B cells expressing antigen receptors or immunoglobulin (Ig) that can recognize foreign antigens.

Mature, peripheral B cells, have been classified into three major subsets: B-1, marginal zone (MZ), and follicular (FO) B cells (Allman and Pillai, 2008). B-1 B cells are innate-like cells generated by the fetal liver and to a lesser extent from the bone marrow, which mainly reside in the pleural and peritoneal cavities (Baumgarth, 2011). B-1 B cells have a less diverse antibody repertoire and largely recognize self-antigens and repetitive pathogen-expressed epitopes. B-2 or conventional B cells are the major subset of B cells, which arise from bone marrow progenitors, migrate to the spleen, and mature through transitional B cell stages (T1 to T3). Then the majority of transitional B cells will become follicular B cells with a minority developing into marginal zone B cells. Marginal zone B cells localize to the marginal sinus of the spleen and like B-1 B cells, are innate-like in their ability to respond rapidly to blood-borne antigens and have a limited antibody repertoire (Cerutti et al., 2013). Follicular B cells are found circulating in the periphery or residing in the follicles of secondary lymphoid organs where they are activated in a T cell-dependent manner and eventually give rise to memory B cells and long-lived plasma cells (McHeyzer-

Williams and McHeyzer-Williams, 2005; Pillai and Cariappa, 2009). As the main agents of the humoral immune response, follicular B cells exhibit an expansive antibody repertoire and are critical for the development of high-affinity B cell memory. In addition to the major mature B cell subsets, under inflammatory conditions, B cells can acquire an immunosuppressive function and develop into regulatory B cells (Bregs), which utilize multiple mechanisms including the production of the regulatory cytokines IL-10 and TGF-β and direct interaction with pathogenic T cells to dampen the immune response (Mizoguchi and Bhan, 2006; Rosser and Mauri, 2015). Thus, mature B cells are capable of multiple immune functions in addition to antibody production, all of which stem from the initial stages of B lymphopoiesis in the bone marrow.

1.2.1) B-lineage specification and commitment

The process of B cell development in the bone marrow initiates from multipotent, self-renewing hematopoietic stem cells (HSCs), which are defined as lineage negative and lack the markers of mature hematopoietic cell lineages while retaining the potential for differentiation into both myeloid and lymphoid cell types. HSCs undergo a series of well-characterized developmental stages, driven by a network of transcription factors and cytokines, during which they gain B-lineage specific genes (B-lineage specification) while conversely losing their ability to differentiate into other myeloid or lymphoid lineages (B-lineage commitment) (Figure 1.1) (Hardy et al., 2007). First, HSCs differentiate into multipotent progenitors (MPPs) and lose their self-renewal capacity while maintaining the ability to differentiate into all hematopoietic cell lineages (Adolfsson et al., 2001). MPPs then differentiate to the lymphoid-primed multipotent progenitor (LMPP) stage, which is characterized by the gradual increase in expression of the tyrosine kinase receptor Flt3. LMPPs retain the potential to differentiate into myeloid or lymphoid lineages but have lost the potential for differentiation into erythrocytes and megakaryocytes (Adolfsson et al.,

2005). The progression from LMPPs to the common lymphoid progenitor (CLP) stage further restricts cells to the lymphoid lineage (B, T, and NK cells) and is characterized by surface expression of the IL-7Rα (Kondo et al., 1997). The CLP stage is further subdivided by expression of Ly6D into the $Ly6D^-$ all-lymphoid progenitors (ALP), which retain the potential for development into all lymphoid lineages in vivo, and the $Ly6D^+$ B-cell-biased lymphoid progenitors (BLP), which act as a B-cell progenitor and have lost most of their potential for differentiation into T cells and NK cells (Inlay et al., 2009). BLPs differentiate into pre-pro B cells, or Fraction A in the Hardy classification of bone marrow B cell subsets, and express B220 (CD45R) (Hardy et al., 1991). Pre-pro B cells are considered the first B-lineage specified progenitor as they express a number of B-lineage associated genes, but still retain a residual capacity for differentiation into T cells and NK cells (Rumfelt et al., 2006). Subsequently, pre-pro B cells differentiate to the pro-B cell stage, characterized by CD19 surface expression, in which cells have lost the potential to differentiate into all other hematopoietic cell lineages (Li et al., 1996). Thus, the pro-B cell stage represents the first committed stage of B lineage progenitors.

The gene expression changes required for the development of $CD19^+$ pro-B cells are mediated by a network of key transcription factors and cytokines critical for B-lineage specification and commitment (Medina et al., 2004; Nutt and Kee, 2007). This network begins to take shape with early lineage fate decisions mediated by Ikaros and PU.1. Ikaros expression is required for lymphoid lineage specification and the development of all lymphocytes (Georgopoulos et al., 1994). In Ikaros-deficient mice, MPPs fail to upregulate the cytokine receptor Flt3 and lose lymphoid potential while retaining the ability to differentiate down the myeloid lineage (Yoshida et al., 2006). PU.1 also regulates Flt3 expression at the MPP stage and PU.1-deficient embryos fail to develop myeloid or lymphoid cells.

Figure 1.1: Developmental stages encompassing B lineage specification and commitment. Diagram depicting the stages of B cell development encompassing B lineage specification from HSCs through B lineage commitment in pro-B cells. Each stage is defined by surface marker expression. The relative expression of each marker in each cell population is delineated by line thickness. HSC=hematopoietic stem cell, MPP=multipotent progenitor, LMPP=lymphoid-primed multipotent progenitor, CLP=common lymphoid progenitor, ALP=all-lymphoid progenitor, BLP=B cell-biased lymphoid progenitor.

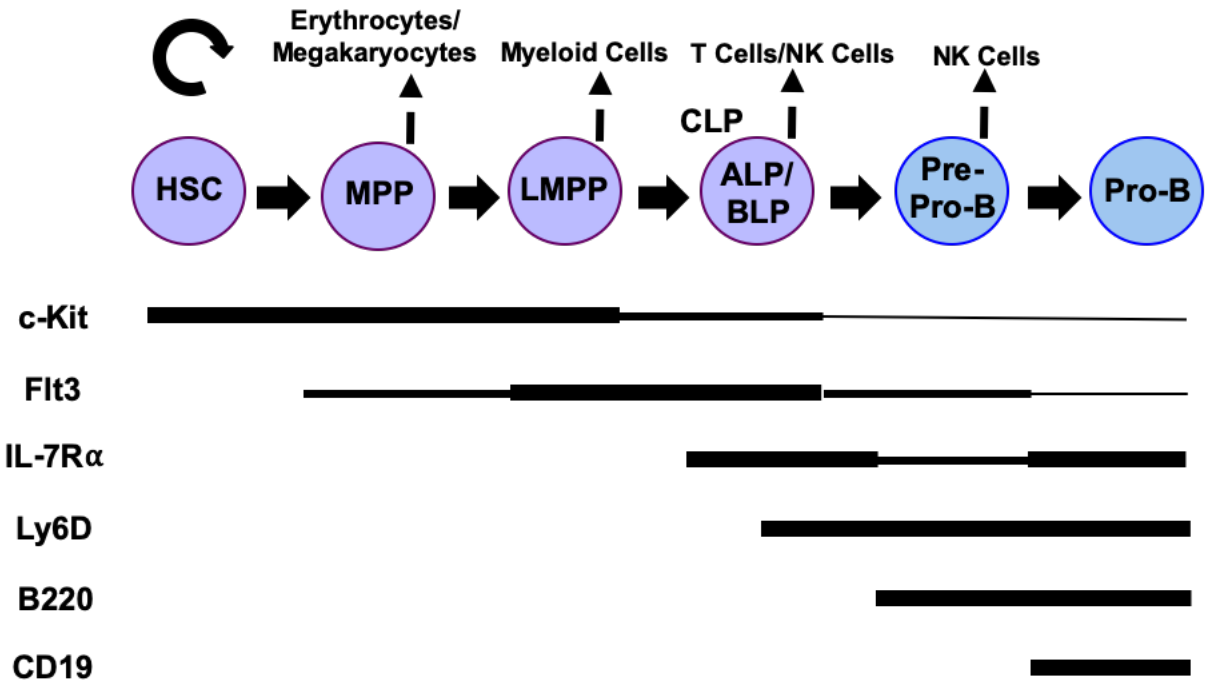
Erythrocytes/
Megakaryocytes
Myeloid Cells
T Cells/NK Cells
NK Cells
CLP
HSC
MPP
LMPP
ALP/
BLP
Pre-
Pro-B
Pro-B
c-Kit
Flt3
IL-7Rα
Ly6D
B220
CD19

Furthermore, in the transition from LMPPs to CLPs, graded expression of PU.1 determines the myeloid versus lymphoid fate through regulation of the IL-7Rα (DeKoter et al., 2002). Thus, Ikaros and PU.1 guide hematopoietic cell development toward the lymphoid lineage by putting into place expression of key signaling receptors needed for lymphocyte and B-lineage development.

From the BLP to pro-B cell stages of development, the transcription factor network that drives B-lineage specification and commitment is established to induce the expression of B-lineage specific genes and repress alternative lineage genes through activity of the transcription factors E2A (*Tcf3*), Ebf1, and Pax5. The E2A gene produces two alternatively spliced proteins, E12 and E47, which are required for the development of CLPs and promote the expression of B-lineage genes including *Cd79a* and *Igll1* (Bain et al., 1997; Borghesi et al., 2005). In addition to E2A, PU.1 and signaling through the IL-7R promote the expression of Ebf1 (Kikuchi et al., 2008; Roessler et al., 2007; Seet et al., 2004). Ebf1 is required for differentiation into pro-B cells and complementation studies have demonstrated that exogenous Ebf1 expression is able to rescue B cell development following loss of Ikaros, PU.1, E2A, or IL-7Rα (Kikuchi et al., 2005; Lin and Grosschedl, 1995; Medina et al., 2004; Reynaud et al., 2008; Seet et al., 2004). Ebf1 also regulates expression of a number of B-lineage genes including *Cd79a*, *Cd79b*, *Igll1*, and *VpreB1* (Lin and Grosschedl, 1995; Zandi et al., 2008). E2A and Ebf1 coordinate to upregulate expression of Pax5 at the pro-B cell stage (O'Riordan and Grosschedl, 1999). The upregulation of Pax5 and the consequent display of CD19 marks commitment to the B cell lineage (Nutt et al., 1999). B cell development in Pax5-deficient mice is blocked at the early pro-B cell stage and are not committed to the B-lineage, retaining the capacity to differentiate into each hematopoietic lineage (Mikkola et al., 2002; Nutt et al., 1999). Ebf1 has also been demonstrated to restrict alternative lineage

potential independently of Pax5, indicating that Ebf1 and Pax5 are both essential factors for B-lineage commitment (Pongubala et al., 2008). Overall, the path leading to the development of $CD19^+$ pro-B cells that are committed to B cell development follows a series of developmental stages driven by cytokine signaling as well as the sequential expression and activation of a network of transcription factors, each with an essential role in B-lineage specification and commitment.

1.2.2) Differentiation of committed B cell progenitors and checkpoints

The developmental stages marking the differentiation of pro-B to immature B cells have been classified based on the expression of surface markers by two major strategies (Figure 1.2). The first, proposed by Hardy and colleagues, characterizes these B cell developmental stages based on the surface expression of B220, IgM, CD43, CD24, and BP-1 (Hardy et al., 1991). The second, proposed by Rolink and colleagues, defines these B cell developmental stages by surface expression of B220, IgM, CD25 (IL-2Rα), and CD117 (c-Kit) (Rolink et al., 1994). In this progression from pro-B to immature B cells, committed B lineage progenitors must pass two developmental checkpoints, which select B cells for continued developed based on successful recombination events at the *Igh* and *Igl* loci. The first checkpoint, the pre-BCR checkpoint, selects pro-B cells for production of a μHC that can bind to the surrogate light chain (SLC) and form a pre-BCR on the surface of large pre-B cells. The second checkpoint selects small pre-B cells for production of a BCR on immature B cells. Recombination at the immunoglobulin heavy chain locus is initiated with D-J_H rearrangements at the pre-pro B cell stage and is completed with V_H-DJ_H rearrangements at the pro-B cell stage resulting in the production of a μ heavy chain (μHC) (Chowdhury and Sen, 2001). However, as this is a random process, nearly 2/3 of these recombination events are non-productive, resulting in out-of-frame rearrangements and leading to cell death by neglect (Decker et al., 1991). Pro-B cells that undergo successful rearrangement at

Figure 1.2: Developmental stages of committed B lineage progenitors in the bone marrow. Diagram depicting the stages of B cell development from B-lineage committed pro-B cells through mature B cells. Each stage is defined by surface marker expression and status of immunoglobulin rearrangements. The relative expression of each marker in each cell population is delineated by line thickness. Imm. B=Immature B

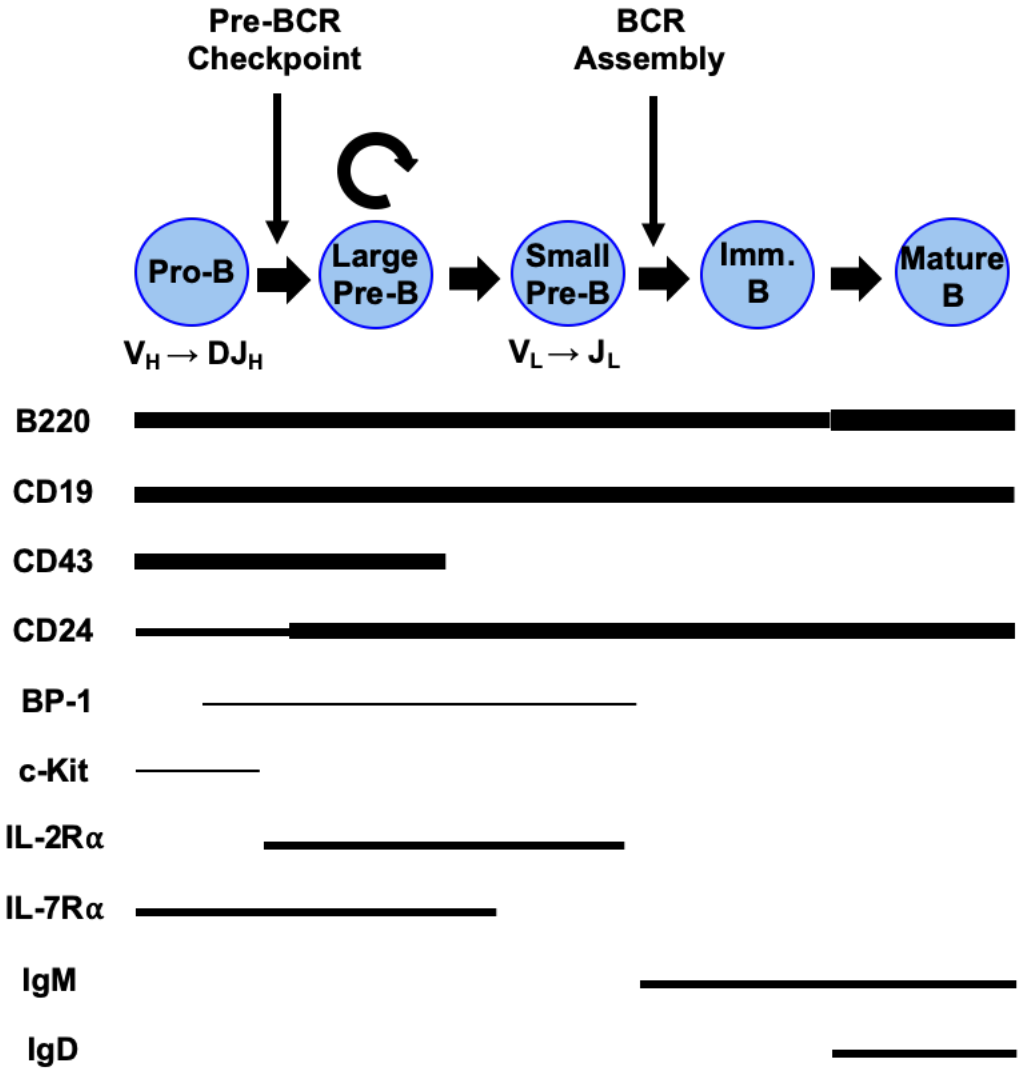
Pre-BCR
Checkpoint
BCR
Assembly
Pro-B
Large
Pre-B
Small
Pre-B
Imm.
B
Mature
B
$V_H \rightarrow DJ_H$
$V_L \rightarrow J_L$
B220
CD19
CD43
CD24
BP-1
c-Kit
IL-2Rα
IL-7Rα
IgM
IgD

the *Igh* locus produce a μH which pairs with the SLC, composed of λ5 and VpreB, and the signaling components Igα and Igβ to form the pre-BCR complex (Hombach et al., 1990; Papavasiliou, 1996). Signaling through the pre-BCR promotes pro-B cell survival and proliferation, facilitates differentiation into the large pre-B cell compartment, and represents the first checkpoint during B cell development, the pre-BCR checkpoint (Geier and Schlissel, 2006). Large pre-B cells undergo a proliferative burst, but after 2-5 rounds of cell division they exit the cell cycle and differentiate into small pre-B cells (Hess et al., 2001; Rolink et al., 2000).

At the small pre-B cell stage, a second B cell developmental checkpoint selects cells for successful rearrangements at the *Igl* loci and expression of a BCR. In small pre-B cells, VJ recombination at the two immunoglobulin light chain loci occurs, first at the at the kappa locus (*Igκ*) and then at the lambda locus (*Igλ*) (Engel et al., 1999). However, recombination at the *Igκ* locus in small pre-B cells is often unsuccessful due to aberrant recombination and the process can repeat, cycling through all available V_κ and J_κ segments before progressing to the *Igλ* locus (Yamagami et al., 1999). Small pre-B cells that fail to produce a functional BCR undergo apoptotic cell death. Thus, while the selective pressure driving the pre-BCR checkpoint ultimately focuses on successful expression and signal transduction through the pre-BCR, the second checkpoint in B cell development focuses on the successful expression of a non-autoreactive BCR (Tussiwand et al., 2009). Cells that pass this checkpoint and produce a BCR in the form of membrane-bound IgM (mIgM) are called immature B cells.

Despite production and expression of mIgM on immature B cells, the process of VJ recombination has the potential to produce B cells with autoreactive BCRs (Nemazee, 2006). Immature B cells that recognize autoantigen undergo selection in the bone marrow or after migration to the spleen after which they are called transitional B cells. These cells face three

potential fates: apoptotic elimination, a non-reactive anergic state, or receptor-editing to generate a new immunoglobulin light chain (Chen et al., 1995; Goodnow et al., 1988; Hartley et al., 1993; Tiegs et al., 1993). Moderate to strong crosslinking of the BCR on immature B cells typically occurs in the bone marrow and leads to receptor editing and possibly apoptotic cell death {Hartley:1993tp}. Weak crosslinking of the BCR on immature B cells typically occurs in the spleen and can induce anergy (Goodnow et al., 1988). However, receptor editing represents the dominant fate of B cells with self-reactive antigen receptors (Retter and Nemazee, 1998). This process involves re-initiation of VJ recombination at the Igl loci, which continues until either a non-self-reactive antigen receptor is produced or no possible rearrangements remain and cells undergo apoptosis (Tiegs et al., 1993). Immature B cells able to successfully overcome this developmental checkpoint and produce a non-self-reactive BCR exit the bone marrow and undergo further maturation in the spleen.

1.3) Signaling Across the pre-BCR Checkpoint

In the developmental stages spanning the pre-BCR checkpoint, pro-B and pre-B cells, key signaling pathways are focused on enforcing the separation of proliferation and immunoglobulin gene rearrangements to distinct sub-populations of B cell progenitors (Hendriks and Middendorp, 2004). Failure to properly segregate these processes can result in leukemic transformation, which is most prevalent at the highly proliferative large pre-B cell stage (Eswaran et al., 2015; Vogler et al., 1978). Two major receptors, the IL-7R and pre-BCR, drive development across the pre-BCR checkpoint through regulation of survival, proliferation, metabolism, and differentiation of pro-B and pre-B cells (Clark et al., 2014; Reth and Nielsen, 2014).

The IL-7 signaling pathway mediates survival, proliferation, and metabolism in pro-B cells (Figure 1.3). The IL-7R is composed of the IL-7Rα, which confers specificity for IL-7, and the

Figure 1.3: IL-7R signaling in pro-B cell development. Pro-B cells rely on signaling through the IL-7R to promote survival, proliferation, and metabolism. Jak1/3 signaling through Stat5 mediates pro-B cell survival through regulating the balance between pro-apoptotic (Mcl1) and anti-apoptotic (Bim and Bmf) family members. Stat5 also promotes pro-B cell proliferation through inducing expression of Ccnd3. IL-7 signaling through Plcγ1/2 signals through the second messenger diacylglycerol (DAG) to activate Pkc and mTORC1 to promote pro-B cell proliferation and metabolism

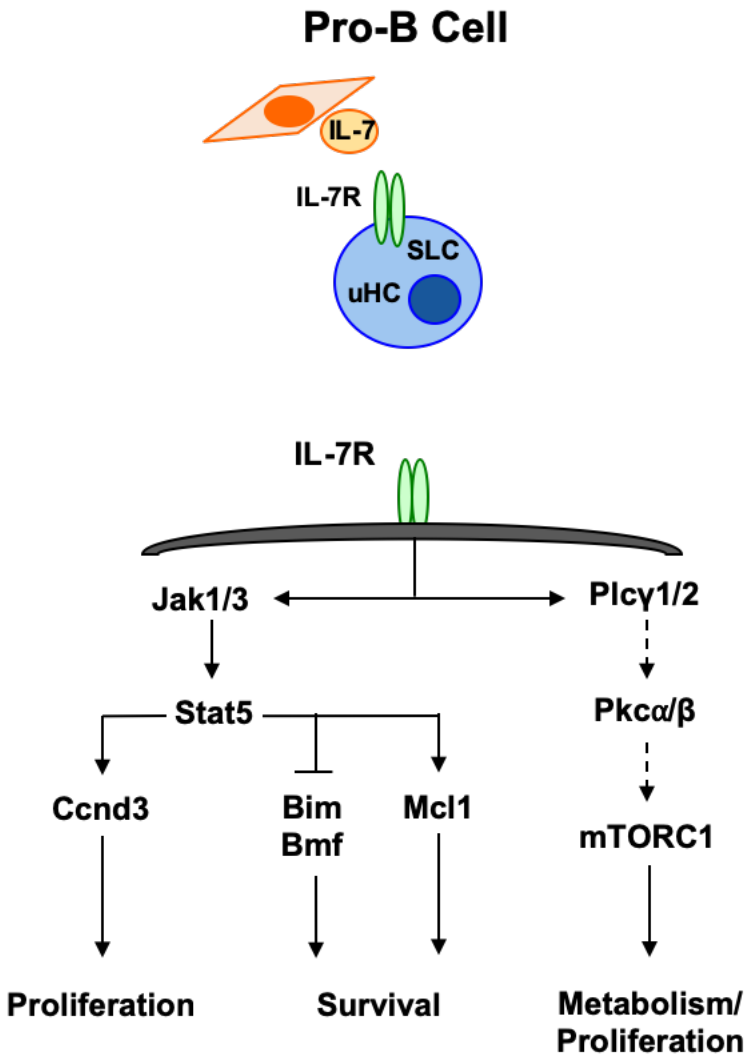
Pro-B Cell
IL-7
IL-7R
SLC
uHC
IL-7R
Jak1/3
Plcγ1/2
Stat5
Pkcα/β
Ccnd3
Bim
Bmf
Mcl1
mTORC1
Proliferation
Survival
Metabolism/
Proliferation

common-γ chain (γc) (Corfe and Paige, 2012). Signaling through the IL-7R activates the Jak/Stat, PI3K/Akt, MAPK/Erk, and Plcγ/Pkc/mTORC1 signaling pathways. However, only the Jak/Stat pathway through Stat5 and the Plcγ/Pkc/mTORC1 pathway appear to be critical for development and maintenance of the pro-B cell compartment. Stat5 signaling mediates pro-B cell survival through regulation of Bcl-2 family members and also contributes to proliferation through induction of cyclin D3 expression (Malin et al., 2010; Ochiai et al., 2012). IL-7-mediated activation of mTORC1 is crucial for maintaining pro-B cell metabolism and is the major contributor to homeostatic proliferation in pro-B cells (Zeng et al., 2018). Pro-B cells must regulate cell division and V(D)J recombination at the *Igh* locus in order to maintain genomic stability and minimize the risk of developing harmful mutations. Thus, pro-B cells modulate IL-7R surface expression to segregate populations undergoing IL-7-mediated proliferation from those undergoing DNA rearrangements (Johnson et al., 2012). Upon productive rearrangement at the *Igh* locus, the mu heavy chain (μHC) rapidly associates with the surrogate light chain, Igα and Igβ to form the pre-BCR. Further rearrangements are prevented in a process called allelic exclusion to ensure that only one μHC is produced so that each B cell has a unique specificity for antigen (Geier and Schlissel, 2006). While the mechanism or signaling pathways required for allelic exclusion has not been determined, it occurs after pre-BCR surface expression and involves chromatin remodeling, which renders the *Igh* locus inaccessible to the Rag recombinase. In addition, signaling downstream of the pre-BCR leads to downregulation of Rag gene expression as B cells enter the proliferative large pre-B cell stage (Kuo and Schlissel, 2009).

Expression of a pre-BCR on the surface lowers the threshold of large pre-B cells for IL-7 and the pre-BCR and IL-7R synergize to induce a burst of proliferation and expand the pool of B cells with productive IgH rearrangements (Figure 1.4) (Hess et al., 2001; Marshall et al., 1998).

Figure 1.4: IL-7R and pre-BCR signaling at the large pre-B cell stage: Upon expression of the pre-BCR on the surface of large pre-B cells, IL-7R and pre-BCR signaling synergize to promote enhanced proliferation and metabolic activity. IL-7R signaling through Stat5 promotes proliferation through induction of Ccnd3 expression. Both the IL-7R and pre-BCR signal through PI3K to activate Mapk/Erk which induces expression of c-Myc. c-Myc promotes proliferation through induction of Ccnd3 and inhibition of the cell cycle inhibitor p27. Signaling through the pre-BCR maintains stability of Ccnd3 protein through a PI3K-dependent mechanism. PI3K signaling also activates Akt, which phosphorylates Foxo1, leading to its degradation. This prevents Foxo1-mediated cell cycle inhibition through p27 and prevents differentiation through Foxo1-mediated induction of Rag expression. Akt also promotes enhanced metabolic activity in large pre-B cells through activation of mTORC1.

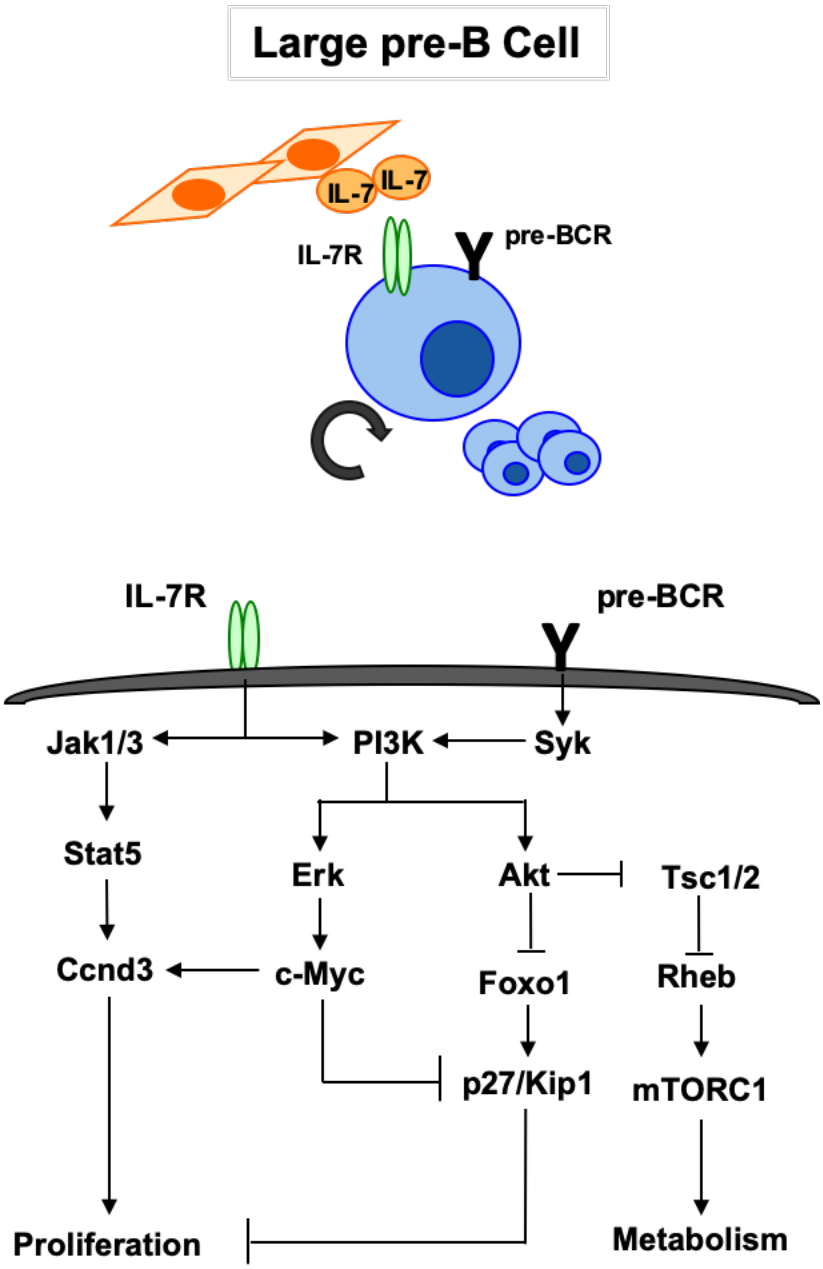
Large pre-B Cell
IL-7
IL-7
IL-7R
pre-BCR
IL-7R
pre-BCR
Jak1/3
PI3K
Syk
Stat5
Erk
Akt
Tsc1/2
Ccnd3
c-Myc
Foxo1
Rheb
p27/Kip1
mTORC1
Proliferation
Metabolism

Both the IL-7R and pre-BCR signal through PI3K/Akt and MAPK/Erk signaling pathways to enhance proliferative expansion as well as the metabolic pathways (see below) needed to fuel this increased cell division in large pre-B cells (Reth and Nielsen, 2014). In addition, downstream of the IL-7R, Stat5 recruits the histone methyltransferase Ezh2 to the *Igk* locus to prevent premature VJ recombination in cycling cells (Mandal et al., 2011).

Transition from the large pre-B cell compartment into small pre-B cells involves attenuation of IL-7R signaling and a shift in pre-BCR signaling from proliferation to differentiation. However, there are two conflicting viewpoints regarding the relative contribution of the IL-7R and pre-BCR to the large to small pre-B cell transition. One camp emphasizes the importance of IL-7 signaling for large pre-B cell proliferation and the necessity to attenuate IL-7-mediated proliferation to allow differentiation into quiescent, small pre-B cells (Clark et al., 2014). The second camp proposes that the IL-7R plays a more passive role and emphasizes the importance of the pre-BCR, initially to enhance proliferative expansion mediated by the IL-7R and then to coordinate attenuation of IL-7R signaling with the expression of genes needed for the large to small pre-B cell transition (Herzog et al., 2009). This second group also argues that many of the studies indicating the importance of the IL-7R for pre-B cell development utilize cells derived from *Irf4/Irf8*$^{-/-}$ mice which accumulate cycling large pre-B cells that are unable to differentiate. However, these cells are heavily reliant on a high concentration of IL-7 to remain viable, and many argue that this skews signaling pathways to be more dependent on signaling through the IL-7R (Abdelrasoul et al., 2018). The differences in these two viewpoints as to the relative importance of the IL-7R or pre-BCR for mediating development past the pre-BCR checkpoint underscores how much work remains to be done to fully understand regulation of the large and small pre-B cell stages of B cell development. What is clear is that IL-7R signaling is attenuated in the transition

from large to small pre-B cells to ensure segregation of proliferating large pre-B cells and small pre-B cells undergoing VJ recombination. This may occur through multiple mechanisms including asymmetric division away from environmental sources of IL-7 and upregulation of members of the suppressor of cytokine signaling (SOCS) family which inhibit proximal signaling through the IL-7R (Corfe et al., 2011; Johnson et al., 2008).

At the large to small pre-B cell transition signaling through the pre-BCR shifts from promoting proliferation to promoting differentiation (Figure 1.5). A critical mediator of this shift is the adaptor protein SLP65 or Blnk. Two mechanisms have been proposed for induction of Blnk expression including loss of Akt activation after attenuation of IL-7R signaling, which relieves repression of Foxo1 that induces Blnk expression (Ochiai et al., 2012). Alternatively, PI3K signaling downstream of the pre-BCR leads to transcription of Pax5, which subsequently induces expression of Blnk (Abdelrasoul et al., 2018). Blnk inhibits PI3K to attenuate pre-BCR mediated proliferative signaling and blocks Jak3 activity and inhibits Jak/Stat5 signaling downstream of the IL-7R (Herzog et al., 2008; Nakayama et al., 2009). In addition, Blnk induces expression of the transcription factors Irf4 and Irf8, which are required for the large to small pre-B cell transition and the recombination at light chain locus (Lu et al., 2003). Furthermore, the Ras/Mek/Erk pathway downstream of the pre-BCR leads to expression of E2A which, upon attenuation of IL-7 signaling through Stat5 that inhibits binding of E2A to the intronic *Igk* enhancer (E_{ki}), is able to induce *Igk* transcription and initiate VJ recombination (Mandal et al., 2009). Irf4/8 induce upregulation of CXCR4, which promotes increased mobility and decreased adhesion of differentiating pre-B cells so that they are not in prolonged contact with IL-7 from the bone marrow microenvironment (Fistonich et al., 2018; Johnson et al., 2008).

Figure 1.5: IL-7R and pre-BCR signaling at the large to small pre-B cell transition: At the large to small pre-B cell transition, signaling from the pre-BCR shifts from promoting proliferation to promoting differentiation. Pre-BCR signaling mediates cell cycle exit through inhibition of pro-proliferative signaling pathways downstream of the IL-7R and pre-BCR by Blnk, which inhibits both Jak1/3 and PI3K. Blnk also upregulates Irf4 and Irf8 that induce expression of Ikaros and Aiolos, which inhibit c-Myc expression as well as the surrogate light chain components of the pre-BCR. Irf4/8 also induce expression of CXCR4, which promotes migration and decreased association with IL-7 producing stromal cells. Loss of IL-7 signaling through Blnk and CXCR4 leads to loss of Stat5-mediated repression of the *Igk* enhancer and allows pre-BCR signaling through Erk to activate E2A, which induces transcription of germ line *Igk* transcripts. In addition, loss of PI3K/Akt activation frees Foxo1 to induce *Rag* expression and initiate VJ recombination at the light chain locus.

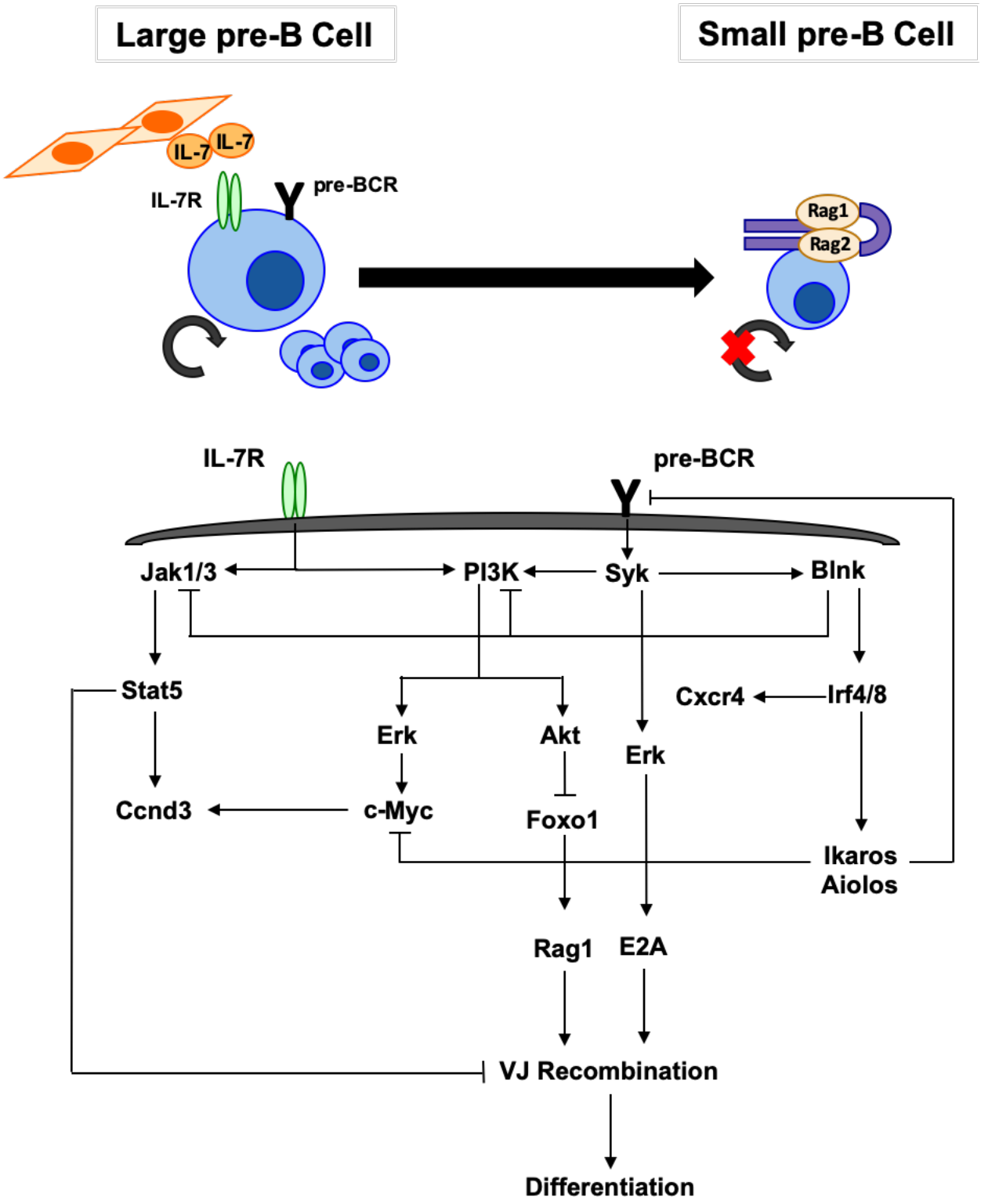
Large pre-B Cell
Small pre-B Cell
IL-7
IL-7
IL-7R
pre-BCR
Rag1
Rag2
IL-7R
pre-BCR
Jak1/3
PI3K
Syk
Blnk
Stat5
Cxcr4
Irf4/8
Erk
Akt
Erk
Ccnd3
c-Myc
Foxo1
Ikaros
Aiolos
Rag1
E2A
VJ Recombination
Differentiation

Irf4/8 also upregulate expression of the transcription factors Ikaros and Aiolos (Ma et al., 2008).Ikaros, in conjunction with its family member Aiolos, regulates a majority of the gene expression changes needed for the large to small pre-B cell transition and, in turn, mediate the phenotypic changes that accompany differentiation (Ferreirós-Vidal et al., 2013; Heizmann et al., 2013; Schwickert et al., 2014). They repress c-Myc to promote cell cycle exit and reduce metabolic activity by repressing Glut1 expression and inducing expression of the Glut1 inhibitor, Txnip which promotes Glut1 internalization and proteasomal degradation (Ferreirós-Vidal et al., 2019; Ma et al., 2010). Ikaros and Aiolos also mediate gene expression changes needed for differentiation including upregulation of key tyrosine kinases downstream of the pre-BCR (Syk, Lyn, Fyn, Blk) and increasing activation of Blnk that promote expression of Foxo1, which induces expression of *Rag1* to enable VJ recombination (Ferreirós-Vidal et al., 2013; Joshi et al., 2014; Schwickert et al., 2014). Finally, Ikaros and Aiolos downregulate the pre-BCR through repression of the surrogate light chain components, which promotes differentiation to small pre-B cells (Ma et al., 2008; Wang et al., 2002). In addition, transgenic expression of the SLC components λ5 and Vpreb1 results in constitutive BCR internalization, continued light chain rearrangements, and a developmental block at the immature B cell stage demonstrating that downregulation of the SLC is important for development beyond the pre-B cell stage (van Loo et al., 2007). Overall, coordinated repression of IL-7R mediated signals and shifting of pre-BCR signals to an anti-proliferation and pro-differentiation function mediates the successful transition from large to small pre-B cells and completion of the pre-BCR checkpoint.

1.3.1) Survival across the pre-BCR checkpoint

Apoptosis is the evolutionarily conserved process of programmed cell death that is necessary for the proper development of metazoans and serves to eliminate unwanted or potentially

dangerous cells (Hengartner, 2000). Apoptotic cells undergo morphological changes including cell shrinkage, membrane blebbing, DNA fragmentation and degradation of cellular structures while maintaining membrane integrity. These apoptotic bodies express surface molecules, which mediate their clearance by phagocytes in a non-inflammatory manner (Grimsley, 2003). Apoptosis can be induced by two pathways referred to as the intrinsic and extrinsic survival pathways. The intrinsic survival pathway is initiated by signals from within the cell such as nutrient starvation, DNA damage, cell cycle defects, loss of pro-survival factors, hypoxia and general cell stress, which converge on the mitochondria and thus is also referred to as the mitochondrial pathway (Chipuk et al., 2010). The intrinsic survival pathway is the critical survival pathway during B lymphopoiesis (Opferman, 2008). The extrinsic survival pathway is initiated by signals from outside the cell that signal through cell surface death receptors and thus is also referred to as the death-receptor pathway (Ashkenazi and Dixit, 1998). This pathway is critical for the maintenance of peripheral B cells but is dispensable for B lymphopoiesis (Imtiyaz et al., 2006). Both the intrinsic and extrinsic survival pathways utilize caspases, aspartate-specific cysteine proteases that mediate breakdown of the cell during apoptosis (Hengartner, 2000). Caspases normally exist within the cell in an inactive form and are referred to as pro-caspases. They are activated by proteolytic cleavage at internal cleavage sites and initiate a catalytic cascade that is amplified through cleavage events activating other caspases and enzymes resulting in irreversible cell death. This cascade begins with initiator caspases, caspase-8 and caspase-9 and proceeds through effector caspases, caspase-3, -6, and -7 that are ultimately responsible for cellular degradation

The intrinsic cell survival pathway

The intrinsic cell survival pathway is controlled by the balance of pro- and anti-apoptotic Bcl-2 family members (Figure 1.6) (Youle and Strasser, 2008). While all family members share

a homologous α-helical Bcl-2 homology (BH) domain, they can be divided into 3 subgroups based on structure and function. The anti-apoptotic members contain 4 BH domains (BH1-4) and include Bcl-2, Bcl-xL, Mcl-1, A1, and Bcl-2. Gain and loss of function approaches have been used to identify roles for all of these proteins but Bcl-w during B cell development (Opferman, 2008). The pro-apoptotic family members are split between proteins with multiple domains and proteins that only contain a single BH3 domain. The multi-domain pro-apoptotic family members contain 3 BH domains and include Bak, Bax, and Bok. Of these, Bak and Bax are the primary members of this subgroup required for B cell development (Takeuchi et al., 2005). The BH3-only pro-apoptotic proteins consist of Bad, Bik, Hrk, Bid, Bim, Bmf, Puma, and Noxa while only Bad, Bik, Bid, Bim, Bmf, and Puma are expressed during B cell development (Strasser, 2005). These proteins have redundant and compensatory functions such that only Bim and Bmf knockout mice have phenotypes during B cell development (Erlacher et al., 2006; Fahl et al., 2009; Labi et al., 2008).

In healthy cells Bak is constitutively associated with the mitochondrial membrane while Bax is sequestered in the cytosol by anti-apoptotic Bcl2 family members (Figure 1.6). This association inhibits oligomerization of Bax and Bak at the mitochondrial membrane which initiates apoptosis (Chipuk et al., 2010). BH3-only family members are activated in response to cell stress and bind to anti-apoptotic family members to prevent their inhibition of Bax and Bak and different BH3-only proteins have varying affinities for different anti-apoptotic proteins (Chen et al., 2005). Bim and Bid have also been found to activate Bax and Bak directly (Gavathiotis et al., 2008; Lovell et al., 2008). Activation of Bax and Bak induces conformational changes that result in their homo-oligomerization and formation of supramolecular pores on the outer mitochondrial membrane. Pore formation then leads to the release of cytochrome c from the mitochondria as well as a loss of mitochondrial membrane potential. Cytochrome-c associates with Apaf-1 and pro-caspase 9 to

Figure 1.6: Model for the intrinsic survival pathway. The intrinsic survival pathway is controlled by the balance of pro-apoptotic and anti-apoptotic Bcl-2 family members. The key mediators of apoptotic cell death in the intrinsic survival pathway are the pro-apoptotic Bak and Bax, which under normal conditions, are inhibited by anti-apoptotic Bcl-2 family members. In response to cellular stress, the BH3-only pro-apoptotic family members are activated. The BH3-only family members can either directly activate Bak and Bax or inhibit interaction of the anti-apoptotic Bcl-2 family members with Bak and Bax. Bak and Bax localize to the mitochondrial membrane, and upon activation, induce permeabilization of the mitochondrial outer membrane and the release of cytochrome c. Cytochrome c, Apaf-1, and pro-caspase 9 form the apoptosome complex, which induces cleavage and activation of caspase 9. Upon activation, caspase 9 catalyzes the cleavage of effector caspases (3, 6, and 7), which leads to apoptosis.

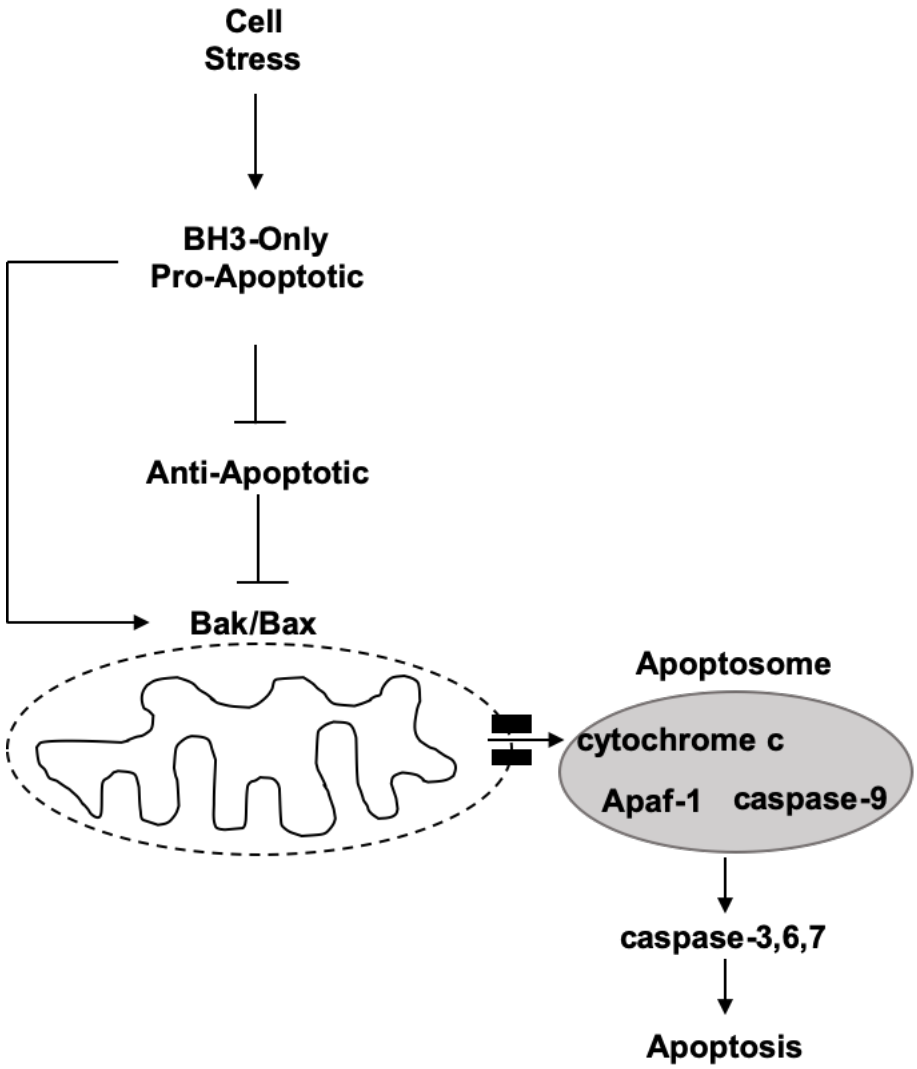
Cell
Stress
BH3-Only
Pro-Apoptotic
Anti-Apoptotic
Bak/Bax
Apoptosome
cytochrome c
Apaf-1
caspase-9
caspase-3,6,7
Apoptosis

assemble the 'apoptosome' complex leading to cleavage and activation of caspase-9 and subsequent activation of downstream effector caspases and apoptosis (Opferman, 2008).

Signaling pathways that control pro-B and pre-B cell survival

Survival at the early stages of B-lymphopoiesis is reliant on cytokines and signaling through cytokine receptors, whereas upon rearrangement of the immunoglobulin antigen receptor genes, survival signals are also provided by the pre-BCR and eventually the BCR (Baird et al., 1999). The cytokine receptor Flt3 promotes survival from the earliest lymphoid progenitors while the IL-7R promotes survival moving forward in development upon its expression at the CLP stage. In pro-B cells, survival is mediated by IL-7 and IL-7R signaling which regulate the balance in pro- and anti-apoptotic Bcl-2 family members (Corfe and Paige, 2012). The IL-7R subunits do not have intrinsic kinase activity and the γc and IL-7Rα are constitutively associated with Janus kinase 3 (Jak3) and Jak1 respectively. Binding of IL-7 induces phosphorylation of Jak1/Jak3 which are then able to recruit SH2-domain containing proteins such as Stat5a/b (O'Shea and Plenge, 2012). IL-7R signaling through Jak/Stat5 promotes survival during the differentiation from CLPs to $CD19^{+}$ pro-B cells differentiation as well as within the pro-B cell compartment through regulation of Mcl-1 expression (Malin et al., 2010). Mcl1 is required for the development and maintenance of B cell progenitors and, in particular, for the development of pro-B cells downstream of IL-7 signaling through Stat5 (Malin et al., 2010; Opferman et al., 2003). Signaling through Stat5 also induces expression of Bcl-2 to promote pro-B cell survival and constitutive expression of Bcl-2 in *Stat5*$^{-/-}$ mice partially rescues B cell development (Clark et al., 2014; Malin et al., 2010). Bcl-2 is highly expressed in pro-B cells and correlates with their ability to resist dexamethasone-mediated cell death (Merino et al., 1994). However, expression of a transgenic Bcl-2 is unable to rescue B

lymphopoiesis in *IL-7R*$^{-/-}$ mice, indicating that Mcl-1 is the major anti-apoptotic protein mediating pro-B cell survival downstream of IL-7 signaling (Maraskovsky et al., 1998).

Signaling through the IL-7R has also been implicated in regulation of pro-apoptotic Bcl-2 family members. IL-7-deficient mice exhibit enhanced pro-B and pre-B cell death as well as an imbalance in expression of Bcl2 and Bax, suggesting that IL-7 signaling regulates expression of Bcl-2 and Bax to favor increased Bcl-2, decreased Bax, and thus to promote survival (Lu et al., 1999). IL-7 signaling is also associated with negative regulation of pro-apoptotic Bim in that loss of Bim promotes survival but not differentiation of pro-B and pre-B cells in response to IL-7 withdrawal *in vitro* (Oliver et al., 2004). Furthermore, *Bim*$^{-/-}$ is able to partially rescue B cell development in the absence of IL-7 *in vivo* (Huntington et al., 2009). We have demonstrated that the transcription factor c-Myb regulates intrinsic pro-B cell survival in the absence of IL-7 through repressing mRNA expression of pro-apoptotic Bim and Bmf (Fahl et al., 2018). Moreover, IL-7R signaling through Stat5 further represses Bim and Bmf expression and thus acts on the base levels set by c-Myb to favor pro-B cell survival. Control of survival at the pro-B cell stage is critical to allow sufficient time for cells to complete V(D)J recombination at the *Igh* locus, but not too much time as to risk the development of transforming mutations or chromosomal translocations. Thus IL-7R signaling in pro-B cells ultimately controls the length of this limited time period in which pro-B cells can attempt V(D)J recombination before ultimately undergoing apoptosis or differentiating into large pre-B cells.

Transition to the large pre-B cell stage is marked by expression of the pre-BCR, which in addition to IL-7 and Stat5-mediated survival cues, provides its own pro-survival signals within the pre-B cell compartment. However, the pro-survival signals downstream of the pre-BCR have not been well-defined. The level of pre-BCR surface expression and signaling as well as its ability to

promote pre-B cell survival, proliferation, and differentiation is primarily determined by the quality of the μHC and its ability to pair with the SLC (Kawano et al., 2006). In particular, the quality of the pre-BCR dictates the ability of downstream signaling pathways to induce expression of pro-survival genes such as Bcl-2 and Bcl-xL in pre-B cells (Wang and Clarke, 2007). Coordinate IL-7R and pre-BCR signaling through MAPK/Erk and PI3K/Akt provides additional survival cues in pre-B cells through inhibition of pro-apoptotic Bcl-2 family members. Signaling through Erk leads to phosphorylation and inhibition of Bim (O'Reilly et al., 2009). In addition, signaling through PI3K/Akt has been demonstrated to promote survival of progenitor and mature lymphocytes (Okkenhaug and Vanhaesebroeck, 2003; Srinivasan et al., 2009). In particular, Akt phosphorylates and sequesters pro-apoptotic Bad to increase B cell survival (Datta et al., 1997). Small pre-B cells are unresponsive to IL-7 signals and downregulate the SLC components of the pre-BCR (λ5 and VpreB) as they initiate DNA rearrangements at the *Igl* loci. Thus, survival of small pre-B cells is primarily mediated by a pathway activated by double-stranded DNA breaks during VJ recombination (Bednarski et al., 2012). The checkpoint kinase ATM is activated as part of the DNA damage response in response to Rag-mediated double-stranded breaks and activates Pim2, which phosphorylates Bad and prevents the initiation of apoptosis. Thus, as in pro-B cells, this pathway provides a window in which small pre-B cells can continue VJ recombination as they attempt to produce productive rearrangements at the immunoglobulin light chain loci.

1.3.2) Proliferation across the pre-BCR checkpoint

Cell division is required for the survival and maintenance of all organisms and is characterized by DNA replication and segregation of replicated chromosomes into separate daughter cells (Civelekoglu-Scholey and Cimini, 2014; Vermeulen et al., 2003). This process was originally divided into two stages which together constitute the cell cycle: mitosis (M) or the

process of nuclear division and interphase or the period between two M phases (Figure 1.7). The cell cycle begins in interphase and completes following equal division of the nuclear material in mitosis. Interphase is further divided into the following phases: G_1, S, and G_2. DNA replication occurs in S-phase and prepares cells for mitotic cell division. Preceding S-phase is a gap referred to as G1 in which the cell is preparing for DNA synthesis and following S phase is a second gap referred to as G2 when the cell is preparing for mitosis. Cells in G_1 can also enter a resting state, G_0, before committing to DNA replication and most non-growing/non-proliferating cells are in this state.

Cell cycle regulation

The orderly transition between each cell cycle phase is regulated by key proteins expressed at specified points in the cycle (Figure 1.7). The main drivers of cell cycle transitions are cyclin-dependent kinases (CDKs) (Malumbres, 2014). Nine CDKs have been identified but just five are active during the cell cycle in the following phases G1 (CDK4, CDK6, and CDK2), S (CDK2), G2 and M (CDK1). CDK protein levels remain stable while protein levels of their cyclin targets rise and fall throughout the cell cycle and thus control activation of CDKs at critical cell cycle transitions (Morgan, 1995). Different cyclins are required at different points in the cell cycle. The D-type cyclins (cyclin D1, cyclin D2, cyclin D3) bind CDK4 and CDK6 and mediate entry into G_1 (Sherr, 1994). Cyclin E associates with CDK2 and mediates the G_1 to S phase transition (Ohtsubo et al., 1995). Cyclin A complexes with CDK2 during S phase and with CDK1 in late G_2 to promote entry into mitosis (Girard et al., 1991). Finally, mitosis is regulated by cyclin B complexed with CDK1 (Arellano and Moreno, 1997). Cyclins A, B, D, and E contain protein sequences required for ubiquitin-mediated degradation, which occurs at the end of each cell cycle phase and ensures the ordered progression of cell cycle stages (Glotzer et al., 1991).

Figure 1.7: Model for cell cycle progression and regulation. The cell cycle can be divided into interphase (composed of G_1, S, and G_2) in which DNA is replicated and mitosis (M), in which the nuclear material is divided between daughter cells. Progression through the cell cycle is regulated by cyclin dependent kinase (CDK)/cyclin interactions, which promote cell cycle progression as well as CDK inhibitors (CKI), which inhibit cell cycle progression. The transition into G_1 is mediated by cyclin D in association with CDK4/6, which phosphorylate retinoblastoma (Rb) protein, preventing its interaction with E2F, which is free to transcribe genes required for entry into S-phase. Then cyclin E and Cdk2 mediate the G_1 to S phase transition, cyclin A complexes with Cdk2 during S phase and Cdk1 in late G_2 to mediate the G_2 to M transition, and cyclin B1 with Cdk1 regulate mitosis. The CKIs p15, p16, p18, and p19 inhibit cell cycle progress by binding to Cdks before association with cyclins and most frequently act on Cdk4/6. The CKIs p21 and p27 inactivate cyclin/Cdk complexes throughout the cell cycle. Cell cycle progression is also regulated by periodic checkpoints (red bars in cycle) in which cells assess internal and external cues to determine if conditions are favorable for cell division or if they will undergo cell cycle arrest.

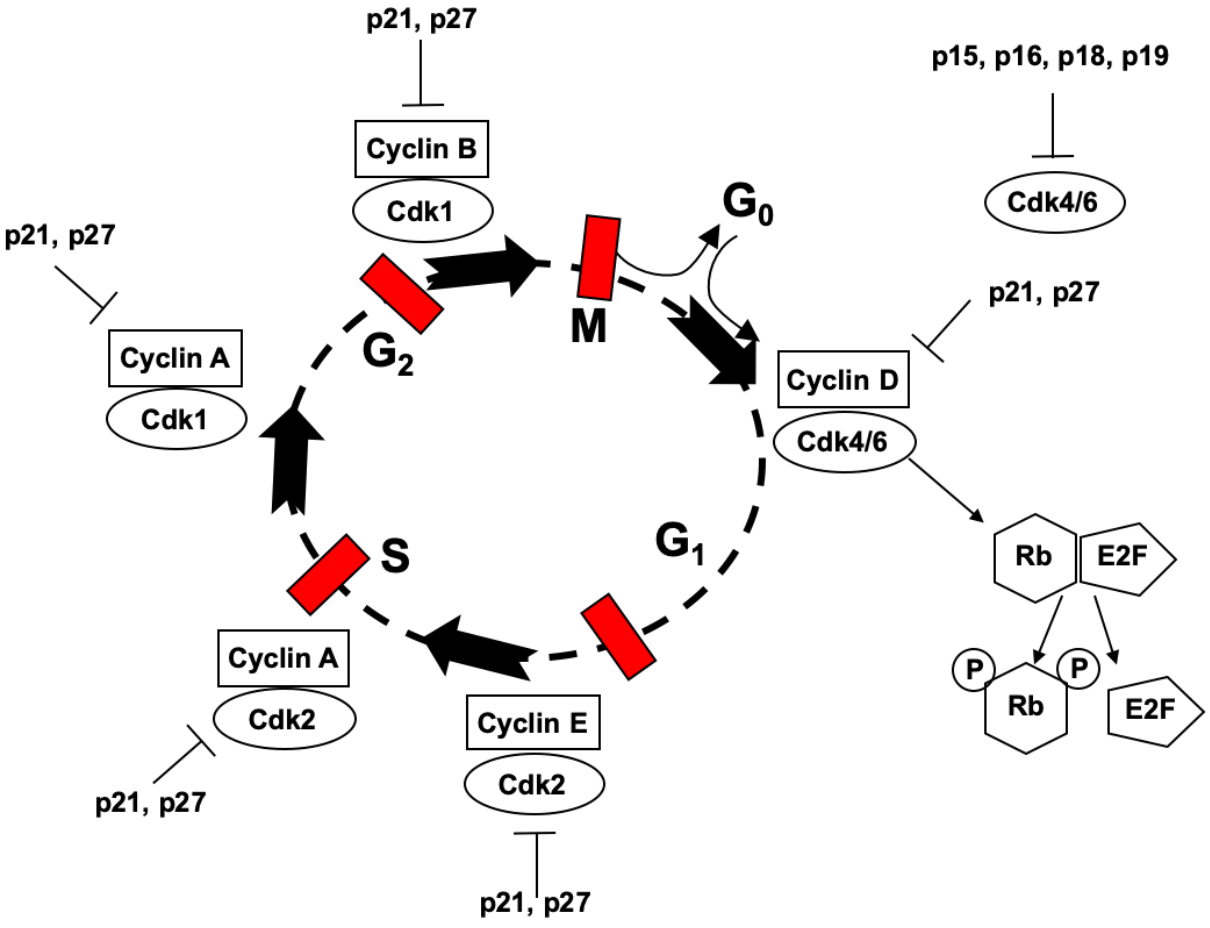
p21, p27
Cyclin B
Cdk1
p15, p16, p18, p19
Cdk4/6
p21, p27
G0
p21, p27
Cyclin A
Cdk1
G2
M
Cyclin D
Cdk4/6
Rb
E2F
S
G1
Cyclin A
Cdk2
Cyclin E
Cdk2
P
P
Rb
E2F
p21, p27
p21, p27

CDK activity is counteracted by cell cycle inhibitory proteins, CDK inhibitors (CKI), which can bind to CDKs or CDK-cyclin complexes. CKIs consist of two main families: the INK4 family and the Cip/Kip family. The INK4 family consists of p15 or INK4b, p16 or INK4a, p18 or INK4c, and p19 or INK4d, which inactivate the G_1 CDKs (CDK4 and CDK6) prior to cyclin binding (Cánepa et al., 2007). The Cip/Kip family includes p21 or Cip1, p27 or Kip1, and p57 or Kip2, which inactivate CDK-cyclin complexes and, like the INK4 family, also typically act on the G_1 CDK4/6-cyclin D complexes (Cerqueira et al., 2014).

Progression through the cell cycle is regulated by a series of checkpoints, in which cells assess internal cues (i.e. nutrient availability and DNA integrity) and external cues (i.e. signals from growth factors) to determine whether conditions are favorable for cell division or if they will undergo cell cycle arrest (Barnum and O'Connell, 2014). The first of these checkpoints referred to as the restriction point (R) is the "point of no return" in G_1 phase, after which cells are committed to enter the cell cycle and undergo DNA replication in S phase. Then, at various points throughout the cell cycle, DNA damage checkpoints arrest cells in order to enable repairs to occur, or to initiate apoptosis if DNA repair is not possible. These status checkpoints occur before cells enter S phase (the G_1-S checkpoint), after DNA replication (the G_2-M checkpoint), or within S and M phases. These cell cycle checkpoints are particularly important to prevent the deregulation of the cell cycle and uncontrolled proliferation associated with cancer (Vermeulen et al., 2003; Williams and Stoeber, 2011).

Balancing proliferation and differentiation at the pre-BCR checkpoint

In developing lymphocytes, it is critical to separate cell proliferation from DNA rearrangements at the immunoglobulin loci to maintain genomic integrity. Across the pre-BCR checkpoint, IL-7R and pre-BCR signaling pathways orchestrates cell proliferation, V(D)J

recombination, and differentiation that occur in the transitions that occur from pro-B to small pre-B cells (Clark et al., 2014; Reth and Nielsen, 2014). In pro-B cells, prior to expression of the pre-BCR, homeostatic proliferation is mediated by signaling through the IL-7R (Corfe and Paige, 2012). IL-7RKO mice exhibit severely impaired B cell lymphopoiesis including decreased proliferative expansion of pro-B cells (Peschon et al., 1994). Pro-B cells undergoing rearrangement at the *Igh* locus, must separate IL-7-mediated homeostatic proliferation from V(D)J recombination. As one method of achieving this, the cyclin A/CDK2 complex phosphorylates Rag2 and targets it for ubiquitination by S phase kinase-associated protein 2 (SKP2) and proteasomal degradation (Jiang et al., 2005). In addition, pro-B cells are heterogeneous for IL-7R surface expression such that it is negatively correlated with the level of Rag expression. Cells with high IL-7R expression undergo IL-7 dependent proliferation while cells with low IL-7R expression able to express Rag and undergo V(D)J recombination (Johnson et al., 2012). Thus, pro-B cells are able to maintain homeostatic proliferation as well as safely initiate rearrangements at the *Igh* locus to facilitate differentiation across the pre-BCR checkpoint.

In pro-B cells, IL-7R signaling through Stat5 promotes proliferation through inducing transcription of cyclin D3, which together with CDK4/6 mediates the G_1/S phase transition of the cell cycle (Mandal et al., 2009). However, cyclin D3 seems to be most critical for the proliferative expansion of large pre-B cells, as *Ccnd3*$^{-/-}$ mice have normal total numbers of pro-B cells and exhibit a moderate reduction in >2n DNA content (Cooper et al., 2006). Subsequent studies demonstrated that cyclin D3 has a proliferation-independent function in pro-B cells mediated by association of cyclin D3 with distinct sub-compartments within the nucleus, each associated with different function (Powers et al., 2012). Cyclin D3 is found in two soluble fractions, one associated with CDK4 that promotes cell cycle progression, and another minor fraction that is sensitive to

inhibition of PI3K but is not important for proliferation. However, the majority of cyclin D3 protein in pro-B cells binds the nuclear matrix and is involved in regulating gene expression including repression of immunoglobulin variable gene segment expression, thus limiting availability for VDJ rearrangement, and induction of cell cycle genes. This discovery represents another mechanism of segregating recombination from proliferation in pro-B cells.

It was previously thought that PI3K/Akt signaling is activated downstream of IL-7R in pro-B cells to promote cell survival and proliferation. However, deletion of the PI3K catalytic subunits p110α and p110δ, treatment with PI3K inhibitors, or deficiency in the regulatory subunit p85α does not significantly affect pro-B cells (Fruman et al., 1999; Powers et al., 2012; Ramadani et al., 2010). Furthermore, a recent report demonstrated that this pathway is not important in pro-B cells and, in fact, that PTEN-mediated repression of PI3K is critical for proper pro-B cell development and to prevent apoptosis (Zeng et al., 2018). However, IL-7R signaling through mTORC1 is critical for pro-B cell proliferation and a second recent report demonstrated that IL-7R signaling activates mTORC1 via Plcγ/Pkc signaling to promote proliferation in a Stat5 independent but c-Myc-dependent manner (Zeng et al., 2018). However, this pathway is not important for pro-B cell survival, suggesting bifurcated roles for Stat5 and mTORC1 in mediating IL-7R-mediated pro-B cell survival and proliferation.

Upon its expression in large pre-B cells, signals from the pre-BCR synergize with IL-7R signaling to induce a limited burst of proliferation. Expression of the pre-BCR lowers the threshold for IL-7 such that large pre-B cells are able to undergo enhanced proliferation even under limited concentrations of IL-7 (Marshall et al., 1998). IL-7R and pre-BCR signaling coordinately activate the PI3K and Mapk/Erk signaling pathways and inhibition of either PI3K or Mek1 inhibits proliferation of pre-BCR$^+$ B cell progenitors (Fleming and Paige, 2001). Downstream of the pre-

BCR, PI3K is activated by spleen tyrosine kinase (Syk), which is important for promoting B-cell proliferation in that Syk-deficient B cells display a developmental block at the pre-B cell stage and fail to undergo proliferative expansion (Cheng et al., 1995). PI3K then signals through Akt to promote activation of the cell growth and bioenergetic machinery needed to support the rapid proliferation of large pre-B cells through aerobic glycolysis (Doughty et al., 2006). One major downstream target of Akt activation in large pre-B cells is mTORC1, which is generally associated with cell growth and increased protein synthesis. *Raptor^{ff} Mb1-cre* mice in which B-cell specific deletion of the mTORC1-specific adapter protein, regulatory-associated protein of mTOR (Raptor), occurs at the pre-pro-B cell stage exhibited a block in early pre-B cells as well as decreased survival and proliferation (Iwata et al., 2016). PI3K/Akt signaling also inhibits Foxo1 and so prevents premature induction of Rag expression and VJ recombination at the immunoglobulin light chain locus. Foxo1 also induces expression of the CKI p27/Kip1 to block the G_1 to S phase transition and Akt is able to counteract p27 expression (Dijkers et al., 2000).

Signaling through both the IL-7R and pre-BCR also activate the Mapk/Erk pathway (Reth and Nielsen, 2014). Inducible *Erk1/Erk2$^{-/-}$* mice exhibit a block in development at the pro-B to pre-B cell transition (Yasuda and Kurosaki, 2008). Deletion of Erk1/Erk2 within the pre-B cell compartment reveals that these cells have normal IL-7R and pre-BCR expression, but are unable to proliferate. However, expression of the downstream target, c-Myc, can bypass loss of Erk and restore proliferation *in vitro* demonstrating the importance of c-Myc expression for large pre-B cell proliferation. Although the mechanism by which IL-7R and pre-BCR signaling activate the MAPK/Erk pathway is not understood, there is crosstalk between PI3K and Mapk/Erk signaling pathways and it has been proposed that PI3K activation by the IL-7R and pre-BCR lies upstream of Mapk/Erk activation (Reth and Nielsen, 2014).

Expression of the transcription factor c-Myc is induced by both PI3K and MAPK/Erk signaling and is crucial for large pre-B cell proliferation (Reth and Nielsen, 2014). c-Myc-deficient mice exhibit defective B cell proliferation while c-Myc transgenic mice develop pre-B cell tumors (Habib et al., 2007; van Lohuizen et al., 1991). In addition, utilizing a c-Myc knock-in GFP reporter gene mouse, it has been demonstrated that the large pre-B cell compartment can be divided into two populations based on c-Myc expression (Sandoval et al., 2013). Early, proliferating large pre-B cells express c-Myc and c-Myc expression is downregulated in a second large pre-B cell subset that appear to be transitioning to the small pre-B cell stage, thus solidifying the link between c-Myc and pre-B cell proliferation. c-Myc also regulates the mRNA expression of other cell cycle proteins through induction of cyclin D3 and repression of the cell cycle inhibitor p27/Kip1 (Ma et al., 2010). Cyclin D3 is another critical cell cycle regulator, which is required for large pre-B cell proliferation in that *Ccnd3*$^{-/-}$ mice exhibit significant decreases in pre-B cell numbers as well as >2n DNA content (Cooper et al., 2006). In particular, signaling downstream of the IL-7R through Stat5 and co-regulation of c-Myc with the pre-BCR activates cyclin D3 transcription while the pre-BCR regulates the stability of cyclin D3 protein. The pre-BCR stabilizes cyclin D3 protein by preventing its proteasomal degradation in a manner dependent on proximal kinase activation (either Src or Syk) and downstream PI3K activity.

After a limited number of divisions, attenuation of IL-7R-mediated proliferation and a shift in pre-BCR signaling from promoting proliferation to promoting differentiation, facilitate the transition from cycling large pre-B cells to quiescent small pre-B cells (Hamel et al., 2014). However, the mechanism of how IL-7R signaling is inhibited and the contribution of the pre-BCR to this process is poorly understood. Attenuation of IL-7 signaling may occur through multiple mechanisms including through asymmetric division away from sources of IL-7 in the bone marrow

microenvironment, which is reinforced by the upregulation of CXCR4 downstream of the pre-BCR that increases cell motility and limits engagement with IL-7 in the microenvironment (Fistonich et al., 2018; Johnson et al., 2008). In addition, signaling downstream of the IL-7R is inhibited by upregulation of SOCS1 and SOCS3 or the adaptor protein Lnk or Sh2b3, which interfere with proximal signaling through direct interaction with the Jak proteins (Cheng et al., 2016; Corfe et al., 2011).

The role of pre-BCR signaling in cell cycle exit at the large to small pre-B cell transition is unclear. Pre-B cells with a pre-BCR lacking tyrosines in the cytoplasmic tail of Igα can still proliferate, but are unable to differentiate, indicating that there are differing requirements for pre-BCR signaling in these processes (Storch et al., 2007). In addition, it has been demonstrated that while the pre-BCR is critical for the initiation of enhanced proliferation in large pre-B cells, downregulation of pre-BCR expression is not required for the cessation of large pre-B cell proliferation. However, downregulation of the pre-BCR expression is required for differentiation, which involves cell cycle exit, thus suggesting that the pre-BCR does play a role in regulating large pre-B cell proliferation (van Loo et al., 2007). In fact, downstream of the pre-BCR, Blnk, has been implicated in mediating repression of IL-7 signaling and differentiation into small pre-B cells. Mice deficient in Blnk expression exhibit aberrant pre-B cell proliferation and development pre-B cell leukemias. Blnk represses pro-proliferative signaling through inhibition of PI3K, induction of Irf4/8 and Ikaros/Aiolos expression which lead to inhibition of c-Myc, and interference with proximal IL-7R signaling through Jak3 (Herzog et al., 2008; Lu et al., 2003; Nakayama et al., 2009). Overall, IL-7R and pre-BCR signaling pathways coordinate the enhanced proliferative expansion of large pre-B cells with exit from the cell cycle in preparation for differentiation into small pre-B cells.

1.3.3) Glucose metabolism across the pre-BCR checkpoint

Cellular metabolism consists of a number of well-conserved pathways which mediate the biochemical reactions required to maintain cellular homeostasis. Both cell extrinsic and intrinsic signals regulate metabolic activity to couple cellular requirements for growth, division, and survival to the metabolic pathways that regulate the production of key macromolecules necessary to fulfill these needs (O'Neill et al., 2016). Metabolic pathways are linked by shared nutrient inputs and the flow of products from one pathway which then serve as precursors of another pathway. Even resting cells have basal energy requirements which are required to maintain their osmotic balance and facilitate replacement biosynthesis of necessary macromolecules (Mason and Rathmell, 2011). Cell populations undergoing increased proliferation (i.e. growth factor-stimulated or cancerous cells) have enhanced nutrient requirements to meet the metabolic demands of increased cell growth and division. In these cells, signaling pathways convey information regarding the nutrient status of the cell so that they can respond appropriately to nutrient sufficient conditions by permitting increased growth and proliferation and nutrient deficient conditions by promoting autophagy or possibly cell death. Signals indicating that there are insufficient nutrients available to promote cell division activate metabolic checkpoints which lead to cell cycle arrest and activation of the intrinsic apoptotic cell death pathway (DeBerardinis et al., 2008).

The major nutrient source fueling cellular metabolism is glucose (Mason and Rathmell, 2011). Cytokine or growth factor signals increase rates of glucose uptake and glycolysis and upregulate downstream metabolic pathways important for cell division in order to satisfy the cell's energetic and biosynthetic requirements. However, under conditions of limiting growth factor or nutrient availability, glycolysis and overall cell metabolism decreases and if these deficiencies persist, cells will eventually succumb to apoptosis. Glucose metabolism is a crucial determinant

of apoptotic initiation and maintaining glucose uptake after growth factor or serum withdrawal can suppress cell death (Rathmell et al., 2003; Zhao et al., 2007, 2008). Furthermore, cancer cells override metabolic checkpoints through oncogenic kinases, which mimic growth signals and facilitate enhanced rates of glucose metabolism needed to support proliferation (DeBerardinis et al., 2008). Thus, proper regulation of glucose uptake and utilization is critical to fulfill the metabolic demands of both normal and transformed cells.

Regulation of glucose uptake and utilization

Glucose uptake is in part controlled by cell-surface expression of glucose transporters which, in mammalian cells, include two protein families, the sodium-driven sugar cotransporters (SGLTs) and glucose transporters (GLUTs) (Augustin, 2010). The GLUT protein family consists of 14 isoforms which can be divided into 3 classes. Among these classes, the class I classical transporters are the best characterized and are comprised of GLUT1-4 and GLUT14. Of the class I transporters, GLUT4 is the most-well known due to its up-regulation by insulin receptor activation. However, GLUT4 is only expressed in muscle, liver, and adipose tissue, and not in hematopoietic lineages. In contrast, GLUT1 is ubiquitously expressed and is the primary source of glucose uptake in lymphocytes (Maciver et al., 2008). In addition, GLUT1 is often overexpressed in cancer to facilitate enhanced glucose uptake in tumor cells (Macheda et al., 2004).

GLUT1 expression is regulated at multiple levels including transcription, transport activity, and cell surface localization (Asano et al., 1991; Bentley et al., 2003; Lachaal et al., 2001; Wieman et al., 2007). Multiple factors have been demonstrated to regulate transcription of Glut1 mRNA including Akt, thioredoxin interacting protein (Txnip), and serum/glucocorticoid regulated kinase 1 (Sgk1) (Barthel et al., 1999; Palmada et al., 2006; Wu et al., 2013). In addition, Txnip inhibits

activity of Glut1 protein by promoting its internalization from the plasma membrane and proteasomal degradation (Sullivan et al., 2018; Waldhart et al., 2017). A series of papers utilized IL-3 dependent hematopoietic cell lines to demonstrate regulation of Glut1 trafficking, including the lymphoid cell line, FL5.12 (Bentley et al., 2003; Kan et al., 1994; Wieman et al., 2007). In these cells, growth factor signaling following IL-3 stimulation, maintained surface GLUT1 levels, promoted recycling of intracellular GLUT1 to the cell surface, and antagonized GLUT1 internalization. The major downstream pathway facilitating glucose transport is through PI3K/Akt (Maciver et al., 2008). Pharmacologic inhibition of PI3K decreases the ability of growth factor and cytokine signaling to increase surface Glut1 levels and a constitutively active form of Akt is able to maintain surface Glut1 in the absence of growth factor (Wieman et al., 2007). Downstream of Akt, mTOR is not important for maintaining surface Glut1 levels, but decreased glucose uptake upon rapamycin-mediated mTOR inhibition suggests that mTOR is important for Glut1 activity. In addition, IL-7 signaling through Stat5 and Akt have been implicated in Glut1 surface localization in T lymphocytes (Wofford et al., 2008).

Upon glucose uptake, the initial step of glucose utilization in the cell is its phosphorylation by the glycolytic enzyme hexokinase and conversion into glucose-6-phosphate (G6P). The hexokinase family consists of four isozymes Type I-IV or Hk1-4 and Type IV is commonly referred to as glucokinase (Wilson, 2003). While there is high sequence similarity between isozymes, they differ in their expression patterns, affinity for glucose, and sensitivity to inhibition by G6P. The isozymes Hk1 and Hk2, also known as mitochondrial hexokinases (mtHks), are able to associate with the outer mitochondrial membrane (Robey and Hay, 2005, 2006). Of the mtHks, Hk1 is ubiquitously expressed, particularly in tissues reliant on glycolysis while Hk2 expression is largely limited to insulin-sensitive tissues such as skeletal muscle and adipose tissue (Wilson,

2003). In addition, Hk1 has a higher affinity for glucose than Hk2 and is more resistant to G6P-mediated inhibition such that Hk1 activity is enhanced during periods of increased metabolic activity. The mtHks largely utilize intramitochondrial sources of ATP to catalyze glucose phosphorylation and thus couple glycolysis and mitochondrial oxidative phosphorylation. Therefore, hexokinase acts as a critical bridge between glucose uptake and its utilization through these two major processes that drive cellular metabolism.

Glycolytic and oxidative metabolism

The key molecule produced from cellular metabolism is adenosine triphosphate (ATP) that provides energy to fuel cellular processes (Donnelly and Finlay, 2015). Two major pathways convert glucose into ATP: glycolysis and oxidative phosphorylation (OxPhos) (Figure 1.8) (Donnelly and Finlay, 2015; Lunt and Vander Heiden, 2011). Following glucose uptake, it is processed through glycolysis, which is inefficient at ATP production, but yields a number of intermediate products that can be utilized in additional biosynthetic growth pathways as well as NADH, a cofactor used by a number of metabolic enzymes. The first committed step of glycolysis is glucose phosphorylation by hexokinase to produce glucose-6-phosphate (G6P). G6P may pass into the pentose phosphate pathway (PPP) for the synthesis of ribose for nucleotides or continue to be processed through the glycolytic pathway, ultimately resulting in the production of pyruvate. Pyruvate may then be reduced to lactate through lactic acid fermentation in order to recycle NADH, maintain NAD+ levels, and maintain flux through the glycolytic pathway. This process is favored by proliferating cell populations in that it perpetuates glycolytic metabolism and increases the accumulation of biosynthetic intermediates. Pyruvate can also be shuttled into the mitochondria as a substrate for the TCA cycle, which produces the reducing agents NADH and FADH2 that fuel oxidative phosphorylation and the mitochondrial electron transport chain. In contrast to glycolysis,

Figure 1.8: Model for glycolytic and oxidative glucose metabolism. Glucose metabolism is initiated following glucose uptake through glucose transporters, mainly Glut1-Glut4. After uptake, glucose is phosphorylated by hexokinase enzymes to produce glucose-6-phosphate, which can be shuttled into the pentose phosphate pathway for nucleotide biosynthesis or continue to be processed through glycolysis. Glycolytic intermediates downstream of glucose-6-phosphate can act as intermediates for the production of lipids and amino acids. The ultimate product of glycolysis is pyruvate, which may be converted into lactate by lactate dehydrogenase to produce NAD^+ ions. The lactate is secreted from the cell, and the NAD^+ ions can feed back into glycolysis. Pyruvate can also be shuttled into the mitochondrial to be utilized in the TCA cycle. The TCA cycle produces the cofactors NADH and $FADH_2$ which fuel oxidative phosphorylation and ATP production.

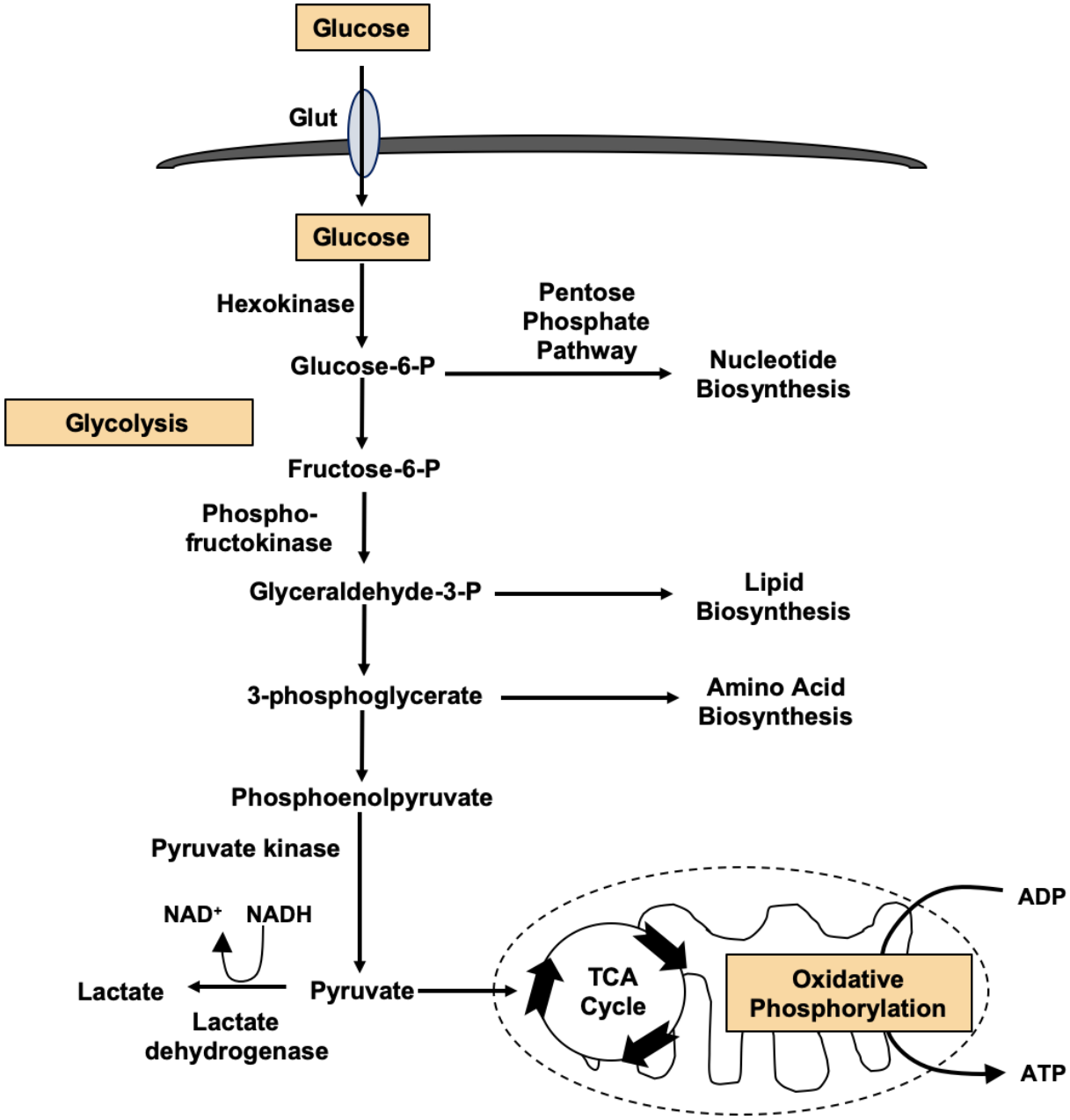
Glucose
Glut
Glucose
Hexokinase
Pentose
Phosphate
Pathway
Glucose-6-P
Nucleotide
Biosynthesis
Glycolysis
Fructose-6-P
Phospho-
fructokinase
Glyceraldehyde-3-P
Lipid
Biosynthesis
3-phosphoglycerate
Amino Acid
Biosynthesis
Phosphoenolpyruvate
Pyruvate kinase
NAD+
NADH
Lactate
Pyruvate
Lactate
dehydrogenase
TCA
Cycle
Oxidative
Phosphorylation
ADP
ATP

this process of oxidative metabolism is focused on ATP generation and thus is favored for maintaining homeostatic metabolism in relatively inert or quiescent cells.

Cancer cells and rapidly proliferating cells exhibit a hybrid metabolism termed aerobic glycolysis, characterized by rapid glycolysis even in the presence of oxygen and mitochondrial oxidative phosphorylation, which, promotes enhanced and sustained growth, proliferation, and survival (Vander Heiden et al., 2009; Lunt and Vander Heiden, 2011). In these cells the majority of pyruvate produced through glycolysis is converted to lactate, which is then secreted from the cell. This process of lactic acid fermentation ultimately recycles pyruvate back into the glycolytic pathway. Signaling through the PI3K/Akt/mTOR pathway and c-Myc link cell proliferation and metabolism and promote aerobic glycolysis (Fan et al., 2010). As a transcription factor, c-Myc induces mRNA expression of glucose transporters and other glycolytic genes (Lewis et al., 2000; Osthus et al., 2000). Activation of Akt typically acts post-transcriptionally to promote glucose transporter surface expression, and enhance activity of glycolytic enzymes including hexokinase and phosphofructokinase (Deprez et al., 1997; Gottlob et al., 2001; Majewski et al., 2003, 2004; Robey and Hay, 2005; Wieman et al., 2007). While aerobic glycolysis is meant to be transiently employed in normal proliferative tissues, it may also be co-opted by cancer cells. The role of c-Myc and PI3K signaling in promoting aerobic glycolysis also means they are vulnerable to mutations that perpetually maintain aerobic glycolysis and fuel the uncontrolled proliferation characteristic of cancer (Elstrom et al., 2004; Goetzman and Prochownik, 2018).

Glucose metabolism and cell survival

In order to balance growth and proliferation with cell death, metabolic pathways receive signals conveying the energy status of the cell and either promote survival under nutrient sufficient conditions, or induce apoptosis in nutrient deficient conditions (Mason and Rathmell, 2011).

Glucose acts as one of the key nutrient signals determining whether cells grow and proliferate or succumb to cell death (Mason and Rathmell, 2011). In particular, if proliferating cells undergoing aerobic glycolysis fail to take up sufficient glucose to meet metabolic and biosynthetic demands, they undergo cell cycle arrest and if nutrients remain limiting, they undergo apoptosis (Altman and Rathmell, 2012). A major energy status sensor that mediates multiple metabolic checkpoints to ensure cells only proliferate when sufficient nutrients are available is AMP activated protein kinase (AMPK) (Hardie et al., 2012). AMPK is a heterotrimeric protein complex which consists of a catalytic α subunit and regulatory β- and γ- subunits and is activated by falling energy status as indicated by an increased ratio of ADP/AMP to ATP. Under limiting glucose conditions, AMPK activates p53 to induce cell cycle arrest and upon complete withdrawal of glucose, apoptosis (Jones et al., 2005; Okoshi et al., 2008).

Under nutrient-deficient conditions cells undergo apoptosis through the Bcl-2 family-mediated intrinsic survival pathway through upregulation of pro-apoptotic Bcl-2 family members (McClintock et al., 2002). In particular, glucose deficiency has been associated with activation of Bax at the mitochondrial membrane while expression of anti-apoptotic Bcl-2 or Bcl-xL, as well as loss of pro-apoptotic Bim or Puma can protect cells from apoptosis upon glucose withdrawal (Chi et al., 2000; Lee et al., 2001; Ouyang and Giffard, 2016; Zhao et al., 2008). Proper glucose metabolism counteracts apoptosis mediated by the intrinsic survival pathway, in part, through maintenance of mitochondrial integrity mediated by the glycolytic enzyme, hexokinase. Growth factor signaling through Akt has been demonstrated to promote survival of the FL5.12 lymphoid cell line and Rat1a fibroblasts through a mechanism dependent on glucose uptake and hexokinase activity (Majewski et al., 2003; Rathmell et al., 2003). In addition, Akt signaling inhibits dissociation of mtHk from the mitochondrial membrane, which is correlated with an impaired

ability of growth factors and Akt to maintain mitochondrial integrity and inhibit apoptosis (Gottlob et al., 2001; Majewski et al., 2004). Thus, deficiencies in glucose uptake and metabolism are directly linked to cell survival.

Regulation of metabolism across the pre-BCR checkpoint

Metabolic regulation during early B cell development across the pre-BCR checkpoint has critical implications for proliferation of normal or leukemic pro-B or pre-B cells (Urbanczyk et al., 2018). However, few studies have been done characterizing metabolism of B cell progenitors across the pre-BCR checkpoint and thus the drivers of pro-B and pre-B cell glucose metabolism are poorly understood. Early studies utilizing 2-deoxyglucose (2-DG), a non-hydrolyzable glucose analog that blocks glycolysis, revealed that pro-B cells and large pre-B cells utilize glucose through the glycolytic pathway while small pre-B cells do not (Kojima et al., 2010). Later work provided a more comprehensive characterization of metabolic readouts from pro-B, large pre-B, and small pre-B cells (Stein et al., 2017). Pro-B cells maintain homeostatic growth mainly through oxidative metabolism over glycolytic metabolism and maintain moderate levels of glucose uptake as compared to large and small pre-B cells (Stein et al., 2017). The shift from pro-B to large pre-B cells is characterized by: reduced mitochondrial mass relative to cell size, which indicates a shift from oxidative to glycolytic metabolism, increased reactive oxygen species (ROS) production that is a normal byproduct of enhanced metabolic activity, and increased glucose uptake to fuel enhanced metabolic activity and cell division (Stein et al., 2017). Then, the shift from large to small pre-B cells returns cells to a more oxidative-reliant metabolism as in pro-B cells, but small pre-B cells exhibit even lower glucose uptake. As compared to pro-B cells, small pre-B cells exhibit a decreased oxygen consumption rate (OCR) and decreased extracellular acidification rate (ECAR), which are measurements performed by the Seahorse extracellular flux analyzer that

assess the status of oxidative phosphorylation and glycolysis respectively (Stein et al., 2017). Furthermore, small pre-B cells have a higher OCR/ECAR ratio indicating an even greater reliance on oxidative versus glycolytic metabolism than in pro-B cells. Furthermore, the decreased mitochondrial membrane potential of small pre-B cells suggests that they have decreased overall metabolic activity through mitochondria, and is in line with their status as a quiescent population.

Pro-B cell metabolism is maintained by IL-7-mediated activation of mTORC1, which coordinates environmental signals from nutrients and growth factors with cell growth and metabolism (Yu et al., 2017; Zeng et al., 2018). Inhibition of mTORC1 results in decreased pro-B cell proliferation and metabolism as measured by extracellular flux analysis of OCR and ECAR, but has no effect on pro-B cell survival. mTORC1 is canonically activated by signaling through PI3K/Akt, which phosphorylates and inhibits TSC1/2, and relieves inhibition of the Ras homolog and GTPase Rheb, which activates mTORC1 (Fruman and Limon, 2012). However, it has been demonstrated that in pro-B cells, IL-7 signaling activates mTORC1 in a PI3K/Akt independent manner and, in fact, that PTEN-mediated inhibition of PI3K is important to allow proper pro-B cell development including expression of the IL-7R, *Igh* rearrangement, and cell survival (Zeng et al., 2018). IL-7 led to mTORC1 activation through Plcg1/2 and specifically through the second messenger DAG and activation of protein kinase C (Pkc). In line with this finding, *Plcg1/2*$^{-/-}$ mice exhibit defects in IL-7 mediated proliferation, metabolism, and decreased mTORC1 activation (Yu et al., 2017).

While the exact mechanism by which mTORC1 mediates pro-B cell metabolism is unclear, this complex has well-documented roles in metabolic processes in numerous cell types, which would be crucial for both pro-B and pre-B cell metabolic pathways. mTORC1 plays an important role in regulating the production of proteins, lipids, and nucleotides required for cell growth and

division as well as in the suppression of autophagy (Saxton and Sabatini, 2017). The major downstream effectors of mTORC1, ribosomal S6K and the eIF4E binding protein (4EBP), mediate a number of mTORC1-dependent functions including protein synthesis. mTORC1 also contributes to lipid synthesis through S6K1-mediated activation of sterol responsive element binding protein (SREBP) transcription factors which control expression of genes important for fatty acid and cholesterol biosynthesis (Düvel et al., 2010). In addition, mTORC1 promotes nucleotide synthesis through S6K1-mediated activation of carbamoyl phosphate synthetase (CAD) involved in pyrimidine synthesis and ATF4-dependent expression of MTHFD2 that is involved in purine synthesis (Ben-Sahra et al., 2013, 2016). Finally, mTORC1 facilitates the shift from oxidative to glycolytic metabolism through increasing translation of the transcription factor HIF1α, which induces expression of a number of glycolytic enzymes (Düvel et al., 2010). These mTORC1 functions are particularly critical for large pre-B cells, in which this glycolytic shift and macromolecule production are required to fuel enhanced proliferative expansion.

At the pro-B to pre-B cell transition, the pre-BCR promotes the shift to a primarily glycolytic metabolism in part through downregulation of the EF-hand domain family member Efhd1 (Stein et al., 2017). Efhd1 is a Ca^{2+} binding protein that localizes to the inner mitochondrial membrane and is expressed in pro-B cells but is downregulated by pre-BCR expression at the pro-B to large pre-B cell transition. Knockdown or knockout of Efhd1 in pro-B cells increases glycolysis and glycolytic capacity and thus decreases the OCR/ECAR ratio, suggesting that Efhd1 functions in limiting glycolytic metabolism at the pro-B cell stage. Expression of Efhd1 beyond the pro-B cell stage in Efhd1 transgenic mice prevents the shift to glycolytic metabolism at the pro-B to pre-B cell transition and leads to decreases in mRNA expression of components of the Akt and Erk pathways as well as Glut1, which are critical mediators of large pre-B cell metabolic

activity. Thus, proper regulation of Efhd1 expression by the pre-BCR is important to facilitate the shift in metabolic pathways at the pro-B to large pre-B cell transition.

Within the pre-B cell compartment, a metabolic checkpoint regulates the shift back to a primarily oxidative metabolism and overall decrease in metabolic activity important for the large to small pre-B cell transition. This pre-B cell metabolic checkpoint is controlled by folliculin interacting protein 1 (Fnip1). Fnip1 forms a complex with AMPK which in turn regulates mTORC1 in response to the energy status of the cell (Iwata et al., 2017). *Fnip1*$^{-/-}$ mice exhibit a block at the large pre-B cell stage due to an imbalance in metabolism through dysregulation of AMPK and mTOR (Park et al., 2012). Large pre-B cells from *Fnip1*$^{-/-}$ mice are able to respond to proliferative signals from the IL-7R and pre-BCR, but are unable to differentiate into small pre-B cells. This leads to excessive cell growth, enhanced sensitivity to apoptosis upon metabolic stress such as nutrient deficiency or oncogene activation, and an overall phenotype of energy exhaustion. In addition, while AMPK is activated in *Fnip1*$^{-/-}$ large pre-B cells, it is unable to inhibit mTOR-mediated cell growth. Thus, Fnip1 functions to maintain metabolic homeostasis within the pre-B cell compartment through interactions with the energy sensor AMPK and modulation of mTORC1 activity during the rapidly proliferating large pre-B cell stage. This discovery emphasizes the importance of mTORC1 for large pre-B cell growth and proliferation as well as the need for proper regulation of mTORC1 to mediate the transition to small pre-B cells.

Control of pre-B cell metabolism has also recently been appreciated as a mechanism of tumor control by B-lineage transcription factors, which act as tumor suppressors counter-acting the development of B cell leukemias (Chan et al., 2017). In particular, Pax5 and Ikaros, which are critical for the commitment and differentiation of B cell progenitors, have been referred to as "metabolic gatekeepers" of B cell development (Muschen, 2019). Pax5 and Ikzf1 are mutated in

over 80% of cases of pre-B cell acute lymphoblastic leukemia (B-ALL) (Chan et al., 2017). Both transcription factors have been demonstrated to enforce a state of glucose and energy deprivation at the pre-B cell stage to rein in metabolic activity at the large to small pre-B cell transition. Thus, regulation of glucose metabolism across the pre-BCR checkpoint is critical to separate cell growth from differentiation and immunoglobulin gene rearrangements to facilitate proper B cell development across this checkpoint as well as to prevent leukemia development.

1.4) c-Myb

The *Myb* locus encodes the transcription factor and proto-oncogene c-Myb, a DNA binding phosphoprotein that acts as an activator and repressor of gene transcription (Zhou and Ness, 2011). c-Myb was originally discovered as the cellular homologue of the v-Myb oncogene found in two avian retroviruses, avian myeloblastosis virus (AMV) and E26 virus, which cause erythroid and myeloid leukemias in chickens (Klempnauer and Bishop, 1984; Leprince et al., 1983). c-Myb differs from virus-encoded v-Myb proteins by the presence of truncations that cause them to become oncogenic and drive leukemia development (Lipsick and Wang, 1999). The discovery of v-Myb in avian leukemia led to the primary association of c-Myb with hematopoietic lineages (Zhou and Ness, 2011). Early studies suggested roles for c-Myb in survival, proliferation, and differentiation of hematopoietic cells (Oh and Reddy, 1999). Experiments utilizing *in vitro* culture systems linked c-Myb expression with inhibiting differentiation and maintaining proliferation of leukemia cell lines. c-Myb expression was downregulated by chemically induced differentiation of myeloid and erythroid leukemia cell lines (Pedrazzoli et al., 1989; Ramsay et al., 1986). In contrast, forced expression of c-Myb inhibited differentiation of erythroid progenitor leukemia cell lines (Chen et al., 2002; Clarke et al., 1988; McClinton et al., 1990). In addition, shRNA-mediated knockdown of c-Myb induced differentiation in a subset of T-ALL (Clappier et al., 2007). Thus,

these preliminary studies suggested that c-Myb plays an important role in the maintenance of leukemia cells, but whether c-Myb is also important in normal hematopoiesis was unknown.

A critical role for c-Myb in normal hematopoiesis was demonstrated by the generation of a *Myb* null allele, which failed to produce homozygous null mice demonstrating that loss of c-Myb was embryonic lethal (Mucenski et al., 1991). The $Myb^{-/-}$ embryos developed normally until embryonic day 13, but by day 15, the embryos were anemic and died in utero. Furthermore, $Myb^{-/-}$ embryos had defects in myeloid development in the fetal liver and failed to switch from fetal to adult-type erythropoiesis. However, while the embryonic lethality of *Myb* null mutations first demonstrated a crucial role for c-Myb during normal adult hematopoiesis, it also impeded study of c-Myb function in the development of each hematopoietic lineage. Therefore, subsequent studies have utilized alternative approaches including hypomorphic mutations, c-Myb knockdown, and conditional deletion models that circumvent the embryonic lethality of *Myb* null mutations and enable continued interrogation of c-Myb function.

In addition to normal hematopoiesis, c-Myb has been implicated as a proto-oncogene acting in the development of both leukemias and solid tumors (Ramsay and Gonda, 2008). Increased c-Myb expression has been detected in murine leukemia models of erythroid, myeloid, and lymphoid cells (Belli et al., 1995; Clarke et al., 1988; Shen-Ong et al., 1989). In these hematopoietic tumors, increased c-Myb expression often retains leukemic cells in an immature, proliferating state and prevents differentiation. In addition, c-Myb has been implicated in murine and human B and T-ALL. Targeting c-Myb via allelic deletion in mouse and human models of BCR/Abl-transformed leukemia and via shRNA mediated knockdown in a human B-ALL cell line results in decreased survival, proliferation, and an overall reduced leukemic aggressiveness (Sarvaiya et al., 2012; Waldron et al., 2012). c-Myb has also been implicated in human T-ALL

and AML through chromosomal translocations and duplications at the *Myb* locus (Clappier et al., 2007; Lahortiga et al., 2007). While the initial characterization of c-Myb focused on hematopoietic cell lineages and leukemias, c-Myb has also been implicated in solid tumors including colon tumors, breast cancers, and head and neck tumors (Miao et al., 2011; Persson et al., 2009; Ramsay et al., 1992). Thus, understanding c-Myb function and identifying c-Myb target genes in normal cell development will inform therapeutic strategies for treating tumors with aberrant c-Myb expression.

1.4.1) Structure and function

The main form of c-Myb expressed in hematopoietic cells is a 75-kDa protein although alternatively spliced variants have been detected in human, mouse, and chicken derived hematopoietic cells (O'Rourke and Ness, 2008; Shen-Ong et al., 1990). Human c-Myb, in particular, undergoes significant alternative splicing and over 60 splice variants have been identified in pre-B-ALL samples (Zhou et al., 2011). However, little is known about the functional importance of these splice variants. The best characterized alternatively spliced *Myb* transcript is an 89-kDa isoform produced by insertion of exon 9A between exons 9 and 10. The 89-kDa isoform constitutes 10-15% of total c-Myb protein in hematopoietic cells and was found to have increased transcriptional activity as compared to the 75-kDa isoform in *in vitro* transactivation potential studies using luciferase reporter plasmids (Klempnauer et al., 1983; Kumar et al., 2003). In addition, expression of the 89-kDa isoform was reported to be important for survival and proliferation of p210-BCR/ABL-transformed cells suggesting that increased transactivation potential of this isoform could also convey greater oncogenic potential (Manzotti et al., 2012). However, deletion of exon 9A in mice did not have any apparent effects on development or hematopoiesis (Baker et al., 2010). Thus, characterization of the 89-kDa isoform of c-Myb reveals

the potential for structurally similar alternative gene products of the *Myb* locus to have differential effects on normal and transformed cells.

c-Myb protein has three major functional domains: an amino-terminal DNA-binding domain (DBD), a central transactivation domain (TAD), and a C-terminal negative regulatory domain (NRD) (Figure 1.9) (Sakura et al., 1989). The DBD is highly conserved throughout all eukaryotic organisms (Biedenkapp et al., 1988). It consists of three imperfect tandem repeats (R1, R2, and R3) that form a helix-turn-helix motif. Three tryptophan residues spaced 18 or 19 amino acids apart maintain the hydrophobic core of the loop and are important for DNA binding (Tanikawa et al., 1993). Of the three tandem repeats, R2 and R3 bind the *Myb* response element (MRE) PyAACG/TG while R1 binds non-specifically to the DNA to stabilize the complex. In the presence of c-Myb, the MRE PyAACG/TG motif can activate transcription of reporter genes (Weston and Bishop, 1989). However, it has also been demonstrated that c-Myb has varying affinity for a number of consensus and non-consensus sites suggesting that c-Myb-DNA interactions are regulated at multiple levels including through interactions with other proteins (Nakagoshi et al., 1992). The DBD interacts with a number of proteins including transcriptional co-activators, co-repressors, and cell cycle proteins. The DBD interacts with Mi-2α/CHD3, which is typically known as a component of the NURD co-repressor complex, as well as FLICE-associated huge protein (FLASH) which act as co-activators of c-Myb transcriptional activity (Alm-Kristiansen et al., 2011; Sæther et al., 2007). In addition, the DBD interacts with the transcriptional co-repressors Ski, nuclear receptor co-repressor 1 (N-CoR), and mSin3A which recruit a histone deacetylase complex that represses c-Myb transcription (Nomura et al., 2004). Furthermore, cyclin D1 and cyclin D3 have been demonstrated to associate with the Myb DBD

Figure 1.9: Structure of v-Myb and c-Myb proteins. Depiction of the functional domains of c-Myb and their alterations in the alternatively spliced transcript c-Myb^{EX9A} and the viral Myb (v-Myb) variants v-Myb^{AMV} and v-Myb^{E26}. These domains include the DNA binding domain (DBD) at the amino-terminus, the central transcriptional activation domain (TAD), and the negative regulatory domain at the carboxyl-terminus (NRD). The DBD contains three tandem repeats R1, R2, and R3. The NRD contains leucine zipper (LZ) and EVES motifs. c-Myb^{EX9A} is an 89-kDa alternatively spliced isoform that includes exon 9A within the leucine zipper motif. The virus-encoded forms of Myb v-Myb^{AMV} and v-Myb^{E26} contain both N- and C-terminal truncations. v-Myb^{AMV} also includes the viral gag protein at the amino-terminus and env protein at the carboxyl-terminus (purple). v-Myb^{E26} also includes the viral gag protein at the amino-terminus and a truncated Ets-1 at the carboxyl-terminus.

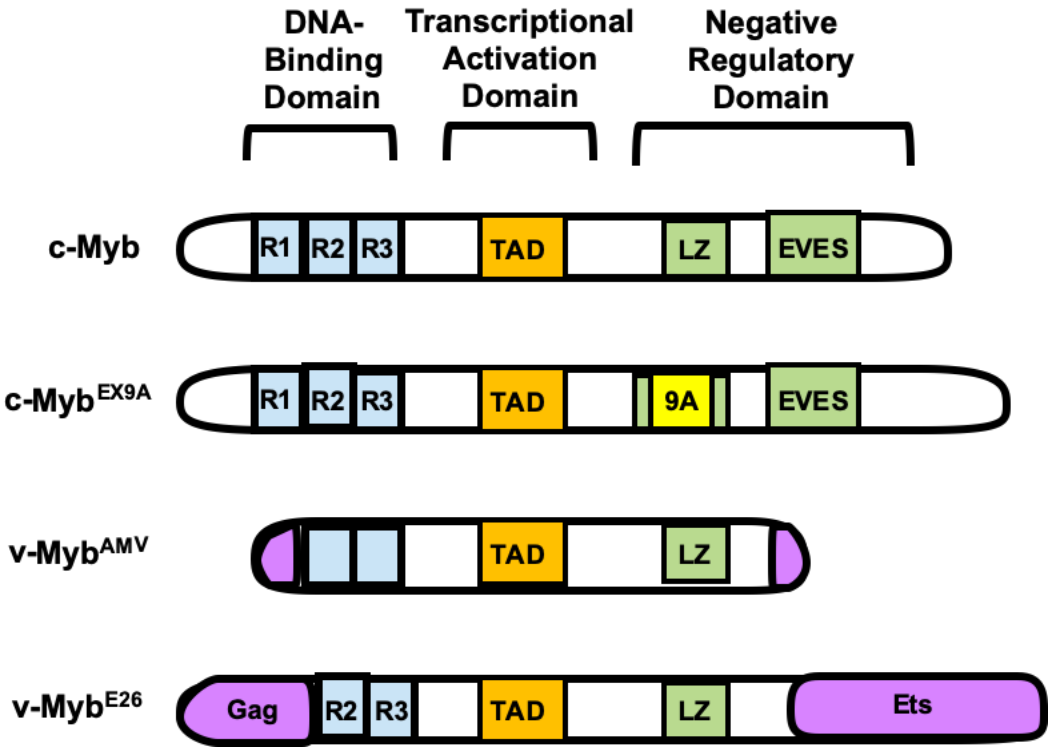
DNA-Binding Domain
Transcriptional Activation Domain
Negative Regulatory Domain
c-Myb
R1
R2
R3
TAD
LZ
EVES
c-Myb EX9A
R1
R2
R3
TAD
9A
EVES
v-Myb AMV
TAD
LZ
v-Myb E26
Gag
R2
R3
TAD
LZ
Ets

and to specifically inhibit transcription through the v-Myb but not c-Myb DBD (Ganter et al., 1998).

The 80 amino acid TAD has not been well characterized but is essential for c-Myb-mediated transcriptional activation (Frampton et al., 1993). The most well-characterized interaction of the TAD is with the histone acetyl transferase p300 (Dai et al., 1996). The importance of this interaction is illustrated by mice with a point mutation at the *Myb* locus ($Myb^{M303V/M303V}$) that interferes with its interaction with p300 and leads to thrombocytosis, megakaryocytosis, anemia and lymphopenia (Sandberg et al., 2005). The TAD also interacts with the co-repressors TIP60 and Menin which recruit HDAC1/2 and the MLL histone methyl transferase complex and alter c-Myb-dependent gene expression (Jin et al., 2010; Zhao et al., 2012). Several studies have also demonstrated that the TAD is important for oncogenic transformation (Cuddihy et al., 1993; Pattabiraman et al., 2014).

The NRD is located at the carboxyl-terminus of c-Myb and plays an important role in the control of c-Myb function. The viral form of c-Myb, v-Myb, lacks a portion of the NRD, which contributes to its role in leukemia development (Klempnauer et al., 1982). This observation first suggested that the NRD is important for regulating c-Myb function. The NRD has been implicated in co-repressor recruitment as deletions at the carboxyl-terminus result in increased DNA binding, transcriptional activation, and cellular transformation (Gonda et al., 1989; Nomura et al., 1993). In addition, transcriptional co-repressors bind to the NRD to inhibit c-Myb transcriptional activity including transcriptional intermediary factor 1 β (TIF1β) and Myb-binding protein 1A (Mybbp1a) (Nomura et al., 2004; Tavner et al., 1998). The NRD consists of a heptad leucine repeat (HLR) sequence at the carboxy-terminus of the c-Myb protein (Kanei-Ishii et al., 1992). Mice expressing a hypomorphic allele of c-Myb (Myb^{Plt4}) with a point mutation in the HLR exhibit reduced

transactivation capacity (Carpinelli et al., 2004; Greig et al., 2010). The NRD also contains a glutamic acid-valine-glutamic acid-serine (EVES) motif found near the carboxyl-terminus of the protein has been implicated in auto-inhibition of c-Myb through interactions with the DBD (Dash et al., 1996). Furthermore, post-translational modifications of the NRD including phosphorylation, acetylation, ubiquitylation, and sumoylation regulate c-Myb protein stability and transactivation activity (see below). Thus, the c-Myb NRD has a critical role in regulation of c-Myb function and to reduce the potential for oncogenic transformation due to enhanced c-Myb activation.

1.4.2) Regulation of c-Myb expression

c-Myb mRNA is expressed in progenitors of each hematopoietic lineage and is greatest in immature progenitor cells, decreasing as cells progress toward terminal differentiation (Bender and Kuehl, 1987; Duprey and Boettiger, 1985; Ess et al., 1999; Greig et al., 2008; Westin et al., 1982). For example, in B cell development when c-Myb expression was initially characterized in pro-B and pre-B cell leukemia cell lines, they were found to contain more *Myb* mRNA than cell lines representing more mature stages of B cell development (immature, mature, and plasma cells) (Bender and Kuehl, 1987). In addition, our lab demonstrated that normal mouse pro-B and pre-B cells expressed more *Myb* than immature and mature B cell subsets (Thomas et al., 2005). Developing hematopoietic cells are also sensitive to levels of c-Myb expression such that overexpression in c-Myb-deficient embryonic stem cells blocks erythrocyte and megakaryocyte differentiation and abolishes B lymphopoiesis *in vitro* (Sakamoto et al., 2006). In addition, $Myb^{+/-}$ mice exhibit partial blocks in B and T cell lineage development and express about 75% of normal c-Myb protein (Xiao et al., 2007).Thus, proper levels of c-Myb expression are critical for decisions regarding hematopoietic lineage development and differentiation. c-Myb is also expressed in other

cell types including: neural retina, tooth buds, hair follicles, neuronal cells, and various epithelial cell types including in the colon, breast and airway (Ess et al., 1999; Malaterre et al., 2007, 2008).

c-Myb expression and function are regulated at multiple levels including transcription, RNA regulation by miRNA, and a variety of post-translational modifications. Levels of c-Myb mRNA are primarily determined by a conditional block to transcriptional elongation within the first intron (Bender and Kuehl, 1987; Hugo et al., 2006). The *Myb* locus is also regulated by distant enhancer or repressor regions. Retroviral insertion of the common murine leukemia virus (MuLV) downstream of the *Myb* locus at the *Ahi-1* locus promotes c-Myb activation in T-cell lymphoma cell lines (Hanlon et al., 2003; Poirier et al., 1988). Distal regulatory regions have also been identified in the *Myb-Hbs1l* intergenic region upstream of the *Myb* locus in erythroid lineage progenitors such that insertion of an erythropoietin receptor transgene reduces c-Myb expression and interaction of the LDB1 complex (Gat1/Tal1/Ldb1) in association with the cofactors Eto2/Mtgr1) with intergenic regions activates c-Myb expression in mouse erythroleukemia (MEL) cells (Mukai et al., 2006; Stadhouders et al., 2011). A number of proteins have been identified as regulators that influence *Myb* expression including Nfkb, E2f, and Ets1, which were implicated in activation of *Myb* and WT-1, which was implicated in repression of *Myb* (McCann et al., 1995; Sala et al., 1994; Sullivan et al., 1997; Toth et al., 1995). More recently, direct regulators that bound to the *Myb* locus were identified including HoxA9, Meis1, Pbx1, and Pbx2 (Dassé et al., 2012). However, the specific role of these proteins in c-Myb function is poorly understood.

Myb is also regulated by a number of microRNAs (miRNA) including miR-15a, miR-34a, miR-150, and miR-200, which appear to regulate translation of c-Myb mRNA (Basso et al., 2012; Cesi et al., 2014; Lu et al., 2008; Navarro et al., 2009; Zhao et al., 2009). Among these, miR-150 has been the most studied. miR-150 binds the 3' untranslated region (UTR) of *Myb* mRNA and

represses c-Myb expression in peripheral B and T cells (Xiao et al., 2007). Expression of miR-150 was also found to be downregulated in granulocytes that over-expressed c-Myb from patients with primary myelofibrosis (PMF), suggesting that miR-150 is critical to regulate c-Myb expression in megakaryocytes and that failure to do so promotes disease (Guglielmelli et al., 2007). In addition, miR-15a binds the c-Myb UTR resulting in decreased c-Myb expression and a cell cycle block in K562 myeloid leukemia cells (Zhao et al., 2009). Thus, post-transcriptional regulation of c-Myb by miRNAs is important for modulating c-Myb expression in multiple hematopoietic cell types and to prevent aberrant c-Myb expression in disease.

Post-translational modifications that affect c-Myb function include acetylation, phosphorylation, ubiquitination, and sumoylation. Acetylation of c-Myb increases its transactivation capacity by increased binding to BCP and p300 (Sano and Ishii, 2001). Phosphorylation by Wnt-1 at multiple sites targets c-Myb for ubiquitination and degradation (Kanei-Ishii et al., 2004). Phosphorylation on serine-528 has differential effects on c-Myb transactivation activity in that it increases the ability of c-Myb to activate the CD34 promoter, but not the c-Myb or Mim1 promoters (Aziz et al., 1995; Miglarese et al., 1996). In addition, phosphorylation at serines 11 and 12 regulates c-Myb DNA binding (Oelgeschläger et al., 1995). Ubiquitination on its carboxyl terminus and sumoylation of the carboxyl terminus by SUMO1 regulate the stability of c-Myb protein (Bies et al., 2002). However, despite identification of these post-translational modifications affecting c-Myb, much of these discoveries have come from *in vitro* experimental models using cells lines or cell-free systems. Thus, due to the lack of data derived from whole animal models, the relevance of these post-translational modifications to c-Myb transcriptional activity is still unclear.

1.4.3) c-Myb in B cell development

Due to the embryonic lethality of germline *Myb* null mutations, it has been difficult to analyze c-Myb function in lineage specified B cell progenitors. In order to bypass the embryonic lethality of c-Myb knockout, early experiments utilized the Rag-deficient blastocyst complementation system in which $Myb^{-/-}$ embryonic stem (ES) cells were injected into $Rag1^{-/-}$ blastocysts which were then implanted into mouse hosts (Allen III et al., 1999). $Rag1^{-/-}$ cells cannot produce mature lymphocytes, therefore, host mice are chimeric for all tissues except antigen receptor rearranged B and T lymphocytes which could only be generated from $Myb^{-/-}$ cells. $Myb^{-/-}$ ES cells could not generate mature B and T lymphocytes or macrophages, and even pro-B cells were all $Rag1^{-/-}$, indicating that c-Myb expression is required for the development of B-lineage cells from HSCs. This experimental system revealed a critical role for c-Myb in B and T lymphocyte development. However, due to the inability to differentiate issues in MPPs from more mature progenitors, these experiments could not identify specific roles for c-Myb in lymphocytes or macrophages and thus, could not be used to study c-Myb function in specified or committed lymphocyte lineage progenitors. The next generation of c-Myb studies utilized hypomorphic *Myb* alleles to circumvent c-Myb-dependent embryonic lethality. In the initial hypomorph, insertion of a neomycin resistance cassette into intron 6 of the murine *Myb* locus resulted in a significant reduction in numbers of $B220^{+}$ B cell progenitors in the bone marrow and suggested that c-Myb is important for B lymphopoiesis (Emambokus et al., 2003). In later studies, additional c-Myb hypomorphs were identified in ENU mutagenesis screens and were characterized by point mutations targeting the DBD, TAD, and NRD domains, which also lead to defects in early B cell development (Carpinelli et al., 2004; Sandberg et al., 2005). However, these early studies could not separate c-Myb-dependent functions in HSCs or early hematopoietic progenitor cells from B-lineage specific functions.

To account for the embryonic lethality of *Myb* null mutations and facilitate stage-specific analysis of c-Myb function, our lab engineered conditional *Myb* knockout mouse models utilizing the Cre/loxP system. Mice were generated in which loxP sites flank exon 2 of the *Myb* locus so that excision by Cre-recombinase prevents the expression of all known *Myb* isoforms and splice variants (Bender et al., 2004). To initially analyze c-Myb function in B cell development, floxed-Myb (Myb^{ff}) mice were crossed with *CD19-cre* mice in which deletion is initiated during the pro-B cell stage (Thomas et al., 2005). In Myb^{ff} *CD19*-cre mice, we found no difference in absolute number of pro-B cells where deletion was ongoing, but significant decreases in pre-B and immature B cells. Interestingly, when $CD19^{+}$ pro-B and pre-B cells were sorted and assessed for deletion efficiency of the floxed *Myb* allele, we noted that the *Myb* allele was efficiently deleted in pro-B cells but not pre-B cells. This result suggested that there is selection against c-Myb deletion in pre-B cells and thus that c-Myb is important for the transition to or maintenance of the pre-B cell compartment. In addition, Myb^{ff} *CD19*-cre mice contained 50% fewer follicular B cells and 85% fewer B-1 B cells, but normal absolute numbers of marginal zone B cells. This reduction was surprising as the block in the pro-B to pre-B cell transition was incomplete and numbers of peripheral B cells would likely be restored by homeostatic proliferation. Therefore, the decreased numbers of mature B cell subsets observed in Myb^{ff} *CD19*-cre mice suggested that c-Myb is important for the maintenance of peripheral B cells. In line with this, we found that c-Myb-deficient splenic B cells were hyporesponsive to the pro-survival factor BAFF due to reduced expression of the BAFF receptor and therefore, exhibited reduced viability.

To further characterize the role of c-Myb in the earliest B lineage progenitors, $Myb^{f/f}$ *Mb1-cre* mice were generated in which inactivation at the *Myb* locus is initiated in pre-pro-B cells and completed in the pro-B cell stage of development. Loss of c-Myb expression in $Myb^{f/f}$ *Mb1-cre*

mice caused a complete block in differentiation from pre-pro-B cells to *CD19*$^{+}$ pro-B cells and c-Myb expression was absolutely required for the development and maintenance of *CD19*$^{+}$ pro-B cells (Fahl et al., 2009; Greig et al., 2010). Deletion of c-Myb in *Myb*$^{f/f}$ *CD19-cre Rag2*$^{-/-}$ mice, which enriches for pro-B cells in which c-Myb ablation is initiated, revealed that c-Myb was also critical for survival within the pro-B cell compartment (Fahl et al., 2009). To identify a potential mechanism for how c-Myb mediates pro-B cell survival, expression of key genes involved in pro-B cell development were assessed and it was demonstrated that c-Myb regulates mRNA and protein expression of the IL-7Rα and mRNA expression of the key B lineage transcription factor Ebf1 (Fahl et al., 2009). However, exogenous expression of IL-7Rα could not rescue survival of c-Myb-deficient pro-B cells suggesting that c-Myb regulates pro-B cell survival independent of IL-7R expression. Expression of exogenous Ebf1 could partially rescue development of *CD19*$^{+}$ pro-B cells during *in vitro* stromal cell culture of c-Myb-deficient progenitors indicating that c-Myb is critical for the differentiation to and survival of *CD19*$^{+}$ pro-B cells.

Characterization of the mechanism of c-Myb-dependent pro-B cell survival revealed that c-Myb regulates both intrinsic and IL-7-dependent survival (Figure 1.10) (Fahl et al., 2018). c-Myb regulated the intrinsic survival of pro-B cells (survival in the absence of IL-7) through repression of the pro-apoptotic Bcl-2 family members Bim and Bmf, which were further repressed by IL-7R signaling. IL-7R signaling through Stat5 repressed both Bim and Bmf and induced expression of the anti-apoptotic Mcl-1. However, expression of exogenous IL-7Rα could not repress Bim and Bmf expression suggesting that c-Myb regulates other components of IL-7R signaling. c-Myb also repressed expression of SOCS3, a negative regulator of IL-7 signaling which binds to the IL-7Rα, Jak1, and Jak3 proteins to prevent their interaction and also targets Jak1 and Jak3 for proteasomal degradation (Croker et al., 2008). Bypassing loss of IL-7R expression and

Figure 1.10: Control of pro-B cell survival by c-Myb. In the absence of IL-7, c-Myb controls the intrinsic survival of pro-B cells by repressing the expression of Bmf and Bim (shaded gray). However, c-Myb also positively regulates the expression of IL-7Rα. Signaling through the IL-7 receptor by binding of IL-7 activates STAT5 and Akt. Activated STAT5 further represses expression of Bmf and Bim as well as increases expression of Mcl- 1. Activated Akt can only repress Bmf and does not induce expression of Mcl-1. Thus, c- Myb serves to set a baseline expression of Bmf and Bim expression in pro-B cells, independent of IL-7 signaling, as well as induce expression of the IL-7 receptor, providing a mechanism to further repress expression of Bim and Bmf, providing a mechanism to regulate the lifespan of pro-B cells. In addition, c-Myb represses expression of SOCS3, which is a negative regulator of IL-7 signaling by inhibiting the activation STAT5 by JAK kinases. Green lines represent positive regulation and red lines represent negative regulation.

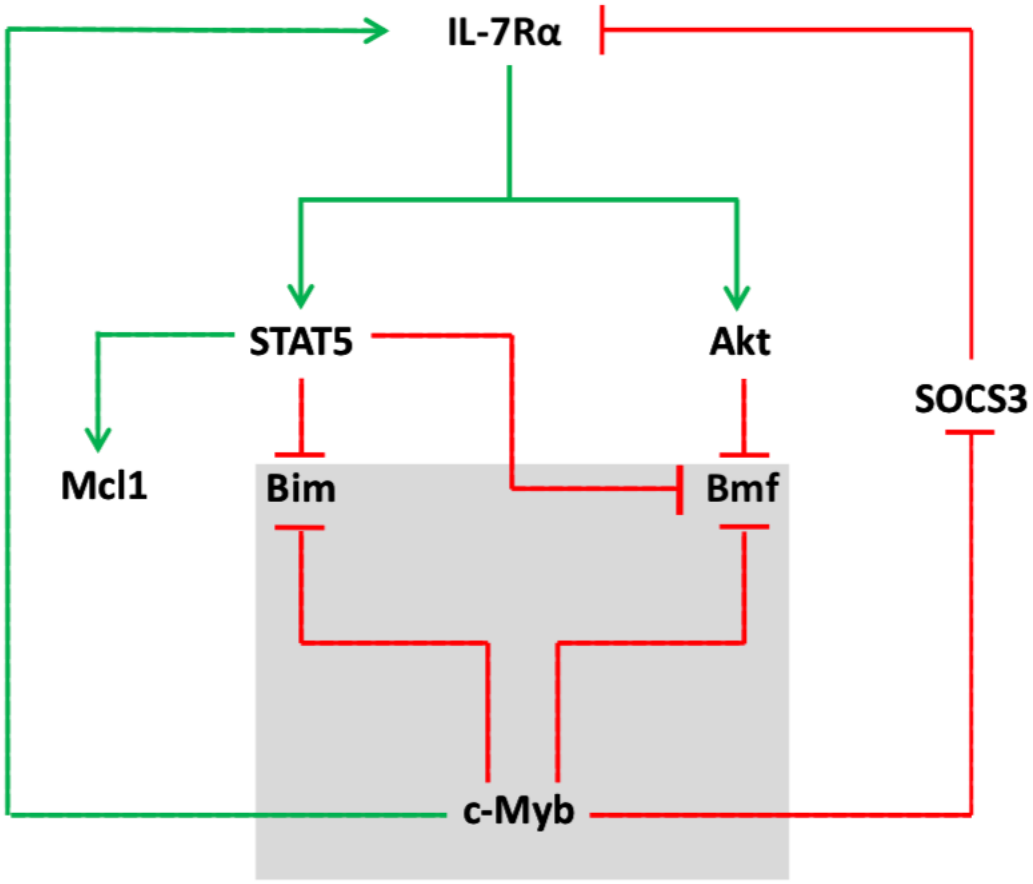
IL-7Rα
STAT5
Akt
SOCS3
Mcl1
Bim
Bmf
c-Myb

signaling by SOCS3 inhibition through expression of a constitutively active Stat5 (CA-Stat5) was unable to rescue recovery of c-Myb-deficient pro-B cells suggesting that c-Myb has additional roles apart from survival that would account for the incomplete rescue. In line with this notion, c-Myb expression was also critical for pro-B cell proliferation.

c-Myb-dependent defects in pro-B cell survival and proliferation as well as previous work indicating that c-Myb is important for the transition to or maintenance of the pre-B cell compartment suggested that c-Myb regulates the expression of genes involved in the pre-BCR checkpoint and large pre-B cell proliferation. In fact, c-Myb coordinated pro-B cell survival with the expression of critical genes important for the pre-BCR checkpoint including the pre-BCR component λ5 (*Igll1)*, the cell cycle regulator cyclin D3 (*Ccnd3*), and the chemokine receptor CXCR4 (Fahl et al., 2018). Furthermore, λ5 was demonstrated to be a direct c-Myb target. Decreased expression of these critical checkpoint genes suggested that c-Myb is important across the pre-BCR checkpoint for the pro-B to large pre-B cell transition. This notion was supported by experiments utilizing a *Bcl2Tg* to rescue pro-B cell survival which rescued numbers of pro-B cells but not large or small pre-B cells. In addition, c-Myb-deficient large pre-B cells exhibited defects in proliferation, suggesting that c-Myb may have a distinct role in the pre-B cell compartment. Overall, utilizing conditional inactivation at the Myb locus at different stages of B cell development with *Mb1-cre* and *CD19-cre* revealed that c-Myb is critical for the development of the earliest stage of committed B cell progenitors and furthermore, that c-Myb is important for the survival, proliferation, and differentiation of multiple stages of B cell development. However, the question remained of whether c-Myb might have specific roles in later stages of B cell differentiation including large and small pre-B cells, as well as immature B cells.

1.5) Thesis Rationale

At the time this project was initiated, it had been established that the transcription factor c-Myb plays critical roles during the development of the earliest B-lineage progenitors. Utilizing conditional deletion at the *Myb* locus in different stages of B cell development, previous work from our lab and others demonstrated that c-Myb expression is absolutely required for the development of pro-B cells as well as for survival within the pro-B cell compartment (Fahl et al., 2009; Greig et al., 2010). Subsequently, our lab identified downstream effectors of c-Myb activity important for mediating pro-B cell survival including pro-apoptotic Bcl-2 family members and multiple components of the major survival pathway in pro-B cells through the IL-7R (Fahl et al., 2018). However, activating pro-survival signaling downstream of the IL-7R through Stat5 failed to fully rescue numbers of c-Myb-deficient pro-B cells. This result suggested that c-Myb has additional, survival-independent functions in pro-B cells and that these functions may be mediated by IL-7 signaling through an alternative pathway. In addition, previous work in the lab demonstrated that c-Myb coordinates regulation of pro-B cell survival with expression of genes critical for proliferation and differentiation across the pre-BCR checkpoint (Fahl et al., 2018). Furthermore, rescuing pro-B cell development and survival revealed additional defects in the numbers of large and small pre-B cells. However, it was still unclear if c-Myb has a distinct role in the pre-B cell compartment or if decreased numbers of large and small pre-B cells were the result of defects in c-Myb-deficient pro-B cells which would impact their ability to cross the pre-BCR checkpoint. In lieu of these observations, the purposes of this project were to identify additional roles for c-Myb in the pro-B cell compartment, to determine if c-Myb is important in the pre-B cell compartment after selection across the pre-BCR checkpoint, and to identify mediators of c-Myb activity that regulate these functions. As a result, this work is the first to

characterize the role of c-Myb in large pre-B cells and has identified a previously unappreciated role for c-Myb in the earliest stages of glucose metabolism in both pro-B and large pre-B cells.

Chapter II. Materials and Methods

2.1) Mice

Mice. *Myb*^{ff} mice have been previously described (Bender et al., 2004). Briefly, exon 2 of the *Myb* locus was flanked by *lox*P sites to generate a floxed *Myb* allele. Recognition of the *lox*P sites by Cre recombinase leads to excision of exon 2, resulting in an out of frame exon1/exon3 splice during transcription of the *Myb* locus, which prevents expression of all known murine c-Myb isoforms. *Rag2*$^{-/-}$ mice (Taconic Farms) were crossed with *Myb*^{ff} mice to generate *Myb*^{ff} *Rag2*$^{-/-}$ mice. *Rag2*$^{-/-}$ mice were generated by replacing a 0.85 kb segment of the *Rag2* open reading frame with PMC1neo (Shinkai et al., 1992). *UBC-Cre-ER*^{T2} mice (Jackson Laboratories) were crossed with *Myb*^{ff} *Rag2*$^{-/-}$ mice to generate *Myb*^{ff} *Rag2*$^{-/-}$ *Cre-ER*^{T2} mice. *UBC-Cre-ER*^{T2} mice were generated by lentitransgenesis using a lentiviral vector expressing human ubiquitin C (UBC) upstream of a Cre-ERT2 fusion gene (Ruzankina et al., 2007). *Bcl2Tg* mice were crossed with *Myb*^{ff} *Rag2*$^{-/-}$ mice to generate *Myb*^{ff} *Rag2*$^{-/-}$ *Bcl2Tg* mice. *Bcl2Tg* mice express human Bcl-2 cDNA driven by the Eμ immunoglobulin heavy chain enhancer and the SV40 promoter so that Bcl-2 expression is directed to both T cell and B cell lineages (Strasser et al., 1991).

Genotyping. Tail biopsies were collected for genotyping, digested in 700 μl tail DNA lysis buffer (100 mM Tris-HCl pH 8.5, 5 mM EDTA pH 8, 200 mM NaCl, 0.2% SDS, 200 μg/ml proteinase K), and left overnight at 55°C. Tail debris was cleared by centrifugation at 14,800 rpm for 5 minutes at room temperature. DNA was precipitated with 700 μl isopropanol, washed with 700 μl 70% ethanol, and re-suspended in 400 μl H_2O. Polymerase chain reaction (PCR) reactions were performed using APEX Taq DNA polymerase (Genessee Scientific) for all reactions except for

YFP PCR, which was performed using HotStart Taq DNA Polymerase (Genessee Scientific). Each reaction used 2 μl of tail DNA in a total volume of 25 μl and was run on a DNA Engine Peltier Thermal Cycler (Bio-Rad). PCR products were run on 1% General Purpose agarose gels except *Myb*^{f} reactions, which were run on 3% Nusieve Agarose gels, and were visualized by ethidium bromide staining. See Table 2.1 for genotyping PCR primers and product sizes. PCR conditions for each reaction were:

Myb^{f} : 94°C 4 minutes, (94°C 1 minute, 58°C 1 minute, 72°C 1 minute) x 30, 72°C 6 minutes, 4°C soak

CD19-cre : 96°C 1 minute, (94°C 30 seconds, 59.5°C 1 minute, 72°C 90 seconds) x 32, 4°C soak

Cre-ER^{T2} : 94°C 4 minutes, (94°C 1 minute, 58°C 1 minute, 72°C 1 minute) x 30, 72°C 6 minutes, 4°C soak

Rag2$^{-/-}$: 94°C 5 minutes, (94°C 1 minute, 67°C 1 minute, 72°C 1 minute) x 40, 72°C 10 minutes, 4°C soak

Bcl2Tg : 94°C 3 minutes, (94°C 30 seconds, 58°C 30 seconds, 72°C 45 seconds) x 36, 72°C 2 minutes, 4°C soak

YFP : 94°C 15 minutes, (94°C 30 seconds, 52°C 1 minute, 72°C 1 minute) x 31, 72°C 7 minutes, 4°C soak

Table 2.1. Genotyping PCR Primers

Reaction	Primer	Sequence	Product Size
c-Myb^{f}	N2	GCATGCCTCTGGAAAGTACCTTAAAC	WT=161bp
	N4	GTCTAGGAGCAAAGTTCTAACAGC	Floxed=194bp
	N6	CAGACAGACAGAACGTGCATTC	Deleted=267bp
CD19cre	cre7	TCAGCTACACCAGAGACGG	WT=450bp
	CD19c	AACCAGTCAACACCCTTCC	Cre=750bp
	CD19d	CCAGACTAGATACAGACCAG	
Cre-ER^{T2}	Cre 531	CGATGCAACGAGTGATGAGG	Cre=250bp
	Cre 819	GCATTGCTGTCACTTGGTCCT	
Rag2	RagA	GGGAGGACACTCACTTGCCAGTA	WT=~300 bp
	RagB	AGTCAGGAGTCTCCATCTCACTGA	KO=~400 bp
	NeoA	CGGCCGGAGAACCTGCGTGCAA	
Bcl2Tg	imr0550	TGGATCCAGGATAACGGAGG	Control=324 bp
	imr0551	TGTTGACTTCACTTGTGGCC	Bcl2=170 bp
	imr0042	CTAGGCCACAGAATTGAAAGATCT	
	imr0043	GTAGGTGGAAATTCTAGCATCATCC	

2.2) Cell Lines and Tissue Culture

Incubator Conditions. All cells were cultured in a humidified incubator at 37°C and with an atmosphere of 5% CO_2.

Cell lines and culture conditions. The HEK 293T cell line was grown in Dulbecco's Modified Eagle Medium (DMEM) supplemented with 10% fetal bovine serum (FBS) (Life Technologies), 100 U/ml penicillin-streptomycin, and 2 mM L-glutamine. The NIH 3T3 cell line was grown in Iscove's Modified Dulbecco's Medium (IMDM) supplemented with 10% FBS, 100 U/ml penicillin-streptomycin, and 2 mM L-glutamine. The OP9 stromal cell line (D. Allman, University of Pennsylvania) was grown in DMEM supplemented with 10% FBS, 100 U/ml penicillin-streptomycin, 2 mM L-glutamine, 1% Sodium pyruvate, 1% 100X HEPES, 0.1% gentamycin, and 50 μM β-mercaptoethanol (2-ME). The *Irf4/8*$^{-/-}$ large pre-B cell line (M. Mandal, University of Chicago) was cultured on an OP9 stromal cell layer in Opti-Minimal Essential Medium (Opti-MEM) supplemented with 10% FBS, 100 U/ml penicillin-streptomycin, 50 μM 2-ME, and 10ng/ml IL-7 (PeproTech). Cells were re-supplemented with 10ng/ml IL-7 every 24 hours in culture.

Pro-B cell culture for metabolism assays. CD19^{+} pro-B cells from *Myb*^{ff} *Rag2*$^{-/-}$*Bcl2Tg (+/-)* mice were positively selected by MACS purification as described in section 2.4. Pro-B cells were re-suspended in Opti-MEM supplemented with 15% FBS, 100 U/ml penicillin-streptomycin, 2 mM L-glutamine, 50 μM 2-ME, and 5 ng/ml IL-7 at 1x10^{6} cells per ml and plated at 1 ml per well of a 24-well plate for retroviral transduction. Following transduction with the indicated

retroviruses, $1x10^6$ cells in 1 ml total volume were re-plated per well of a 24-well plate and incubated for the indicated time points before analysis for glucose uptake and hexokinase activity.

Retroviral supernatant production. Retroviral supernatants were produced by $CaPO_4$ transduction of HEK293T cells with the desired expression vector and the RetroMax packaging vector pCl-Eco (Pear, 2001). HEK293T cells were seeded at $2x10^6$ cells and 4 ml total volume per 60 mm plate and incubated for 24 hours. A retrovirus transfection cocktail was prepared by combining 10 μg of the desired expression vector, 10 μg of pCl-Eco, 50 μl 2.5M $CaCl_2$ solution pH 7.2 (2.5 M $CaCl_2$, 10 mM HEPES) and TE pH 7.3 (10 mM Tris-HCl, 1 mM EDTA) to a final volume of 500 μl per 60 mm transfection plate. The transfection cocktail solution was added to 500 μl of 2X HBS pH 7.2 (50 mM HEPES, 10 mM KCl, 0.28 M NaCl, 1.2 mM Dextrose, 1.5 mM $Na_2PO_4 \cdot 7H_2O$), dropwise while bubbling air into the combined solution through a Pasteur pipette. This solution was added to the HEK293T cell 60 mm plates, dropwise at 1 ml per plate (total volume 5 ml per plate) and incubated for 24 hours. The transfection cocktail was aspirated from the plates and replaced with 3 ml Opti-MEM supplemented with 15% FBS, 100 U/ml penicillin-streptomycin, 2 mM L-glutamine, and 50 μM 2-ME. At 24 and 48 hours later, viral supernatant was harvested, filtered through a 0.45 μm Whatman syringe filter (GE Healthcare), and stored at -80°C.

Retroviral titer. Retroviral titer was determined by transduction of NIH3T3 cells. NIH3T3 cells were seeded at $2x10^5$ cells and 2 ml total volume per well of a 6-well plate and cultured for 24 hours. Each well was then supplemented with 2ml medium plus 4 μg/ml polybrene and for each retrovirus preparation 1 μl, 10 μl and 100 μl of retroviral supernatant was added to 3 wells of

NIH3T3 cells. The cells were then centrifuged at 2,000 rpm for 90 minutes at room temperature and then incubated for 24 hours. Cells were harvested by trypsinization and for NGFR and NGFR-Cre retroviruses, were stained for expression of NGFR, after which flow cytometry was performed to determine the proportion of GFP^+ or $NGFR^+$ cells. The approximate concentration of viral particles was calculated using the volumes of viral supernatant that produced a linear proportion of GFP^+ or $NGFR^+$ cells using the following formula:

$$\frac{(\%\ GFP^+/100) \times 8x10^5}{\text{Volume of viral supernatant added}}$$

$8x10^5$ represents the approximate number of NIH3T3 cells present on the day of flow cytometry. The viral titer is calculated in units of number of infectious particles per ml.

2.3) Retroviral Plasmids and Transduction

Retroviral vectors. The retroviral vectors pMIG-R1, pMSCV-IRES-tNGFR, pMSCV-IRES-tNGFR-Cre, pMIG-17.2.25, pSIREN-RetroQ-shLuc-IRES-eGFP, pSIREN-RetroQ-shMyb, pMIG-IkWT, pMIG-Ik159A, pMSCV-IRES-tNGFR-Glut1, and pMSCV-IRES-tNGFR-Hk1 have been previously described (Ferreirós-Vidal et al., 2013; Guloglu et al., 2005; Hess et al., 2006; Izon et al., 2001; Nitta et al., 2006; Pear et al., 1993; Wieman et al., 2007). pMIG-R1 and pMSCV-IRES-NGFR were provided by Warren Pear, University of Pennsylvania. pMIG-17.2.25 was provided by Christopher Roman, SUNY Downstate Medical Center. pSIREN-RetroQ-shLuc-IRES-GFP was provided by Takeshi Nitta, University of Tokushima. c-Myb-targeting shRNA (shMyb) was provided by Robert Slany, University Erlangen. pMIG-IkWT and pMIG-Ik159A were provided by Dr. Stephen Smale, University of California Los Angeles. pMSCV-IRES-tNGFR-Glut1 and pMSCV-IRES-tNGFR-Hk1 were provided by Dr. J. Rathmell, Vanderbilt

University. Plasmids were transfected into OneShot Top10 competent cells (Invitrogen), grown in 100 ml selection medium overnight at 37°C, and purified using the Qiagen Maxiprep Kit per manufacturer's instructions.

pMSCV-IRES-tNGFR-Cre. Cre cDNA was excised from pSP72-Cre as an *Xho*I/*Eco*RI fragment and cloned into the pLITMUS28 *Xho*I/*Eco*RI site to generate pLITMUS28-Cre. Cre cDNA was then excised from pLITMUS28-Cre as a *Bgl*II/*Eco*RI fragment and cloned into the pMSCV-IRES-NGFR *Bgl*II/*Eco*RI site to generate pMSCV-Cre-IRES-NGFR.

pSIREN-RetroQ-shMyb. shMyb was excised from pSIREN-RetroQ as a *Bste*II fragment and cloned into the *Bste*II site of pSIREN-RetroQ-IRES-eGFP.

pSIREN-RetroQ-shMyb-IRES-tNGFR. IRES-tNGFR was excised from pMSCV-IRES-tNGFR as a *Bgl*II/*Xho*I fragment and cloned into the *Bgl*II/*Xho*I site of pLITMUS28. IRES-tNGFR was excised from pLITMUS28 as a *EcoR*V fragment and cloned into the *EcoR*V site of pSIREN-RetroQ-shMyb.

CD19$^+$ pro-B cell transduction. CD19$^+$ pro-B cells from *Myb^{ff} Rag2$^{-/-}$* or *Myb^{ff} Rag2$^{-/-}$ Bcl2Tg* mice were positively selected by MACS purification as described in section 2.4. Pro-B cells were re-suspended in Opti-MEM supplemented with 15% FBS, 100 U/ml penicillin-streptomycin, 2 mM L-glutamine, 50 μM 2-ME, and 5 ng/ml IL-7 at 1x10^6 cells per ml and plated at 1 ml per well of a 24-well plate for retroviral transduction. Pro-B cells were transduced with the indicated retroviruses at a multiplicity of infection (MOI) of 10:1 and a total volume of 1 ml retroviral supernatant per well. If a volume less than 1 ml was necessary to reach the desired MOI, the volume was brought up to 1 ml using Opti-MEM supplemented with 15% FBS, 100 U/ml penicillin-streptomycin, 2 mM L-glutamine, and 50 μM 2-ME. Then recombinant IL-7 was added

at a concentration of 5 ng/ml and polybrene at a concentration of 8 μg/ml per well. Pro-B cells were centrifuged at 2,000 rpm for 90 minutes at room temperature and incubated for 2 hours. Pro-B cells were harvested from the plate into 15 ml conical tubes, centrifuged at 1,800 rpm and 10°C, and seeded for glucose uptake and hexokinase activity assays as described above.

De-novo generation of pre-B cells (μHC-transduced pro-B cells). $CD19^+$ pro-B cells from *Myb*^{ff} *Rag2*$^{-/-}$ or *Myb*^{ff} *Rag2*$^{-/-}$ *Bcl2Tg* mice were positively selected by MACS purification as described in section 2.4. Pro-B cells were re-suspended in Opti-MEM supplemented with 15% FBS, 100 U/ml penicillin-streptomycin, 2 mM L-glutamine, 50 μM 2-ME, and 5 ng/ml IL-7 at $1x10^6$ cells per ml and plated at 1 ml per well of a 24-well plate for retroviral transduction. Cells were then transduced as described above, with pMIG-R1 or pMIG-17.2.25, returned to culture for 24 hours, transduced with pMSCV-IRES-tNGFR or pMSCV-IRES-tNGFR-Cre, and returned to culture for the indicated time points before analysis by flow cytometry.

***Irf4/8*$^{-/-}$ large pre-B cell transductions.** *Irf4/8*$^{-/-}$ large pre-B cells were maintained in culture on an OP9 stromal cell layer in Opti-MEM supplemented with 10% FBS, 100 U/ml penicillin-streptomycin, 50 μM 2-ME, and 10 ng/ml IL-7. At 24 hours pre-transduction, OP9 cells were seeded in a 24-well plate at 25,000 cells and 1 ml per well for *Irf4/8*$^{-/-}$ cell transduction and in a 24-well plate at 20,000 cells and 1ml per well or a 96-well plate at 2,500 cells and 100 μl per well for *Irf4/8*$^{-/-}$ cell post-transduction. For transduction, *Irf4/8*$^{-/-}$ large pre-B cells were seeded on the OP9 24-well transduction plate at $1x10^6$ cells and 1 ml per well in Opti-MEM supplemented with 10% FBS, 100 U/ml penicillin-streptomycin, 50 μM 2-ME, and 10 ng/ml IL-7. *Irf4/8*$^{-/-}$ large pre-B cells were transduced with the indicated retroviruses at a multiplicity of infection (MOI) of 10:1

and a total volume of 1 ml retroviral supernatant per well. If a volume less than 1 ml was necessary to reach the desired MOI, the volume was brought up to 1 ml using Opti-MEM supplemented with 10% FBS, 100 U/ml penicillin-streptomycin, 50 μM 2-ME, and 10 ng/ml IL-7. Then recombinant IL-7 was added at a concentration of 10 ng/ml and polybrene at a concentration of 8 μg/ml per well. *Irf4/8*$^{-/-}$ large pre-B cells were centrifuged at 2,000 rpm for 90 minutes at room temperature and incubated for 2 hours. *Irf4/8*$^{-/-}$ large pre-B cells were harvested from the plate into 15 ml conical tubes, centrifuged at 1,800 rpm and 10°C, and seeded on OP9 post-transduction 24-well or 96-well plates at $1x10^6$ cells and 1 ml per well or at $1.5x10^5$ cells and 150 μl per well respectively and incubated for the indicated time points.

2.4) Flow Cytometry and Cell Sorting

Isolation of single cell suspension from bone marrow. Single cell suspensions from bone marrow of *Myb*^{ff} *Rag2*$^{-/-}$ or *Myb*^{ff} *Rag2*$^{-/-}$ *Bcl2Tg* mice were prepared from 6-8 week old mice. Femurs and tibias were harvested, the ends were trimmed with a razor blade, and bone marrow was flushed out with DMEM supplemented with 5% FBS, 2 mM L-glutamine, and 100 U/ml penicillin-streptomycin (DMEM$^+$). Single cell suspensions were centrifuged at 1800 rpm for 5 minutes at 10°C (this program was used for all subsequent centrifugations). The supernatant was aspirated and erythrocytes were lysed by incubation in 5 ml Ammonium-Chloride-Potassium (AKC) lysis buffer (0.15 M NH_4Cl, 10 mM $KHCO_3$, 0.1 mM Na_2EDTA (pH 7.2-7.4)) for 3 minutes on ice. The lysis reaction was quenched with 5ml of DMEM$^+$, cells were centrifuged, the supernatant was aspirated, cells were re-suspended in the desired medium or buffer, and filtered through a 100 μm nylon cell strainer. Cells were counted on a hemocytometer using trypan blue exclusion.

Magnet Activated Cell Sorting (MACS). To isolate $CD19^+$ pro-B cells from *Rag2*$^{-/-}$ mice, bone marrow was isolated into a single cell suspension and counted as described above. Bone marrow cells were re-suspended in $1x10^7$ cells per 90 µl PBS supplemented with 0.5% BSA and 2 mM EDTA (MACS buffer). Prior to use, MACS buffer was sterile filtered through a 0.2 µm filter and degassed. Then 10 µl CD19 magnetic beads (Miltenyi) were added and cells were incubated for 15 minutes at 4°C. Cells were washed with 5ml MACS buffer and centrifuged at 1800 rpm for 5 minutes at 10°C (this program was used for all subsequent centrifugations). Cells were then re-suspended in 1 ml MACS buffer and positively selected over LS MACS columns per the manufacturer's protocol. In brief, each column was equilibrated with 3 ml MACS buffer, the cell suspension was added, and each column was washed 2 times with 3 ml MACS buffer. Each column was then removed from the magnet and $CD19^+$ cells were eluted by plunging the column with 5ml MACS buffer. Cells were counted on a hemocytometer using trypan blue exclusion and seeded for cell culture as described above.

Flow cytometry and Fluorescence Activated Cell Sorting (FACS). $1\text{-}2x10^6$ cells were stained in 50 µl phosphate buffered saline (PBS) containing 0.5% bovine serum albumin (BSA) and 0.01% NaN_3 (PBA) with pre-titered fluorochrome- or biotin-conjugated antibodies (Table 2.2). For experiments conducted in 96-well plates with fewer cells, they were stained in a 25 µl volume. For experiments using a fixable cell viability dye, cells were stained in a low BSA PBS solution (PBS containing 0.01% BSA). Dead cells were identified using the DNA intercalating dye 4',6-diamidino-2-phenylindole (DAPI) (Sigma-Aldrich) or the amine-reactive Zombie Aqua Fixable Viability Dye. Cells were analyzed on a FACSCanto II (BD Biosciences, CytoFLEX (Beckman

Coulter), or the Attune NxT (Thermo Fisher Scientific). Data were analyzed using FlowJo software (Tree Star). For isolation of transduced or co-transduced GFP^+, $NGFR^+$, or $GFP^+/NGFR^+$ pro-B or *Irf4/8*$^{-/-}$ large pre-B cells for RNA, genomic DNA, cDNA, or protein lysate preparation, cells were stained as described above and cell sorting was performed using either a FACSVantage SE Turbo Sorter with DIVA Option (BD Biosciences) or BD Influx Cell Sorter (BD Immunocytometry Systems).

Quantitation of cell counts for relative recovery by counting beads. To determine the total number of cells per sample, 50 μl of 5 μm AccuCount Blank Particles (Spherotech) of a known concentration were added to triplicate wells per sample condition. Cells were then harvested, stained as desired, and analyzed by flow cytometry. To determine the total number of cells per well using AccuCount Blank Particles, the following formula was used:

$$\frac{\#\text{ particles seeded} \times \#\text{ cells collected}}{\#\text{ particles collected}}$$

α-active Caspase 3 Staining. Prior to staining, cells set aside for α-active Caspase-3 compensation were treated with Dexamethasone at 10 μM and incubated for 3 hours. Then cells were surface stained as described above and fixed using the BD Cytofix/Cytoperm Kit per the manufacturer's protocol. Briefly, after the final wash in PBA, cells were re-suspended in 100 μl Cytofix/Cytoperm (BD Pharmingen) and incubated, covered and on ice for 20 minutes. Cells were washed with 200 μl 1X Perm/Wash Buffer (BD Pharmingen), re-suspended in 100 μl α-active Caspase-3 staining solution (5 μl α-active Caspase-3 and 95 μl Perm/Wash Buffer), and incubated 30 minutes, covered and at room temperature. Cells were washed with 200 μl 1X Perm/Wash Buffer, re-suspended in 200 μl 1X Perm/Wash Buffer, and analyzed by flow cytometry.

Table 2.2. Flow cytometry antibodies

Marker	Clone	Fluorochromes	Source
α-Active Caspase-3	C92-605	AlexaFluor 647	BD Pharmingen
CD2	RM2-5	PE	eBioscience
NGFR	ME20.4-1.H4	Biotin	Miltenyi
NGFR	ME20.4	APC	BioLegend
Streptavidin		PE	BD Pharmingen
Zombie Aqua			BioLegend

Click-iT EdU vs. 7AAD Staining. To assess cell proliferation, DNA synthesis and DNA content were analyzed by simultaneously measuring EdU uptake and 7AAD DNA staining. EdU uptake was analyzed using the Click-iT Plus EdU Alexa Fluor 647 Flow Cytometry Assay Kit (Life Technologies) per the manufacturer's protocol. Briefly, cells were incubated for 2 hours with 10 μM EdU, then surface stained as described above. Cells were re-suspended in 50 μl Click-iT Fixative and incubated 15 minutes, covered and at room temperature. Then, cells were washed with 200 μl Click-iT Fix/Perm Buffer, re-suspended in 100 μl Click-iT Fix/Perm Buffer, and stored at 4°C. On the day of flow cytometry analysis, the Click-iT Plus reaction cocktail was prepared according to the manufacturer's instructions, 500 μl of Click-iT Plus reaction cocktail was added to each sample, and cells were incubated for 30 minutes, covered and at room temperature. Cells were washed with 500 μl Click-iT Fix/Perm Buffer and re-suspended in 7AAD (eBioscience) diluted in Click-iT Fix/Perm Buffer at 8 μl 7AAD staining solution per 200 μl buffer before analysis by flow cytometry.

2-NBDG Glucose Uptake Assay. Glucose uptake was analyzed using the 2-NBDG Glucose Uptake Assay Kit (BioVision) per the manufacturer's protocol. Cells were harvested, counted, and aliquots of $2x10^5$ cells were prepared in triplicate for each sample. Then, cells were surface stained as described above and re-suspended in 400 μl Opti-MEM supplemented with 0.5% FBS, re-plated on a 24-well plate, and incubated for 1 hour at 37°C and 5% CO_2. As a control for glucose uptake, cells were re-suspended in 400 μl Opti-MEM supplemented with 0.5% FBS and the glucose uptake inhibitor Phloretin at a 1:100 dilution. For each well, 400 μl of glucose uptake mix was prepared per the manufacturer's instructions and for the glucose uptake control, Phloretin was added as above. Cells were incubated for 30 minutes at 37°C and 5% CO_2, harvested to Eppendorf tubes

and washed with 500 μl 1X Analysis Buffer (BioVision). Cells were re-suspended in 300 μl 1X Analysis Buffer (BioVision) and analyzed by flow cytometry.

2.5) RNA/DNA Preparations and Quantitative Real-Time PCR (qRT-PCR)

Deletion efficiency PCR. μHC-transduced pro-B cells were electronically sorted based on co-expression of GFP/NGFR as well as CD2, and genomic DNA was isolated. Cells were lysed in 500 μl TSE lysis buffer (10 mM Tris, 150 mM NaCl, 10 mM EDTA, 0.2% SDS, 600 μg/ml proteinase K) at 55°C overnight. Lysates were cleared by centrifugation at 14,800 rpm for 5 minutes at room temperature. Genomic DNA was precipitated with 500 μl isopropanol, washed with 500 μl 70% ethanol, and re-suspended in 200 μl dH_2O. The *Myb* genotyping reaction was performed as described above.

RNA extraction and reverse transcription (RT). Total cellular RNA was isolated using the TRIZOL reagent (Invitrogen) according to the manufacturer's protocol. Treatment with RNase-free DNase I (Invitrogen) was used to remove contaminating DNA and the SuperScript III First-Strand Synthesis System (Invitrogen) was used to prepare cDNA by the manufacturer's protocol. For RNA-seq, total cellular RNA from electronically sorted, GFP^+ *Irf4/8*$^{-/-}$ large pre-B cells was isolated using the TRIZOL reagent (Invitrogen) and purified using the Qiagen RNeasy Kit (Qiagen) by the manufacturer's protocol.

Quantitative RT-PCR (qRT-PCR). qRT-PCR was performed on a MyiQ Single Color Real-Time PCR Detection System (Bio-Rad) using Titanium Taq DNA polymerase (Clonetech) and 1X SYBR Green (Invitrogen) using the following conditions:

95°C for 3 minutes

40 cycles of 95°C for 40 seconds

66°C for 20 seconds

72°C for 30 seconds

Extension at 72°C for 1 minute

Melt curve analysis was performed to ensure melting temperatures were appropriate and equivalent. Primer sequences are listed in Table 2.3. Each sample was normalized to expression of *HPRT* and relative expression was calculated using the 2-ΔΔCT method as previously described (Pfaffl, 2001).

2.6) Protein Preparation and Immunoblotting

Western blotting. To determine c-Myb knockdown efficiency, transduced *Irf4/8*$^{-/-}$ large pre-B cells were electronically sorted based on GFP expression as described above and lysed in the following lysis buffer (20 mM Tris pH 7.2, 100 mM NaCl, 10 mM EDTA, 1 mM EGTA, 1% Triton X-100) (Emambokus et al., 2003) supplemented with an EDTA-free protease inhibitor cocktail (Roche) and 1mM PMSF (Sigma-Aldrich). Fifteen micrograms of protein were run on a 15% SDS-polyacrylamide gel and transferred to a Protran nitrocellulose transfer membrane (Whatman). Membranes were then blocked for 1 hour in PBS supplemented with 0.05% Tween-20 (PBS-T) containing 5% non-fat dry milk powder and incubated overnight with the c-Myb targeting primary antibody in PBS-T at 4°C. Membranes were washed 3 times with PBS-T and

Table 2.3. Quantitative Real Time PCR Primers

Gene	Sequence
Ccnd3	ATGCTGGAGGTGTGTGAGGA
	CCACAGCCTGGTCCGTATAG
Foxo1	AAGGATAAGGGCGACAGCAA
	TGGATTGAGCATCCACCAAG
Hk1	GCCACGCCTCGGTGCCATCTT
	GGTCTTGTGGAACCGCCGGG
Hprt	TGCCGAGGATTTGGAAAAAGTG
	CACAGAGGGCCACAATGTGATG
Ikzf1	GGAGGCACAAGTCTGTTGAT
	CATTTCACAGGCACGCCCATTCT
Ikzf3	GCCGAGATGGGAAGTGAGAG
	CCGGGATTGTAGTTGGCATC
IL7Rα	AGGATGGGATCCTGTCTTGC
	GGGGAGACTAGGCCATACGA
mTOR	CCATCCAATCTGATGCTGGA
	GGTGTGGCATGTGGTTCTGT
Myc	CGAAACTCTGGTGCATAAACTG
	GAACCGTTCTCCTTAGCTCTCA
Plcγ1	CTGTTCCACAGACGAATGCCCA
	GAGTTAGGCTCATTGCGTTTCCG
Rag1	GGGGAGTGGGGTTGAAAGTA
	TCCTCCAATCCTGCCTCCTA
Slc2a1	AGCCCTGCTACAGTGTAT
	AGGTCTCGGGTCACATC
Txnip	CGAGTCAAAGCCGTCAGGAT
	TTCATAGCGCAAGTAGTCCAAAGT

incubated with anti-Rabbit HRP secondary antibody in PBS-T containing 5% non-fat dry milk for 2 hours at room temperature. Again, membranes were washed 3 times with PBS-T and proteins were detected using the Western Lightning Plus-ECL enhanced chemiluminescence substrate (Perkin Elmer) on HyBlot CL film (Denville Scientific). As a loading control, membranes were incubated with β-Actin-HRP antibody in PBS-T for 1 hour at room temperature and detected on film as above. Signals were quantified using ImageQuant TL 2005 software and normalized to the β-Actin signal. Antibodies used for western blotting are detailed in Table 2.4.

Hexokinase activity assay. $CD19^{+}$ pro-B cells were transduced with pMSCV-IRES-tNGFR or pMSCV-IRES-tNGFR-Cre and electronically sorted based on the expression of tNGFR at 48 hours post-transduction. *Irf4/8*$^{-/-}$ large pre-B cells were transduced with pSIREN-RetroQ-shLuc-IRES-eGFP or pSIREN-RetroQ-shMyb-IRES-eGFP and electronically sorted based on the expression of GFP at 72 hours post-transduction. The enzymatic activity of hexokinase (HK) was measured using the Hexokinase enzyme assay kit (Biomedical Research Service and Clinical Application or BMR; E-111) per the manufacturer's protocol. Briefly, cells were lysed in 50 μl 1X Cell Lysis Solution (BMR), incubated 5 minutes on ice, and centrifuged at 13,000 rpm for 3 minutes at 4°C. Protein concentrations between samples were normalized to 0.5 μg/μl and, if needed, were diluted with 1X Cell Lysis Solution (BMR). For each sample condition, 10 μl of lysate was added to a 96-well plate in two sets of triplicate wells. Control and reaction solutions were prepared with 500 μl of HK Assay Solution with or without 10 μl of HK Substrate and 50 μl of each solution was added to triplicate wells for each sample condition. Cells were incubated for 1 hour at 37°C and 50 μl of 3% Acetic Acid was added to stop the reaction. For each well, the OD_{492nm} was measured and the

Table 2.4. Western blot antibodies

Protein	Clone	Species	Source
c-Myb	EP769Y	Rabbit	Epitomics
β-actin-HRP	AC-15	Mouse	Sigma-Aldrich
Rabbit HRP			GE Healthcare

measurements for control wells were subtracted from the measurements for sample wells. Then hexokinase enzyme activity was calculated using the following formula:

$$1U/L = OD_{492nm} \times 16.98$$

2.7) Microarray and RNA-seq

Microarray. Pro-B cells from *Myb^{ff} Rag2$^{-/-}$* and *Myb^{ff} Rag2$^{-/-}$ Cre-ER^{T2}* mice were cultured for 24 hours, treated with 4-hydroxytamoxifen (4-OHT) at 0.6 μM and the pan-caspase inhibitor Q-VD-OPH (SM Biochemicals) at 100 μM, and returned to culture for 48 hours. Total RNA was homogenized using QIAshredder spin columns (Qiagen) and prepared using the RNeasy Plus Micro Kit (Qiagen) according to the manufacturer's protocol. Quantity of total RNA was measured using a NanoView (GE Health Systems) at UV 260 nm and quality was assessed on the Agilent Technologies 4200 TapeStation. Double stranded cDNA and biotin-labeled cRNA were synthesized according to Affymetrix recommendations. Biotin-labeled cRNA was hybridized to Mouse Genome 430 2.0 Gene ChIP (Affymetrix) for 16 hours and scanned with the Affymetrix Gene-Array Scanner as previously described (Gallagher et al., 2005). Synthesis of cRNA, ChIP hybridization, data collection, and production of CEL files were performed by the University of Virginia Genome Analysis and Technology Core. The CEL files were then imported into R version 3.0.1 using the oligo package (Carvalho and Irizarry, 2010). Differential expression analysis was performed using the R/Bioconductor limma package (Ritchie et al., 2015).

RNA-seq. Retrovirus-transduced *Irf4/8$^{-/-}$* large pre-B cells were electronically sorted based on GFP expression and total cellular RNA was prepared as described above.

Library preparation. Quantity of total RNA was measured using a NanoView (GE Health Systems) at UV 260 nm and quality was assessed on the Agilent Technologies 4200 TapeStation. Samples with RNA integrity numbers of 7.7 and above were selected to prepare libraries using the NEBNext Ultra II Directional RNA Library Prep Kit for Illumina (New England BioLab) following the manufacturer's protocols. Briefly, 1 microgram of total RNA was used to isolate mRNA using NEBNext Poly(A) mRNA Magnetic Isolation Module, followed by fragmentation and poly-A priming. First & second-strand cDNA synthesis followed.The resulting cDNA was end-repaired dA tailed before ligated to the i5 and i7 sequencing adapters. To allow multiplexing of the libraries, unique barcodes had been incorporated to the ligation products via PCR, and the final purified libraries were quantified by a Qubit 3 Fluorometer (Fisher Scientific) and sized by Agilent TapeStation.

Next-Generation sequencing run and quality control. Individually barcoded libraries were adjusted to equal molar concentration and pooled to a 4 nM solution, which was then denatured in 0.1N sodium hydroxide, following the Illumina recommended procedure. Before each run, the denatured pool was diluted to 1.2 pM before loading on the Illumina NextSeq 150 High Output sequencing kit reagent cartridge. Sequencing run was carried out on the Illumina NextSeq 500 for paired-end sequencing (R1=R2=75 cycles). Demultiplexing of the barcoded sequences was performed on line in BaseSpace. Quality assessment of the sequencing reads was performed by running the FASTQC *Andrews S. (2010). FastQC: a quality control tool for high throughput sequence data. Available online at:* *http://www.bioinformatics.babraham.ac.uk/projects/fastqc*

Differential Gene Expression Analysis. The fastq files were first quality filtered and then aligned to the mouse transcriptome mm10 using STAR following by gene counting with HTSeq (Anders et al., 2015; Dobin et al., 2013). The count data were then imported into R-Bioconductor

for differential expression analysis using DESeq2 (Love et al., 2014). RNA-seq library preparation, next generation sequencing, quality control, genome alignment, and gene counting were performed by the University of Virginia Genome Analysis and Technology Core.

Gene set analysis. Gene set analysis was performed utilizing the investigate function of the Molecular Signatures Database (MSigDb) (Liberzon et al., 2011, 2015; Subramanian et al., 2005). Microarray results at a threshold of $p<0.05$ and RNA-seq results at a threshold of $p<0.0001$ were used to compute overlaps with curate gene set collections for KEGG pathways nad Gene Ontolog (GO) gene sets for Biological Processes at an FDR q-value below 0.05.

2.8) Statistics.

Differences between data sets were analyzed using the two-tailed Student t test at a confidence level of 95% for all experiments. Error bars represent standard error of the mean (SEM). Data sets were analyzed and figures were prepared with Prism v.7.0 and Prism v.8.0 (GraphPad Software).

Chapter III. c-Myb regulates IL-7R signaling to promote pro-B cell proliferation and glucose metabolism

3.1) Introduction

B cell development initiates in the bone marrow from hematopoietic stem cells (HSCs), which undergo a series of developmental stages to gain B-lineage specific genes while conversely losing the potential for differentiation into other myeloid or lymphoid cell lineages (Hardy et al., 2007). The $CD19^+$ pro-B cell stage marks the first stage of B-lineage committed progenitors. At the pro-B cell stage, V(D)J recombination occurs at the *Igh* locus, resulting in the production of a μHC, which combines with the surrogate light chain and signaling molecules Igα and Igβ to form the pre-BCR. Regulation of survival during the pro-B cell stage is critical to ensure that cells have enough time to successfully complete V(D)J rearrangements at the *Igh* locus, while not too much time as to allow failed rearrangements to result in mutations or chromosomal translocations (Opferman, 2008). Pro-B cell survival is regulated by the intrinsic survival pathway and the balance in pro-apoptotic and anti-apoptotic members of the Bcl-2 protein family. Apoptosis through the intrinsic survival pathway occurs following oligomerization of the pro-apoptotic Bcl-2 family members Bax and Bak at the mitochondrial membrane, which is inhibited by anti-apoptotic Bcl-2 family members, including Bcl-2 and Mcl-1, which are in turn, inhibited by the pro-apoptotic BH3-only proteins, including Bim, Bmf, Bid, and Bad (Strasser, 2005). The relative expression of these pro-apoptotic and anti-apoptotic proteins is responsive to levels of cellular stress such as growth factor or nutrient deprivation and thus ensure that B cell progenitors that are unfit to continue in development are removed.

The major nutrient source in pro-B cells is glucose, which is processed to fuel cellular metabolism through two major pathways: glycolysis and oxidative phosphorylation (Donnelly and Finlay, 2015). A more glycolytic metabolism is favored by activated or proliferating cells while a more oxidative metabolism is used to maintain homeostasis in less active or quiescent cells (Donnelly and Finlay, 2015; Lunt and Vander Heiden, 2011). Pro-B cells maintain moderate levels of proliferation while alternating between dividing populations engaged with IL-7-producing stromal cells and non-dividing populations undergoing DNA rearrangements at the *Igh* locus (Clark et al., 2014). To do this, pro-B cells primarily utilize oxidative metabolism and to a lesser extent glycolytic metabolism to generate sufficient energy and macromolecules to maintain homeostatic proliferation (Urbanczyk et al., 2018).

Signaling through the IL-7R is crucial for the survival, proliferation, and metabolism of pro-B cells. Signaling through the IL-7R in pro-B cells, activates the Jak/STAT and the Plcγ/Pkc/mTORC1 signaling pathways (Malin et al., 2010; Mandal et al., 2009; Yu et al., 2017). Jak1/3 signaling through Stat5 mediates pro-B cell survival through regulating the balance between pro- and anti-apoptotic Bcl-2 family members. In addition, Stat5 contributes to pro-B cell proliferation through inducing expression of the cell cycle regulator *Ccnd3* (Mandal et al., 2009). Plcγ signals through the second messenger DAG to activate Pkc and ultimately mTORC1 and this pathway has been demonstrated to be critical for pro-B cell proliferation and metabolism (Yu et al., 2017; Zeng et al., 2018). Upon deletion of Plcγ1/2 or rapamycin-mediated inhibition of mTORC1, pro-B cells are unable to respond to IL-7 signaling resulting in decreases in pro-B cell proliferation and metabolic readouts of oxidative phosphorylation and glycolysis. Activation of mTORC1 does not affect pro-B cell survival and acts independently of IL-7 signaling through

Stat5, indicating that these two pathways through mTORC1 and Stat5 mediate separate processes important for maintaining the pro-B cell compartment.

Previous work from our lab and others revealed critical roles for c-Myb in differentiation to pro-B cells as well as pro-B cell survival (Fahl et al., 2009; Greig et al., 2010). We subsequently investigated the mechanism of c-Myb-mediated pro-B cell survival and demonstrated that c-Myb regulates the intrinsic survival of pro-B cells, in the absence of IL-7, through repression of the pro-apoptotic Bcl-2 family members Bim and Bmf (Fahl et al., 2018). In addition, signaling downstream of the IL-7R through Stat5 further repressed expression of Bim and Bmf and increased expression of the anti-apoptotic Mcl-1 to skew the balance of Bcl-2 family members in favor of survival. However, restoring this IL-7-mediated pro-B cell survival pathway through expression of a constitutively active Stat5 (CA-Stat5) led to a significant but incomplete rescue of c-Myb-deficient pro-B cell numbers, suggesting that c-Myb has an additional function(s) in pro-B cells. In line with this, we demonstrated that c-Myb is important for mRNA expression of cyclin D3 and that c-Myb-deficient pro-B cells exhibited decreased >2n DNA content when cultured in the absence of IL-7 as compared to c-Myb-sufficient cells indicating a defect in proliferation. However, while expression of CA-Stat5 restored mRNA expression of cyclin D3, this was unable to rescue proliferation or recovery of c-Myb-deficient pro-B cell numbers. This result suggests that c-Myb regulates pro-B cell proliferation through a Stat5-independent mechanism and also raises the possibility that c-Myb has yet other function(s) within the pro-B cell compartment.

We have now demonstrated additional roles for c-Myb in the earliest stages of pro-B cell glucose metabolism at the level of glucose uptake and utilization. Gene set analysis of a microarray comparing c-Myb-sufficient and -deficient pro-B cells revealed that c-Myb-regulated genes were highly enriched in pathways and processes related to glucose. c-Myb-deficient pro-B cells

exhibited decreased glucose uptake accompanied by decreased mRNA expression of the glucose transporter Glut1 (*Slc2a1*) as well as decreased hexokinase activity accompanied by decreased mRNA expression of hexokinase 1 (*Hk1*). In addition, microarray analysis revealed that expression of a number of components of the Plcγ/Pkc/mTORC1 signaling pathway important for IL-7 mediated proliferation and metabolism in pro-B cells were significantly decreased upon loss of c-Myb. Thus, this work demonstrates a previously unappreciated role for c-Myb in glucose uptake and utilization and suggests that loss of IL-7R signaling contributes to c-Myb-dependent regulation of glucose metabolism in pro-B cells.

3.2) Results

Genome-wide analysis reveals a role for c-Myb in pro-B cell glucose metabolism

We have previously reported that c-Myb expression is critical for pro-B cell survival and proliferation, in part, via regulation of signaling downstream of the IL-7R through Stat5 (Fahl et al., 2018). However, expression of CA-Stat5 was unable to completely rescue recovery of c-Myb-deficient pro-B cell numbers suggesting that c-Myb has other function(s) in pro-B cells and/or that c-Myb may act through a Stat5-independent pathway. To identify additional roles for c-Myb in pro-B cells, we performed microarray analysis to compare gene expression of c-Myb-sufficient and -deficient pro-B cells. We utilized an inducible deletion system in *Cre-ER^{T2}* mice, which express a Cre recombinase and mutated estrogen receptor fusion protein with high affinity for the synthetic estrogen ligand 4-hydroxytamoxifen (4-OHT). Following treatment with 4-OHT, Cre translocates into the nucleus to induce recombination at *lox*P sites (Ruzankina et al., 2007). Pro-B cells from *Myb^{ff} Rag2$^{-/-}$ Cre-ER$^{T2+/-}$* mice were treated with 4-OHT to ablate c-Myb expression and global gene expression changes were assessed 48 h after treatment (Figure 3.1A). In addition, cells were treated with the pan-caspase inhibitor Q-VD-OPH to rescue pro-B cell survival as we

have previously reported that the rapid cell death that occurs upon loss of c-Myb can limit the detection of some c-Myb-regulated genes (Fahl et al., 2018). Microarray differential expression analysis yielded 906 genes that were significantly changed with a false discovery rate (FDR) of $p<0.05$, 40 genes with a log2 fold change>1, and 38 genes that met both thresholds (Figure 3.1B). Thus, loss of c-Myb expression in pro-B cells appeared to have broad effects on a large number of genes, but few of these gene expression changes resulted in a substantial increase or decrease in fold change.

To identify additional pathways and processes associated with c-Myb-dependent gene expression changes in pro-B cells that would account for the incomplete rescue after restoring IL-7 signaling through Stat5, we performed gene set analysis with gene sets from the molecular signatures database (MSigDb) (Figure 3.2). Notably, c-Myb-dependent differentially expressed genes (MDGs) were enriched in gene sets related to glucose metabolism including glycolysis, oxidative phosphorylation, and pathways involved in macromolecular biosynthesis. Among these were a number of downregulated MDGs including enzymes important for glucose utilization including *Hk1, Pfkm,* and *Fbp1*, nutrient transporters important for maintaining homeostasis of glucose and other metabolites including *Slc26a2, Slc37a4, Slc27a4,* and *Slc37a1*, as well as *Efhd1* which has been demonstrated to promote oxidative over glycolytic metabolism in pro-B cells. Therefore, this result suggested that a previously unappreciated role for c-Myb in glucose metabolism could account for persistent defects in recovery of c-Myb-deficient pro-B cells.

Recently published work identified a pathway downstream of the IL-7R through Plcγ/Pkc/mTORC1, which is critical for mediating IL-7-dependent pro-B cell metabolism and proliferation (Yu et al., 2017; Zeng et al., 2018). We found that MDGs involved in both IL-7 signaling including the IL-7Rα subunit (*Il7r*) and mTORC1 signaling including multiple

Figure 3.1: Microarray profiling of c-Myb-dependent gene expression changes in pro-B cells.

Experimental system used to analyze genome-wide c-Myb-dependent gene expression changes by microarray. $CD19^{+}$ pro-B cells were positively selected on magnetic beads from *Myb^{ff} Rag2$^{-/-}$ Cre-ER^{T2} (+/-)* and cultured for 24 h in the presence of IL-7. Cells were then treated with 200uM Q-VD-OPH and 0.6uM 4-OHT. At 48 h after treatment, total cellular RNA was harvested from *Cre-ER$^{T2(-)}$* (control) and *Cre-ER$^{T2(+)}$* (c-Myb-deficient) cells for microarray analysis. **(B)** Volcano plot of c-Myb-dependent differentially expressed genes (MDGs) displayed as fold change (log2FC; x-axis) versus statistical significance (adjusted p-value (padj); y-axis). Each gene is represented as one dot and is colored based on a threshold padj < 0.05 (red), log2FC > 1 (blue), and the genes that satisfy both of these parameters (yellow). Select genes are labeled and denoted by black dots.

A.

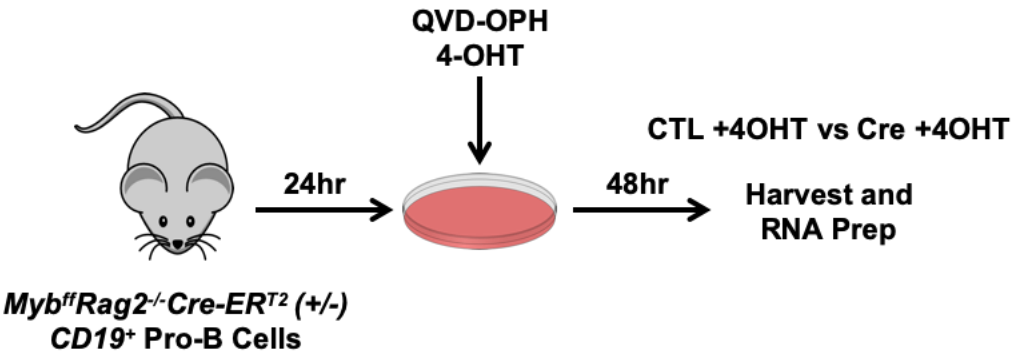
QVD-OPH
4-OHT
CTL +4OHT vs Cre +4OHT
24hr
48hr
Harvest and
RNA Prep
Mybff Rag2-/- Cre-ERT2 (+/-)
CD19+ Pro-B Cells

B.

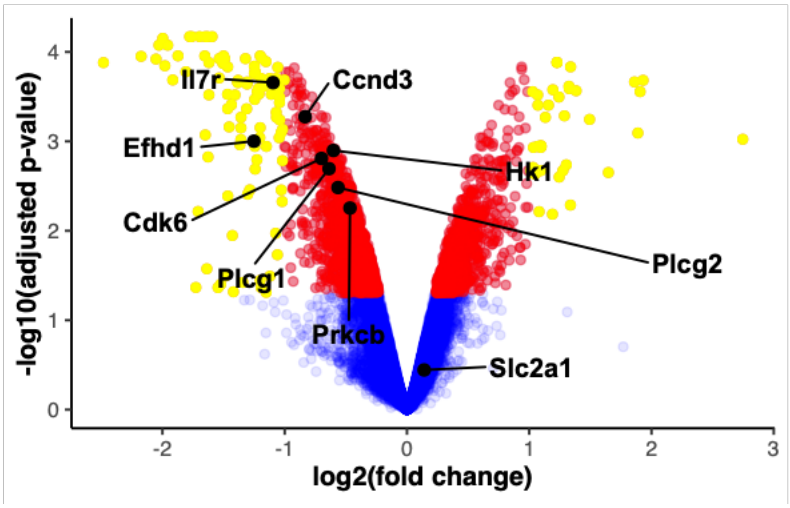
Il7r
Ccnd3
Efhd1
Hk1
Cdk6
Plcg1
Plcg2
Prkcb
Slc2a1
-log10(adjusted p-value)
log2(fold change)
0
1
2
3
4
-2
-1
0
1
2
3

Figure 3.2: Gene set analysis of MDGs from pro-B cell microarray analysis. Gene set analysis of the pro-B cell microarray experiment described in Figure 3.1A utilizing the Hallmark, Reactome, and KEGG pathway gene sets from the molecular signatures database (MSigDb). Overlap between MDGs with a padj < 0.05 and selected gene sets was determined using the MSigDb investigate gene sets function with a false discovery rate (FDR) threshold for enrichment of 0.05.

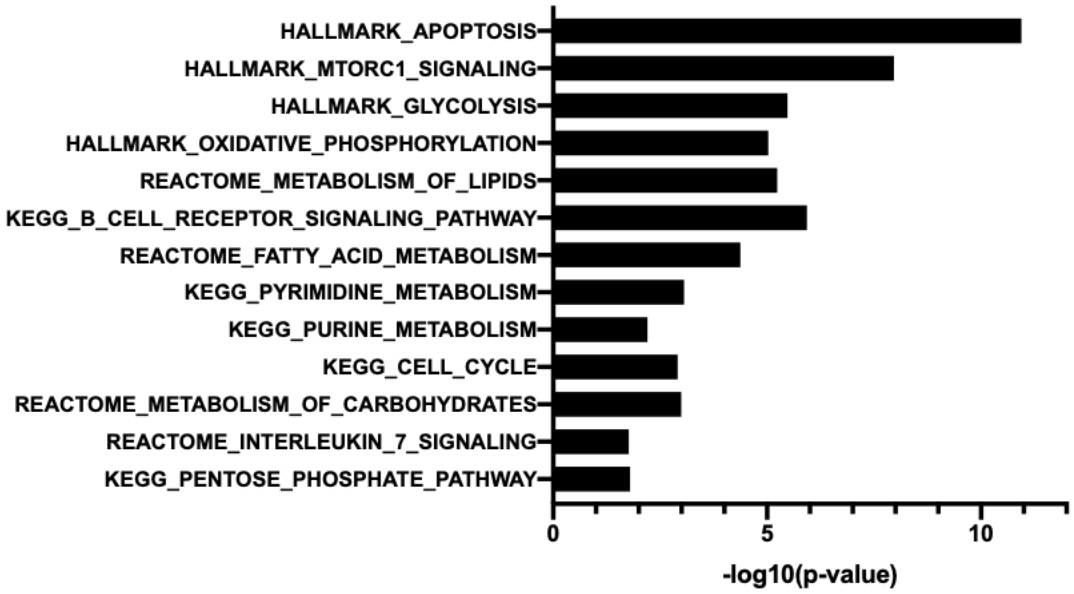
HALLMARK_APOPTOSIS
HALLMARK_MTORC1_SIGNALING
HALLMARK_GLYCOLYSIS
HALLMARK_OXIDATIVE_PHOSPHORYLATION
REACTOME_METABOLISM_OF_LIPIDS
KEGG_B_CELL_RECEPTOR_SIGNALING_PATHWAY
REACTOME_FATTY_ACID_METABOLISM
KEGG_PYRIMIDINE_METABOLISM
KEGG_PURINE_METABOLISM
KEGG_CELL_CYCLE
REACTOME_METABOLISM_OF_CARBOHYDRATES
REACTOME_INTERLEUKIN_7_SIGNALING
KEGG_PENTOSE_PHOSPHATE_PATHWAY
0
5
10
-log10(p-value)

components of this recently characterized pathway (*Plcg1, Plcg2, Prkcb*, and *mTOR*), were all downregulated upon loss of c-Myb (Figure 3.2). Consistent with previously published data, MDGs were also enriched in gene sets related to cell cycle progression including the cell cycle regulator *Ccnd3* and one of its associated cyclin dependent kinases *Cdk6* (Cogswell et al., 1993; Fahl et al., 2018). Overall, these results suggest that c-Myb-mediated regulation of IL-7R signaling through mTORC1 is important for pro-B cell proliferation and glucose metabolism.

To validate our microarray data, we performed qRT-PCR on a panel of key genes involved in mTORC1 signaling and glucose metabolism (Figure 3.3). To do this, pro-B cells were transduced with retroviruses encoding a tNGFR reporter or tNGFR and a *Myb* mRNA targeting shRNA (tNGFR-shMyb) (Fahl et al., 2009; Hess et al., 2006). Knockdown of c-Myb mRNA with shMyb behaves similarly to c-Myb hypomorphic mutations that induce a similar but less drastic phenotype than *Myb* null mutations and thus acts similarly to Q-VD-OPH treatment and enables us to detect gene expression changes masked by cell death upon loss of c-Myb expression (Carpinelli et al., 2004; Sandberg et al., 2005). Interestingly, we found that in addition to downregulated mRNA expression of IL-7Rα, Plcg1, mTOR, and Hk1, expression of the major glucose transporter in B cell progenitors, *Slc2a1* (Glut1), was also decreased upon loss of c-Myb. Failure to detect a statistically significant decrease in Glut1 mRNA expression in our pro-B cell microarray could be due to a number of factors including the efficiency of deletion at the *Myb* locus upon tamoxifen treatment and differences in the Cre-mediated knockout and shRNA-mediated knockdown approaches (see Discussion). Regardless, this result demonstrates that c-Myb regulates the expression of multiple components of this critical mTORC1 pathway mediating IL-7-dependent proliferation and metabolism in pro-B cells as well as multiple factors critical for the earliest processes involved in glucose utilization.

Figure 3.3: c-Myb-dependent expression of genes important for pro-B cell glucose metabolism. $CD19^{+}$ pro-B cells were positively selected on magnetic beads from *Myb*^{ff} *Rag2*$^{-/-}$ mice and cultured for 24 h in the presence of IL-7. Cells were subsequently transduced with tNGFR or tNGFR-shMyb and cultured for 48 h in the presence of IL-7. Total RNA was prepared and mRNA expression of selected genes related to pro-B cell glucose metabolism was analyzed by qRT-PCR. Gene expression was normalized to the expression of Hprt and genes were analyzed in triplicate per condition. *$p < 0.05$, **$p < 0.005$, ***$p < 0.0005$.

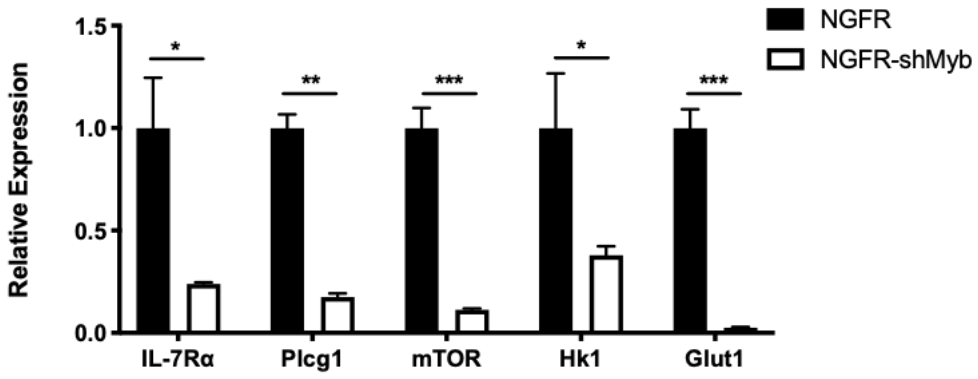
NGFR
NGFR-shMyb
Relative Expression
1.5
1.0
0.5
0.0
*
**
***
*
***
IL-7Rα
Plcg1
mTOR
Hk1
Glut1

c-Myb is critical for pro-B cell glucose uptake and hexokinase activity

Upon glucose uptake by transporters at the plasma membrane, intracellular glucose is phosphorylated by hexokinase to produce glucose-6-phosphate (G6P), which is either shuttled into the pentose phosphate pathway for nucleotide synthesis or is converted into other downstream glycolytic intermediates (Donnelly and Finlay, 2015). Our microarray gene set analysis indicated that loss of c-Myb expression would lead to defects in pro-B cell glucose metabolism. Furthermore, our differential gene expression analysis indicated that loss of c-Myb would lead to defects in the ability of pro-B cells to take up glucose through Glut1 and to convert glucose to G6P via Hk1-mediated phosphorylation (Figure 3.3). To determine whether c-Myb is important for glucose uptake in pro-B cells, we transduced *Myb*^{ff} *Rag2*$^{-/-}$ *CD19*$^{+}$ pro-B cells with retroviruses encoding tNGFR or tNGFR and Cre (tNGFR-Cre) and 48 h post-transduction, incubated them with the fluorescent glucose analog 2-deoxy-2-[(7-nitro-2,1,3-benzoxadiazol-4-yl) amino]-D-glucose (2-NBDG) (Figure 3.4A). We detected a 50% decrease in 2-NBDG uptake in the tNGFR-Cre transduced pro-B cells as compared to controls, suggesting that loss of c-Myb and Glut1 mRNA expression lead to decreased transport of glucose into the cell. Then, to determine if c-Myb is important for glucose utilization through hexokinase-mediated phosphorylation, we measured total hexokinase activity. By 48 h post-transduction we found that the tNGFR-Cre transduced pro-B cells exhibited an approximately 75% decrease in overall hexokinase activity (Figure 3.4B). Thus, loss of c-Myb expression in pro-B cells and the concomitant decrease in Hk1 and Glut1 mRNA expression results in decreased glucose uptake and modification for use in metabolic pathways. With this result, we can propose a model in which c-Myb regulates IL-7R signaling through mTORC1, which is critical for maintaining homeostatic metabolism and proliferation of pro-B cells (Figure 3.5). In particular, loss of c-Myb and IL-7R signaling through mTORC1, leads

Figure 3.4: c-Myb-deficient pro-B cells exhibit defects in glucose uptake and hexokinase activity. CD19+ pro-B cells were positively selected on magnetic beads from Mybff Rag2-/- mice and cultured for 24 h in the presence of IL-7. Cells were subsequently transduced with tNGFR or tNGFR-Cre and cultured for 48 h in the presence of IL-7. **(A)** At 48 h post-transduction, NGFR+ cells were incubated for 30 min with the 2-NBDG glucose uptake mix and 2-NBDG mean fluorescence intensity (MFI) was measured by flow cytometry. The glucose uptake inhibitor phloretin was used as a negative control for 2-NBDG uptake. **(B)** At 48 h post-transduction, NGFR+ cells were electronically sorted and protein lysate was prepared for analysis of hexokinase enzymatic activity. Enzyme activity was determined by colorimetric assay and absorbance at 492nm. All retrovirus transductions were performed with three replicates per condition. *$p < 0.05$, **$p < 0.005$.

A.

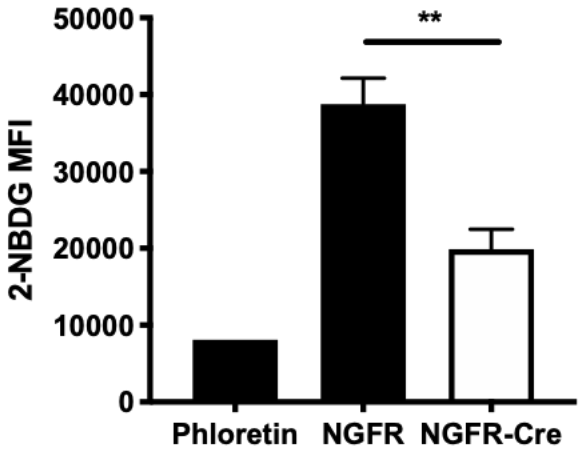
50000
40000
30000
20000
10000
0
2-NBDG MFI
**
Phloretin
NGFR
NGFR-Cre

B.

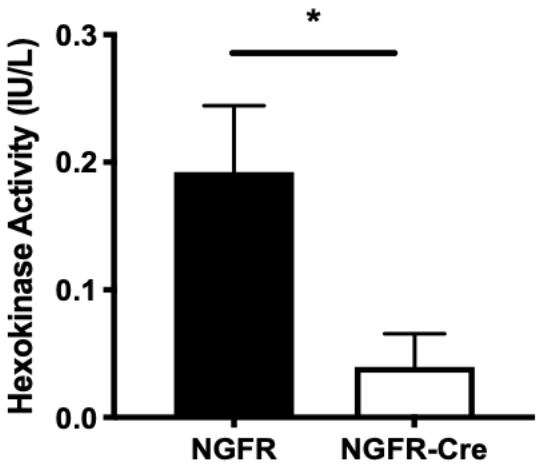
0.3
0.2
0.1
0.0
Hexokinase Activity (IU/L)
*
NGFR
NGFR-Cre

Figure 3.5: Regulation of pro-B cell glucose metabolism by c-Myb. Proposed model for c-Myb regulation of pro-B cell glucose metabolism. c-Myb positively regulates expression of the IL-7Rα as well as multiple components of downstream signaling through mTORC1 including Plcγ1/2, Pkcb, and mTOR. IL-7/IL-7R signaling activates Plcγ1/2 which signals through the second messenger DAG to activate Pkcβ, which leads to activation of mTORC1. This pathway is critical for pro-B cell proliferation and to maintain pro-B cell metabolism, which primarily utilizes glucose to produce ATP through oxidative phosphorylation. c-Myb also regulates multiple genes important for glucose metabolism including Glut1, the major glucose transporter in B cell progenitors, and Hk1, the enzyme responsible for catalyzing the initial step of glucose processing in the cell. Proper glucose uptake and phosphorylation by hexokinase are critical upstream processes required for glucose utilization in downstream metabolic pathways including glycolysis and oxidative phosphorylation. c-Myb-regulated genes identified by microarray and qRT-PCR are represented by blue ovals.

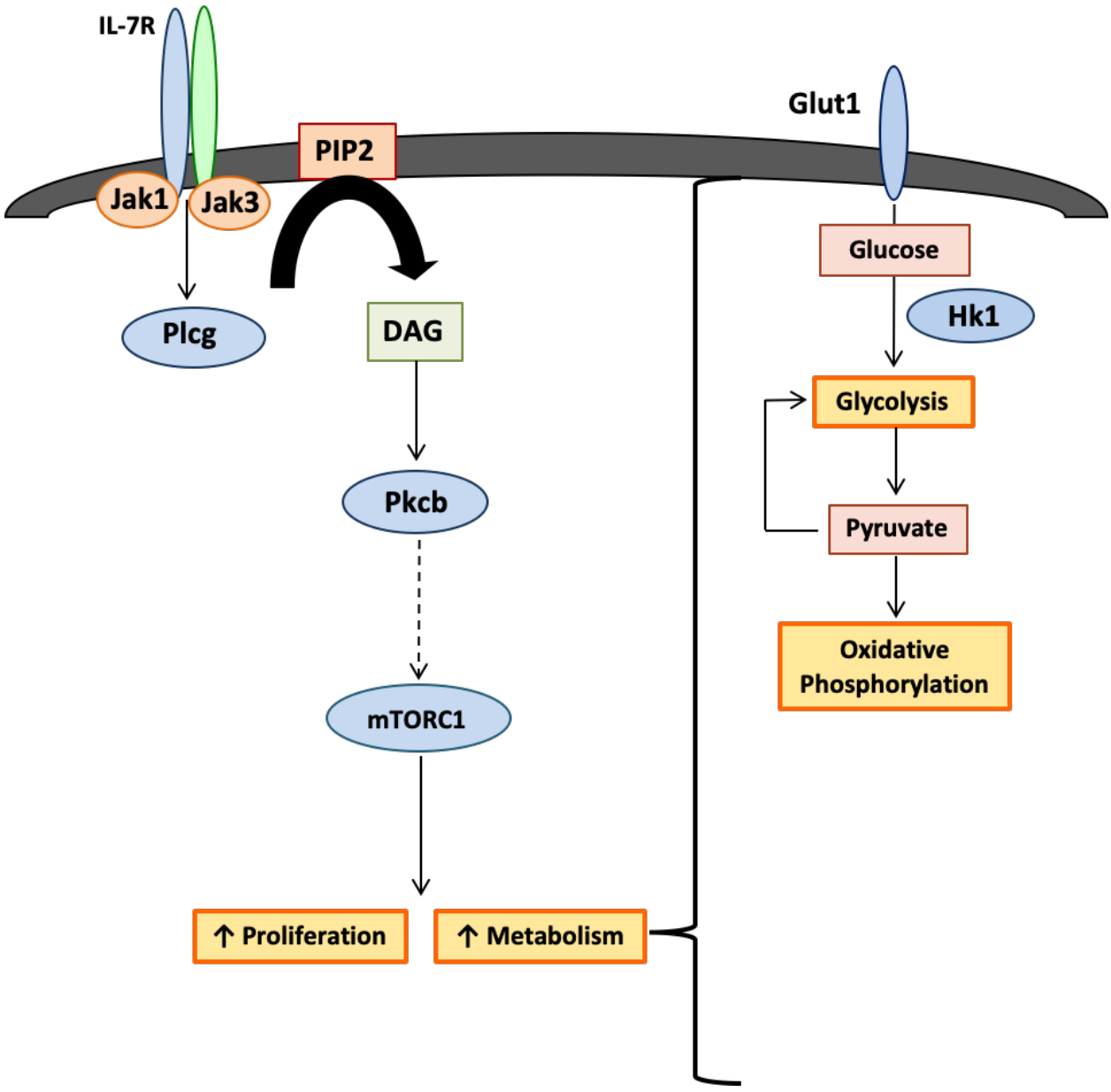
IL-7R
Jak1
Jak3
PIP2
Plcg
DAG
Pkcb
mTORC1
↑ Proliferation
↑ Metabolism
Glut1
Glucose
Hk1
Glycolysis
Pyruvate
Oxidative Phosphorylation

to defects in the earliest steps of glucose uptake and hexokinase-mediated phosphorylation, which are critical to allow further utilization of glucose through downstream metabolic pathways such as glycolysis and oxidative phosphorylation.

3.3) Discussion

The IL-7 signaling pathway is the major mediator of survival, proliferation, and metabolism in pro-B cells (Corfe and Paige, 2012; Yu et al., 2017; Zeng et al., 2018). We have previously reported that the transcription factor c-Myb is critical for pro-B cell survival, proliferation, and regulation of multiple components of IL-7 signaling (Fahl et al., 2018). However, while targeting signaling downstream of the IL-7R through expression of CA-Stat5 was able to restore c-Myb-dependent pro-survival gene expression changes and expression of *Ccnd3*, this was unable to rescue pro-B cell proliferation or recovery of c-Myb-deficient pro-B cell numbers suggesting that c-Myb has additional functions in pro-B cells and that these functions are mediated by a Stat5-independent mechanism. We have now identified a previously unappreciated role for c-Myb in pro-B cell glucose metabolism and specifically for glucose uptake and phosphorylation through hexokinase activity as well as mRNA expression of Glut1 and Hk1, loss of which would preclude glucose utilization in downstream metabolic pathways.

We have utilized a microarray comparing c-Myb-sufficient and c-Myb deficient pro-B cells to demonstrate that MDGs are enriched in gene sets related to glucose metabolism. However, in the process of validating changes in MDGs from the microarray, we noted that mRNA expression of Glut1 (*Slc2a1*) was significantly decreased upon shRNA-mediated knockdown of c-Myb as measured by qRT-PCR but was not among the significantly changed genes on the microarray at a threshold of $p<0.05$. This could be due to a number of factors including the deletion efficiency of the *Myb* allele as well as differences in our knockout and knockdown approaches. The

experimental design for the microarray compared *Myb*^{ff} *Rag2*$^{-/-}$ *Cre-ER*$^{T2+/-}$ mice following treatment with tamoxifen to delete c-Myb expression. However, the deletion efficiency at the *Myb* locus was never assessed for this experiment and remains unknown. Thus, as hematopoietic cells are acutely sensitive to levels of c-Myb expression, it is likely that variations in deletion efficiency could impact the results of microarray differential gene expression analysis (Sakamoto et al., 2006). In addition, our lab has demonstrated that the severe survival defect in c-Myb-deficient cells can limit detection of c-Myb regulated genes, which is why we have employed methods to rescue survival including expression of Bcl-2 or treatment with a pan-caspase inhibitor (Fahl et al., 2009). Therefore, it is possible that utilizing an shRNA-mediated knockdown approach to validate MDGs had a similar effect to Bcl-2 expression or caspase inhibitor treatment and uncovered an additional c-Myb-regulated gene (Glut1) that was not detected by microarray in c-Myb-deficient pro-B cells treated with Q-VD-OPH. It also remains possible that there are additional c-Myb-regulated genes that were not statistically significant within the threshold we set in our microarray analysis, which emphasizes the fact that subtle shifts in c-Myb expression can impact the result of studies of c-Myb function.

We have also demonstrated that c-Myb regulates mRNA expression of multiple components of the IL-7R signaling pathway through Plcγ/Pkc/mTORC1, which is critical for pro-B cell proliferation and metabolism but not for pro-B cell survival. In addition, this Plcγ/Pkc/mTORC1 signaling pathway acts independently of Stat5 signaling (Zeng et al., 2018). Thus, it appears that c-Myb regulation of signaling through the IL-7R regulates pro-B cell survival through the Jak/Stat5 signaling pathway and pro-B cell proliferation and metabolism through the Plcγ/Pkc/mTORC1 signaling pathway. However, the exact mechanism by which activation of mTORC1 promotes pro-B cell glucose metabolism and specifically glucose uptake and hexokinase

activity has not been defined. One possibility is that mTORC1 acts through activation of the transcription factor hypoxia inducible factor 1 subunit alpha (HIF1α), which acts as a master regulator of the homeostatic response to hypoxia, in part, through activating transcription of genes involved in metabolism (Liu et al., 2012). Although the mechanism is not completely understood, activation of mTORC1 promotes transcription of HIF1α and enhances translation of HIF1α gene targets (Zeng and Chi, 2014). In addition, the HIF1α transcription factor MSigDb gene set from the pathway interaction database (PID_HIF1_TFPATHWAY) includes *Slc2a1* and *Hk1,* indicating that both genes have been identified as targets of HIF1α transcription factor activity (Schaefer et al., 2009). Thus, it is possible that mTORC1 activation of HIF1α could mediate transcription of Glut1 and Hk1 mRNA in pro-B cells.

Pro-B cells maintain homeostatic levels of metabolism and are minimally proliferative, relying primarily on oxidative metabolism to produce energy in the form of ATP (Urbanczyk et al., 2018). Limiting proliferation at the pro-B cell stage is particularly important to separate cell division from DNA rearrangements at the *Igh* locus by V(D)J recombination in order to reduce the risk of developing mutations. Then, upon surface expression of the pre-BCR, pro-B cells transition into large pre-B cells and undergo a limited proliferative burst of proliferation to expand the pool of B cells with productive IgH rearrangements. Therefore, the role we have described for c-Myb in pro-B cell glucose metabolism raises the question of what implications this finding would have for the proliferative burst across the pre-BCR checkpoint at the large pre-B cell stage of development. Large pre-B cells exhibit enhanced metabolic demands for biosynthetic intermediates to facilitate cell division and shift to a primarily glycolytic metabolism called aerobic glycolysis in which they also utilize oxidative phosphorylation, but at a lower level than pro-B cells. In this shift to aerobic glycolysis, large pre-B cells exhibit increased glucose uptake and rely

more heavily on glucose utilization than pro-B cells as well. Thus, while it is possible that c-Myb has a different function in the large pre-B cell compartment, it is likely that the role we have demonstrated for c-Myb in glucose uptake and utilization in pro-B cells would have a major impact on the more metabolically active large pre-B cell.

Chapter IV. c-Myb expression is critical to maintain proliferation and glucose metabolism of large pre-B cells

4.1) Introduction

Upon commitment to the B-cell lineage at the $CD19^+$ pro-B cell stage, progenitors face two major developmental checkpoints defined by products of V(D)J recombination events at the *Igh* and *Igl* loci resulting in the production of a B-cell receptor (BCR). The first of these checkpoints, the pre-BCR checkpoint, selects pro-B cells based on successful rearrangement at the *Igh* locus, production of a μ heavy chain (μHC), and expression on the cell surface with the surrogate light chain (SLC) and signaling molecules Igα and Igβ to form the pre-BCR. Upon expression of the pre-BCR, pro-B cells differentiate to large pre-B cells, which undergo a transient proliferative burst, exit the cell cycle, and differentiate into quiescent, small pre-B cells (Clark et al., 2014; Reth and Nielsen, 2014). The second developmental checkpoint selects small pre-B cells for successful completion of VJ recombination at the *Igκ* L chain locus to produce a L chain that pairs with the μHC and forms membrane IgM on the surface of immature B cells.

The successive differentiation from pro-B to large pre-B to small pre-B cells involves changes in proliferative and metabolic status, in particular changes in their reliance on glucose uptake and metabolism (Stein et al., 2017; Urbanczyk et al., 2018). In pro-B cells, glucose uptake is primarily utilized through oxidative phosphorylation over glycolysis (Urbanczyk et al., 2018). Subsequently, with expression of the pre-BCR, large pre-B cells exhibit increased glucose uptake and increased overall metabolic activity to fuel their proliferative expansion. Similar to other highly proliferative cell types, large pre-B cells shift the majority of glucose utilization to glycolysis and the production of macromolecules to facilitate increased proliferation (Lunt and Vander Heiden, 2011; Urbanczyk et al., 2018). Then, after approximately 5 or 6 divisions, large

pre-B cells exit the cell cycle and repress glucose metabolism in preparation for differentiation into quiescent small pre-B cells. Repression of proliferation and metabolism is critical to minimize the risk of possible mutations that can occur during the process of VJ recombination in small pre-B cells.

Signaling through the IL-7R and pre-BCR are the major drivers of development across the pre-BCR checkpoint including changes in gene expression and shifts in proliferative and metabolic status (Clark et al., 2014; Reth and Nielsen, 2014). Pro-B cells mainly rely on IL-7R signaling for cell survival and to maintain cell proliferation and metabolism (Malin et al., 2010; Mandal et al., 2009; Yu et al., 2017; Zeng et al., 2018). Upon its expression on large pre-B cells, the pre-BCR initially synergizes with the IL-7R to increase sensitivity to IL-7 (Hess et al., 2001; Marshall et al., 1998). Activation of Jak/Stat5 signaling downstream of the IL-7R in combination with PI3K/Akt signaling downstream of the IL-7R and pre-BCR lead to the expression of cyclin D3 and activation of c-Myc and mTORC1 to promote enhanced proliferation and metabolism (Cooper et al., 2006; Habib et al., 2007; Iwata et al., 2016). Subsequently, a threshold level of pre-BCR signaling shifts large pre-B cells from a focus on proliferation to differentiation. In particular, pre-BCR-mediated induction and activation of Blnk (SLP-65) inhibits PI3K/Akt proliferative signaling and activates Irf4, which induces expression of the Ikaros transcription factor family members Ikaros (*Ikzf1*) and Aiolos (*Ikzf3*) (Heizmann et al., 2013). Ikaros family members form homo- or heterodimers to facilitate optimal DNA binding and activity and, together, Ikaros and Aiolos mediate the majority of gene expression changes that occur at the large to small pre-B cell transition (Ferreirós-Vidal et al., 2013; Georgopoulos, 2017).

Loss of c-Myb expression in *Myb*$^{f/f}$ *CD19-cre* mice, where Cre-mediated deletion occurs in late pro-B cells, results in a partial block to differentiation beyond the pro-B cell stage and a

decreased number of large and small pre-B cells as well as immature B cells (Thomas et al., 2005). We recently reported that c-Myb is required for the survival of $CD19^{+}$ pro-B cells where c-Myb sets baseline expression of the pro-apoptotic proteins Bim and Bmf and is further required for expression of IL-7Rα, which suppresses expression of Bim and Bmf, thus regulating the lifespan of pro-B cells (Fahl et al., 2018). However, rescue of c-Myb-deficient pro-B cell survival with a Bcl-2 transgene does not rescue the large and small pre-B cell compartments. c-Myb also controls the expression of genes that are required for the pre-BCR checkpoint including components of the SLC and cyclin D3 (Fahl et al., 2018). However, it is not known if c-Myb is important in the large pre-B cell compartment or differentiation to the small pre-B cell compartment.

We have now demonstrated that c-Myb plays a distinct role in the large pre-B cell compartment and found that loss of c-Myb expression lead to decreased large pre-B cell proliferation and survival. Genome-wide analysis of c-Myb function by RNA-seq revealed enrichment of c-Myb-regulated genes in pathways related to metabolism and glucose utilization. Furthermore, exogenous expression of Glut1, the major glucose transporter expressed in B cell progenitors, and Hk1, a critical mediator of glucose utilization and glucose-dependent survival, restored recovery and decreased apoptosis of c-Myb-deficient large pre-B cells. We also identified a role for c-Myb in repression of Ikaros and Aiolos and found that our c-Myb-dependent transcriptional profile was highly enriched in Ikaros targets important for mediating cell cycle exit and the large to small pre-B cell transition. However, while expression of a dominant negative Ikaros mutant was able to reverse gene expression changes induced by c-Myb knockdown and increased Ikaros expression, it was insufficient to fully rescue recovery of c-Myb deficient large pre-B cells, suggesting that increased Ikaros expression cannot account for all aspects of the c-Myb-dependent large pre-B cell phenotype. We found that c-Myb regulated Hk1 mRNA

expression and thus, glucose utilization and glucose-dependent survival, in an Ikaros-independent manner. Thus, c-Myb exhibits both Ikaros-dependent and Ikaros-independent functions in large pre-B cells in order to maintain large pre-B cell metabolism and proliferation while preventing the premature initiation of gene expression changes that promote differentiation.

4.2) Results

c-Myb is critical for the proliferative expansion of large pre-B cells

We previously reported that c-Myb coordinates pro-B cell survival and proliferation with the expression of genes that are critical for initiation of the pre-BCR checkpoint (Fahl et al., 2018). However, it is not known if c-Myb is important in the large pre-B cell compartment or transition to the small pre-B cell compartment. Due to the transient nature of the large pre-B cell compartment it is difficult to isolate this population for study *in vivo*. Thus, to examine c-Myb function in large pre-B cells, we have utilized two model systems. In the first model, *Myb*^{ff} *Rag2*$^{-/-}$ pro-B cells were transduced in cell culture with a retrovirus (MIG-17.2.25) that encodes a rearranged mu heavy chain (μHC) and a GFP reporter as a bicistronic mRNA (μHC–GFP) to promote differentiation into large pre-B cells (Guloglu et al., 2005). Subsequently, these cells were transduced 24 hours later with retroviruses encoding a tNGFR reporter or the tNGFR reporter and Cre (Cre-tNGFR) to ablate c-Myb expression (Figure 4.1A). Transition to the large pre-B cell compartment was demonstrated by an increase in cell size and cell number of μHC/tNGFR co-transduced cells over the time course of the experiment as compared to empty-vector-transduced pro-B cell controls (Figure 4.2A and B). To determine if c-Myb is important in large pre-B cells, the relative recovery of MIG-μHC/tNGFR (μHC) and MIG-μHC/tNGFR-Cre (μHC/Cre) transduced pro-B cells was assessed over a 72 h time course (Figure 4.1B). We found that the relative recovery of μHC/Cre transduced pro-B cells was decreased by approximately 80%

Figure 4.1. c-Myb deletion in *Myb^{ff}Rag2$^{-/-}$ uHC*-Transduced pro-B cells leads to decreased cell recovery. (A) Experimental model for in vitro generation of pre-B cells. CD19^{+} pro-B cells were positively selected on magnetic beads from *Myb^{ff} Rag2$^{-/-}$* mice and cultured for 24 h with 10ng/ml IL-7. These cells were subsequently transduced with MIG-17.2.25 (uHC) or the empty GFP reporter vector (MIG-R1) and 24 h later with NGFR-Cre or the empty NGFR reporter vector. Following retrovirus transduction, pre-B cells were cultured with 10ng/ml IL-7 and every 24 h, co-transduced GFP^{+} NGFR^{+} cells were analyzed for total cell numbers. To determine relative recovery, the total number of co-transduced cells was set as 1 and relative recovery was calculated as a ratio compared with the number of GFP^{+} NGFR^{+} cells at the 24 h time point. **(B)** Co-transduced GFP^{+} NGFR^{+} cells was analyzed at 24, 48, and 72 h post-transduction by flow cytometry and relative recovery was determined.

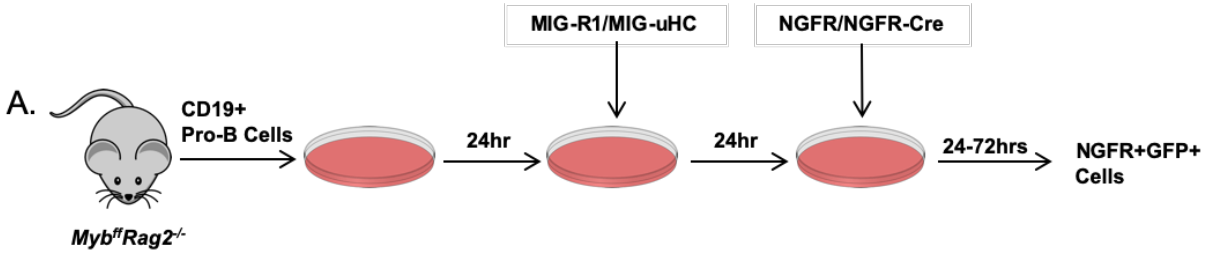
A.
CD19+
Pro-B Cells
Myb^ff Rag2^-/-
24hr
MIG-R1/MIG-uHC
24hr
NGFR/NGFR-Cre
24-72hrs
NGFR+GFP+
Cells

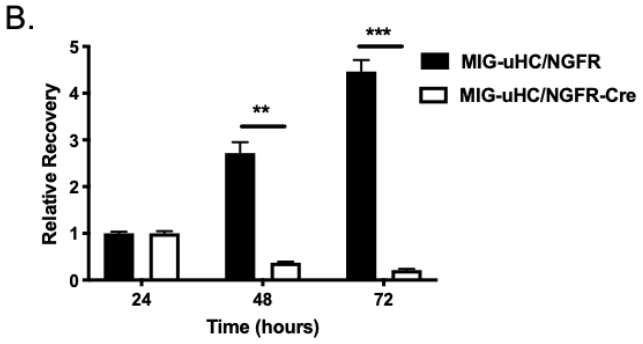
B.
Relative Recovery
0
1
2
3
4
5
**
***
24
48
72
Time (hours)
MIG-uHC/NGFR
MIG-uHC/NGFR-Cre

Figure 4.2. Efficacy of the μHC transduction large pre-B cell model. Pro-B cells from *Myb*^{ff} *Rag2*$^{-/-}$ mice were co-transduced with MIG-R1 or MIG-17.2.25 (uHC) and NGFR or NGFR-Cre and cultured with 10ng/ml IL-7. **(A)** Total numbers of co-transduced GFP^{+} NGFR^{+} cells was analyzed 24, 48, and 72 h post-transduction by flow cytometry. Relative recovery was determined by normalization to the total number of co-transduced cells at the 24 h time point. Retrovirus transductions were done in triplicate. *$p < 0.05$, **$p < 0.005$. **(B)** Forward scatter (FSC) histograms of co-transduced GFP^{+} NGFR^{+} cells from (A). The solid line represents MIG-uHC/NGFR transduced cells (pre-B) and the dotted line represents MIG-R1/NGFR transduced cells (pro-B).

A.

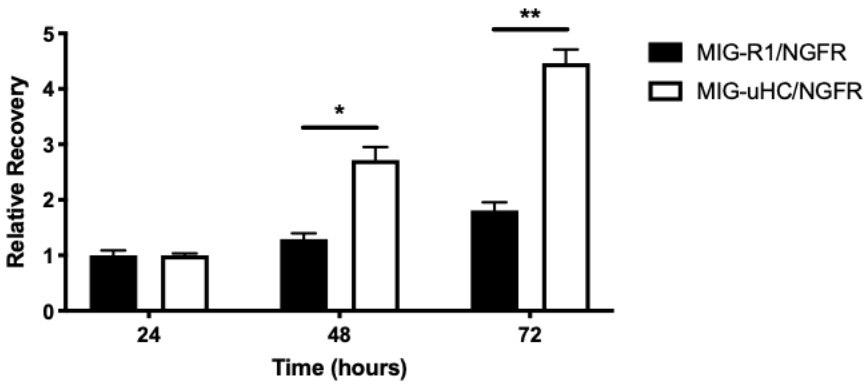
Relative Recovery
5
4
3
2
1
0
*
**
24
48
72
Time (hours)
MIG-R1/NGFR
MIG-uHC/NGFR

B.

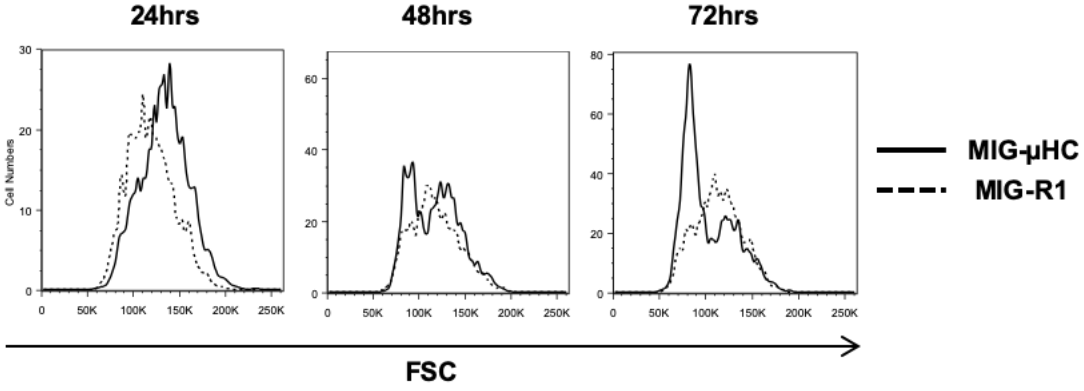
24hrs
48hrs
72hrs
Cell Numbers
30
20
10
0
60
40
20
80
60
40
0
50K
100K
150K
200K
250K
FSC
MIG-μHC
MIG-R1

compared to μHC transduced pro-B cells 48 h after transduction and >90% by 72 h post-transduction. Thus, c-Myb appears to be crucial for continued proliferative expansion of μHC-transduced pro-B cells. In this model, large pre-B cells continued to differentiate and by 48 h post transduction with μHC, a population of small pre-B cells appeared (Figure 4.2B). Since the μHC-transduction model ultimately produces a heterogeneous population of large and small pre-B cells, we also examined the *Irf4*$^{-/-}$ *Irf8*$^{-/-}$ double deficient (*Irf4/8*$^{-/-}$) large pre-B cell line as a second model that represents large pre-B cells (Lu et al., 2003). This cell line is derived from *Irf4/Irf8*$^{-/-}$ mice that accumulate cycling large pre-B cells in the bone marrow that fail to differentiate and undergo recombination at the IgL locus. However, as *Irf4/8*$^{-/-}$ large pre-B cells are not on a *Myb*^{ff} background, they were transduced with retroviruses that co-produce a GFP reporter and a *Myb* mRNA targeting shRNA (shMyb), or a GFP reporter and a control *Luciferase* mRNA targeting shRNA (shLuc) (Fahl et al., 2009; Hess et al., 2006). Transduction of *Irf4/8*$^{-/-}$ large pre-B cells with shMyb resulted in approximately an 80% knock-down of c-Myb protein (Figure 4.3A). In addition, shMyb transduction resulted in a 30% decrease in relative recovery at 72 h post-transduction compared to shLuc transduced *Irf4/8*$^{-/-}$ large pre-B cells. Due to the differences in phenotype between the shMyb-mediated knockdown and Cre-mediated knockout approaches, we extended the relative recovery time course from 72 h to 120 h in the shMyb-transduced *Irf4/8*$^{-/-}$ large pre-B cell model. With these additional time points, we found a 50-60% decrease in recovery of shMyb-transduced *Irf4/8*$^{-/-}$ large pre-B cells at 96 and 120 h post-transduction compared to shLuc transduced controls (Figure 4.3B). Thus, the shMyb knockdown model in *Irf4/8*$^{-/-}$ large pre-B cells behaves similar to a hypomorphic c-Myb mutant and is consistent with results obtained with c-Myb hypomorphic mutations that are viable but have a less drastic phenotype than *Myb* null

Figure 4.3. c-Myb knockdown in *Irf4/8*$^{-/-}$ large pre-B cells leads to decreased cell recovery. *Irf4/8*$^{-/-}$ large pre-B cells were transduced with shLuc-GFP or shMyb-GFP cultured with 10ng/ml IL-7. **(A)** GFP^{+} cells were electronically sorted at 72 h post-transduction and knockdown efficiency of c-Myb protein was analyzed by Western blot. β-Actin was used as a loading control. Representative of 3 independent experiments. **(B)** Total numbers of GFP^{+} cells was analyzed every 24 h post-transduction over a 120 h time course by flow cytometry. Relative recovery was determined as described in Figure 4.2A. All retrovirus transductions were performed with three replicates per condition. *$p < 0.05$, **$p < 0.005$, ***$p < 0.0005$.

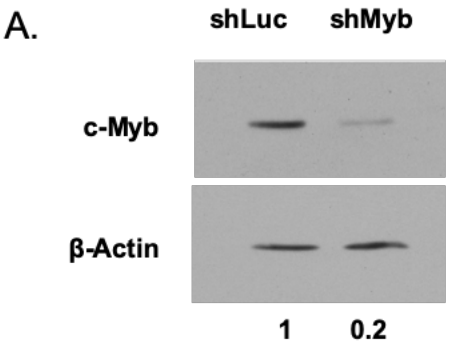
A.
shLuc
shMyb
c-Myb
β-Actin
1
0.2

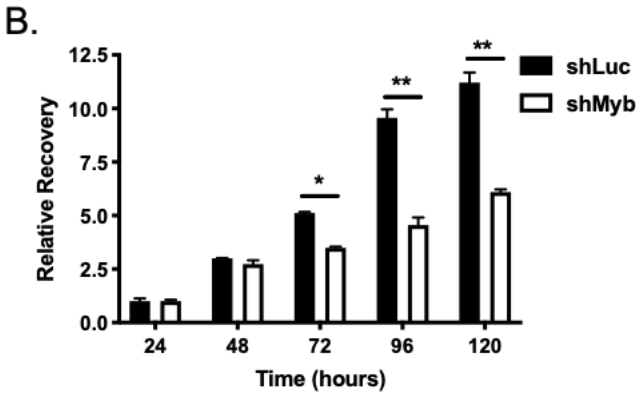
B.
Relative Recovery
12.5
10.0
7.5
5.0
2.5
0.0
24
48
72
96
120
Time (hours)
*
**
**
shLuc
shMyb

mutations (Carpinelli et al., 2004; Sandberg et al., 2005). Taken together, these experiments demonstrate that c-Myb is important for the proliferative expansion of large pre-B cells.

c-Myb is important for pre-B cell survival, proliferation, and accumulation of CD2$^+$ small pre-B cells

Large pre-B cells undergo a limited number of divisions, exit the cell cycle and differentiate into CD2$^+$ small pre-B cells. The deficit in relative recovery that we observed in both the μHC-transduction and *Irf4/8*$^{-/-}$ large pre-B cell models upon loss of c-Myb expression (Figure 4.1B and 4.3B) could be due to increased apoptosis, lack of proliferation, premature differentiation from large to small pre-B cells or all three. To address these questions, we examined the ability of c-Myb deficient μHC-transduced pro-B cells to differentiate into small, CD2$^+$ pre-B cells. *Myb*$^{f/f}$ *Rag2*$^{-/-}$ pro-B cells were transduced with MIG-μHC and 24 h later transduced with tNGFR (control) or tNGFR-Cre (Cre) retroviruses and cultured for an additional 24-72 h (Figure 4.4A). At 24 h, the control μHC-transduced pro-B cells were mostly large pre-B cells, based on FSC, though a small proportion appeared to be small pre-B cells (Figure 4.4A). By 48 and 72 h, the control μHC-transduced pro-B cell population increased the fraction of small pre-B cells. In contrast, the entire population of μHC/Cre transduced pro-B cells was smaller than the control cells 24 h post-transduction. By 48 and 72 h post-transduction the vast majority of μHC/Cre transduced pro-B cells were small. Furthermore, by 72 h post-transduction the μHC/Cre transduced cells displayed lower FSC than the control μHC-transduced pro-B cells. Thus, the μHC/Cre transduced pro-B cell population failed to maintain a large pre-B cell population. In addition, while control μHC transduced pro-B cells decreased in cell size, as measured by forward scatter (FSC), they also gradually acquired expression of the small pre-B cell marker CD2 over the 72 h time course. In contrast, the μHC/Cre transduced pro-B cell population contained a higher proportion of CD2$^+$ cells at 48 and 72 h although the relative recovery of μHC/Cre transduced pro-

B cells was much smaller at these time points (Figure 4.4A), suggesting the possibility that the c-Myb deficient population quickly differentiated into small $CD2^+$ pre-B cells. To determine if the floxed *Myb* locus was deleted in the $CD2^+$ μHC/Cre-transduced pro-B cell population, we electronically sorted the $CD2^+$ and $CD2^-$ populations and measured the deletion efficiency at the $Myb^{f/f}$ loci by PCR as we have previously described (Bender et al., 2004; Thomas et al., 2005). Deletion at the $Myb^{f/f}$ locus was very efficient (92%) in the $CD2^-$ fraction (Figure 4.4B). In contrast, deletion efficiency was poor (13%) in the $CD2^+$ fraction, demonstrating a strong selection against loss of the floxed *Myb* allele in the $CD2^+$ fraction, suggesting that c-Myb deficient large pre-B cells fail to transit to or survive in the $CD2^+$ small pre-B cell fraction.

To better understand the nature of the defect in μHC-transduced pro-B cells, we measured apoptotic cell death by flow cytometry to detect active Caspase 3^+ cells using our two model systems. Loss of c-Myb in μHC-transduced pro-B cells resulted in a 2 to 3-fold increase in the proportion of active Caspase 3^+ cells 24 and 48 h after tNGFR-Cre transduction (Figure 4.5A). Similarly, c-Myb knockdown in $Irf4/8^{-/-}$ large pre-B cells resulted in a 2-fold increase in active Caspase 3^+ cells by 72 h and 96 h post-transduction with shMyb (Figure 4.5B). These data indicated that ablation of c-Myb expression increased pre-B cell death. We also assessed DNA synthesis and DNA content by simultaneously measuring EdU uptake and 7AAD DNA staining. By 24 and 48 h post-transduction, we detected a >80% reduction in the proportion of S-phase μHC-transduced pro-B cells that were actively synthesizing new DNA compared to controls. This result demonstrated a severe defect in proliferation following c-Myb deletion (Figure 4.6A). We also noted an increased number of c-Myb-deficient cells that by DNA content appeared to be in S-phase but did not label with EdU, possibly representing cells that have undergone an intra-S-phase cell cycle arrest, which typically occurs due to the activation of a DNA damage checkpoint

Figure 4.4. Defects in proliferation and selection against differentiation of c-Myb-deficient pre-B cells. Pre-B cells were generated by retrovirus transduction of *Myb*^{ff} *Rag2*$^{-/-}$ pro-B cells as described in Figure 4.1. **(A)** Representative histograms of FSC and CD2 expression of co-transduced GFP^{+} NGFR^{+} cells from the 48 h time point of the relative recovery time course in Figure 1B. **(B)** GFP^{+} NGFR^{+} CD2^{+} cells were electronically sorted and deletion efficiency of the floxed *Myb* allele was analyzed by PCR.

\

A.

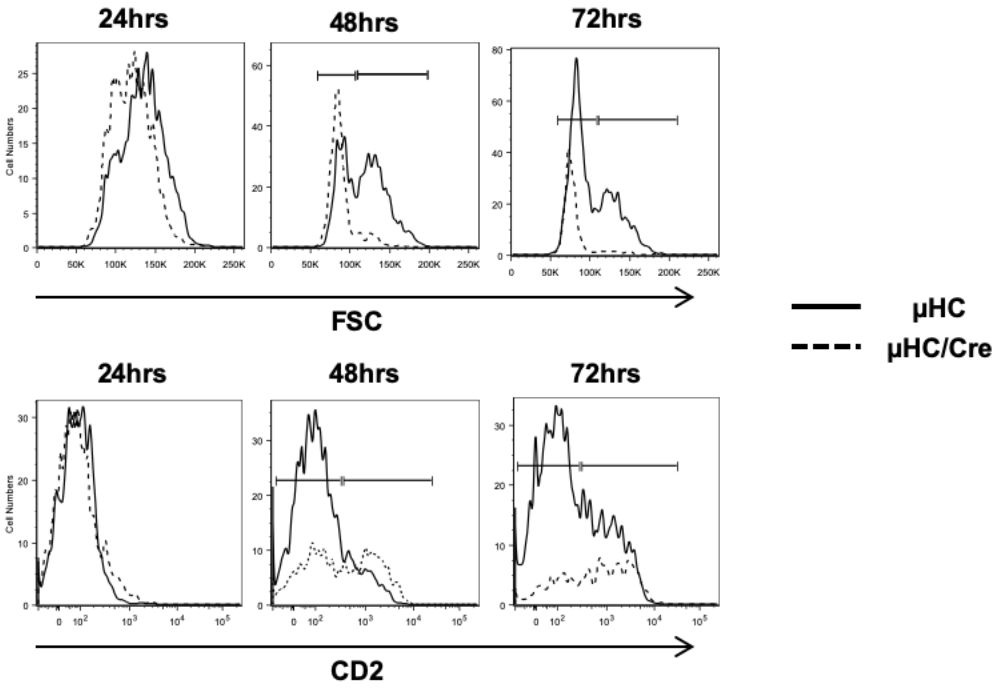
24hrs
48hrs
72hrs
Cell Numbers
FSC
μHC
μHC/Cre
CD2

B.

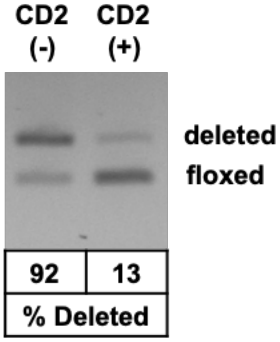
CD2 (-)
CD2 (+)
deleted
floxed
92
13
% Deleted

Figure 4.5. c-Myb deletion in uHC-transduced pro-B cells and knockdown in *Irf4/8*$^{-/-}$ large pre-B cells leads to decreased cell survival. (A) Pre-B cells were generated by retrovirus transduction of *Myb*^{ff} *Rag2*$^{-/-}$ pro-B cells as described in Figure 4.1. Following retrovirus transduction, pre-B cells were cultured with 10ng/ml IL-7 and the proportion of co-transduced GFP^{+} NGFR^{+} active Caspase 3^{+} pre-B cells was analyzed 24 and 48 h post-transduction by flow cytometry. **(B)** *Irf4/8*$^{-/-}$ large pre-B cells were transduced with shLuc-GFP or shMyb-GFP and cultured with 10ng/ml IL-7. The proportion of GFP^{+} active Caspase 3^{+} *Irf4/8*$^{-/-}$ large pre-B cells was analyzed 48, 72, 96, and 120 h post-transduction by flow cytometry. All retrovirus transductions were performed with three replicates per condition. *$p < 0.05$, **$p < 0.005$, ***$p < 0.0005$.

A.

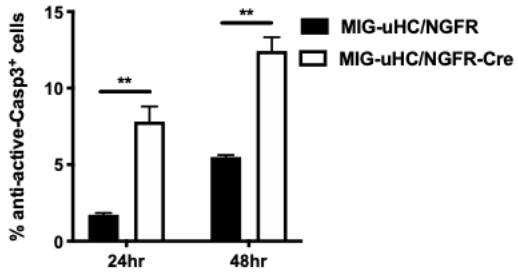
% anti-active-Casp3+ cells
15
10
5
0
**
**
24hr
48hr
MIG-uHC/NGFR
MIG-uHC/NGFR-Cre

B.

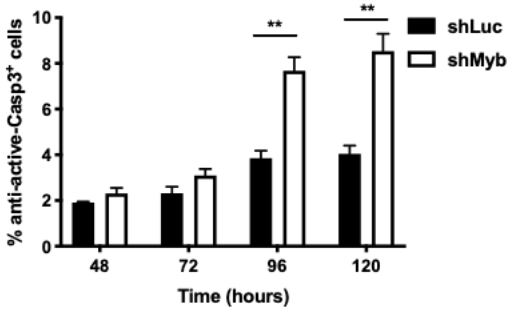
% anti-active-Casp3+ cells
10
8
6
4
2
0
**
**
48
72
96
120
Time (hours)
shLuc
shMyb

(Iyer and Rhind, 2017). In the *Irf4/8*$^{-/-}$ large pre-B cell model, we also detected an approximately 30% reduction in the proportion of S-phase cells that were actively synthesizing new DNA compared to controls at 96 h and 120 h after shMyb transduction (Figure 4.6B). Thus, c-Myb is important for the survival and continued proliferation of large pre-B cells. Taken together, these results suggest that loss of c-Myb in large pre-B cells results in rapid loss of proliferation, cell death, and a failure to transit to the CD2^{+} small pre-B cell compartment.

c-Myb-dependent gene expression changes in large pre-B cells correlate with an Ikaros-dependent pro-differentiation gene signature

We have previously reported that rapid cell death after acute deletion at the *Myb*$^{f/f}$ locus can limit detection of some genes that are regulated by c-Myb (Fahl et al., 2018). To avoid this problem, we compared gene expression in *Irf4/8*$^{-/-}$ large pre-B cells 72 h after transduction with shMyb or shLuc as this is the first time point where we detected a statistically significant decrease in relative recovery of shMyb transduced cells (Figure 4.3B). Results showed that 5,895 genes were significantly changed with a false discovery rate of $p<0.05$, with 2,979 genes having a log2 fold change > 1, and 725 genes that met both of these thresholds (Figure 4.7A). These data demonstrate that loss of c-Myb expression has broad effects on global gene expression which is consistent with other reports (Dias et al., 2017; Quintana et al., 2011a; Zhao et al., 2011). To identify major processes that were impacted by the loss of c-Myb, we performed gene set analysis utilizing KEGG pathway and biological process gene ontology (GO-BP) gene sets and validated a panel of key genes involved in these processes by qRT-PCR (Figure 4.7B). Consistent with our phenotypic data, we identified pathways and processes related to proliferation that were enriched in downregulated genes. These downregulated genes included a number of cyclins and cyclin-dependent kinases (Cdks) that drive cell cycle progression (Figure 4.8A). In particular, we identified *Cdk4* (Cdk4) and its target *Ccnd3* (cyclin D3), which is required for the proliferation of

Figure 4.6. c-Myb deletion in uHC-transduced pro-B cells and knockdown in *Irf4/8*$^{-/-}$ large pre-B cells leads to decreased cell proliferation. (A) Pre-B cells were generated by retrovirus transduction of *Myb*^{ff} *Rag2*$^{-/-}$ pro-B cells as described in Figure 4.1. Following retrovirus transduction, pre-B cells were cultured with 10ng/ml IL-7. At 24 h and 48 h post-transduction pre-B cells were labeled with EdU for 2 h and cell cycle analysis was performed by flow cytometry after staining with the Click-iT Plus EdU reaction cocktail to assess DNA synthesis and 7AAD to assess DNA content. The proportion of GFP^{+} NGFR^{+} S-phase cells was determined at each time point. Representative EdU versus 7AAD plots for each condition and time point are shown. **(B)** *Irf4/8*$^{-/-}$ large pre-B cells were transduced with shLuc-GFP or shMyb-GFP and cultured with 10ng/ml IL-7. At 96 h and 120 h post-transduction *Irf4/8*$^{-/-}$ cells were labeled with EdU for 2 h and cell cycle analysis was performed by flow cytometry after staining with the Click-iT Plus EdU reaction cocktail and 7AAD. The proportion of GFP^{+} S-phase cells was determined at each time point. Representative EdU versus 7AAD plots for each condition and time point are shown. All retrovirus transductions were performed with three replicates per condition. *$p < 0.05$, **$p < 0.005$, ***$p < 0.0005$.

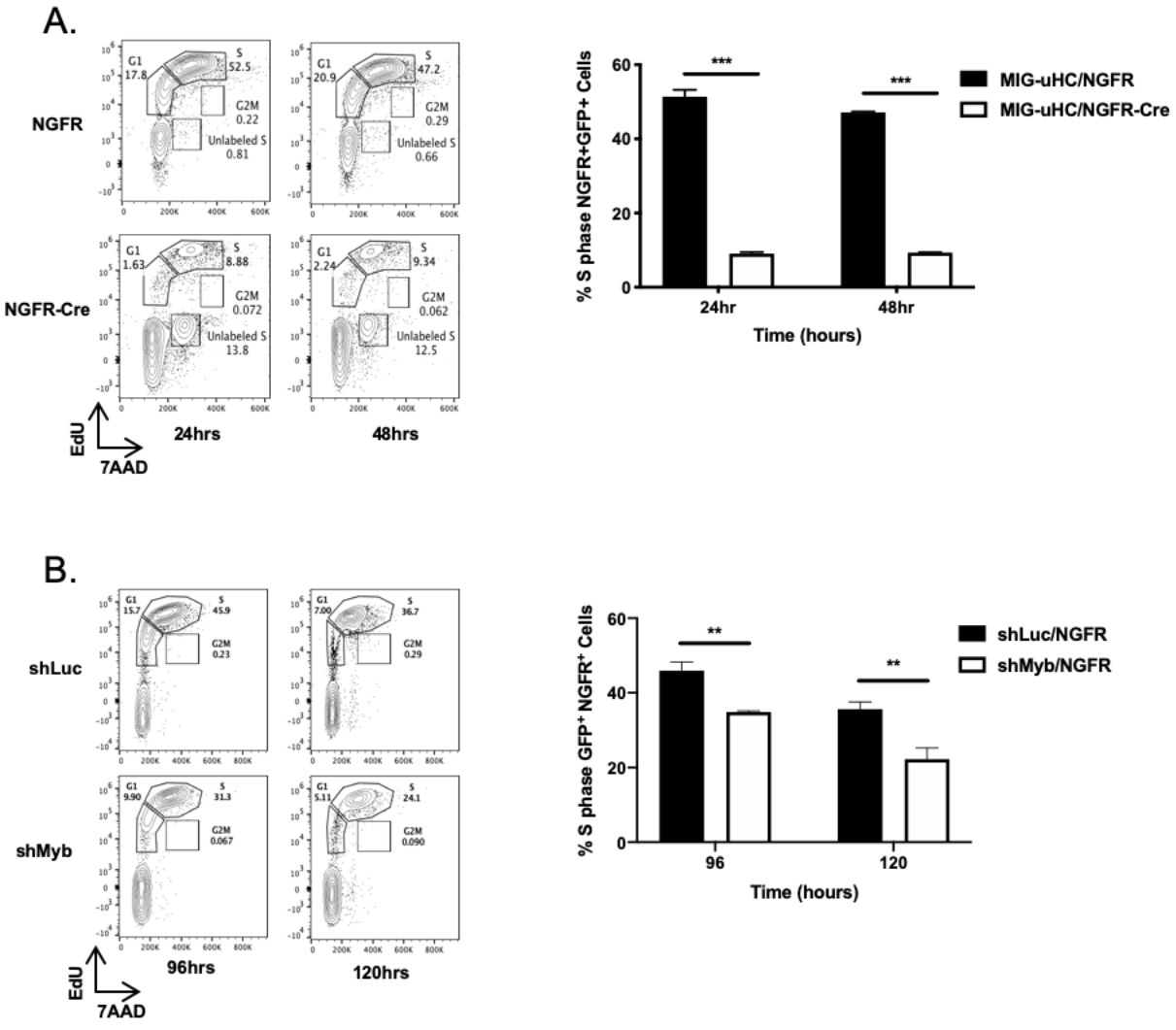
A.
NGFR
NGFR-Cre
G1
17.8
S
52.5
G2M
0.22
Unlabeled S
0.81
G1
20.9
S
47.2
G2M
0.29
Unlabeled S
0.66
G1
1.63
S
8.88
G2M
0.072
Unlabeled S
13.8
G1
2.24
S
9.34
G2M
0.062
Unlabeled S
12.5
EdU
7AAD
24hrs
48hrs
% S phase NGFR+GFP+ Cells
60
40
20
0
***
***
24hr
48hr
Time (hours)
MIG-uHC/NGFR
MIG-uHC/NGFR-Cre
B.
shLuc
shMyb
G1
15.7
S
45.9
G2M
0.23
G1
7.00
S
36.7
G2M
0.29
G1
9.90
S
31.3
G2M
0.067
G1
5.11
S
24.1
G2M
0.090
EdU
7AAD
96hrs
120hrs
% S phase GFP+ NGFR+ Cells
60
40
20
0
**
**
96
120
Time (hours)
shLuc/NGFR
shMyb/NGFR

Figure 4.7. c-Myb-dependent RNA-seq and gene set analysis of shMyb-transduced *Irf4/8*$^{-/-}$ large pre-B cells. *Irf4/8*$^{-/-}$ large pre-B cells were transduced with shLuc-GFP or shMyb-GFP and cultured with 10ng/ml IL-7. At 72 h post-transduction, GFP^{+} cells were electronically sorted and total RNA was prepared for genome-wide gene expression profiling by RNA-seq. **(A)** Volcano plot of differentially expressed (DE) genes displayed as fold change (log2FC; x-axis) versus statistical significance (p-value; y-axis). Each gene is represented as one dot and is colored based on a threshold adjusted p-value (padj) < 0.05 (red), log2FC > 1 (blue), and the genes that satisfy both of these parameters (yellow). **(B)** Gene set analysis of DE genes with a padj < 0.0001 utilizing KEGG pathway and GO-BP ontology gene sets. The analysis was divided between downregulated and upregulated DE genes.

A.

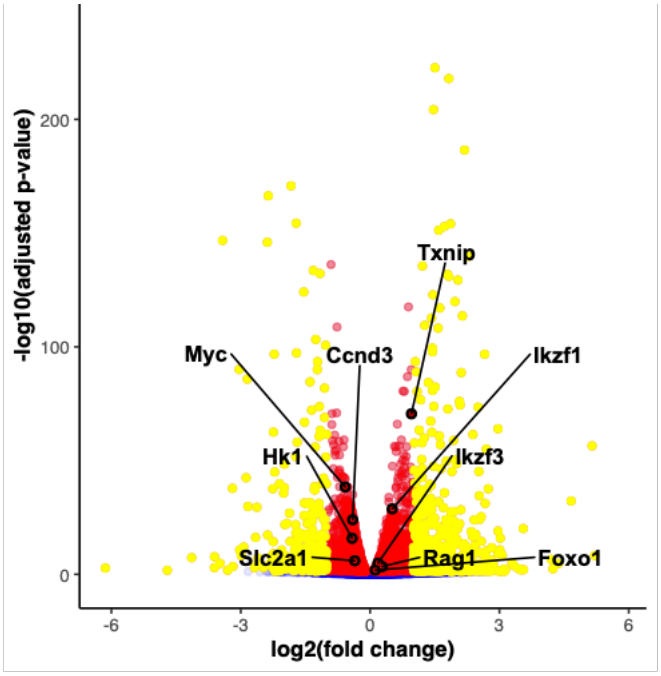
-log10(adjusted p-value)
200
100
0
-6
-3
0
3
6
log2(fold change)
Txnip
Myc
Ccnd3
Ikzf1
Hk1
Ikzf3
Slc2a1
Rag1
Foxo1

B.

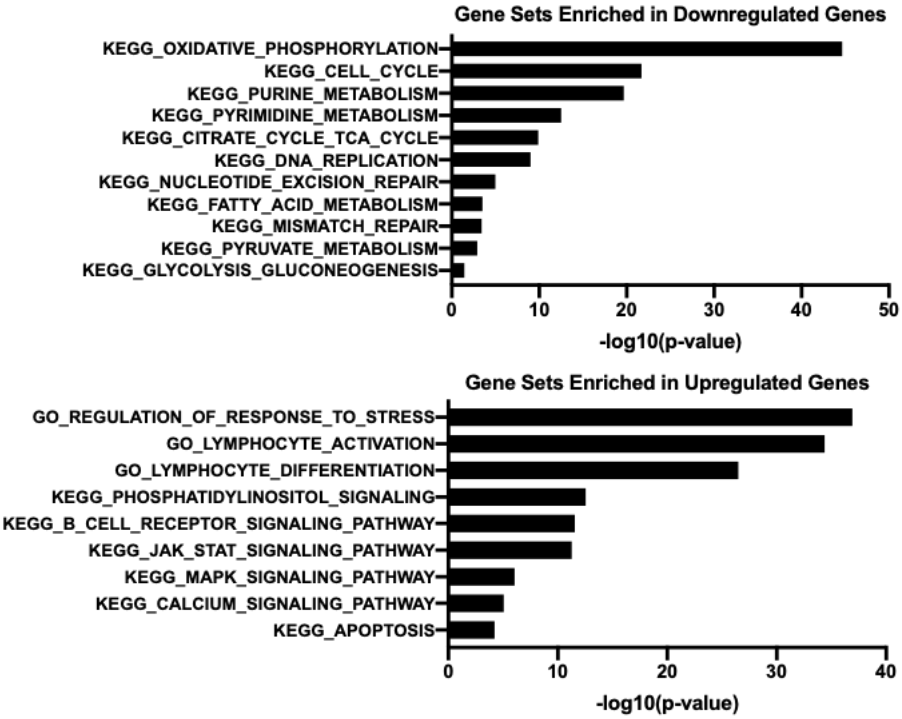
Gene Sets Enriched in Downregulated Genes
KEGG_OXIDATIVE_PHOSPHORYLATION
KEGG_CELL_CYCLE
KEGG_PURINE_METABOLISM
KEGG_PYRIMIDINE_METABOLISM
KEGG_CITRATE_CYCLE_TCA_CYCLE
KEGG_DNA_REPLICATION
KEGG_NUCLEOTIDE_EXCISION_REPAIR
KEGG_FATTY_ACID_METABOLISM
KEGG_MISMATCH_REPAIR
KEGG_PYRUVATE_METABOLISM
KEGG_GLYCOLYSIS_GLUCONEOGENESIS
0
10
20
30
40
50
-log10(p-value)
Gene Sets Enriched in Upregulated Genes
GO_REGULATION_OF_RESPONSE_TO_STRESS
GO_LYMPHOCYTE_ACTIVATION
GO_LYMPHOCYTE_DIFFERENTIATION
KEGG_PHOSPHATIDYLINOSITOL_SIGNALING
KEGG_B_CELL_RECEPTOR_SIGNALING_PATHWAY
KEGG_JAK_STAT_SIGNALING_PATHWAY
KEGG_MAPK_SIGNALING_PATHWAY
KEGG_CALCIUM_SIGNALING_PATHWAY
KEGG_APOPTOSIS
0
10
20
30
40
-log10(p-value)

large pre-B cells. We also detected decreased mRNA expression of the transcription factor c-Myc, which is important both to promote transcription of cell cycle genes as well as repress transcription of cell cycle inhibitors. In particular, the cell cycle inhibitor and c-Myc target *Cdkn1b* (p27 or Kip1) was upregulated in our analysis (Cooper et al., 2006; Habib et al., 2007; Ma et al., 2010). Interestingly, we also found that downregulated genes were enriched in metabolic pathways and processes needed to maintain cell growth and division (Figure 4.8B and C). In particular, expression of the glucose transporter *Slc2a1* (Glut1), and the hexokinase isoform *Hk1* (HK1), which mediates the initial step of glucose processing in the cell, were significantly decreased. In addition, expression of the Glut1 inhibitor *Txnip* (thioredoxin interacting protein) was significantly increased upon loss of c-Myb. *Txnip* inhibits transcription of Glut1 mRNA and promotes Glut1 internalization and proteasomal degradation, suggesting that c-Myb controls the initial steps of glucose metabolism in large pre-B cells (Vander Heiden et al., 2001; Rathmell et al., 2003). Consistent with this notion, downregulated genes were significantly enriched in metabolic pathways downstream of glucose uptake that utilize products of glucose catabolism. These metabolic pathways included glycolysis, biosynthesis of macromolecules such as nucleic acids and fatty acids, and the production of pyruvate which feeds into the TCA cycle and mitochondrial oxidative phosphorylation (Lunt and Vander Heiden, 2011). Thus, analysis of gene sets enriched in downregulated genes suggests that c-Myb might have a previously unappreciated role in the regulation of glucose metabolism. This role would be particularly significant in large pre-B cells, which rely heavily on glucose to fuel their rapid proliferation, and thus is likely to be important to the phenotype of c-Myb-deficient large pre-B cells.

Pathways and processes related to cell stress and apoptosis and, interestingly to B cell activation and/or differentiation including BCR signaling, MAPK signaling, PI3K signaling, and

calcium flux were enriched in upregulated genes (Figure 4.8D). Notably, key genes associated with differentiation from large to small pre-B cells were upregulated including *Foxo1* and *Rag1* (Figure 4.9A), which are important for the initiation of VJ recombination. In addition, the transcription factor *Irf4* and its downstream targets *Ikzf1* and *Ikzf3* (Figure 4.9A), which mediate many of the gene expression changes needed for the large to small pre-B cell transition were upregulated. Furthermore, we detected increased expression of *Sh2b3,* which is a direct Ikaros target gene that inhibits IL-7R signaling through interaction with the proximal kinase Jak3 (Cheng et al., 2016; Clark et al., 2014; Ferreirós-Vidal et al., 2013; Ge et al., 2016). Overall, the results of gene set analysis suggest that shMyb-transduced large pre-B cells are receiving opposing signals from the downregulation of genes involved in cell growth, proliferation, and metabolism, which typically accompany differentiation to small pre-B cells, and the upregulation of genes promoting cell activation, which would typically increase these same cell growth and proliferation pathways. As we also observe upregulation of cell stress and apoptosis associated genes, these results suggest that a failure to reconcile conflicting gene expression changes might increase cell stress and, if unresolved, could ultimately result in cell death.

Our RNA-seq differential gene expression data and gene set analysis suggested that c-Myb expression is important for maintaining the expression of genes involved in proliferation and metabolism while suppressing the expression of genes involved in transition to the small pre-B cell stage such as the transcription factors Irf4, Ikaros, and Aiolos that were upregulated upon *Myb* knockdown. Downstream of pre-BCR signaling, Irf4 induces expression of Ikaros and Aiolos that mediate gene expression changes important for the large to small pre-B cell transition. In particular, Ikaros and Aiolos-mediated gene expression changes lead to decreased metabolism, exit from the cell cycle, and initiation of changes in chromatin structure necessary for VJ

Figure 4.8. Gene set enrichment of c-Myb-dependent differentially expression genes (MDGs) in large pre-B cells. c-Myb-dependent gene expression changes in large pre-B cells were identified by RNA-seq of *Irf4/8*$^{-/-}$ large pre-B cells after shMyb transduction as described in Fig. 4. Differential expression of genes identified from gene set analysis described in Fig. 4B in the Cell_Cycle **(A),** Glycolysis_Gluconeogenesis **(B),** and Oxidative_Phosphorylation **(C)** KEGG pathway gene sets and the Lymphocyte_Differentiation **(D)** GO gene set is shown. Genes upregulated upon c-Myb knockdown are shown in black and genes downregulated upon c-Myb knockdown are shown in red.

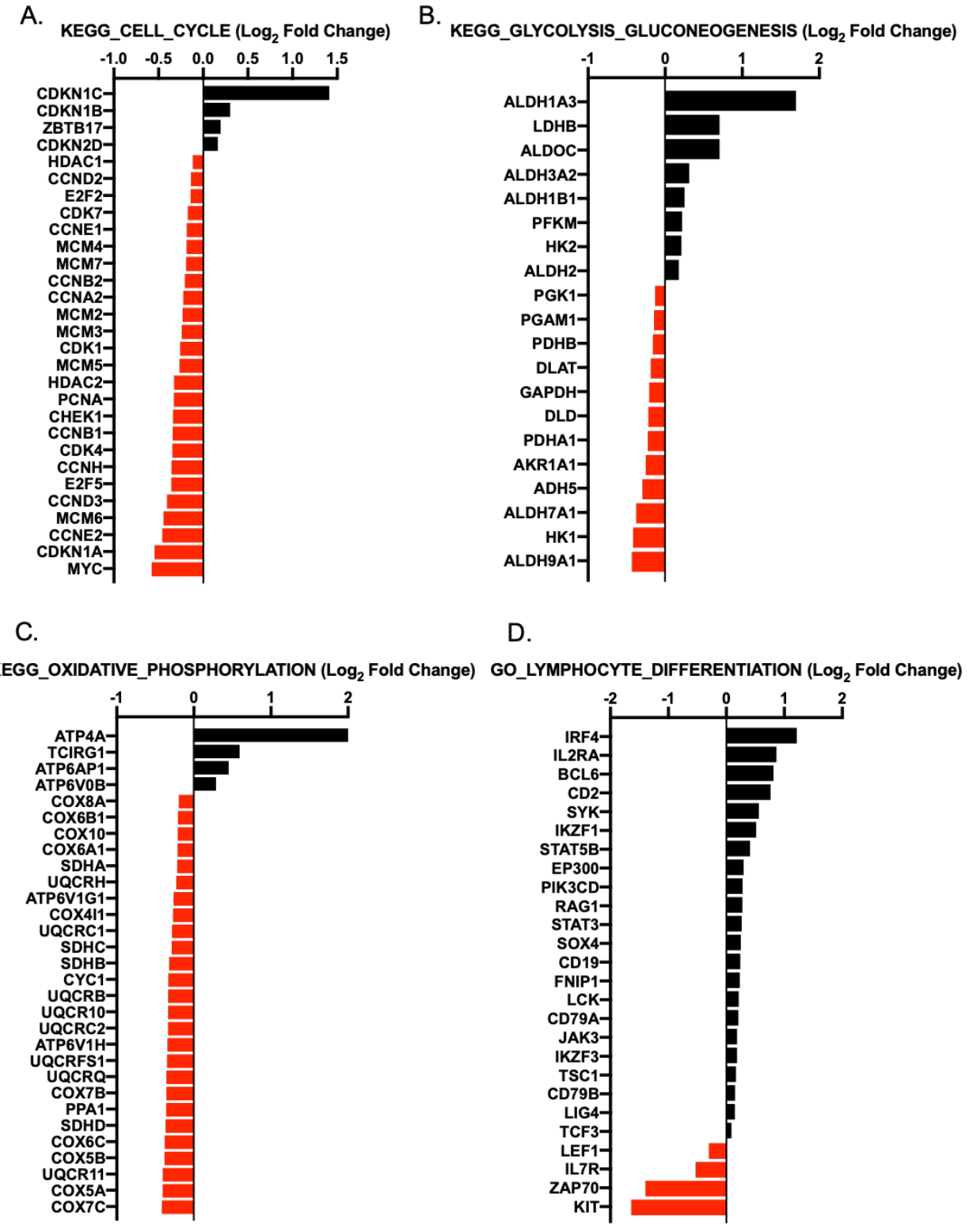
A.
KEGG_CELL_CYCLE (Log2 Fold Change)
-1.0 -0.5 0.0 0.5 1.0 1.5
CDKN1C
CDKN1B
ZBTB17
CDKN2D
HDAC1
CCND2
E2F2
CDK7
CCNE1
MCM4
MCM7
CCNB2
CCNA2
MCM2
MCM3
CDK1
MCM5
HDAC2
PCNA
CHEK1
CCNB1
CDK4
CCNH
E2F5
CCND3
MCM6
CCNE2
CDKN1A
MYC
B.
KEGG_GLYCOLYSIS_GLUCONEOGENESIS (Log2 Fold Change)
-1 0 1 2
ALDH1A3
LDHB
ALDOC
ALDH3A2
ALDH1B1
PFKM
HK2
ALDH2
PGK1
PGAM1
PDHB
DLAT
GAPDH
DLD
PDHA1
AKR1A1
ADH5
ALDH7A1
HK1
ALDH9A1
C.
KEGG_OXIDATIVE_PHOSPHORYLATION (Log2 Fold Change)
-1 0 1 2
ATP4A
TCIRG1
ATP6AP1
ATP6V0B
COX8A
COX6B1
COX10
COX6A1
SDHA
UQCRH
ATP6V1G1
COX4I1
UQCRC1
SDHC
SDHB
CYC1
UQCRB
UQCR10
UQCRC2
ATP6V1H
UQCRFS1
UQCRQ
COX7B
PPA1
SDHD
COX6C
COX5B
UQCR11
COX5A
COX7C
D.
GO_LYMPHOCYTE_DIFFERENTIATION (Log2 Fold Change)
-2 -1 0 1 2
IRF4
IL2RA
BCL6
CD2
SYK
IKZF1
STAT5B
EP300
PIK3CD
RAG1
STAT3
SOX4
CD19
FNIP1
LCK
CD79A
JAK3
IKZF3
TSC1
CD79B
LIG4
TCF3
LEF1
IL7R
ZAP70
KIT

Figure 4.9. c-Myb-dependent gene expression changes in *Irf4/8*$^{-/-}$ large pre-B cells correlate with an Ikaros-dependent gene signature. RNA-seq analysis of shMyb-transduced *Irf4/8*$^{-/-}$ large pre-B cells was performed as described in Figure 4.7. **(A)** qRT-PCR validation of selected DE genes from GFP^{+} *Irf4/8*$^{-/-}$ cells electronically sorted at 72 h post-transduction. Gene expression was normalized to expression of *HPRT* and genes were analyzed in triplicate per condition. *$p < 0.05$, **$p < 0.005$, ***$p < 0.0005$. **(B)** Heatmap depicting merged gene signatures of DE genes from shLuc/shMyb transduced *Irf4/8*$^{-/-}$ large pre-B cells and direct Ikaros targets differentially expressed at the large to small pre-B cell transition as reported by Ferreiros-Vidal et al. (2013). The overlap in genes that are downregulated or upregulated in both the c-Myb-dependent and Ikaros-dependent gene signatures are indicated by black boxes.

A.

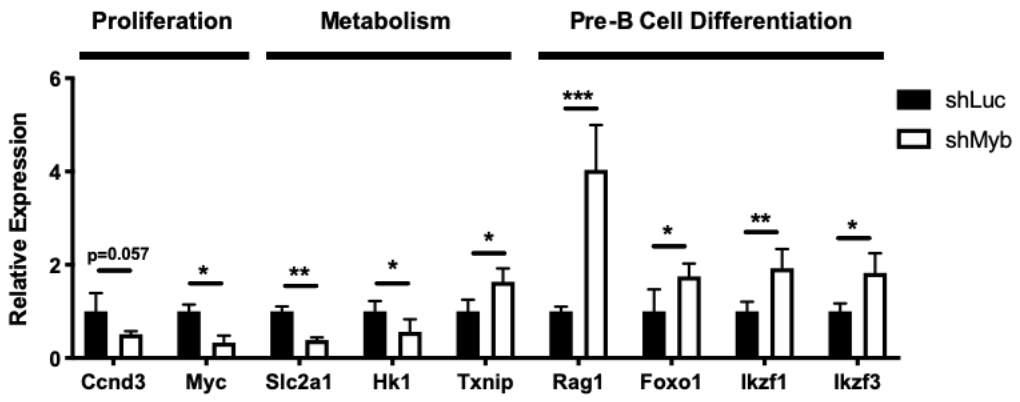
Proliferation
Metabolism
Pre-B Cell Differentiation
Relative Expression
6
4
2
0
shLuc
shMyb
p=0.057
*
**
*
*
***
*
**
*
Ccnd3
Myc
Slc2a1
Hk1
Txnip
Rag1
Foxo1
Ikzf1
Ikzf3

B.

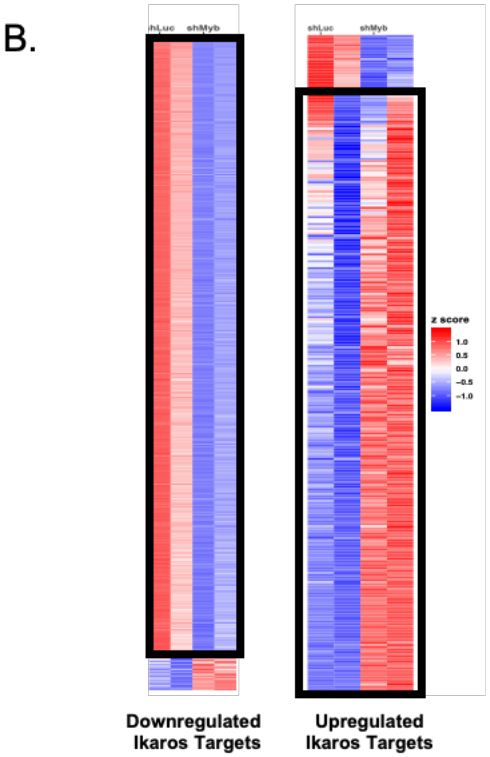
shLuc
shMyb
z score
1.0
0.5
0.0
−0.5
−1.0
Downregulated Ikaros Targets
Upregulated Ikaros Targets

recombination at the IgL locus (Georgopoulos, 2017). Thus, c-Myb-mediated repression of Ikaros and Aiolos expression could be responsible for many of the gene expression changes related to proliferation, metabolism, and differentiation we detect upon c-Myb knockdown in large pre-B cells. In fact, comparison of c-Myb-dependent differentially expressed genes with a published Ikaros footprint revealed that approximately 70% of the direct Ikaros targets that are important for the large to small pre-B cell transition were also changed by c-Myb knockdown (Figure 4.9B) (Ferreirós-Vidal et al., 2013). Among the c-Myb and Ikaros co-regulated genes were those we had already identified as genes that have crucial roles in the proliferation (*Ccnd3* and *Myc*), metabolism (*Slc2a1* and *Txnip*), and differentiation (*Foxo1* and *Sh2b3*) of large pre-B cells. This result suggests the failure to repress Ikaros and Aiolos expression in c-Myb-deficient large pre-B cells could lead to decreased metabolism, decreased proliferation, and trigger the implementation of a gene expression program promoting differentiation into small pre-B cells.

c-Myb is critical for large pre-B cell glucose uptake and hexokinase activity

The increased biosynthetic demands of large pre-B cells are predominantly met by increased glucose uptake and processing through glycolysis, which provides critical intermediates for the production of macromolecules needed for cell division (Lunt and Vander Heiden, 2011). Our RNA-seq gene set analysis suggested that c-Myb knockdown in large pre-B cells would result in substantial defects in glucose metabolism. In particular, mRNA expression of Glut1 (*Slc2a1*) and hexokinase 1 (*Hk1*) were significantly decreased upon loss of c-Myb (Figure 4.9A). Failure to take up and phosphorylate sufficient glucose due to loss of Glut1 and Hk1 expression would preclude glucose utilization in downstream metabolic pathways. To determine whether c-Myb is important for glucose uptake in large pre-B cells, we transduced *Irf4/8*$^{-/-}$ large pre-B cells with shLuc or shMyb and 72 h later incubated them with the fluorescent glucose analog, 2-deoxy-2-

[(7-nitro-2,1,3-benzoxadiazol-4-yl) amino]-D-glucose (2-NBDG) (Figure 4.10A). By 72 h post-transduction, the time point at which we begin to detect a significant decrease in relative recovery of shMyb transduced *Irf4/8*$^{-/-}$ large pre-B cells, we detected an approximately 50% decrease in 2-NBDG uptake. Thus, this result suggested that the c-Myb-dependent decrease in Glut1 mRNA expression resulted in decreased glucose transport into the cell. To determine if c-Myb is also important for glucose processing, we measured hexokinase activity of shMyb-transduced *Irf4/8*$^{-/-}$ large pre-B cells and found, similar to glucose uptake, that c-Myb knockdown resulted in a 50% decrease in overall hexokinase activity by 72 h post-transduction (Figure 4.10B). Thus, c-Myb is important for maintaining expression of critical upstream components of glucose metabolism involved in glucose uptake (Glut1) and utilization (Hk1) in large pre-B cells.

Expression of Glut1 or Hk1 rescues relative recovery and survival of c-Myb-deficient large pre-B cells

To determine the contribution of c-Myb mediated regulation of glucose uptake/utilization to the *Myb*-dependent large pre-B cell phenotype, *Irf4/8*$^{-/-}$ large pre-B cells were co-transduced with GFP-shLuc or GFP-shMyb and either tNGFR (control), tNGFR-Glut1 or tNGFR-Hk1 and the relative recovery of shMyb^{+} NGFR^{+} cells was determined over a 96 h time course (Figure 4.11A). Expression of exogenous Glut1 had little effect on the relative recovery of c-Myb sufficient cells (shLuc/Glut1) (Figure 4.11B). However, Glut1 rescued the relative recovery of *Irf4/8*$^{-/-}$ large pre-B cells 72 h post-transduction such that the recovery of shMyb/Glut1 transduced cells was comparable to control, shLuc/NGFR transduced cells. Thus, increasing the capacity of *Irf4/8*$^{-/-}$ large pre-B cells to take up glucose after c-Myb knockdown is sufficient to restore their relative recovery.

Transduction with Hk1 increased the relative recovery of c-Myb-sufficient (shLuc/tNGFR) *Irf4/8*$^{-/-}$ large pre-B cells by approximately 1.5-fold suggesting that Hk1 overexpression increased

the efficiency of glucose utilization resulting in increased relative recovery of *Irf4/8*$^{-/-}$ large pre-B cells (Figure 4.11C). This is consistent with the high affinity of Hk1 for glucose and greater activity as compared to other hexokinase isoforms (Wilson, 2003). Importantly, expression of exogenous Hk1 increased recovery of *Irf4/8*$^{-/-}$ large pre-B cells after c-Myb knockdown (shMyb/HK1) to a level comparable to that of shLuc/tNGFR or shLuc/Hk1 transduced control cells. Thus, forced expression of the key mediators of glucose uptake and utilization, Glut1 and Hk1, completely rescued the relative recovery resulting from c-Myb knockdown in *Irf4/8*$^{-/-}$ large pre-B cells. In addition, the increased relative recovery induced by exogenous Hk1 expression as compared to Glut1 expression suggests that Hk1 activity is the limiting factor in the ability of large pre-B cells to utilize glucose. Overall, this result indicates that c-Myb-dependent regulation of glucose uptake and utilization through hexokinase activity are crucial to maintain the large pre-B cell compartment.

In addition to fueling metabolism and proliferation, glucose uptake and utilization through hexokinase activity is critical for cell survival (Majewski et al., 2003; Rathmell et al., 2003). Hk1 associates with mitochondria and interferes with binding of pro-apoptotic Bcl-2 family members, maintains mitochondrial membrane integrity, and prevents the release of cytochrome c associated with apoptosis in the FL5.12 lymphoid cell line. To determine if exogenously supplied Glut1 or Hk1 could decrease apoptosis in *Irf4/8*$^{-/-}$ large pre-B cells after c-Myb knockdown, the proportion of active Caspase 3^{+} cells was assessed in *Irf4/8*$^{-/-}$ large pre-B cells 96 h after co-transduction (Figure 4.12). While *Irf4/8*$^{-/-}$ large pre-B cells transduced with Glut1 decreased the proportion of active Caspase 3^{+} cells after c-Myb knockdown to a proportion comparable to control cells (GFP/tNGFR), expression of Hk1 resulted in an even further decrease in active Caspase 3^{+} cells.

Figure 4.10. c-Myb knockdown leads to defects in *Irf4/8*$^{-/-}$ large pre-B cell glucose uptake and hexokinase activity. *Irf4/8*$^{-/-}$ large pre-B cells were transduced with NGFR or NGFR-shMyb **(A)** or shLuc-GFP or shMyb-GFP **(B)** and cultured for 72 h with 10ng/ml IL-7. **(A)** At 72 h post-transduction, NGFR^{+} cells were incubated 30 min with the 2-NBDG glucose uptake mix and 2-NBDG MFI was measured by flow cytometry. The glucose uptake inhibitor phloretin was used as a negative control for 2-NBDG uptake. **(B)** At 72 h post-transduction GFP^{+} cells were electronically sorted and protein lysate was prepared for analysis of hexokinase enzymatic activity. Enzyme activity was determined by colorimetric assay and absorbance at 492nm. All retrovirus transductions were performed with three replicates per condition. N = 3, *$p < 0.05$, **$p < 0.005$, ***$p < 0.0005$.

A.

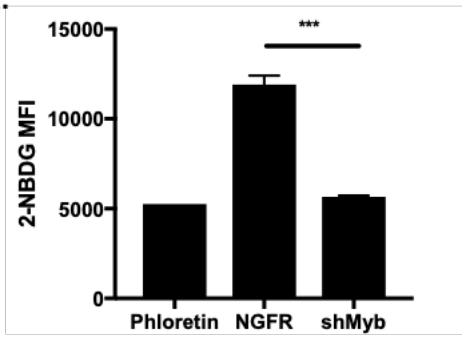
15000
10000
5000
0
2-NBDG MFI
***
Phloretin
NGFR
shMyb

B.

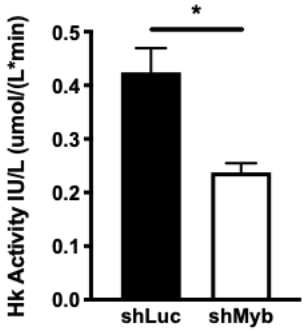
0.5
0.4
0.3
0.2
0.1
0.0
Hk Activity IU/L (umol/(L*min)
*
shLuc
shMyb

Figure 4.11. Expression of Glut1 or Hk1 rescues recovery of c-Myb-deficient *Irf4/8*$^{-/-}$ large pre-B cells. (A) Experimental design used to determine the role of Glut1 and Hk1 expression in large pre-B cells. *Irf4/8*$^{-/-}$ large pre-B cells were co-transduced with shLuc-GFP or shMyb-GFP and NGFR, NGFR-Glut1, or NGFR-Hk1 and cultured with 10ng/ml IL-7. Every 24 h post-transduction over a 96 h time course, co-transduced GFP^{+} NGFR^{+} cells were analyzed for total cell numbers and at 96 h post-transduction they were analyzed for cell survival. **(B&C)** Co-transduced GFP^{+} NGFR^{+} cells were analyzed at 24, 48, 72, and 96 h post-transduction by flow cytometry and relative recovery was determined as described in Figure 1. The numbers of shLuc/shMyb-GFP^{+} cells co-transduced with the NGFR empty vector control were compared to co-transduction with NGFR-Glut1 **(B)** or NGFR-Hk1 **(C).**

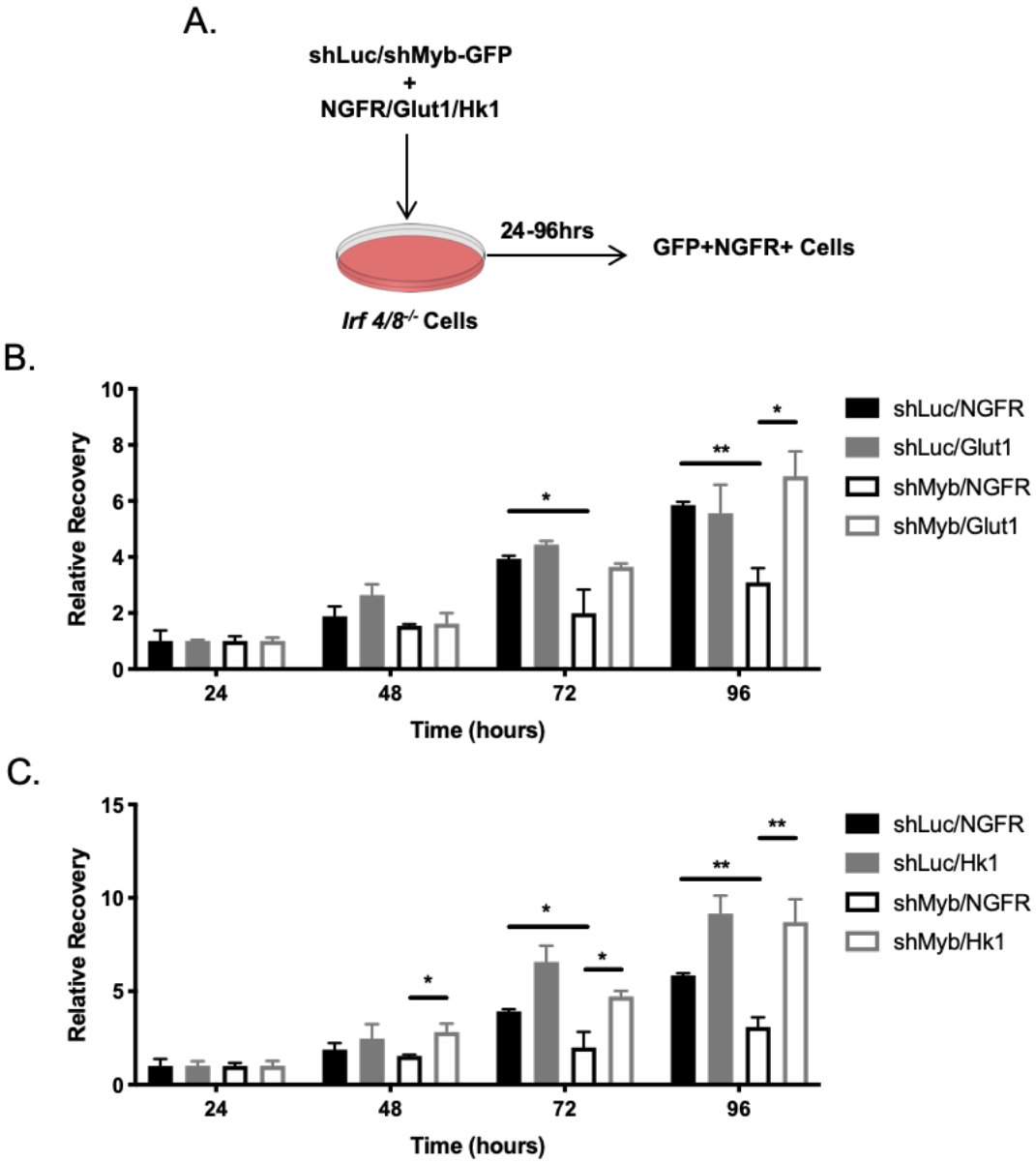
A.
shLuc/shMyb-GFP
+
NGFR/Glut1/Hk1
24-96hrs
GFP+NGFR+ Cells
Irf 4/8-/- Cells
B.
Relative Recovery
Time (hours)
24
48
72
96
shLuc/NGFR
shLuc/Glut1
shMyb/NGFR
shMyb/Glut1
C.
Relative Recovery
Time (hours)
shLuc/NGFR
shLuc/Hk1
shMyb/NGFR
shMyb/Hk1

Figure 4.12. Expression of Glut1 or Hk1 rescues glucose-dependent survival of c-Myb-deficient *Irf4/8*$^{-/-}$ large pre-B cells. *Irf4/8*$^{-/-}$ large pre-B cells were co-transduced with shLuc-GFP or shMyb-GFP and NGFR, NGFR-Glut1, or NGFR-Hk1 and cultured with 10ng/ml IL-7. The proportion of co-transduced GFP^{+} NGFR^{+} active Caspase 3^{+} cells was analyzed 96h post-transduction by flow cytometry.

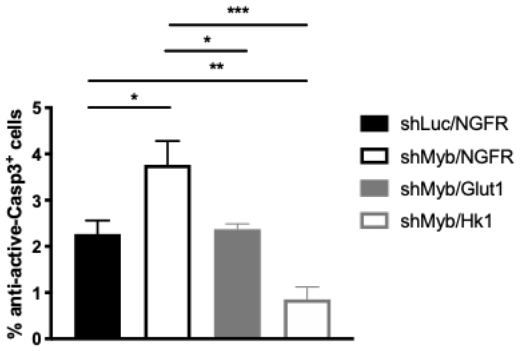
***
*
**
*
% anti-active-Casp3+ cells
0
1
2
3
4
5
shLuc/NGFR
shMyb/NGFR
shMyb/Glut1
shMyb/Hk1

Thus, these results reveal a previously unreported mechanism for c-Myb-dependent survival and, more generally, for large pre-B cell survival through regulation of key mediators of glucose metabolism, Glut1 and Hk1, as exogenous expression of Glut1 and Hk1 rescues large pre-B cell survival after c-Myb knockdown.

Ikaros-dependent and Ikaros-independent functions of c-Myb in large pre-B cells

To transition from cycling large pre-B cells to quiescent small pre-B cells, large pre-B cells exit the cell cycle and significantly decrease metabolic activity (Clark et al., 2014; Reth and Nielsen, 2014). The transcription factor Ikaros and its family member Aiolos mediate most of the gene expression changes needed for the large to small pre-B cell transition. We have found, approximately 70% of the Ikaros targets important for this transition were also differentially expressed upon c-Myb knockdown in *Irf4/8*$^{-/-}$ large pre-B cells (Figure 4.9B). Many of the gene expression changes induced by both c-Myb knockdown and Ikaros are also critical for mediating the phenotype we have observed in c-Myb-deficient large pre-B cells including decreased proliferation as well as decreased glucose uptake/utilization. Furthermore, we have demonstrated that exogenous expression of genes important for glucose uptake/utilization, Glut1 and Hk1, rescues survival of shMyb-transduced *Irf4/8*$^{-/-}$ large pre-B cells (Figure 4.12). These results suggest that failures to repress Ikaros expression in c-Myb-deficient large pre-B cells could account for the defects in proliferation, metabolism, and survival we have observed upon c-Myb knockdown. Therefore, we determined whether inhibition of Ikaros activity could rescue defects in recovery of large pre-B cells after c-Myb knockdown.

Ikaros undergoes alternative splicing to produce isoforms with variable DNA binding capability. Isoforms of Ikaros that are unable to bind DNA have a dominant negative effect on Ikaros function (Molnár and Georgopoulos, 1994; Sun et al., 1996). To determine if repression of

Ikaros and Aiolos could rescue the decreased relative recovery that we observed upon c-Myb knockdown in *Irf4/8*$^{-/-}$ large pre-B cells, we utilized a DNA binding domain point-mutant of Ikaros (Ik159A), which acts similarly to the naturally occurring dominant negative Ikaros isoforms (Ferreirós-Vidal et al., 2013). *Irf4/8*$^{-/-}$ large pre-B cells were co-transduced with tNGFR/MIG-R1, tNGFR/MIG-IK159A, shMyb/MIG-R1 or shMyb/MIG-Ik159A and the relative recovery of each co-transduced pair was assessed every 24 h over a 96 h time course (Figure 4.13A). Expression of the Ik159A mutant had little or no effect on the relative recovery of c-Myb-sufficient cells (compare tNGFR/MIG-R1 with tNGFR/MIG-Ik159A) while shMyb/MIG-R1 transduction resulted in approximately a 60% and 70% decrease in relative recovery at 72 h and 96 h post-transduction respectively (Figure 4.13B). However, while we did detect a small increase in relative recovery of shMyb/MIG-Ik159A transduced cells, this was not sufficient to fully restore relative recovery to a level comparable to tNGFR/MIG-R1 transduced controls. Thus, inhibition of Ikaros activity using the Ik159A mutant is unable to account for the entire phenotype induced by c-Myb knockdown in *Irf4/8*$^{-/-}$ large pre-B cells, suggesting that there are Ikaros dependent and independent changes in gene expression that contribute to the decreased proliferative expansion in this model.

Failure of the dominant negative Ik159A mutant to fully rescue the relative recovery of shMyb transduced *Irf4/8*$^{-/-}$ large pre-B cells suggested that inhibition of Ikaros activity is insufficient to restore all aspects of the c-Myb-dependent large pre-B cell phenotype. Following this result, we considered 2 major possibilities: 1) Ik159A was not expressed in sufficient amounts to sequester Ikaros, or 2) an Ikaros-independent role for c-Myb in large pre-B cells prevented complete recovery after Ikaros neutralization. To address these possibilities, we determined if Ik159A could restore Ikaros-dependent gene expression changes in large pre-B cells following

Figure 4.13. Expression of Ik159A fails to rescue recovery of c-Myb-deficient *Irf4/8*$^{-/-}$ large pre-B cells. (A) Experimental design used to determine the role of dominant negative mutant Ikaros (Ik159A) expression in large pre-B cells. *Irf4/8*$^{-/-}$ large pre-B cells were co-transduced with NGFR or NGFR-shMyb and MIG-R1 or MIG-Ik159A and cultured with 10ng/ml IL-7. Every 24 h post-transduction over a 96 h time course, co-transduced NGFR^{+} GFP^{+} cells were analyzed for total cell numbers and at 72 h post-transduction gene expression changes were analyze. **(B)** Co-transduced NGFR^{+} GFP^{+} cells were analyzed at 24, 48, 72, and 96 h post-transduction by flow cytometry and relative recovery was determined as described in Figure 1. The numbers of NGFR/NGFR-shMyb^{+} cells co-transduced with the MIG-R1 empty vector control were compared to co-transduction with MIG-Ik159A.

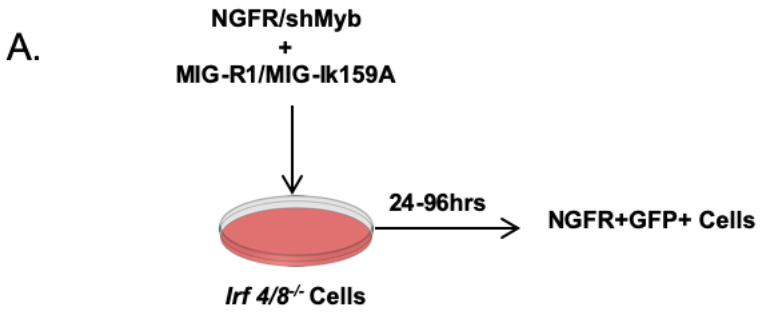
A.
NGFR/shMyb
+
MIG-R1/MIG-Ik159A
24-96hrs
NGFR+GFP+ Cells
Irf 4/8-/- Cells

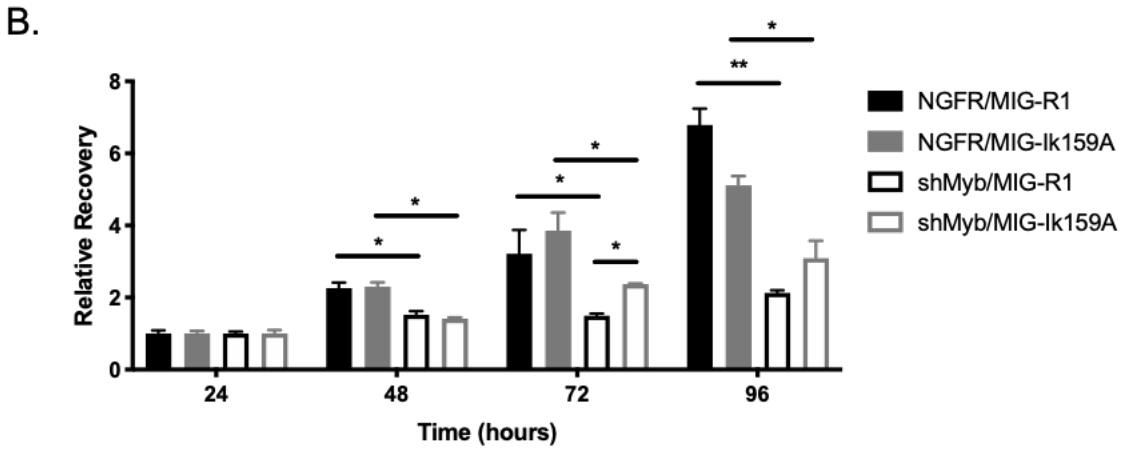
B.
Relative Recovery
0
2
4
6
8
24
48
72
96
Time (hours)
*
*
*
*
*
**
NGFR/MIG-R1
NGFR/MIG-Ik159A
shMyb/MIG-R1
shMyb/MIG-Ik159A

c-Myb knockdown. *Irf4/8*$^{-/-}$ large pre-B cells were co-transduced with tNGFR, tNGFR-shMyb, tNGFR/MIG-Ik159A or shMyb/MIG-Ik159A and both tNGFR^{+} and tNGFR^{+} GFP^{+} cells were electronically sorted at 72 h post-transduction. We then determined mRNA expression of a panel of genes differentially expressed upon c-Myb knockdown in *Irf4/8*$^{-/-}$ large pre-B cells that have been reported to be Ikaros targets. In each case we would expect the Ik159A mutant to reverse expression mediated by Ikaros upon c-Myb knockdown (Figure 4.14A) (Ferreirós-Vidal et al., 2013).

c-Myc mRNA expression was downregulated upon c-Myb knockdown in *Irf4/8*$^{-/-}$ large pre-B cells (Figure 4.14A) and is repressed by direct Ikaros binding (Ma et al., 2010). We found that transduction with the Ik159A mutant resulted in increased *Myc* mRNA expression in c-Myb-sufficient *Irf4/8*$^{-/-}$ large pre-B cells, consistent with a dominant negative function in counteracting Ikaros-mediated repression of *Myc*. Furthermore, co-transduction with shMyb and the Ik159A mutant resulted in a level of *Myc* mRNA expression comparable to the control (c-Myb-sufficient *Irf4/8*$^{-/-}$ cells), indicating that Ik159A is able to inhibit Ikaros function to oppose the decreased expression of *Myc* resulting from c-Myb knockdown and the resultant increase in Ikaros. *Foxo1* and *Txnip* mRNA expression are positively regulated by direct Ikaros binding (Ferreirós-Vidal et al., 2013) and were also upregulated upon c-Myb knockdown in *Irf4/8*$^{-/-}$ large pre-B cells (Figure 4.14A). Transduction with the Ik159A mutant produced the opposite result and resulted in increased *Foxo1* and *Txnip* mRNA expression in c-Myb sufficient *Irf4/8*$^{-/-}$ large pre-B cells. Again, co-transduction with shMyb and the Ik159A mutant resulted in *Foxo1* and *Txnip* mRNA expression comparable to control *Irf4/8*$^{-/-}$ cells. Thus, *Myc, Foxo1* and *Txnip* mRNA appear to be controlled in *Irf4/8*$^{-/-}$ large pre-B cells by Ikaros in a c-Myb dependent fashion, demonstrating that the dominant negative Ik159A was able to reverse c-Myb-dependent gene expression changes in

Irf4/8$^{-/-}$ large pre-B cells. Furthermore, this is in agreement with a previous study (Ferreirós-Vidal et al., 2013) that examined Ikaros dependent gene expression in the mouse B3 pre-B cell line (Figure 4.14B).

As expected, *Slc2a1* (Glut1) expression, which is repressed by direct Ikaros binding (Ferreirós-Vidal et al., 2013, 2019), was also repressed by transduction with shMyb (Figure 4.14A). However, unexpectedly, expression of *Slc2a1* was also repressed after transduction with Ik159A. Furthermore, co-transduction of *Irf4/8*$^{-/-}$ large pre-B cells with both shMyb and Ik159A resulted in a further decrease in Glut1 mRNA expression compared to transduction with shMyb or Ik159A alone. This result is consistent with previous work utilizing the Ik159A mutant to assess Ikaros mediated gene expression in the B3 pre-B cell line, in which transduction with Ik159A also appeared to decrease Glut1 mRNA expression, although it was not statistically significant (Figure 4.14B)(Ferreirós-Vidal et al., 2013). Thus, the unexpected effect of the Ik159A mutant on Glut1 mRNA expression indicates that Ik159A does not exert a dominant negative function in all cases of Ikaros-regulated gene expression.

In contrast to the genes regulated by c-Myb and Ikaros, Hk1 mRNA expression was decreased with c-Myb knockdown, but was unaffected by Ik159A alone or when co-transduced with shMyb, suggesting that *Hk1* is regulated by c-Myb in an Ikaros-independent manner (Figure 4.14A). This is consistent with previous reports that Ikaros has no or little effect on Hk1 expression (Ferreirós-Vidal et al., 2013, 2019) as summarized in Figure 4.14B. Thus, in the context of c-Myb knockdown, restoration of Ikaros-dependent gene expression changes using Ik159A is insufficient to rescue Hk1 expression, demonstrating that c-Myb has both Ikaros dependent and independent effects on genes in large pre-B cells. Taken together, our results demonstrate that c-Myb plays a crucial role in balancing the expression of genes that are important for maintaining the large

Figure 4.14. .Ikaros-dependent and Ikaros-independent gene expression changes mediated by c-Myb in *Irf4/8*$^{-/-}$ large pre-B cells. (A) *Irf4/8*$^{-/-}$ large pre-B cells were co-transduced with NGFR or NGFR-shMyb and MIG-R1 or MIG-Ik159A and cultured with 10ng/ml IL-7. At 72 h post-transduction single-transduced NGFR^{+} and co-transduced NGFR^{+} GFP^{+} cells were electronically sorted and total RNA was prepared for qRT-PCR. Gene expression was normalized to expression of *HPRT* and genes were analyzed in triplicate per condition. **(B)** Microarray differential expression analysis of B3 pre-B cells transduced with pMSCV, IkWT, or Ik159A was performed as described in Ferreiros-Vidal et al, Blood (2013). Log2 fold change values comparing pMSCV empty vector transduced cells to IkWT or Ik159A transduced cells were converted to fold changes with the empty vector control set as 1. Significance was determined by Benjamini-Hochberg adjusted p-value comparing the pMSCV empty vector to fold changes induced by IkWt or Ik159A transduction. *$p < 0.05$, **$p < 0.005$, ***$p < 0.0005$.

A.

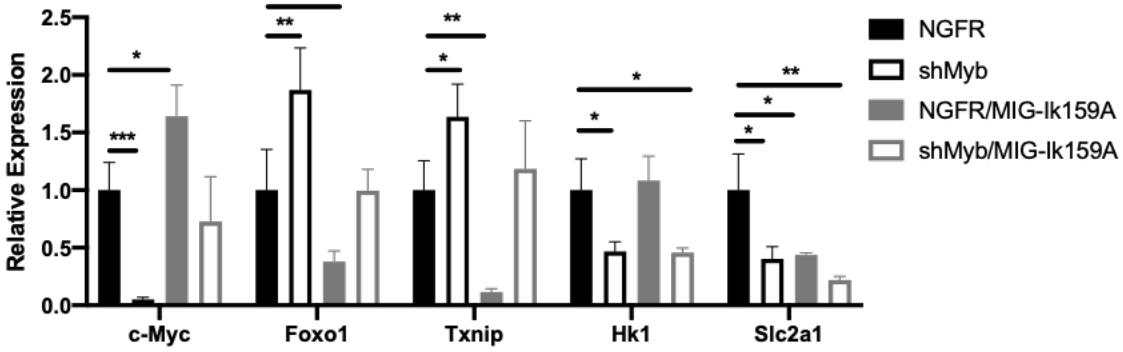
Relative Expression
2.5
2.0
1.5
1.0
0.5
0.0
c-Myc
Foxo1
Txnip
Hk1
Slc2a1
NGFR
shMyb
NGFR/MIG-Ik159A
shMyb/MIG-Ik159A

B.

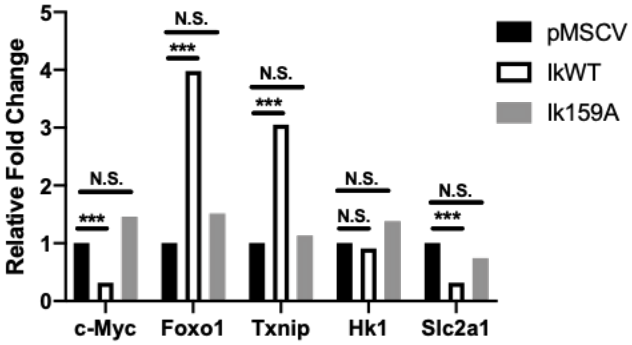
Relative Fold Change
5
4
3
2
1
0
N.S.
c-Myc
Foxo1
Txnip
Hk1
Slc2a1
pMSCV
IkWT
Ik159A

Figure 4.15. c-Myb regulation of glucose metabolism, proliferation, and differentiation in large pre-B cells. c-Myb expression is important for maintaining the large pre-B cell compartment while suppressing premature expression of genes important for quiescence and differentiation into small pre-B cells. c-Myb represses expression of Ikaros and Aiolos, to prevent premature implementation of a pro-differentiation gene expression program important for the large to small pre-B cell transition. c-Myb regulates genes important for proliferation (Ccnd3 and c-Myc), glucose metabolism (Txnip and Glut1), and differentiation (Irf4, Foxo1, Rag1, and the SLC of the pre-BCR) in an Ikaros-dependent manner. As a whole, these gene expression changes prevent premature cell cycle exit, a reduction in metabolic activity, and initiation of VJ recombination, which typically accompany large pre-B cell differentiation. However, inhibition of Ikaros activity is unable to restore all aspects of the c-Myb-dependent large pre-B cell phenotype. c-Myb regulates expression of other genes such as the glycolytic enzyme, Hk1, which is critical for glucose utilization, in an Ikaros-independent manner. Expression of Glut1 or Hk1 was able to restore recovery of c-Myb-deficient large pre-B cells and rescue large pre-B cell survival. Purple symbols/boxes represent downregulated genes and processes and green symbols/boxes represent upregulated genes and processes in c-Myb-deficient large pre-B cells.

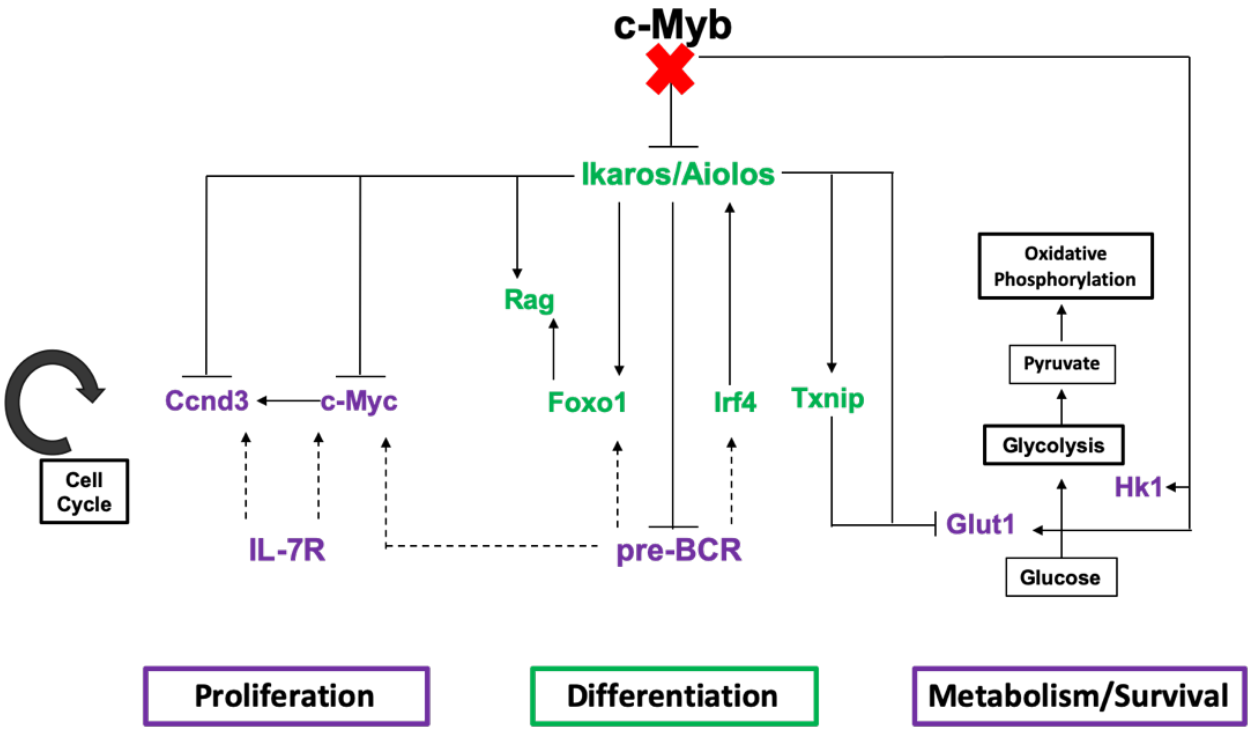
c-Myb
Ikaros/Aiolos
Rag
Foxo1
Irf4
Txnip
Ccnd3
c-Myc
Cell Cycle
IL-7R
pre-BCR
Glut1
Oxidative Phosphorylation
Pyruvate
Glycolysis
Hk1
Glucose
Proliferation
Differentiation
Metabolism/Survival

pre-B cell compartment while suppressing the premature expression of genes that are important for quiescence and differentiation to the small pre-B cell compartment (Figure 4.15).

4.3) Discussion

c-Myb is crucial for pro-B cell survival as well as transition to the large pre-B cell compartment (Fahl et al., 2009; Greig et al., 2010). However, it was not known if c-Myb plays additional roles within the pre-B cell compartment. Rapidly cycling large pre-B cells are dependent on glucose uptake and the production of glycolytic intermediates to facilitate cell division (Stein et al., 2017; Urbanczyk et al., 2018). We demonstrate that c-Myb plays a crucial and unappreciated role in regulating glucose uptake and utilization in the large pre-B cell compartment that is critical to maintain proliferation and prevent apoptosis. c-Myb promotes glucose metabolism in large pre-B cells at the level of both glucose uptake and utilization through hexokinase activity. c-Myb regulates glucose uptake through the glucose transporter Glut1. Loss of c-Myb leads to decreased expression of Glut1 mRNA as well as increased expression of the Glut1 inhibitor Txnip. Txnip has multiple metabolism-related functions including inhibiting Glut1 by promoting its internalization from the plasma membrane to the lysosome and subsequent proteasomal degradation as well as regulating Glut1 mRNA levels (Sullivan et al., 2018; Waldhart et al., 2017; Wu et al., 2013). Downstream of glucose uptake, c-Myb regulates glucose phosphorylation through the glycolytic enzyme Hk1, which mediates the initial step of glucose metabolism, conversion of glucose into glucose-6-phosphate for downstream applications such as glycolysis (Wilson, 2003). c-Myb knockdown in large pre-B cells leads to decreased Hk1 mRNA expression and a significant reduction in overall hexokinase activity. Notably, c-Myb regulation of the initial steps in glucose metabolism is critical for the c-Myb-dependent large pre-B cell phenotype as exogenous expression of Glut1 or Hk1 is able to fully restore recovery of large pre-

B cells after c-Myb knockdown. We further demonstrate that c-Myb represses mRNA expression of Ikaros, which is critical to prevent the premature initiation of a gene expression program that promotes differentiation to the small pre-B cell compartment. Taken together, our results demonstrate an important role for c-Myb in maintaining homeostasis across the pre-BCR checkpoint by controlling key mediators of glucose uptake and utilization while preventing premature differentiation by repressing Ikaros expression (Figure 4.15).

Role of glucose metabolism in large pre-B cell survival

Control of glucose metabolism by c-Myb in large pre-B cells has critical implications for cell survival. Proper glucose metabolism is crucial to maintain mitochondrial integrity and ultimately to prevent apoptotic cell death. In particular, growth factor receptor signaling through Akt has been reported to promote survival of the B3 pre-B cell line and Rat1a fibroblasts through a mechanism dependent on glucose uptake and hexokinase activity (Majewski et al., 2003; Rathmell et al., 2003). The hexokinase isoforms Hk1 and Hk2, also known as mitochondrial hexokinases (mtHk), are able to associate with the outer mitochondrial membrane (Robey and Hay, 2005, 2006). Furthermore, mtHks largely utilize intramitochondrial sources of ATP to catalyze glucose phosphorylation and thus couple glycolysis and oxidative phosphorylation. Akt signaling has been reported to inhibit dissociation of mtHks from the mitochondrial membrane in Rat1a fibroblasts and mtHk dissociation is correlated with an impaired ability of growth factors and Akt to maintain mitochondrial integrity and inhibit apoptosis (Gottlob et al., 2001; Majewski et al., 2004). This survival pathway appears to be independent of Bcl-2 family member expression as mtHk dissociation induces cytochrome c release even in the absence of the pro-apoptotic proteins Bax and Bak (Majewski et al., 2004). Thus, activation of Akt downstream of IL-7R and pre-BCR signaling coordinates large pre-B cell proliferation and survival in a manner dependent on glucose

uptake and hexokinase-mitochondria interaction (Herzog et al., 2009; Majewski et al., 2003, 2004). Our data is consistent with a pro-survival function for mtHKs as we found that in addition to rescuing large pre-B cell relative recovery, exogenous expression of Hk1 also decreased the proportion of active Caspase 3^+ cells (Fig. 6D), indicating that Hk1 reduces apoptosis and promotes survival of large pre-B cells after loss of c-Myb expression. Therefore, while our RNA-seq and gene set analysis did not indicate that expression of Akt was altered by c-Myb knockdown, defects in glucose uptake and hexokinase activity would compromise the ability of Akt to promote large pre-B cell survival. Thus c-Myb-dependent deficiencies in large pre-B cell glucose metabolism are directly linked to defects in cell survival.

Ikaros-dependent and Ikaros-independent functions of c-Myb in large pre-B cells

The transcription factor Ikaros and its family member Aiolos are critical for initiating the pro-differentiation gene expression program and associated decreases in proliferation and metabolic activity that are important for the large to small pre-B cell transition (Heizmann et al., 2013; Ma et al., 2006, 2010). We found that approximately 70% of genes included in a genomic footprint of Ikaros targets important for the large to small pre-B cell transition were also differentially expressed upon c-Myb knockdown in large pre-B cells (Ferreirós-Vidal et al., 2013). Among the genes represented in both the Ikaros footprint and our c-Myb-dependent RNA-seq data were those with roles in proliferation (*Ccnd3* and *Myc*), metabolism (*Slc2a1* and *Txnip*), and differentiation to small pre-B cells (*Foxo1* and *Rag1*). These results suggest that failure to repress Ikaros expression could account for the defects we have observed upon c-Myb knockdown in large pre-B cells. However, we found that expression of a dominant negative Ikaros mutant (Ik159A) failed to rescue recovery of c-Myb-deficient large pre-B cells, suggesting that inhibition of Ikaros activity is unable to account for the entire phenotype induced by c-Myb knockdown and that c-Myb

exhibits an Ikaros-independent role(s) in large pre-B cells. We have demonstrated that expression of the Ik159A mutant restored mRNA expression of c-Myc, Foxo1, and Txnip to the level of c-Myb-sufficient *Irf4/8*$^{-/-}$ large pre-B cell controls indicating that expression of these genes in c-Myb-deficient large pre-B cells is dependent on loss of c-Myb-mediated repression of Ikaros. However, transduction with Ik159A failed to restore mRNA expression of Hk1 and Glut1 in c-Myb-deficient *Irf4/8*$^{-/-}$ large pre-B cells indicating that expression of these genes in c-Myb-deficient large pre-B cells is independent of c-Myb-mediated repression of Ikaros.

Hk1 mRNA expression is not significantly affected by Ikaros activity and, consistent with this, we found that *Hk1* expression was decreased upon c-Myb knockdown, but unaffected by Ik159A (Ferreirós-Vidal et al., 2019). In contrast to Hk1, it has been demonstrated that mRNA expression of Glut1 is repressed by direct Ikaros binding, however, we also found that Glut1 mRNA expression was decreased after transduction with the dominant negative Ik159A mutant and was further decreased after Ik159A/shMyb co-transduction in *Irf4/8*$^{-/-}$ large pre-B cells. It is possible that there was insufficient Ik159A expressed to fully repress Ikaros activity at the *Slc2a1* (Glut1) locus, but this is unlikely as expression of Ik159A was sufficient to inhibit Ikaros activity at other loci (see above). Another possible explanation is that Ik159A transduction was not sufficient to overcome suppression of Glut1 mediated by another c-Myb-dependent factor, however, this is also unlikely as expression of Ik159A decreased mRNA expression of Glut1 in both c-Myb-sufficient and -deficient large pre-B cells. Altogether, the results with Glut1 indicate that the Ik159A mutant does not function as a dominant negative in all cases of Ikaros-regulated gene expression. In addition, our gene expression results following transduction with Ik159A are consistent with a previous study utilizing this dominant negative Ikaros mutant in the B3 pre-B cell line (Ferreirós-Vidal et al., 2013) (Figure 4.14B). Overall, the ability of the Ik159A mutant to

restore certain c-Myb-dependent gene expression changes related to proliferation and differentiation (*Myc, Foxo1, Txnip*) but not others related to glucose uptake/utilization (*Slc2a1, Hk1*) suggests that c-Myb exhibits Ikaros-dependent and Ikaros-independent functions in large pre-B cells.

Role for c-Myb at the large to small pre-B cell transition

c-Myb expression has long been linked with the immature stages of hematopoietic cell differentiation (Zhou and Ness, 2011). Early studies utilizing myeloid and erythroid leukemia cell lines, linked c-Myb with inhibiting differentiation and maintaining proliferation as c-Myb expression was downregulated by chemically induced differentiation, while forced expression of c-Myb inhibited differentiation (Clarke et al., 1988; Hoffman-Liebermann and Liebermann, 1991; McClinton et al., 1990; Pedrazzoli et al., 1989). We have demonstrated that c-Myb has a similar role in large pre-B cells, maintaining them in an immature, proliferating state and inhibiting differentiation as c-Myb-deficient pro-B cells exhibit many of the gene expression changes associated with the large to small pre-B cell transition, including increased expression of the transcription factors Ikaros and Aiolos. At the pre-B cell stage, Ikaros and Aiolos act together to initiate changes in gene expression that are critical for large pre-B cells to exit the cell cycle and differentiate into small pre-B cells (Ma et al., 2008, 2010). Thus, repression of Ikaros and Aiolos expression by c-Myb is consistent with an established role for c-Myb in antagonizing differentiation and promoting proliferation of hematopoietic cells. A role for c-Myb in opposing differentiation from large to small pre-B cells would also suggest that c-Myb and/or c-Myb activity must be decreased or modified to permit differentiation from large to small pre-B cells. Therefore, it will be important to how c-Myb activity is regulated in the small pre-B cell compartment and if c-Myb is effectively altered at the level of transcription or post-translational mechanisms to enable

continued B cell development. We also noted that c-Myb-deficient large pre-B cells exhibited a block in differentiation into $CD2^+$ small pre-B cells, which suggests that c-Myb expression is important to facilitate differentiation into small pre-B cells. However, this differentiation block may also represent enhanced apoptosis due to the Ikaros-independent role for c-Myb in regulating glucose uptake and utilization as well as glucose-dependent survival (see above). In this scenario, despite increasing expression of Ikaros and Aiolos, decreased expression of c-Myb fails to induce large pre-B cell differentiation and rather, leads to cell death. Thus, it is likely that some level of c-Myb expression is required to maintain survival while the shift in pre-BCR signaling that accompanies the large to small pre-B cell transition leads to a sufficient increase in Ikaros expression to overcome c-Myb-mediated repression and thus to permit differentiation.

Role for c-Myb in genomic stability of large pre-B cells

In addition to metabolism, proliferation, and survival, we noted that a number of pathways related to DNA replication and repair were downregulated in our RNA-seq gene set analysis, which suggests that genomic stability may be affected by loss of c-Myb expression in large pre-B cells. This notion is supported by the result of EdU uptake vs. 7AAD staining in the μHC-transduced pro-B cell model, which suggests that c-Myb-deficient large pre-B cells might have undergone intra-S-phase cell cycle arrest due to the activation of a DNA damage checkpoint (Figure 4.6A). In addition, a number of genes with known roles in DNA replication and maintenance of genomic stability are represented in the c-Myb and Ikaros co-regulated gene signature. Among these genes are the maintenance DNA methyltransferase Dnmt1, the Myb transcription factor family member B-Myb (*Mybl2*), and proliferating cell nuclear antigen (PCNA). Dnmt1 associates with replication forks during cell division to transfer methylation marks to daughter cells and has been associated with intra-S-phase arrest after knockdown in the A549 lung cancer cell line (Milutinovic et al.,

2004). The ubiquitously expressed B-Myb is important for S phase progression in association with the DREAM complex and B-Myb knockdown has been implicated in chromosomal instability of megakaryocytes (García and Frampton, 2006; Guiley et al., 2015; Tarasov et al., 2008). Like Dnmt1, PCNA is also associated with the replication fork and is an important co-factor for a number of protein-protein interactions (including with Dnmt1) that ensure proper DNA replication and repair during cell division (Fridman et al., 2010). Thus, it is possible that deregulated expression of one or more of these genes could compromise the genomic stability of c-Myb-deficient large pre-B cells. It is also interesting to consider that these indicators of genomic instability are present in the context of increased *Rag1* expression, which induces DNA breaks in conjunction with the initiation of VJ recombination. Thus, it is also possible that upregulation of the Rag recombinase among other pro-differentiation gene expression changes important for VJ recombination in the context of proliferating, large pre-B cells contributes to the signifiers of genomic instability we have observed upon c-Myb ablation.

Implications of c-Myb function in normal large pre-B cells for B-ALL

Due to the rapid proliferation of large pre-B cells and the tight regulation needed to coordinate cell cycle exit with differentiation and the initiation of VJ recombination, the pre-B cell stage is particularly prone to the accumulation of transforming mutations that result in the development of B-cell acute lymphoblastic leukemia (B-ALL) (Eswaran et al., 2015). Overall, these transforming mutations promote survival and proliferation and inhibit cell cycle arrest and differentiation, perpetually maintaining cells in a large pre-B cell state. Notably, we have demonstrated a similar role for c-Myb in normal large pre-B cells (see above), suggesting that c-Myb would have a similar role in leukemias arising at the large pre-B cell stage of development. In fact, c-Myb has been implicated as an oncogene promoting the development of B-ALL in both mouse and human model

systems (Sarvaiya et al., 2012; Waldron et al., 2012). A key hallmark of cancer cells is their altered metabolism, which shifts to aerobic glycolysis and promotes enhanced and sustained growth, proliferation and survival (Vander Heiden et al., 2009). While a role for c-Myb in cancer cell metabolism has not been described, it is interesting to speculate on the implications that a role for c-Myb in maintaining glucose metabolism of normal large pre-B cells would have for understanding c-Myb function in B-ALL. Ikaros has also been implicated in the development of B-ALL and functions as a tumor suppressor that is inactivated in over 80% of cases of BCR-ABL$^+$ B-ALL (Kastner et al., 2013; Mullighan et al., 2008). In addition, Ikaros has been demonstrated to exert its tumor suppressor function in B-ALL by acting as a "metabolic gatekeeper" to enforce a chronic state of energy deprivation as a safeguard against autoimmunity and leukemic transformation (Chan et al., 2017). Therefore, c-Myb regulation of early steps of glucose metabolism as well as c-Myb-mediated repression of Ikaros expression at the large pre-B cell stage have critical implications for B-ALL. Our findings suggest that increased c-Myb could contribute to the development and maintenance of B-ALL through repression of Ikaros expression and prevention of Ikaros-mediated cell cycle exit, metabolic inhibition, and differentiation. Thus, this work provides a novel rationale for targeting c-Myb as a therapeutic strategy for cases of B-ALL both as a means of interfering with cancer metabolism as well as to relieve repression of Ikaros and enable its functions as a tumor suppressor and pro-differentiation factor in large pre-B cells.

Chapter V. Summary and Future Directions

At the time this project was initiated, previous work had demonstrated a critical role for c-Myb in survival of the earliest committed B-lineage progenitors and identified mediators of c-Myb function in the pro-B cell compartment and the pro-B to pre-B cell transition (Fahl et al., 2009, 2018; Greig et al., 2010; Thomas et al., 2005). In pro-B cells, we established that c-Myb expression was critical both for intrinsic survival, in the absence of cytokine, and for IL-7 mediated survival, largely via signaling through Stat5 (Fahl et al., 2018). However, failure to fully rescue relative recovery of c-Myb-deficient pro-B cells after rescuing Stat5 signaling downstream of the IL-7R through expression of a constitutively active Stat5 (CA-STAT5) suggested that c-Myb has additional function(s) within the pro-B cell compartment. This work also established a role for c-Myb in expression of genes important for the pre-BCR checkpoint and for the pro-B to pre-B cell transition. However, it is unclear whether c-Myb has a distinct role in cycling, large pre-B cells that is separate from c-Myb function in the pro-B cell compartment and in mediating differentiation across the pre-BCR checkpoint.

In this thesis, genome-wide analysis of pro-B and pre-B cells has been used to identify additional c-Myb functions in pro-B cells and to characterize c-Myb function in the large pre-B cell compartment. In pro-B cells, I have identified a role for c-Myb in the early steps of glucose metabolism and identified a number of c-Myb targets within the Plcγ/Pkc/mTORC1 pathway, which acts downstream of IL-7 signaling and regulates proliferation and metabolism at the pro-B cell stage. In large pre-B cells, I have demonstrated that c-Myb plays a critical role in regulating the expression of genes important for maintaining homeostasis in the large pre-B cell compartment and suppressing the premature expression of genes important for differentiation into the small pre-B cell compartment. This work has provided new insights into how c-Myb controls B cell

development across the pre-BCR checkpoint and raises significant questions. These questions include whether c-Myb-regulated genes represent direct targets, the mechanism by which c-Myb-regulated genes mediate c-Myb function in pro-B and large pre-B cells, and what are the implications of this work for human disease. In addition, utilizing genomic analysis of c-Myb-dependent gene expression in pro-B and large pre-B cells, this work has generated a resource of c-Myb-dependent gene expression changes that could be used for future studies of c-Myb function in B cell development. This chapter will discuss the rationale behind these questions and provide potential strategies for addressing them in future studies.

What c-Myb-regulated genes are direct targets in pro-B and large pre-B cells?

To understand how c-Myb carries out its functions in pro-B and pre-B cells, it is crucial to identify direct c-Myb targets, which will allow one to build c-Myb-controlled gene networks across the pre-BCR checkpoint. However, identifying direct c-Myb binding regions in the context of chromatin has been a fundamental challenge in the field to understanding how c-Myb functions. This challenge is, in part, due to the fact that c-Myb is a component of large protein complexes that is thought to result in epitope masking and thus contribute to the lack of effective commercially available antibodies. Early chromatin immunoprecipitation (ChIP) studies identified a number of direct c-Myb targets, but these experiments were largely conducted using transformed cell lines and focused on c-Myb binding to the proximal promoters of selected genes (Berge et al., 2007; Lang et al., 2005; Wang et al., 2000). Then, later studies sought to identify global c-Myb targets by ChIP-seq, but these studies were problematic due to the use of epitope-tagged and overexpressed, exogenously supplied c-Myb to facilitate detection of binding peaks (Quintana et al., 2011b, 2011a; Zhao et al., 2011). Since these ChIP-seq studies were conducted, a new

commercial antibody has been developed by Bethyl Laboratories, which seems to work more consistently. Using this new antibody, I have had some success with ChIP and ChIP-seq experiments, the results of which correlated with several known direct c-Myb target genes. However, due to the potential for epitope masking it is difficult to say whether these approaches are able to successfully detect all potential c-Myb binding sites on a global scale. Taken together, the results of previous studies to detect direct c-Myb target genes suggest that these promoter-directed or antibody-dependent approaches may limit identification of c-Myb binding sites to a subset in the genome that can be recognized by the currently available antibodies.

To account for the limitations of ChIP and ChIP-seq approaches for the identification of direct c-Myb target genes, recent studies have utilized a procedure developed by the ENCODE Consortium termed digital genomic footprinting (DGF) (Neph et al., 2012). DGF utilizes massively parallel sequencing of DNase I treated cells to map proteins associated with particular DNA sequences of "open" chromatin and has been used to map c-Myb binding sites in human blood cell types as well as Treg cells (Bengtsen et al., 2015; Dias et al., 2017). The Assay for Transposase Accessible Chromatin with high-throughput sequencing (ATAC-seq) is a relatively recent technique developed for mapping genome-wide chromatin accessibility with the advantage over DNase-seq of requiring small numbers of cells. Thus, ATAC-seq provides an unbiased, antibody-independent approach to identify c-Myb binding sites in B lineage cells (Buenrostro et al., 2015; Li et al., 2019; Liu et al., 2019). In particular, ATAC-seq could be used to compare c-Myb-dependent chromatin occupancy profiles of pro-B and large pre-B cells with and without c-Myb expression.

In the ATAC-seq procedure, a genomic footprint is generated by the Tn5 transposase, which detects regions of open chromatin and inserts adapters, which are then sequenced to provide

a map of global chromatin accessibility (Buenrostro et al., 2015). Sequencing reads are then used to infer regions of transcription factor (TF) binding, which prevents enzyme cleavage and results in "footprints" at various regulatory elements such as promoters, enhancers, and repressors. Then, a number of computational methods, such as the recently developed HINT-ATAC approach, can be used to scan open chromatin profiles to find footprints and predict transcription factor binding sites (TFBS) (Li et al., 2019). Applying this ATAC-seq protocol to c-Myb-sufficient and -deficient pro-B and large pre-B cells could identify promising c-Myb binding sites at footprint regions that contain a canonical *Myb* response element (MRE). These sites could then be mapped to our previously generated microarray and RNA-seq gene expression data in order to match c-Myb-dependent transcriptional changes with potential sites of c-Myb occupancy.

If a portion of the c-Myb-dependent footprints fail to contain a c-Myb binding motif, these sites could be scanned for co-localization with binding sites of known c-Myb interaction partners. In addition, HINT-ATAC analysis could potentially uncover sites of new binding partners that may be critical for c-Myb function at these loci. These sites would be characterized by the presence of binding sequences specific to genes that have not been identified as c-Myb interaction partners that could subsequently be validated as true interaction partners through co-immunoprecipitation experiments. Then CRISPR-mediated mutagenesis of these sites and/or shRNA-mediated knockdown of these potential binding partners could be utilized to assess the effects on c-Myb-dependent gene expression. To better understand how c-Myb functions in concert with other proteins/complexes on a global scale, co-localization of c-Myb footprints with publicly available TF ChIP-seq peak datasets could be analyzed. Selection of TF ChIP-seq data sets would be informed by TFBS analysis of c-Myb-dependent footprints as described above. Thus, comparison of c-Myb-dependent footprints from pro-B and large pre-B cells with publicly available ChIP-seq

data could provide valuable insights into the impact of each c-Myb footprint on potential target genes and how interactions of c-Myb with co-regulatory proteins could modulate c-Myb function.

Chromatin occupancy data from ATAC-seq analysis of c-Myb-sufficient and -deficient pro-B and large pre-B cells could also be used to characterize whether c-Myb-dependent sites of open chromatin represent promoters of proximal genes or potential regulatory regions of proximal or distal genes. To do this, c-Myb footprints could be compared to ChIP-seq data for histone marks in pro-B and large pre-B cells, which could be used to identify different regulatory sequences. These histone modifications include the transcriptional activation marker H3K4me3 (Barski et al., 2007), the enhancer markers H3K4me1 and H3K9ac (Heintzman et al., 2007), and the repressive marker H3K27me3 (Boyer et al., 2006). These comparisons would provide insight into the function of each c-Myb footprint as a transcriptional activator, repressor, or distal enhancer region. Overall, ATAC-seq analysis could be used to provide a genomic footprint of c-Myb binding sites in pro-B and large pre-B cells. In combination with publicly available ChIP-seq data for histone modifications and binding sites for other TFs, this genomic footprint could provide insight into the mechanism of c-Myb function at each footprint region. In combination with global gene expression data through microarray or RNA-seq, this genomic footprint could be used to identify which of these c-Myb-regulated genes are direct targets.

Integrated genome-wide chromatin accessibility (ATAC-seq) and gene expression (microarray and RNA-seq) data sets could be used to build a network of c-Myb-regulated genes across the pre-BCR checkpoint during the pro-B and large pre-B cell stages of development. To do this, pathway gene set analysis could be performed on genes containing c-Myb footprints at promoter or previously validated distal regulatory sequences that were also differentially expressed in c-Myb-deficient pro-B or large pre-B cells. This would identify signaling pathways or processes

enriched in direct c-Myb target genes, which would likely be critical for c-Myb function. Then the remaining genes constituting each of these pathway gene sets could be cross-referenced with c-Myb-dependent gene expression changes (MDGs) that were not identified as direct c-Myb targets. This analysis could identify components of each pathway downstream of c-Myb activity, that were also dysregulated in c-Myb-deficient pro-B and large pre-B cells. Then the impact of c-Myb activity on each pathway could be determined by correlating the effect of c-Myb activity on each gene target (whether c-Myb induces or represses their mRNA expression) with the role of that gene target in the pathway as a whole. Finally, critical downstream components of each pathway could be expressed or knocked down in c-Myb-deficient pro-B or large pre-B cells to test for their ability to rescue c-Myb-mediated functions. Altogether, the combination of microarray/RNA-seq gene expression and ATAC-seq chromatin accessibility data have the potential to identify key c-Myb target genes important for pro-B and pre-B cell development as well as critical pathways impacted by these genes and ultimately to construct a network of c-Myb-regulated genes and functions across the pre-BCR checkpoint.

How do loss of IL-7R signaling and defects in glucose metabolism impact relative recovery of c-Myb-deficient pro-B cells?

This thesis has uncovered a previously unknown role for c-Myb in pro-B cell glucose metabolism. Gene set analysis of our pro-B cell microarray revealed that c-Myb-dependent differentially expressed genes (MDGs) were enriched in gene sets related to multiple steps in glucose processing including glycolysis, the biosynthesis of macromolecules, and mitochondrial oxidative phosphorylation (Figure 3.2). We identified decreased mRNA expression of Glut1 and Hk1 as the most upstream components of these pathways and demonstrated decreased glucose

uptake and processing. However, the role that loss of Glut1/Hk1 expression plays in the overall phenotype of c-Myb-deficient pro-B cells remains unknown. In addition, it is unclear exactly how c-Myb-dependent expression of Glut1/Hk1 as well as glucose uptake/utilization are regulated in pro-B cells. One possible mechanism is through c-Myb-dependent regulation of IL-7 signaling through the Plcγ/Pkc/mTORC1 signaling pathway which has been demonstrated to promote IL-7-mediated proliferation and metabolism in pro-B cells (Yu et al., 2017; Zeng et al., 2018). Furthermore, our microarray gene set analysis revealed that MDGs were enriched in IL-7 signaling and mTORC1 signaling gene sets (Figure 3.5), which suggested that c-Myb-mediated regulation of IL-7R signaling through mTORC1 could be important for pro-B cell glucose metabolism. However, it is unknown whether mTORC1 activation is important for expression of Glut1/Hk1 or for glucose uptake/utilization in pro-B cells. This section will explore possible approaches to investigate the impact of Glut1/Hk1 expression, glucose metabolism, and IL-7/mTORC1 signaling on the c-Myb-dependent large pre-B cell phenotype.

To determine the relative contribution of glucose uptake and utilization to decreased recovery of c-Myb-deficient pro-B cells, initial experiments could be done to determine whether Glut1 and Hk1 are important in normal, c-Myb-sufficient pro-B cells. These experiments would separate deficiencies in the pro-B cell compartment due to decreased expression of Glut1 or Hk1 from other c-Myb-dependent gene expression changes. To do this, Glut1 and Hk1 could be targeted by shRNA-mediated knockdown and assessed for relative recovery, glucose uptake, and hexokinase activity. These experiments would demonstrate whether loss of Glut1/Hk1 expression results in a similar phenotype to what we have observed in c-Myb-deficient pro-B cells. Then, one could determine whether loss of Glut1/Hk1 also impacts the expression of genes involved in downstream metabolic pathways that were dysregulated upon loss of c-Myb expression such as

those depicted in Figure 5.1. Then, the activity of these downstream metabolic pathways after Glut1/Hk1 knockdown could be assessed. To do this, glycolysis and oxidative phosphorylation could be analyzed using the Seahorse Extracellular Flux Analyzer to determine the extracellular acidification rate (ECAR) and oxygen consumption rate (OCR), which act as measures of glycolysis and oxidative phosphorylation respectively. These experiments would determine whether expression of Glut1/Hk1 and glucose uptake/utilization are necessary for downstream metabolic pathways in pro-B cells. In addition, these experiments would indicate whether loss of Glut1/Hk1 alone could account for the defects in glucose uptake/utilization as well as pathways important for the utilization of glucose downstream of hexokinase activity that we observed in c-Myb-deficient pro-B cells. To assess this, one could determine whether expression of Glut1/Hk1 is sufficient to restore relative recovery and readouts of glucose metabolism in c-Myb-deficient pro-B cells. To do this, retroviral co-transductions with Cre and exogenous Glut1 or Hk1 could be performed as described for large pre-B cells (Figure 4.11) to determine whether expression of Glut1 or Hk1 can restore defects in relative recovery, glucose uptake/utilization, and downstream metabolic pathways (glycolysis and oxidative phosphorylation) of c-Myb-deficient pro-B cells. After determining the relative contribution of Glut1/Hk1 and their effects on glucose metabolism to the phenotype of c-Myb-deficient pro-B cells, it will be important to determine how expression of Glut1/Hk1, glucose uptake/utilization, and downstream metabolic pathways are regulated.

Due to the demonstrated roles for c-Myb in regulating expression of the IL-7Rα and for IL-7/mTORC1 signaling in mediating pro-B cell metabolism, it is likely that this pathway is

Figure 5.1. Gene set enrichment of c-Myb-dependent differentially expression genes (MDGs) in pro-B cells. c-Myb-dependent gene expression changes in pro-B cells were identified by microarray analysis as described in Figure 3.1A. Differential expression of genes identified from gene set analysis described in Figure 3.2 in the Hallmark_Glycolysis (A), Hallmark_Oxidative_Phosphorylation (B), Reactome_Fatty_Acid_Metabolism (C) and Kegg_Purine Metabolism and Kegg_Pyrimidine_Metabolism (D) gene set is shown. Genes upregulated upon c-Myb deletion are shown in black and genes downregulated upon c-Myb deletion are shown in red.

A.

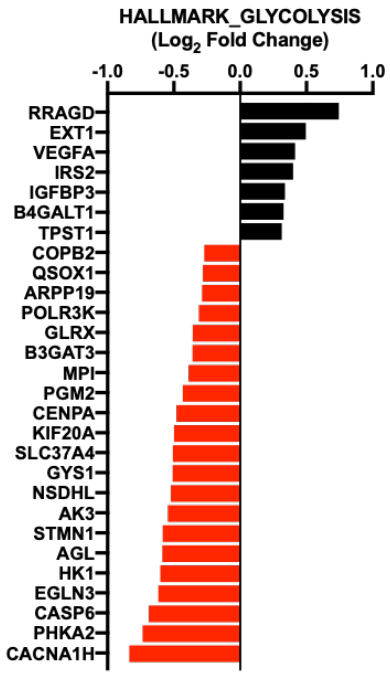
HALLMARK_GLYCOLYSIS
(Log2 Fold Change)
-1.0
-0.5
0.0
0.5
1.0
RRAGD
EXT1
VEGFA
IRS2
IGFBP3
B4GALT1
TPST1
COPB2
QSOX1
ARPP19
POLR3K
GLRX
B3GAT3
MPI
PGM2
CENPA
KIF20A
SLC37A4
GYS1
NSDHL
AK3
STMN1
AGL
HK1
EGLN3
CASP6
PHKA2
CACNA1H

B.

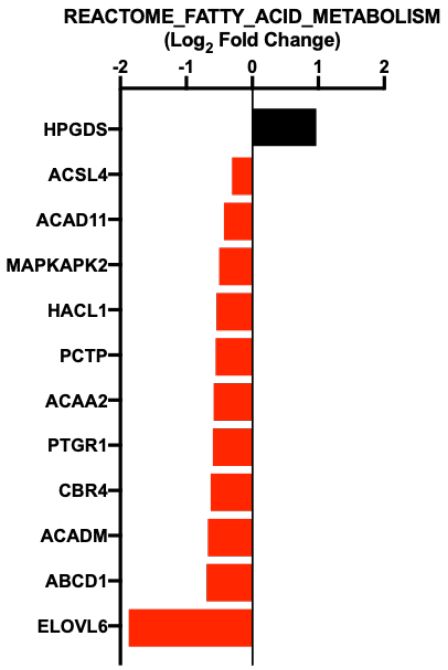
REACTOME_FATTY_ACID_METABOLISM
(Log2 Fold Change)
-2
-1
0
1
2
HPGDS
ACSL4
ACAD11
MAPKAPK2
HACL1
PCTP
ACAA2
PTGR1
CBR4
ACADM
ABCD1
ELOVL6

C.

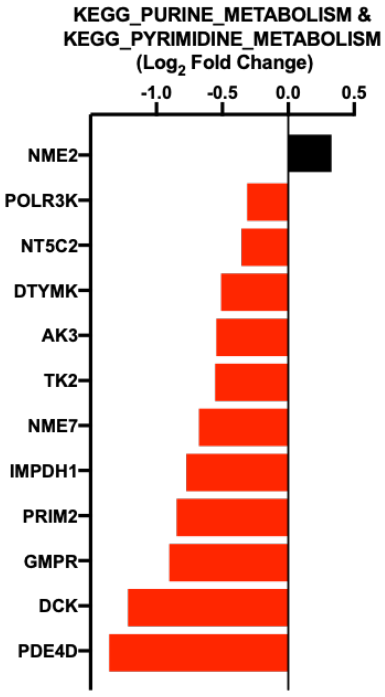
KEGG_PURINE_METABOLISM &
KEGG_PYRIMIDINE_METABOLISM
(Log2 Fold Change)
-1.0
-0.5
0.0
0.5
NME2
POLR3K
NT5C2
DTYMK
AK3
TK2
NME7
IMPDH1
PRIM2
GMPR
DCK
PDE4D

D.

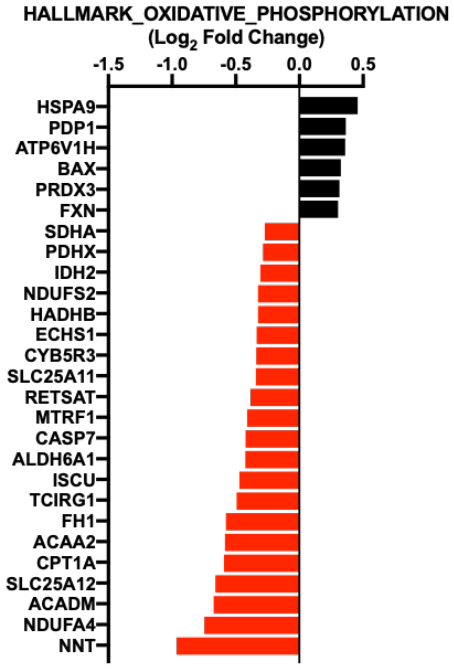
HALLMARK_OXIDATIVE_PHOSPHORYLATION
(Log2 Fold Change)
-1.5
-1.0
-0.5
0.0
0.5
HSPA9
PDP1
ATP6V1H
BAX
PRDX3
FXN
SDHA
PDHX
IDH2
NDUFS2
HADHB
ECHS1
CYB5R3
SLC25A11
RETSAT
MTRF1
CASP7
ALDH6A1
ISCU
TCIRG1
FH1
ACAA2
CPT1A
SLC25A12
ACADM
NDUFA4
NNT

important for c-Myb-dependent regulation of pro-B cell glucose metabolism (Fahl et al., 2009; Yu et al., 2017; Zeng et al., 2018). To determine the relative contribution of IL-7 signaling through mTORC1 to defects in glucose metabolism and decreased recovery of c-Myb-deficient pro-B cells, one could initially determine if decreased activity of mTORC1 induces a similar phenotype to loss of c-Myb expression. To do this, mTORC1 could be inhibited by treatment with rapamycin in c-Myb-sufficient pro-B cells. Then, it could be determined if loss of mTORC1 leads to decreased mRNA expression of Glut1/Hk1, decreased glucose uptake/utilization, decreased ECAR/OCR, decreased proliferation, and overall decreased recovery. These experiments would demonstrate whether IL-7/mTORC1 signaling is important for expression of Glut1/Hk1 and downstream pathways important for glucose metabolism. Then, to determine the overall impact of IL-7 signaling through the Plcγ/Pkc/mTORC1 on the phenotype of c-Myb-deficient pro-B cells, retroviral co-transductions could be done with the Pkcβ catalytic domain (Pkcβ-CAT), which acts like a constitutively active form of Pkcβ, to rescue activation of mTORC1 downstream of IL-7 signaling (Soh and Weinstein, 2003; Yu et al., 2017). It could then be determined if Pkcβ-CAT transduction is able to rescue defects in relative recovery and glucose metabolism as described above in c-Myb-deficient pro-B cells.

Altogether, these experiments could specifically link IL-7-mediated activation of mTORC1 through the Plcγ/Pkc/mTORC1 pathway to deficiencies in Glut1/Hk1 expression and glucose metabolism in c-Myb-deficient pro-B cells. However, the exact mechanism by which mTORC1 might induce Glut1/Hk1 expression and impact additional metabolic pathways in pro-B cells has not been established. Studies identifying the role of this pathway in IL-7-mediated metabolism utilized the Seahorse Extracellular Flux Analyzer to show decreased readouts of glycolysis and oxidative phosphorylation, but the role of mTORC1 in activating these metabolic

pathways was not identified. One possible connection between mTORC1 activation and metabolic pathways in pro-B cells is the transcription factor HIF1α. Activation of mTORC1 has been demonstrated to promote translation of HIF1α, which, in turn, induces expression of a number of metabolic genes including Glut1 and Hk1 (Düvel et al., 2010). To determine the relative contribution of HIF1α to expression of Glut1/Hk1 in c-Myb-deficient pro-B cells, protein levels of HIF1α could be determined. This would demonstrate whether c-Myb-dependent loss of signaling through IL-7/mTORC1 leads to decreased translation of HIF1α protein in pro-B cells. Then, transduction with a retroviral vector encoding HIF1α, could be used to determine whether exogenous expression of HIF1α can rescue Glut1/Hk1 mRNA expression as well as glucose uptake/utilization in c-Myb-deficient pro-B cells. Overall, the experiments outlined in this section will greatly expand on the few studies that have analyzed pro-B cell metabolism and will build off of previous work in our lab to provide a more comprehensive picture of how c-Myb and signaling pathways downstream of the IL-7R regulate pro-B cell development. Furthermore, understanding how c-Myb functions in the context of normal pro-B cell development can provide insight into how these processes may apply to B-lymphoid tumors.

What other c-Myb-regulated pathways or processes may be revealed by genome-wide analysis of pro-B cells?

Gene set analysis of our microarray comparing c-Myb-sufficient and -deficient pro-B cells provided evidence for additional functions of c-Myb in the pro-B cell compartment that represent interesting lines of investigation to pursue in future studies. Identifying additional functions for c-Myb will contribute to understanding B-lymphopoiesis and could have implications for the development and maintenance of leukemias arising from the pro-B cell stage. For example, MDGs

were enriched in gene sets related to cell migration and adhesion. Pro-B cells are essentially non-motile and largely remain in contact with IL-7^{+} stromal cells to maintain IL-7 signaling and promote pro-B cell survival and proliferation (Fistonich et al., 2018). In addition, IL-7 signaling promotes CXCR4 expression to facilitate movement away from IL-7-high environments in the bone marrow. These alternating states of engagement and separation from IL-7^{+} stromal cells promote separation of IL-7-mediated proliferation from V(D)J recombination (Clark et al., 2014). Thus, a role for c-Myb in pro-B cell migration/adhesion could provide an additional mechanism by which c-Myb regulates IL-7 signaling through interactions of pro-B cells with IL-7 cytokine in the bone marrow microenvironment. In addition, our microarray gene set analysis indicated that c-Myb-regulated genes were involved in cell stress pathways. We have previously demonstrated a role for c-Myb in pro-B cell survival through regulating the balance in pro-apoptotic and anti-apoptotic Bcl-2 family members, in particular, through repression of pro-apoptotic Bim and Bmf (Fahl et al., 2018). Bim and Bmf are among the BH3-only subset of Bcl-2 family members that directly or indirectly activate Bak or Bax to induce apoptosis in response to cellular stress (Figure 1.6). Therefore, a role for c-Myb in regulating the cellular stress response could provide further insight into how c-Myb promotes pro-B cell survival. These examples of additional pathways and processes enriched in c-Myb-regulated genes from our microarray analysis illustrate the untapped potential of this data set to instigate future studies of c-Myb function in the pro-B cell compartment.

Among the potential c-Myb functions suggested by microarray gene set analysis and perhaps the most critical for the overall development of B cell progenitors in the bone marrow is V(D)J recombination. Our lab has demonstrated that c-Myb is important for *Tcrβ* rearrangement in developing T lymphocytes and other groups have demonstrated that c-Myb also plays a role in

Tcrδ rearrangement (Bender et al., 2004; Hernandez-Munain and Krangel, 1994). Previous attempts to assess V(D)J recombination in c-Myb-deficient pro-B cells failed to yield observable differences (Greig et al., 2010). However, we have demonstrated that loss of c-Myb expression in pro-B cells leads to rapid cell death, which may preclude detection of changes in V(D)J recombination or may lead to a skewed repertoire due to cell death before rearrangements at distal J segments can occur (Fahl et al., 2018; Yuan et al., 2010). Thus, the possibility remains that c-Myb plays a role in rearrangements at the *Igh* locus. The results of our c-Myb-dependent pro-B cell microarray provided evidence of a role for c-Myb in V(D)J recombination. MDGs derived from the pro-B cell microarray included components of the recombination machinery (*Rag2*, *Xrcc6*, *Lig4*, *Dntt*), transcripts of the heavy chain locus (*Igh-VJ558, Ighg3, Ikhv1-72, Ighm*), and genes with known roles in regulating V(D)J recombination (*Pax5, Ezh2*). In addition, gene set analysis revealed that MDGs were enriched in gene sets related to chromatin and double-stranded break repair including: REACTOME_CHROMOSOME_MAINTENANCE, GO_CHROMATIN_ORGANIZATION, and KEGG_NON_HOMOLOGOUS_END_JOINING. Thus, the results of our pro-B cell microarray suggest that c-Myb may play a role in V(D)J recombination. To determine if c-Myb plays a role in V(D)J recombination in pro-B cells, YFP^+ pro-B cells could be electronically sorted from *Myb^{ff} CD19-cre YFP Bcl2Tg* mice in which c-Myb deletion is initiated in the pro-B cell compartment and expression of a *Bcl2Tg* is used to rescue the c-Myb-dependent pro-B cell survival defect. Then PCR of the *Igh* locus in YFP^+, c-Myb-deficient pro-B cells followed by southern blot could be used to detect rearrangements as our lab has done in the past (Bender et al., 2004; Yuan et al., 2010)

A role for IL-7 signaling through Stat5 in V(D)J recombination has been described, although there are conflicting reports as to the exact role of this pathway in regulating

immunoglobulin rearrangements. An initial publication reported that Stat5 promoted germline transcription at the heavy chain locus, histone acetylation to increase locus accessibility, and recombination of distal V_H segments (Bertolino et al., 2005). However, a later report found V_H recombination was normal in Stat5-deficient and IL-7Rα-deficient pro-B cells, but that Stat5 was important to repress rearrangements at the light chain locus (Malin et al., 2010). Thus, while the exact role of IL-7 signaling in V(D)J recombination in pro-B cells is unclear, c-Myb-regulation of IL-7R expression and signaling could implicate c-Myb in this process as well. In addition, examination of c-Myb regulation of V(D)J recombination would provide insight into the question of whether IL-7 signaling in pro-B cells is important for DNA rearrangements at the heavy chain locus or if the major function of IL-7 signaling is to maintain pro-B cell survival in order to provide sufficient time for these rearrangements to occur.

What role does c-Myb have in regulation of IL-7R and pre-BCR signaling in large pre-B cells and how does this impact glucose metabolism?

Our genome-wide expression analysis of shMyb-transduced *Irf4/8*$^{-/-}$ large pre-B cells by RNA-seq, provided insight into how c-Myb activity integrates with IL-7R and pre-BCR signaling and ultimately effects large pre-B cell function. We found that c-Myb regulates mRNA expression of both the IL-7Rα and the surrogate light chain (SLC) components of the pre-BCR, λ5 and VpreB1. In addition, c-Myb knockdown in *Irf4/8*$^{-/-}$ large pre-B cells resulted in broad changes in gene expression (nearly 6,000 MDGs at $p<0.05$ and nearly 3,000 with log2 FC>1) which were enriched in gene sets related to downstream functions of IL-7R and pre-BCR signaling in glucose metabolism, proliferation, survival, and differentiation (Figure 4.7). However, following this work, it is unclear exactly how c-Myb regulation of the IL-7R and pre-BCR as well as components

of downstream signaling pathways might impact glucose uptake/utilization, proliferation, and survival in large pre-B cells. In addition, it is unclear how co-expression of the IL-7R and pre-BCR in large pre-B cells might alter the mechanism of c-Myb regulation of glucose uptake/utilization as compared to pro-B cells, which do not yet express a pre-BCR. To address the role of defects in expression of the IL-7R and pre-BCR in the c-Myb-dependent large pre-B cell phenotype, it is tempting to utilize retroviral transduction rescue experiments to express the IL-7Rα and the SLC of the pre-BCR in c-Myb-deficient large pre-B cells. However, due to deregulated expression of downstream signaling factors as well as negative regulators of the IL-7R and pre-BCR, it is unlikely that exogenous expression of these receptors alone will be sufficient to rescue defects in c-Myb-deficient large pre-B cells. Therefore, future studies could utilize shRNA-mediated knockdown of negative regulators and exogenous expression of downstream signaling components to determine the contribution of these c-Myb-regulated genes to IL-7R and pre-BCR-mediated functions in the large pre-B cell compartment. The following section will propose methods of investigating the contribution of c-Myb regulation of IL-7R and pre-BCR signaling to the phenotype of c-Myb-deficient large pre-B cells.

With expression of the pre-BCR, activation of the PI3K/Akt pathway promotes large pre-B cell metabolism, proliferation, and survival. A major downstream mediator of PI3K/Akt signaling in large pre-B cells is mTORC1, which integrates nutrient sensing with regulation of cell growth and glycolytic metabolism in order to support proliferative expansion (Dibble and Cantley, 2015; Dibble and Manning, 2013; Fruman and Limon, 2012). As discussed in the Introduction section 1.3.3, the function of FNIP1 provides evidence for the importance of mTORC1 to large pre-B cell metabolism and the "metabolic checkpoint" that occurs between large and small pre-B cells. It has been demonstrated that FNIP1 mediates this checkpoint through interaction with

AMPK, which promotes AMPK-mediated inhibition of mTORC1. In *Fnip1*$^{-/-}$ large pre-B cells, while AMPK is activated, it is unable to inhibit mTORC1 and this leads to excessive cell growth, increased sensitivity to apoptosis, and a block at the large to small pre-B cell transition. Thus, the known role of mTORC1 as a nutrient sensor that in the presence of sufficient nutrient signals, promotes cell metabolism and proliferation suggests that it would have a critical role in coordinating increased glucose uptake with increased metabolic activity and proliferative expansion in large pre-B cells. However, how mTORC1 regulates components of glucose metabolism in large pre-B cells is unknown and, as discussed above, the best candidate for mediating a potential link between mTORC1 activation and regulation of glucose uptake/utilization through Glut1 and Hk1 expression is HIF1α.

In addition to activation of mTORC1, signaling through Akt has been implicated in glucose transporter surface expression and increasing the activity of glycolytic enzymes including hexokinase in the FL5.12 lymphoid cell line (Majewski et al., 2003, 2004; Wieman et al., 2007). Furthermore, Akt has been demonstrated to promote survival of lymphoid cells through a mechanism dependent on glucose uptake, association of hexokinase with the mitochondrial membrane, and hexokinase activity (Majewski et al., 2003; Rathmell et al., 2003). Therefore, while regulation of survival in large pre-B cells has not been characterized, my work suggests that large pre-B cell survival is intimately linked with their ability to utilize glucose. We found that exogenous expression of Glut1 or Hk1 in shMyb-transduced *Irf4/8*$^{-/-}$ large pre-B cells was able to completely restore cell recovery and oppose the increase in apoptosis induced by c-Myb knockdown (Figure 4.11 and 4.12). Thus, it appears that large pre-B cells, which exhibit increased metabolic activity to fuel their rapid proliferation, are engineered to couple this increased glucose uptake and metabolism with survival. To determine the role of PI3K/Akt signaling in the c-Myb-

dependent large pre-B cell phenotype, retroviral transduction with the plasma-membrane targeted, constitutively active PI3K subunit p110-CAAX or constitutively active Akt (CA-Akt) could be utilized to determine if rescuing this pathway as a whole can restore glucose uptake/utilization, proliferation, and survival in c-Myb-deficient large pre-B cells (Fahl et al., 2018). These experiments would provide an initial characterization of how PI3K/Akt signaling contributes to c-Myb-dependent functions in large pre-B cells.

In addition to the PI3K/Akt pathway, coordinated signaling through the IL-7R and pre-BCR also activate the Mapk/Erk pathway, which induces expression of *Myc* in large pre-B cells. Similar to PI3K/Akt signaling, c-Myc activity links pre-B cell proliferation and metabolism to promote aerobic glycolysis (Fan et al., 2010). c-Myc promotes proliferation through inducing mRNA expression of the cell cycle regulator *Ccnd3* and repressing the cell cycle inhibitor p27/Kip1 and also regulate mRNA expression of a number of metabolic genes including Glut1 (Lewis et al., 2000; Ma et al., 2010; Osthus et al., 2000). In addition, a recent publication has linked c-Myc to the mRNA expression of genes important to maintain "housekeeping" functions in large pre-B cells, which encompass proliferation and metabolism (Ferreirós-Vidal et al., 2019). In this study, repression of c-Myc by pre-BCR-mediated activation of Ikaros was critical for the decreased expression of cell cycle and metabolic genes and corresponding decrease in proliferation and metabolic activity that occurs at the large to small pre-B cell transition. We found that mRNA expression of c-Myc was decreased upon c-Myb knockdown in *Irf4/8*$^{-/-}$ large pre-B cells and thus, c-Myc represents another promising candidate for mediating c-Myb-dependent regulation of glucose metabolism and proliferation in large pre-B cells. Furthermore, we also observed increased mRNA expression of Ikaros and expression of the dominant negative Ik159A mutant was able to counteract the decrease in c-Myc expression upon c-Myb knockdown and increased Ikaros

Figure 5.2. Proposed model of c-Myb function in large pre-B cells. c-Myb expression is critical for maintaining large pre-B cell survival, proliferation, and glucose metabolism while suppressing premature differentiation into small pre-B cells. c-Myb induces expression of the IL-7Rα and the SLC components of the pre-BCR (λ5 and VpreB1). Coordinated signaling through the IL-7R and pre-BCR activates PI3K/Akt and Mapk/Erk signaling to promote large pre-B cell proliferation and metabolism. Signaling through Mapk/Erk induces expression of c-Myc which promotes proliferation through inducing *Ccnd3* expression and inhibiting expression of the cell cycle inhibitor p27/Kip1. PI3K/Akt signaling promotes proliferation through inhibition of Foxo1 and metabolism through activation of mTORC1. mTORC1 promotes translation of Hif1α, which in turn induces transcription of a number of metabolic genes including Glut1 and Hk1. mTORC1 activity is regulated by Fnip1, which associates with AMPK to enforce a metabolic checkpoint within the pre-B cell compartment and facilitate decreased metabolic activity at the large to small pre-B cell transition. c-Myb is also important to repress expression of Ikaros/Aiolos, which promote the large to small pre-B cell transition, in part through inhibiting expression of c-Myc and the pre-BCR. Thus, loss of c-Myb in large pre-B cells leads to decreased expression of the IL-7R and pre-BCR, increased expression of Ikaros/Aiolos, and overall to decreased proliferation, glucose metabolism, and glucose-dependent survival. Purple text represents downregulated genes and processes and green text represents upregulated genes and processes in c-Myb-deficient large pre-B cells.

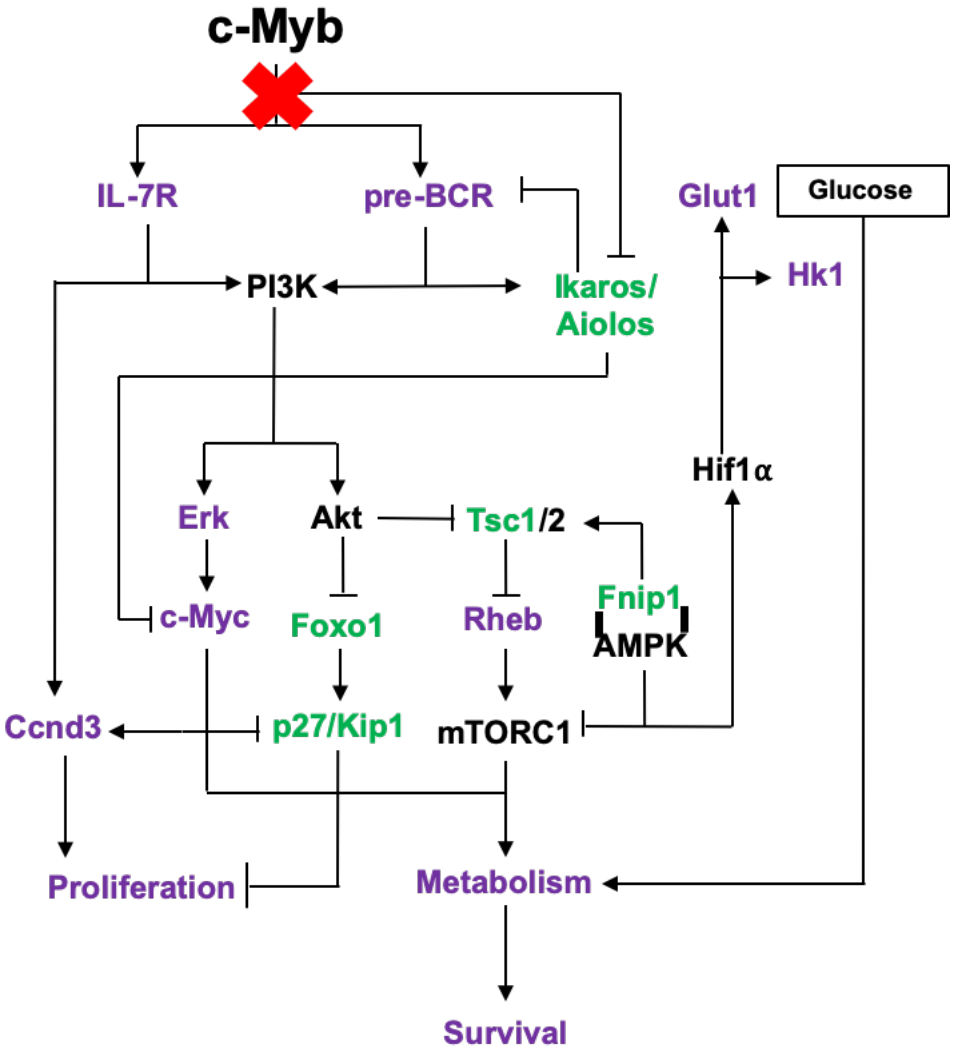
c-Myb
IL-7R
pre-BCR
Glut1
Glucose
PI3K
Ikaros/
Aiolos
Hk1
Hif1α
Erk
Akt
Tsc1/2
c-Myc
Foxo1
Rheb
Fnip1
AMPK
Ccnd3
p27/Kip1
mTORC1
Proliferation
Metabolism
Survival

expression. Thus, it is possible that repression of Ikaros by c-Myb is important to prevent Ikaros-mediated repression of c-Myc and acts as a critical mechanism to maintain glucose metabolism and proliferative expansion in large pre-B cells. Following the work described in this thesis, one can propose a model depicting how loss of components of the IL-7R and pre-BCR could be important for c-Myb-dependent regulation of glucose metabolism, proliferation, and survival in large pre-B cells, which remains a question to address in future studies (Figure 5.2).

What is the role of c-Myb in the large to small pre-B cell transition?

From the earliest characterization of v-Myb and c-Myb proteins, the *Myb* locus has been closely associated with differentiation, in particular, in immature hematopoietic cells (Bender and Kuehl, 1987; Duprey and Boettiger, 1985; Ess et al., 1999; Westin et al., 1982). *Myb* expression is greatest in immature progenitor cells and decreases as cells progress toward terminal differentiation. In addition, early work linked c-Myb with inhibiting differentiation and maintaining proliferation in myeloid and erythroid leukemia cell lines (McClinton et al., 1990; Pedrazzoli et al., 1989). Previous work from our lab has demonstrated that c-Myb is absolutely required for differentiation from pre-pro B cells to B-lineage committed pro-B cells and that c-Myb coordinates pro-B cell survival with the expression of genes important for differentiation across the pre-BCR checkpoint (Fahl et al., 2009, 2018). This role for c-Myb in differentiation of hematopoietic cells and, specifically, B-lineage progenitors, suggests that c-Myb may also function in the large to small pre-B cell transition. The work in this thesis is the first to characterize c-Myb function in large pre-B cells and to implicate c-Myb in regulating changes in gene expression important for differentiation into small pre-B cells. As discussed above, the exact mechanism for how attenuation of IL-7R signaling and the shift in pre-BCR signaling from

promoting proliferation to promoting differentiation is coordinated to facilitate the large to small pre-B cell transition has not been determined. Thus, understanding how c-Myb functions in the large to small pre-B cell transition will provide crucial insight into normal B cell development, the pre-BCR checkpoint, and have significant implications for pre-B-ALL.

Our work in the μHC-transduced pro-B cell knockout model, provided our first indication that c-Myb expression may play a role in large pre-B cell differentiation. In this model, large pre-B cells generated upon expression of a μHC in pro-B cells continue to differentiate into small pre-B cells as measured by decrease in cell size and increase in expression of the small pre-B cell marker CD2. c-Myb ablation appeared to accelerate large pre-B cell differentiation as we observed decreased cell size and increased CD2 expression occurred earlier in μHC/Cre-transduced pro-B cells as compared to control μHC-transduced pro-B cells. However, we observed selection against c-Myb deletion specifically in cells with increased CD2 expression that appeared to differentiate. With these results, we cannot discern whether c-Myb-deficient large pre-B cells are unable to differentiate or if this apparent selection against differentiation is due to increased apoptosis in either the large or small pre-B cell fractions of the pre-B cell compartment. To address this, these experiments in μHC/Cre-transduced pro-B cells could be conducted in the context of *Bcl2Tg* expression or treatment with the pan-caspase inhibitor Q-VD-OPH. If rescuing survival of μHC/Cre-transduced pro-B cells also rescues their ability to become $CD2^+$ small pre-B cells, this would indicate that the apparent block in differentiation we have observed is due to increased cell death in c-Myb-deficient large pre-B cells. If rescuing survival of μHC/Cre-transduced pro-B cells fails to rescue differentiation into $CD2^+$ small pre-B cells, this would indicate that expression of c-Myb is important for the large to small pre-B cell transition. As a whole, these experiments would clarify the role of c-Myb in large pre-B cell differentiation within this model. Then, to

pursue a potential role for c-Myb in the large to small pre-B cell transition, RNA-seq could be performed comparing μHC and μHC/Cre-transduced pro-B cells express a *Bcl2Tg* to determine if the gene expression program important for large pre-B cell differentiation is in place in μHC/Cre-transduced pro-B cells. A particular focus would be placed on expression of Ikaros/Aiolos and the Ikaros-dependent footprint depicted in Figure 4.9B. Then, if deficiencies in expression of genes important for the large to small pre-B cell transition are detected one could determine if exogenous expression of c-Myb is able to rescue this gene expression program and differentiation of μHC/Cre-transduced pro-B cells into $CD2^+$ small pre-B cells. This result would be particularly interesting if c-Myb knockout in this model leads to a block in differentiation while the results of c-Myb knockdown in *Irf4/8*$^{-/-}$ large pre-B cells indicated that c-Myb is important to repress differentiation and could reveal that the level of c-Myb expression is an important factor in determining the ability of large pre-B cells to transition to the small pre-B cell compartment.

In contrast to our work in pro-B cells, which indicates that c-Myb is important to induce expression of genes necessary for differentiation across the pre-BCR checkpoint, our work in large pre-B cells indicates that c-Myb is important to repress the gene expression program mediating the transition from large to small pre-B cells. The transcription factors Ikaros and Aiolos are critical mediators of this gene expression program and we have demonstrated that c-Myb represses mRNA expression of Ikaros and Aiolos in *Irf4/8*$^{-/-}$ large pre-B cells. Loss of c-Myb expression in *Irf4/8*$^{-/-}$ large pre-B cells led to increased expression of Ikaros and Aiolos and induced gene expression changes that encompassed approximately 70% of Ikaros target genes important for the large to small pre-B cell transition. With this result, one would hypothesize that the c-Myb-dependent increase in Ikaros/Aiolos expression would induce large pre-B cell differentiation. However, the results in μHC/Cre-transduced pro-B cells discussed above suggest that induction of this Ikaros-

dependent gene expression program is insufficient to promote the transition into small pre-B cells and results in apoptotic cell death. We propose this is due to an Ikaros-independent function of c-Myb in regulating glucose uptake and utilization in that exogenous expression of Glut1/Hk1 rescued recovery and survival of shMyb-transduced *Irf4/8*$^{-/-}$ large pre-B cells. To determine the relative contributions of c-Myb-dependent regulation of Ikaros/Aiolos and Glut1/Hk1 to differentiation of *Irf4/8*$^{-/-}$ large pre-B cells, initial experiments would be needed to establish that expression of Ikaros is able to induce differentiation of c-Myb-sufficient but not c-Myb-deficient *Irf4/8*$^{-/-}$ large pre-B cells as measured by decreased cell size and increased expression of CD2. Then, differentiation status could be assessed following c-Myb knockdown and increased Ikaros expression in combination with caspase inhibitor treatment or expression of Glut1/Hk1. These experiments would determine whether rescuing survival alone is sufficient to enable Ikaros-mediated differentiation or whether c-Myb-deficient large pre-B cells require Glut1/Hk1 expression and activity to complete the transition into small pre-B cells.

If rescuing survival of c-Myb-deficient large pre-B cells in a Glut1/Hk1-dependent or -independent manner still fails to enable differentiation this would indicate that Ikaros expression is insufficient to support differentiation in the context of c-Myb knockdown. It is possible that while the majority of the Ikaros-mediated gene expression changes needed for the large to pre-B cell transition were also induced by c-Myb knockdown, that a critical factor(s) needed for differentiation was not induced or was repressed and that this prevented large pre-B cell differentiation. Thus, investigating the portion of the Ikaros-dependent gene signature that was not represented in our c-Myb-dependent RNA-seq data as well as genes that were differentially regulated by c-Myb and Ikaros could yield insight into additional gene expression changes needed to complete differentiation into small pre-B cells. To do this, gene set analysis could be utilized to

assist in identification of Ikaros-mediated pro-differentiation gene expression changes that were not changed upon c-Myb knockdown or were differentially regulated by c-Myb knockdown that might prevent differentiation of c-Myb-deficient large pre-B cells. Then targeting these genes via exogenous expression or shRNA-mediated knockdown alone or in combination could be used to determine which of these factors is able to promote the large to small pre-B cell transition. Taken together, these proposed studies would provide crucial insight into the network of genes that coordinate differentiation within the pre-B cell compartment.

What are the implications of c-Myb function in pro-B and large pre-B cells to B-ALL?

Due to the proliferative expansion of large pre-B cells and the importance of coordinating cell cycle exit with differentiation and the initiation of DNA rearrangements at the *Igl* locus, the pre-B cell stage is particularly prone to transforming mutations resulting in the development of B-ALL (Eswaran et al., 2015). pre-B-ALL commonly arises from mutations in B-lineage precursors, which promote survival and proliferation and arrest development at the cycling large pre-B cell stage. We have demonstrated a similar role for c-Myb in normal large pre-B cells, retaining cells in an immature, proliferating state and blocking differentiation, suggesting that c-Myb may have an analogous role in pre-B-ALL. Cancer cells also alter their cellular metabolism, which shifts to aerobic glycolysis to fuel sustained proliferative expansion. In particular, this shift has been demonstrated in cases of pre-B-ALL which exhibit higher expression of Glut1, excessive lactate production, and enhanced sensitivity to glycolytic inhibition (Boag et al., 2006). Thus, the role we have demonstrated for c-Myb in maintaining proliferation and glucose uptake/utilization in normal pro-B and large pre-B cells could have critical implications for c-Myb function in pre-B-ALL.

In addition to glucose uptake/utilization, the role we have demonstrated for c-Myb in repressing Ikaros expression also has implications for c-Myb function in pre-B-ALL. Ikaros functions as a tumor suppressor and is inactivated in over 80% of cases of BCR-ABL$^+$ B-ALL (Kastner et al., 2013; Mullighan et al., 2008). Ikaros mutations in B-ALL block differentiation and retain leukemic cells in an immature, cycling state. In addition, it has more recently been demonstrated that Ikaros exhibits a "metabolic gatekeeper" function through regulation of glucose metabolism. Thus, Ikaros exerts its tumor suppressor function to enforce a chronic state of energy deprivation, which acts as a safeguard against autoimmunity and leukemic transformation (Chan et al., 2017). Based on our work, an aberrant increase in c-Myb expression could contribute to the development of B-ALL through repression of Ikaros which would prevent differentiation and Ikaros-mediated inhibition of tumor cell metabolism. This function of c-Myb in repressing Ikaros expression could also be exploited for the treatment of pre-B-ALL. In tumors that exhibit increased expression of c-Myb, knockdown or inhibition of c-Myb could lead to increased expression of Ikaros, which would decrease tumor cell proliferation and metabolism and promote differentiation. In addition, overexpression of Ikaros could potentially be used to counteract increased expression of c-Myb in pre-B-ALL. Thus, the work described in this thesis on the function of c-Myb in normal large pre-B cells suggests that targeting c-Myb could be an effective treatment for cases of pre-B-ALL and potential strategies to do this are discussed below.

The essential function of c-Myb for normal adult hematopoiesis initially suggested that targeting c-Myb for cancer therapies may not be possible. However, the subsequent development of hypomorphic mutant mouse models demonstrated that reduced levels of c-Myb expression and activity are tolerable (Carpinelli et al., 2004; Sandberg et al., 2005). These observations indicate that a therapeutic index for modulating levels of c-Myb expression and activity could be beneficial

to cancer patients and provide efficacy for targeting c-Myb in human disease. The complexities of c-Myb regulation and function provide a number of approaches by which c-Myb could be targeting including at the level of transcriptional elongation, interactions with other co-regulatory proteins, or post-translational modifications.

Transcription at the *Myb* locus is primarily determined by a conditional block to transcriptional elongation within the first intron, suggesting that targeting c-Myb at the level of transcriptional elongation could be an effective method of reducing c-Myb expression in pre-B-ALL to a level sufficient to allow increased Ikaros expression (Bender and Kuehl, 1987; Hugo et al., 2006). Furthermore, there is evidence that tumor cells have employed mechanisms to relieve this block to *Myb* transcriptional elongation. In breast cancer cells, the estrogen receptor bound to estradiol relieves elongation arrest through direct interaction with the *Myb* locus and recruitment of the positive transcription elongation factor (P-Tefb) complex (Drabsch et al., 2007; Mitra et al., 2012). In addition, the p50/RelB NF-kB complex has been implicated in overcoming this elongation block in erythroleukemia and colon cancer cells (Pereira et al., 2015; Suhasini and Pilz, 1999; Toth et al., 1995). In colon cancer cells, combined treatment with inhibitors targeting NF-kB as well as the catalytic subunit of the P-Tefb complex, demonstrated that both are necessary for c-Myb transcription (Pereira et al., 2015). Furthermore, NF-kB has been demonstrated to promote transcriptional elongation of IL-8 through recruitment of P-Tefb in the CV-1 cell line (Barboric et al., 2001). Thus, c-Myb-directed therapies for pre-B-ALL could target these protein complexes involved in the relief of the *Myb* transcription elongation block or interactions between these complexes and the *Myb* locus. However, due to the other critical functions of NF-kB including in cell survival, it has been proposed that targeting P-Tefb may be more therapeutically beneficial in treating breast cancer and colon cancer (Mitra, 2018; Pattabiraman and Gonda, 2013).

Therefore, if PTef-b plays a similar role in promoting transcriptional elongation in pre-B-ALL, treatment with the PTef-b catalytic subunit inhibitors DRB or Flavopiridol could be effective therapies for pre-B-ALL as well.

Protein interactions or processes that modify c-Myb also represent potential therapeutic targets for regulating c-Myb activity in pre-B-ALL. One example of a successfully targeted c-Myb interaction partner is the transcriptional co-activator p300, which interacts with the c-Myb TAD through its KIX domain (Zor et al., 2004). In recent years, a number of small molecule inhibitors targeting c-Myb/p300 interactions have been identified as potential treatments for acute myeloid leukemia (AML). One of these inhibitors, Celastrol, interferes with the c-Myb/p300 interaction by binding to the p300 KIX domain, and was found to decrease AML cell proliferation and prolonged survival of mice in an *in vivo* AML model (Uttarkar et al., 2016a). Another inhibitor, Plumbagin, which interferes with the c-Myb/p300 interaction by binding the c-Myb TAD, inhibited proliferation and promoted differentiation of AML cells (Uttarkar et al., 2016b). These studies in AML suggest that use of these compounds to inhibit the c-Myb/p300 interaction may also be useful for treating pre-B-ALL. To test this, a variety of pre-B-ALL cell lines such as Nalm6 cells could be treated with Celastrol or Plumbagin to determine their ability to reduce proliferation and promote differentiation of leukemia cells. The success of targeting the c-Myb/p300 interaction also suggests that targeting other c-Myb protein-protein interactions may be therapeutically beneficial for treatment of leukemia.

Another potential co-activator of c-Myb that could be exploited to target c-Myb function in pre-B-ALL is C/EBP-β, which has been demonstrated to be essential for activation of myeloid specific genes such as *mim-1* via interactions with both c-Myb and v-Myb (Mink et al., 1996; Ness et al., 1993). As C/EBP-β has primarily been associated with myeloid-specific gene expression,

the interaction between c-Myb and C/EBP-β could be verified in large pre-B cells through *in vitro* co-immunoprecipitation experiments. Then, experiments to identify small molecule inhibitors targeting this interaction in pre-B-ALL could be initiated with compounds that have previously been identified as inhibitors of C/EBP-β. In fact, Klempnauer and colleagues have identified a role for Celastrol as well as two other compounds, Withaferin A, and Helenalin Acetate in interfering with interactions of C/EBP-β with both c-Myb and p300 (Coulibaly et al., 2018; Falkenberg et al., 2017; Jakobs et al., 2016). As another approach to more specifically target the interaction of C/EBP-β with c-Myb and thus, minimize potential off-target effects, a peptidomimetic inhibitor could be designed as previously reported (Ramaswamy et al., 2018). Briefly, one could utilize knowledge of the crystal structure of the c-Myb and C/EBP-β interaction as previously described (Tahirov et al., 2002) to identify critical residues of c-Myb important for binding to C/EBP-β which could be used to design a peptidomimetic inhibitor that would specifically interfere with these residues. The c-Myb and C/EBP-β interaction occurs through the R2 subdomain of the c-Myb DBD and it was demonstrated that mutations to the I91, L106, and V117 residues prevented binding to C/EBP-β such that a peptide could be designed to compete with binding to this region of c-Myb. Then, the ability of the previously characterized small molecule inhibitors or peptidomimetic inhibitor described above to control c-Myb activity and proliferation/differentiation of pre-B-ALL cells could be assayed as described above for p300. Altogether, this approach could be applied to other co-activator proteins that interact with c-Myb such as p100 to exploit these interactions as a method of modulating c-Myb activity in pre-B-ALL.

The c-Myb protein is modified by a number of post-translational modifications including phosphorylation, acetylation, ubiquitination, and sumoylation (Aziz et al., 1995; Bies et al., 2002; Miglarese et al., 1996; Sano and Ishii, 2001). However, the outcomes of many of these

modifications on c-Myb function and, in particular, to c-Myb function in leukemia are poorly understood and represent potentially druggable targets for pre-B-ALL. For example, c-Myb is phosphorylated at Ser528 of the NRD by $p42^{MAPK}$ *in vitro,* and mutation of this site alters the ability of c-Myb to transactivate different target promoters, suggesting that it may be an important for c-Myb function *in vivo* (Aziz et al., 1995; Miglarese et al., 1996). Pim1 has been demonstrated to phosphorylate the c-Myb DBD and also to interact with p100 and promote c-Myb transcriptional activity in a p100-dependent manner (Leverson et al., 1998; Winn et al., 2003). In addition, phosphorylation adjacent to a sumoylation site at Thr486 by $p38^{MAPK}$ led to repression of c-Myb sumoylation and prevented negative regulation of c-Myb transcriptional activity under conditions of cellular stress (Bies et al., 2013). For each of these kinases, there are commercially available inhibitors which could be tested for their ability to interfere with post-translational modification of c-Myb. In addition, the sites themselves could be targeted directly through CRISPR-mediated mutagenesis. Then these approaches could be tested for their ability to alter c-Myb activity, decrease proliferation, and promote differentiation of pre-B-ALL cells. In addition, testing the effect of interfering with post-translational modifications of c-Myb for leukemia therapy could help to better understand their overall role in c-Myb function.

In conclusion, the work in this thesis utilizes genome-wide analysis to identify critical roles for c-Myb in survival, proliferation, metabolism, and differentiation during early B cell development at the pro-B and large pre-B cell stages. This work is the first to characterize a role for c-Myb in maintaining glucose uptake/utilization, proliferation, and survival within the large pre-B cell compartment while preventing premature differentiation to the small pre-B cell compartment. In addition, this thesis describes a previously unappreciated function of c-Myb in regulating the initial steps of glucose metabolism across the pre-BCR checkpoint. Future studies

to determine which of the c-Myb-regulated genes we have identified are direct targets that mediate c-Myb activity in early B cell developmental stages will be crucial to develop the network of c-Myb-regulated genes throughout B-lineage development. Furthermore, understanding how c-Myb-regulated genes function in the development and maintenance of B-cell leukemias will likely be important for the development of targeted therapies for c-Myb-mediated leukemogenesis.

References

Abdelrasoul, H., Werner, M., Setz, C.S., Okkenhaug, K., and Jumaa, H. (2018). PI3K induces B-cell development and regulates B cell identity. Sci. Rep. *8*, 1–15.

Adolfsson, J., Johan Borge, O., Bryder, D., Theilgaard-Monch, K., Astrand-Grundstrom, I., Sitnicka, E., Sasaki, Y., and Jacobsen, S.E.W. (2001). Upregulation of Flt3 Expression within the Bone Marrow Lin-Sca1+c-kit+ Stem Cell Compartment Is Accompanied by Loss of Self-Renewal Capacity. Immunity *15*, 659–669.

Adolfsson, J., Mansson, R., Buza-Vidas, N., Hultquist, A., Liuba, K., Jensen, C.T., Bryder, D., Yang, L., Borge, O.J., Thoren, L.A.M., et al. (2005). Identification of Flt3+ Lympho-Myeloid Stem Cells Lacking Erythro-Megakaryocytic Potential. Cell *121*, 295–306.

Allen III, R.D., Bender, T.P., and Siu, G. (1999). c-Myb is essential for early T cell development. Genes & Dev. *13*, 1073–1078.

Allman, D., and Pillai, S. (2008). Peripheral B cell subsets. Curr. Opin. Immunol. *20*, 149–157.

Alm-Kristiansen, A.H., Lorenzo, P.I., Molværsmyr, A.-K., Matre, V., Ledsaak, M., Sæther, T., and Gabrielsen, O.S. (2011). PIAS1 interacts with FLASH and enhances its co-activation of c-Myb. Mol. Cancer *10*, 21.

Alt, F.W., Yancopoulos, G.D., Blackwell, T.K., Wood, C., Thomas, E., Boss, M., Coffman, R., Rosenberg, N., Tonegawa, S., and Baltimore, D. (1984). Ordered rearrangement of immunoglobulin heavy chain variable region segments. EMBO J. *3*, 1209–1219.

Altman, B.J., and Rathmell, J.C. (2012). Metabolic stress in autophagy and cell death pathways. Cold Spring Harb. Perspect. Biol. *4*, a008763–a008763.

Anders, S., Pyl, P.T., and Huber, W. (2015). HTSeq--a Python framework to work with high-

throughput sequencing data. Bioinformatics *31*, 166–169.

Arellano, M., and Moreno, S. (1997). Regulation of CDK/cyclin complexes during the cell cycle. Int. J. Biochem. & Cell Biol. *29*, 559–573.

Asano, T., Katagiri, H., Takata, K., Lin, J.L., Ishihara, H., Inukai, K., Tsukuda, K., Kikuchi, M., Hirano, H., and Yazaki, Y. (1991). The role of N-glycosylation of GLUT1 for glucose transport activity. J. Biol. Chem. *266*, 24632–24636.

Ashkenazi, A., and Dixit, V.M. (1998). Death receptors: signaling and modulation. Science (80-.). *281*, 1305–1308.

Augustin, R. (2010). The protein family of glucose transport facilitators: It's not only about glucose after all. IUBMB Life *447*, NA-NA.

Aziz, N., Miglarese, M.R., Hendrickson, R.C., Shabanowitz, J., Sturgill, T.W., Hunt, D.F., and Bender, T.P. (1995). Modulation of c-Myb-induced transcription activation by a phosphorylation site near the negative regulatory domain. Proc. Natl. Acad. Sci. *92*, 6429–6433.

Bain, G., Robanus Maandag, E.C., te Riele, H.P., Feeney, A.J., Sheehy, A., Schlissel, M., Shinton, S.A., Hardy, R.R., and Murre, C. (1997). Both E12 and E47 allow commitment to the B cell lineage. Immunity *6*, 145–154.

Baird, A.M., Gerstein, R.M., and Berg, L.J. (1999). The role of cytokine receptor signaling in lymphocyte development. Curr. Opin. Immunol. *11*, 157–166.

Baker, S.J., Kumar, A., and Reddy, E.P. (2010). p89c-Myb is not required for fetal or adult hematopoiesis. Genesis *48*, 309–316.

Barboric, M., Nissen, R.M., Kanazawa, S., Jabrane-ferrat, N., Peterlin, B.M., and Francisco, S. (2001). NF- κ B Binds P-TEFb to Stimulate Transcriptional Elongation by RNA Polymerase II

University of California at San Francisco Medical Faculty of the University of Ljubljana. Mol. Cell *8*, 327–337.

Barnum, K.J., and O'Connell, M.J. (2014). Cell Cycle Regulation by Checkpoints. In Cell Cycle Control, (New York, NY: Springer New York), pp. 29–40.

Barski, A., Cuddapah, S., Cui, K., Roh, T.Y., Schones, D.E., Wang, Z., Wei, G., Chepelev, I., and Zhao, K. (2007). High-Resolution Profiling of Histone Methylations in the Human Genome. Cell *129*, 823–837.

Barthel, A., Okino, S.T., Liao, J., Nakatani, K., Li, J., Whitlock, J.P., and Roth, R.A. (1999). Regulation of GLUT1 gene transcription by the serine/threonine kinase Akt1. J. Biol. Chem. *274*, 20281–20286.

Basso, K., Schneider, C., Shen, Q., Holmes, A.B., Setty, M., Leslie, C., and Dalla-Favera, R. (2012). BCL6 positively regulates AID and germinal center gene expression via repression of miR-155. J. Exp. Med. *209*, 2455–2465.

Baumgarth, N. (2011). The double life of a B-1 cell: self-reactivity selects for protective effector functions. Nat. Publ. Gr. *11*, 34–46.

Bednarski, J.J., Nickless, A., Bhattacharya, D., Amin, R.H., Schlissel, M.S., and Sleckman, B.P. (2012). RAG-induced DNA double-strand breaks signal through Pim2 to promote pre-B cell survival and limit proliferation. J. Exp. Med. *209*, 11–17.

Belli, B., Wolff, L., Nazarov, V., and Fan, H. (1995). Proviral activation of the c-myb proto-oncogene is detectable in preleukemic mice infected neonatally with Moloney murine leukemia virus but not in resulting end stage T lymphomas. J. Virol. *69*, 5138–5141.

Ben-Sahra, I., Howell, J.J., Asara, J.M., and Manning, B.D. (2013). Stimulation of de novo

pyrimidine synthesis by growth signaling through mTOR and S6K1. Science (80-.). *339*, 1323–1328.

Ben-Sahra, I., Hoxhaj, G., Ricoult, S.J.H., Asara, J.M., and Manning, B.D. (2016). mTORC1 induces purine synthesis through control of the mitochondrial tetrahydrofolate cycle. Science (80-.). *351*, 728–733.

Bender, T.P., and Kuehl, W.M. (1987). Differential expression of the c-myb proto-oncogene marks the pre-B cell/B cell junction in murine B lymphoid tumors. J. Immunol. *139*, 3822–3827.

Bender, T.P., Kremer, C.S., Kraus, M., Buch, T., and Rajewsky, K. (2004). Critical functions for c-Myb at three checkpoints during thymocyte development. Nat. Immunol. *5*, 721–729.

Bengtsen, M., Klepper, K., Gundersen, S., Cuervo, I., Drabløs, F., Hovig, E., Sandve, G.K., Gabrielsen, O.S., and Eskeland, R. (2015). c-Myb Binding Sites in Haematopoietic Chromatin Landscapes. PLoS One *10*, e0133280.

Bentley, J., Itchayanan, D., Barnes, K., McIntosh, E., Tang, X., Downes, C.P., Holman, G.D., Whetton, A.D., Owen-Lynch, P.J., and Baldwin, S.A. (2003). Interleukin-3-mediated Cell Survival Signals Include Phosphatidylinositol 3-Kinase-dependent Translocation of the Glucose Transporter GLUT1 to the Cell Surface. J. Biol. Chem. *278*, 39337–39348.

Berge, T., Matre, V., Brendeford, E.M., Sæther, T., Lüscher, B., and Gabrielsen, O.S. (2007). Revisiting a selection of target genes for the hematopoietic transcription factor c-Myb using chromatin immunoprecipitation and c-Myb knockdown. Blood Cells, Mol. Dis. *39*, 278–286.

Bertolino, E., Reddy, K., Medina, K.L., Parganas, E., Ihle, J., and Singh, H. (2005). Regulation of interleukin 7-dependent immunoglobulin heavy-chain variable gene rearrangements by transcription factor STAT5. Nat. Immunol. *6*, 836–843.

Biedenkapp, H., Borgmeyer, U., Sippel, A.E., and Klempnauer, K.H. (1988). Viral myb oncogene encodes a sequence-specific DNA-binding activity. Nat. … *335*, 835–837.

Bies, J., Markus, J., and Wolff, L. (2002). Covalent Attachment of the SUMO-1 Protein to the Negative Regulatory Domain of the c-Myb Transcription Factor Modifies Its Stability and Transactivation Capacity. J. Biol. Chem. *277*, 8999–9009.

Bies, J., Sramko, M., and Wolff, L. (2013). Stress-induced phosphorylation of Thr486 in c-Myb by p38 mitogen-activated protein kinases attenuates conjugation of SUMO-2/3. J. Biol. Chem. *288*, 36983–36993.

Boag, J.M., Beesley, A.H., Firth, M.J., Freitas, J.R., Ford, J., Hoffmann, K., Cummings, A.J., de Klerk, N.H., and Kees, U.R. (2006). Altered glucose metabolism in childhood pre-B acute lymphoblastic leukaemia. Leukemia *20*, 1731–1737.

Boehm, T., and Swann, J.B. (2014). Origin and Evolution of Adaptive Immunity. Annu. Rev. Anim. Biosci. *2*, 259–283.

Borghesi, L., Aites, J., Nelson, S., Lefterov, P., James, P., and Gerstein, R. (2005). E47 is required for V(D)J recombinase activity in common lymphoid progenitors. J. Exp. Med. *202*, 1669–1677.

Boyer, L.A., Plath, K., Zeitlinger, J., Brambrink, T., Medeiros, L.A., Lee, T.I., Levine, S.S., Wernig, M., Tajonar, A., Ray, M.K., et al. (2006). Polycomb complexes repress developmental regulators in murine embryonic stem cells. Nature *441*, 349–353.

Brubaker, S.W., Bonham, K.S., Zanoni, I., and Kagan, J.C. (2015). Innate Immune Pattern Recognition: A Cell Biological Perspective. Annu. Rev. Immunol. *33*, 257–290.

Buenrostro, J.D., Wu, B., Chang, H.Y., and Greenleaf, W.J. (2015). ATAC-seq: A Method for Assaying Chromatin Accessibility Genome-Wide. Curr. Protoc. Mol. Biol. *109*, 21.29.1-9.

Cánepa, E.T., Scassa, M.E., Ceruti, J.M., Marazita, M.C., Carcagno, A.L., Sirkin, P.F., and Ogara, M.F. (2007). INK4 proteins, a family of mammalian CDK inhibitors with novel biological functions. IUBMB Life *59*, 419–426.

Carpinelli, M.R., Hilton, D.J., Metcalf, D., Antonchuk, J.L., Hyland, C.D., Mifsud, S.L., Di Rago, L., Hilton, A.A., Willson, T.A., Roberts, A.W., et al. (2004). Suppressor screen in Mpl-/- mice: c-Myb mutation causes supraphysiological production of platelets in the absence of thrombopoietin signaling. Proc. Natl. Acad. Sci. *101*, 6553–6558.

Carvalho, B.S., and Irizarry, R.A. (2010). A framework for oligonucleotide microarray preprocessing. Bioinformatics *26*, 2363–2367.

Cerqueira, A., Martín, A., Symonds, C.E., Odajima, J., Dubus, P., Barbacid, M., and Santamaría, D. (2014). Genetic characterization of the role of the Cip/Kip family of proteins as cyclin-dependent kinase inhibitors and assembly factors. Mol. Cell. Biol. *34*, 1452–1459.

Cerutti, A., Cols, M., and Puga, I. (2013). Marginal zone B cells: virtues of innate- like antibody-producing lymphocytes. Nat. Publ. Gr. *13*, 118–132.

Cesi, V., Casciati, A., Sesti, F., Tanno, B., Calabretta, B., and Raschellà, G. (2014). TGFβ-induced c-Myb affects the expression of EMT-associated genes and promotes invasion of ER +breast cancer cells. Cell Cycle *10*, 4149–4161.

Chan, L.N., Chen, Z., Braas, D., Lee, J.-W., Xiao, G., Geng, H., Cosgun, K.N., Hurtz, C., Shojaee, S., Cazzaniga, V., et al. (2017). Metabolic gatekeeper function of B-lymphoid transcription factors. Nat. Publ. Gr. *542*, 479–483.

Chen, C., Nagy, Z., Radic, M.Z., Hardy, R.R., Huszar, D., Camper, S.A., and Weigert, M. (1995). The site and stage of anti-DNA B-cell deletion. Nat. … *373*, 252–255.

Chen, J., Kremer, C.S., and Bender, T.P. (2002). A Myb dependent pathway maintains Friend murine erythroleukemia cells in an immature and proliferating state. Oncogene *21*, 1859–1869.

Chen, L., Willis, S.N., Wei, A., Smith, B.J., Fletcher, J.I., Hinds, M.G., Colman, P.M., Day, C.L., Adams, J.M., and Huang, D.C.S. (2005). Differential targeting of prosurvival Bcl-2 proteins by their BH3-only ligands allows complementary apoptotic function. Mol. Cell *17*, 393–403.

Cheng, A.M., Rowley, B., Pao, W., Hayday, A., Bolen, J.B., and Pawson, T. (1995). Syk tyrosine kinase required for mouse viability and B-cell development. Nat. … *378*, 303–306.

Cheng, Y., Chikwava, K., Wu, C., Zhang, H., Bhagat, A., Pei, D., Choi, J.K., and Tong, W. (2016). LNK/SH2B3 regulates IL-7 receptor signaling in normal and malignant B-progenitors. J. Clin. Invest. *126*, 1267–1281.

Chi, M.M.-Y., Pingsterhaus, J., Carayannopoulos, M., and Moley, K.H. (2000). Decreased Glucose Transporter Expression Triggers BAX-dependent Apoptosis in the Murine Blastocyst. J. Biol. Chem. *275*, 40252–40257.

Chipuk, J.E., Moldoveanu, T., Llambi, F., Parsons, M.J., and Green, D.R. (2010). The BCL-2 family reunion. Mol. Cell *37*, 299–310.

Chowdhury, D., and Sen, R. (2001). Stepwise activation of the immunoglobulin mu heavy chain gene locus. EMBO J. *20*, 6394–6403.

Civelekoglu-Scholey, G., and Cimini, D. (2014). Modelling chromosome dynamics in mitosis: a historical perspective on models of metaphase and anaphase in eukaryotic cells. Interface Focus *4*, 20130073–20130079.

Clappier, E., Cuccuini, W., Kalota, A., Crinquette, A., Cayuela, J.-M., Dik, W.A., Langerak, A.W., Montpellier, B., Nadel, B., Walrafen, P., et al. (2007). The C-MYB locus is involved in

chromosomal translocation and genomic duplications in human T-cell acute leukemia (T-ALL), the translocation defining a new T-ALL subtype in very young children. Blood *110*, 1251–1261.

Clark, M.R., Mandal, M., Ochiai, K., and Singh, H. (2014). Orchestrating B cell lymphopoiesis through interplay of IL-7 receptor and pre-B cell receptor signalling. Nat. Rev. Immunol. *14*, 69–80.

Clarke, M.F., Kukowska-Latallo, J.F., Westin, E., Smith, M., and Prochownik, E. V (1988). Constitutive expression of a c-myb cDNA blocks Friend murine erythroleukemia cell differentiation. Mol. Cell. Biol. *8*, 884–892.

Cogswell, J.P., Cogswell, P.C., Kuehl, W.M., Cuddihy, A.M., Bender, T.M., Engelke, U., Marcu, K.B., and Ting, J.P. (1993). Mechanism of c-myc regulation by c-Myb in different cell lineages. Mol. Cell. Biol. *13*, 2858–2869.

Cooper, A.B., Sawai, C.M., Sicinska, E., Powers, S.E., Sicinski, P., Clark, M.R., and Aifantis, I. (2006). A unique function for cyclin D3 in early B cell development. Nat. Immunol. *7*, 489–497.

Corfe, S.A., and Paige, C.J. (2012). The many roles of IL-7 in B cell development; mediator of survival, proliferation and differentiation. Semin. Immunol. *24*, 198–208.

Corfe, S.A., Rottapel, R., and Paige, C.J. (2011). Modulation of IL-7 Thresholds by SOCS Proteins in Developing B Lineage Cells. J. Immunol. *187*, 3499–3510.

Coulibaly, A., Haas, A., Steinmann, S., Jakobs, A., Schmidt, T.J., and Klempnauer, K.H. (2018). The natural anti-tumor compound Celastrol targets a Myb-C/EBP?-p300 transcriptional module implicated in myeloid gene expression. PLoS One *13*, 1–18.

Croker, B.A., Kiu, H., and Nicholson, S.E. (2008). SOCS regulation of the JAK/STAT signalling pathway. Semin. Cell & Dev. Biol. *19*, 414–422.

Cuddihy, A.E., Brents, L.A., Aziz, N., Bender, T.P., and Kuehl, W.M. (1993). Only the DNA binding and transactivation domains of c-Myb are required to block terminal differentiation of murine erythroleukemia cells. Mol. Cell. Biol. *13*, 3505–3513.

Dai, P., Akimaru, H., Tanaka, Y., Hou, D.X., Yasukawa, T., Kanei-Ishii, C., Takahashi, T., and Ishii, S. (1996). CBP as a transcriptional coactivator of c-Myb. Genes & Dev. *10*, 528–540.

Dash, A.B., Orrico, F.C., and Ness, S.A. (1996). The EVES motif mediates both intermolecular and intramolecular regulation of c-Myb. Genes & Dev. *10*, 1858–1869.

Dassé, E., Volpe, G., Walton, D.S., Wilson, N., Del Pozzo, W., O'Neill, L.P., Slany, R.K., Frampton, J., and Dumon, S. (2012). Distinct regulation of c-myb gene expression by HoxA9, Meis1 and Pbx proteins in normal hematopoietic progenitors and transformed myeloid cells. Blood Cancer J. *2*, e76–e76.

Datta, S.R., Dudek, H., Tao, X., Masters, S., Fu, H., Gotoh, Y., and Greenberg, M.E. (1997). Akt phosphorylation of BAD couples survival signals to the cell-intrinsic death machinery. Cell *91*, 231–241.

DeBerardinis, R.J., Lum, J.J., Hatzivassiliou, G., and Thompson, C.B. (2008). The Biology of Cancer: Metabolic Reprogramming Fuels Cell Growth and Proliferation. Cell Metab. *7*, 11–20.

Decker, D.J., Boyle, N.E., and Klinman, N.R. (1991). Predominance of nonproductive rearrangements of VH81X gene segments evidences a dependence of B cell clonal maturation on the structure of nascent H chains. J. Immunol. *147*, 1406–1411.

DeKoter, R.P., Lee, H.-J., and Singh, H. (2002). PU.1 regulates expression of the interleukin-7 receptor in lymphoid progenitors. Immunity *16*, 297–309.

Deprez, J., Vertommen, D., Alessi, D.R., Hue, L., and Rider, M.H. (1997). Phosphorylation and

activation of heart 6-phosphofructo-2-kinase by protein kinase B and other protein kinases of the insulin signaling cascades. J. Biol. Chem. *272*, 17269–17275.

Desiderio, S. V, Yancopoulos, G.D., Paskind, M., Thomas, E., Boss, M.A., Landau, N., Alt, F.W., and Baltimore, D. (1984). Insertion of N regions into heavy-chain genes is correlated with expression of terminal deoxytransferase in B cells. Nat. … *311*, 752–755.

Dias, S., D'Amico, A., Cretney, E., Liao, Y., Tellier, J., Bruggeman, C., Almeida, F.F., Leahy, J., Belz, G.T., Smyth, G.K., et al. (2017). Effector Regulatory T Cell Differentiation and Immune Homeostasis Depend on the Transcription Factor Myb. Immunity *46*, 78–91.

Dibble, C.C., and Cantley, L.C. (2015). Regulation of mTORC1 by PI3K signaling. Trends Cell Biol. *25*, 545–555.

Dibble, C.C., and Manning, B.D. (2013). Signal integration by mTORC1 coordinates nutrient input with biosynthetic output. Nat. Publ. Gr. *15*, 555–564.

Dijkers, P.F., Medema, R.H., Pals, C., Banerji, L., Thomas, N.S., Lam, E.W., Burgering, B.M., Raaijmakers, J.A., Lammers, J.W., Koenderman, L., et al. (2000). Forkhead transcription factor FKHR-L1 modulates cytokine-dependent transcriptional regulation of p27(KIP1). Mol. Cell. Biol. *20*, 9138–9148.

Dobin, A., Davis, C.A., Schlesinger, F., Drenkow, J., Zaleski, C., Jha, S., Batut, P., Chaisson, M., and Gingeras, T.R. (2013). STAR: ultrafast universal RNA-seq aligner. Bioinformatics *29*, 15–21.

Donnelly, R.P., and Finlay, D.K. (2015). Glucose, glycolysis and lymphocyte responses. Mol. Immunol. *68*, 513–519.

Doughty, C.A., Bleiman, B.F., Wagner, D.J., Dufort, F.J., Mataraza, J.M., Roberts, M.F., and Chiles, T.C. (2006). Antigen receptor–mediated changes in glucose metabolism in B lymphocytes:

role of phosphatidylinositol 3-kinase signaling in the glycolytic control of growth. Blood *107*, 4458–4465.

Drabsch, Y., Hugo, H., Zhang, R., Dowhan, D.H., Miao, Y.R., Gewirtz, A.M., Barry, S.C., Ramsay, R.G., and Gonda, T.J. (2007). Mechanism of and requirement for estrogen-regulated MYB expression in estrogen-receptor-positive breast cancer cells. Proc. Natl. Acad. Sci. U. S. A. *104*, 13762–13767.

Duprey, S.P., and Boettiger, D. (1985). Developmental regulation of c-myb in normal myeloid progenitor cells. Proc. Natl. Acad. Sci. *82*, 6937–6941.

Düvel, K., Yecies, J.L., Menon, S., Raman, P., Lipovsky, A.I., Souza, A.L., Triantafellow, E., Ma, Q., Gorski, R., Cleaver, S., et al. (2010). Activation of a Metabolic Gene Regulatory Network Downstream of mTOR Complex 1. *39*, 171–183.

Elstrom, R.L., Bauer, D.E., Buzzai, M., Karnauskas, R., Harris, M.H., Plas, D.R., Zhuang, H., Cinalli, R.M., Alavi, A., Rudin, C.M., et al. (2004). Akt stimulates aerobic glycolysis in cancer cells. Cancer Res. *64*, 3892–3899.

Emambokus, N., Vegiopoulos, A., Harman, B., Jenkinson, E., Anderson, G., and Frampton, J. (2003). Progression through key stages of haemopoiesis is dependent on distinct threshold levels of c-Myb. EMBO J. *22*, 4478–4488.

Engel, H., Rolink, A., and Weiss, S. (1999). B cells are programmed to activate kappa and lambda for rearrangement at consecutive developmental stages. Eur. J. Immunol. *29*, 2167–2176.

Erlacher, M., Labi, V., Manzl, C., Böck, G., Tzankov, A., Häcker, G., Michalak, E., Strasser, A., and Villunger, A. (2006). Puma cooperates with Bim, the rate-limiting BH3-only protein in cell death during lymphocyte development, in apoptosis induction. J. Exp. Med. *203*, 2939–2951.

Ess, K.C., Witte, D.P., Bascomb, C.P., and Aronow, B.J. (1999). Diverse developing mouse lineages exhibit high-level c-Myb expression in immature cells and loss of expression upon differentiation. Oncogene *18*, 1103–1111.

Eswaran, J., Sinclair, P., Heidenreich, O., Irving, J., Russell, L.J., Hall, A., Calado, D.P., Harrison, C.J., and Vormoor, J. (2015). The pre-B-cell receptor checkpoint in acute lymphoblastic leukaemia. Leukemia *29*, 1623–1631.

Fahl, S.P., Crittenden, R.B., Allman, D., and Bender, T.P. (2009). c-Myb is required for pro-B cell differentiation. J. Immunol. *183*, 5582–5592.

Fahl, S.P., Daamen, A.R., Crittenden, R.B., and Bender, T.P. (2018). c-Myb Coordinates Survival and the Expression of Genes That Are Critical for the Pre-BCR Checkpoint. J. Immunol. ji1302303.

Falkenberg, K.D., Jakobs, A., Matern, J.C., Dörner, W., Uttarkar, S., Trentmann, A., Steinmann, S., Coulibaly, A., Schomburg, C., Mootz, H.D., et al. (2017). Withaferin A, a natural compound with anti-tumor activity, is a potent inhibitor of transcription factor C/EBPβ. Biochim. Biophys. Acta - Mol. Cell Res. *1864*, 1349–1358.

Fan, Y., Dickman, K.G., and Zong, W.-X. (2010). Akt and c-Myc differentially activate cellular metabolic programs and prime cells to bioenergetic inhibition. J. Biol. Chem. *285*, 7324–7333.

Ferreirós-Vidal, I., Carroll, T., Taylor, B., Terry, A., Liang, Z., Bruno, L., Dharmalingam, G., Khadayate, S., Cobb, B.S., Smale, S.T., et al. (2013). Genome-wide identification of Ikaros targets elucidates its contribution to mouse B-cell lineage specification and pre-B-cell differentiation. Blood *121*, 1769–1782.

Ferreirós-Vidal, I., Carroll, T., Zhang, T., Lagani, V., Ramirez, R.N., Ing-Simmons, E., Gómez-

Valadés, A.G., Cooper, L., Liang, Z., Papoutsoglou, G., et al. (2019). Feedforward regulation of Myc coordinates lineage-specific with housekeeping gene expression during B cell progenitor cell differentiation. PLoS Biol. *17*, e2006506-28.

Fistonich, C., Zehentmeier, S., Bednarski, J.J., Miao, R., Schjerven, H., Sleckman, B.P., and Pereira, J.P. (2018). Cell circuits between B cell progenitors and IL-7 +mesenchymal progenitor cells control B cell development. J. Exp. Med. *163*, jem.20180778-15.

Fleming, H.E., and Paige, C.J. (2001). Pre-B cell receptor signaling mediates selective response to IL-7 at the pro-B to pre-B cell transition via an ERK/MAP kinase-dependent pathway. Immunity *15*, 521–531.

Frampton, J., Kouzarides, T., Doderlein, G., Graf, T., and Weston, K. (1993). Influence of the v-Myb transactivation domain on the oncoprotein's transformation specificity. EMBO J. *12*, 1333–1341.

Francisco A Bonilla MD, P., and Hans C Oettgen MD, P. (2010). Adaptive immunity. J. Allergy Clin. Immunol. *125*, S33–S40.

Fridman, Y., Palgi, N., Dovrat, D., Ben-Aroya, S., Hieter, P., and Aharoni, A. (2010). Subtle Alterations in PCNA-Partner Interactions Severely Impair DNA Replication and Repair. PLoS Biol. *8*, e1000507-15.

Fruman, D.A., and Limon, J.J. (2012). Akt and mTOR in B Cell Activation and Differentiation. Front. Immunol. *3*, 1–12.

Fruman, D.A., Snapper, S.B., Yballe, C.M., Davidson, L., Yu, J.Y., Alt, F.W., and Cantley, L.C. (1999). Impaired B Cell Development and Proliferation in Absence of Phosphoinositide 3-Kinase p85alpha. Science (80-.). *283*, 1–6.

Gallagher, P., Bao, Y., Serrano, S.M.T., Laing, G.D., Theakston, R.D.G., Gutierrez, J.M., Escalante, T., Zigrino, P., Moura-da-Silva, A.M., Nischt, R., et al. (2005). Role of the snake venom toxin jararhagin in proinflammatory pathogenesis: in vitro and in vivo gene expression analysis of the effects of the toxin. Arch. Biochem. Biophys. *441*, 1–15.

Ganter, B., Fu, S. l, and Lipsick, J.S. (1998). D-type cyclins repress transcriptional activation by the v-Myb but not the c-Myb DNA-binding domain. EMBO J. *17*, 255–268.

García, P., and Frampton, J. (2006). The transcription factor B-Myb is essential for S-phase progression and genomic stability in diploid and polyploid megakaryocytes. J. Cell Sci. *119*, 1483–1493.

Gavathiotis, E., Suzuki, M., Davis, M.L., Pitter, K., Bird, G.H., Katz, S.G., Tu, H.-C., Kim, H., Cheng, E.H.Y., Tjandra, N., et al. (2008). BAX activation is initiated at a novel interaction site. Nat. … *455*, 1076–1081.

Ge, Z., Gu, Y., Xiao, L., Han, Q., Li, J., Chen, B., Yu, J., Kawasawa, Y.I., Payne, K.J., Dovat, S., et al. (2016). Co-existence of IL7R high and SH2B3 low expression distinguishes a novel high-risk acute lymphoblastic leukemia with Ikaros dysfunction. Oncotarget *7*, 46014–46027.

Geier, J.K., and Schlissel, M.S. (2006). Pre-BCR signals and the control of Ig gene rearrangements. Semin. Immunol. *18*, 31–39.

Georgopoulos, K. (2017). The making of a lymphocyte: the choice among disparate cell fates and the IKAROS enigma. Genes & Dev. *31*, 439–450.

Georgopoulos, K., Bigby, M., Wang, J.H., Molnár, A., Cell, P.W., and 1994 (1994). The Ikaros gene is required for the development of all lymphoid lineages. Elsevier *79*, 143–156.

Girard, F., Strausfeld, U., Fernandez, A., and Lamb, N.J. (1991). Cyclin A is required for the onset

of DNA replication in mammalian fibroblasts. Cell *67*, 1169–1179.

Glotzer, M., Murray, A.W., and Kirschner, M.W. (1991). Cyclin is degraded by the ubiquitin pathway. Nat. … *349*, 132–138.

Goetzman, E.S., and Prochownik, E. V (2018). The Role for Myc in Coordinating Glycolysis, Oxidative Phosphorylation, Glutaminolysis, and Fatty Acid Metabolism in Normal and Neoplastic Tissues. Front. Endocrinol. (Lausanne). *9*, 25–54.

Gonda, T.J., Buckmaster, C., and Ramsay, R.G. (1989). Activation of c-myb by carboxy-terminal truncation: relationship to transformation of murine haemopoietic cells in vitro. EMBO J. *8*, 1777–1783.

Goodnow, C.C., Crosbie, J., Adelstein, S., Lavoie, T.B., Smith-Gill, S.J., Brink, R.A., Pritchard-Briscoe, H., Wotherspoon, J.S., Loblay, R.H., and Raphael, K. (1988). Altered immunoglobulin expression and functional silencing of self-reactive B lymphocytes in transgenic mice. Nat. … *334*, 676–682.

Gottlob, K., Majewski, N., Kennedy, S., Kandel, E., Robey, R.B., and Hay, N. (2001). Inhibition of early apoptotic events by Akt/PKB is dependent on the first committed step of glycolysis and mitochondrial hexokinase. Genes & Dev. *15*, 1406–1418.

Greig, K.T., Carotta, S., and Nutt, S.L. (2008). Critical roles for c-Myb in hematopoietic progenitor cells. Semin. Immunol. *20*, 247–256.

Greig, K.T., de Graaf, C.A., Murphy, J.M., Carpinelli, M.R., Pang, S.H.M., Frampton, J., Kile, B.T., Hilton, D.J., and Nutt, S.L. (2010). Critical roles for c-Myb in lymphoid priming and early B-cell development. Blood *115*, 2796–2805.

Grimsley, C. (2003). Cues for apoptotic cell engulfment: eat-me, don't eat-me and come-get-me

signals. Trends Cell Biol. *13*, 648–656.

Guglielmelli, P., Tozzi, L., Pancrazzi, A., Bogani, C., Antonioli, E., Ponziani, V., Poli, G., Zini, R., and Ferrari, S. (2007). MicroRNA expression profile in granulocytes from primary myelofibrosis patients. *35*, 1708–1718.

Guiley, K.Z., Liban, T.J., Felthousen, J.G., Ramanan, P., Litovchick, L., and Rubin, S.M. (2015). Structural mechanisms of DREAM complex assembly and regulation. Genes & Dev. *29*, 961–974.

Guloglu, F.B., Bajor, E., Smith, B.P., and Roman, C.A.J. (2005). The Unique Region of Surrogate Light Chain Component 5 Is a Heavy Chain-Specific Regulator of Precursor B Cell Receptor Signaling. J. Immunol. *175*, 358–366.

Habib, T., Park, H., Tsang, M., de Alboran, I.M., Nicks, A., Wilson, L., Knoepfler, P.S., Andrews, S., Rawlings, D.J., Eisenman, R.N., et al. (2007). Myc stimulates B lymphocyte differentiation and amplifies calcium signaling. J. Cell Biol. *179*, 717–731.

Hamel, K.M., Mandal, M., Karki, S., and Clark, M.R. (2014). Balancing Proliferation with Igκ Recombination during B-lymphopoiesis. Front. Immunol. *5*, 139.

Hanlon, L., Barr, N.I., Blyth, K., Stewart, M., Haviernik, P., Wolff, L., Weston, K., Cameron, E.R., and Neil, J.C. (2003). Long-Range Effects of Retroviral Insertion on c-myb: Overexpression May Be Obscured by Silencing during Tumor Growth In Vitro. J. Virol. *77*, 1059–1068.

Hardie, D.G., Ross, F.A., and Hawley, S.A. (2012). AMPK: a nutrient and energy sensor that maintains energy homeostasis. Nat. Rev. Mol. Cell Biol. *13*, 251–262.

Hardy, R.R., Carmack, C.E., Shinton, S.A., Kemp, J.D., and Hayakawa, K. (1991). Resolution and characterization of pro-B and pre-pro-B cell stages in normal mouse bone marrow. J. Exp. Med.

173, 1213–1225.

Hardy, R.R., Kincade, P.W., and Dorshkind, K. (2007). The protean nature of cells in the B lymphocyte lineage. Immunity *26*, 703–714.

Hartley, S.B., Cooke, M.P., Fulcher, D.A., Harris, A.W., Cory, S., Basten, A., and Goodnow, C.C. (1993). Elimination of self-reactive B lymphocytes proceeds in two stages: arrested development and cell death. Cell *72*, 325–335.

Vander Heiden, M.G., Plas, D.R., Rathmell, J.C., Fox, C.J., Harris, M.H., and Thompson, C.B. (2001). Growth Factors Can Influence Cell Growth and Survival through Effects on Glucose Metabolism. Mol. Cell. Biol. *21*, 5899–5912.

Vander Heiden, M.G., Cantley, L.C., and Thompson, C.B. (2009). Understanding the Warburg effect: the metabolic requirements of cell proliferation. Science (80-.). *324*, 1029–1033.

Heintzman, N.D., Stuart, R.K., Hon, G., Fu, Y., Ching, C.W., Hawkins, R.D., Barrera, L.O., Van Calcar, S., Qu, C., Ching, K.A., et al. (2007). Distinct and predictive chromatin signatures of transcriptional promoters and enhancers in the human genome. Nat. Genet. *39*, 311–318.

Heizmann, B., Kastner, P., and Chan, S. (2013). Ikaros is absolutely required for pre-B cell differentiation by attenuating IL-7 signals. J. Exp. Med. *210*, 2823–2832.

Helmink, B.A., and Sleckman, B.P. (2012). The Response to and Repair of RAG-Mediated DNA Double-Strand Breaks. *30*, 175–202.

Hendriks, R.W., and Middendorp, S. (2004). The pre-BCR checkpoint as a cell-autonomous proliferation switch. Trends Immunol. *25*, 249–256.

Hengartner, M.O. (2000). The biochemistry of apoptosis. Nat. … *407*, 770–776.

Hernandez-Munain, C., and Krangel, M.S. (1994). Regulation of the T-cell receptor delta enhancer by functional cooperation between c-Myb and core-binding factors. Mol. Cell. Biol. *14*, 473–483.

Herzog, S., Hug, E., Meixlsperger, S., Paik, J.-H., DePinho, R.A., Reth, M., and Jumaa, H. (2008). SLP-65 regulates immunoglobulin light chain gene recombination through the PI(3)K-PKB-Foxo pathway. Nat. Immunol. *9*, 623–631.

Herzog, S., Reth, M., and Jumaa, H. (2009). Regulation of B-cell proliferation and differentiation by pre-B-cell receptor signalling. Nat. Rev. Immunol. *9*, 195–205.

Hess, J., Werner, A., Wirth, T., Melchers, F., Jack, H.M., and Winkler, T.H. (2001). Induction of pre-B cell proliferation after de novo synthesis of the pre-B cell receptor. Proc. Natl. Acad. Sci. *98*, 1745–1750.

Hess, J.L., Bittner, C.B., Zeisig, D.T., Bach, C., Fuchs, U., Borkhardt, A., Frampton, J., and Slany, R.K. (2006). c-Myb is an essential downstream target for homeobox-mediated transformation of hematopoietic cells. Blood *108*, 297–304.

Hoffman-Liebermann, B., and Liebermann, D.A. (1991). Interleukin-6- and leukemia inhibitory factor-induced terminal differentiation of myeloid leukemia cells is blocked at an intermediate stage by constitutive c-myc. Mol. Cell. Biol. *11*, 2375–2381.

Hombach, J., Tsubata, T., Leclercq, L., Stappert, H., and Reth, M. (1990). Molecular components of the B-cell antigen receptor complex of the IgM class. Nat. … *343*, 760–762.

Hugo, H., Cures, A., Suraweera, N., Drabsch, Y., Purcell, D., Mantamadiotis, T., Phillips, W., Dobrovic, A., Zupi, G., Gonda, T.J., et al. (2006). Mutations in the MYB intron I regulatory sequence increase transcription in colon cancers. Genes, Chromosom. & Cancer *45*, 1143–1154.

Huntington, N.D., Labi, V., Cumano, A., Vieira, P., Strasser, A., Villunger, A., Di Santo, J.P., and Alves, N.L. (2009). Loss of the pro-apoptotic BH3-only Bcl-2 family member Bim sustains B lymphopoiesis in the absence of IL-7. Int. Immunol. *21*, 715–725.

Imtiyaz, H.Z., Rosenberg, S., Zhang, Y., Rahman, Z.S.M., Hou, Y.-J., Manser, T., and Zhang, J. (2006). The Fas-Associated Death Domain Protein Is Required in Apoptosis and TLR-Induced Proliferative Responses in B Cells. J. Immunol. *176*, 6852–6861.

Inlay, M.A., Bhattacharya, D., Sahoo, D., Serwold, T., Seita, J., Karsunky, H., Plevritis, S.K., Dill, D.L., and Weissman, I.L. (2009). Ly6d marks the earliest stage of B-cell specification and identifies the branchpoint between B-cell and T-cell development. Genes & Dev. *23*, 2376–2381.

Iwata, T.N., Ramírez, J.A., Tsang, M., Park, H., Margineantu, D.H., Hockenbery, D.M., and Iritani, B.M. (2016). Conditional Disruption of Raptor Reveals an Essential Role for mTORC1 in B Cell Development, Survival, and Metabolism. J. Immunol. 1600492.

Iwata, T.N., Ramírez-Komo, J.A., Park, H., and Iritani, B.M. (2017). Control of B lymphocyte development and functions by the mTOR signaling pathways. Cytokine & Growth Factor Rev. *35*, 47–62.

Iyer, D., and Rhind, N. (2017). The Intra-S Checkpoint Responses to DNA Damage. Genes (Basel). *8*, 25–74.

Izon, D.J., Punt, J.A., Xu, L., Karnell, F.G., Allman, D., Myung, P.S., Boerth, N.J., Pui, J.C., Koretzky, G.A., and Pear, W.S. (2001). Notch1 regulates maturation of CD4+ and CD8+ thymocytes by modulating TCR signal strength. Immunity *14*, 253–264.

Jakobs, A., Steinmann, S., Henrich, S.M., Schmidt, T.J., and Klempnauer, K.H. (2016). Helenalin

acetate, a natural sesquiterpene lactone with anti-inflammatory and anti-cancer activity, disrupts the cooperation of CCAAT box/enhancer-binding protein β (C/EBPβ) and co-activator p300. J. Biol. Chem. *291*, 26098–26108.

Jiang, H., Chang, F.-C., Ross, A.E., Lee, J., Nakayama, K., Nakayama, K., and Desiderio, S. (2005). Ubiquitylation of RAG-2 by Skp2-SCF Links Destruction of the V(D)J Recombinase to the Cell Cycle. Mol. Cell *18*, 699–709.

Jin, S., Zhao, H., Yi, Y., Nakata, Y., Kalota, A., and Gewirtz, A.M. (2010). c-Myb binds MLL through menin in human leukemia cells and is an important driver of MLL-associated leukemogenesis. J. Clin. Invest. *120*, 593–606.

Johnson, K., Hashimshony, T., Sawai, C.M., Pongubala, J.M.R., Skok, J.A., Aifantis, I., and Singh, H. (2008). Regulation of immunoglobulin light-chain recombination by the transcription factor IRF-4 and the attenuation of interleukin-7 signaling. Immunity *28*, 335–345.

Johnson, K., Chaumeil, J., Micsinai, M., Wang, J.M.H., Ramsey, L.B., Baracho, G. V, Rickert, R.C., Strino, F., Kluger, Y., Farrar, M.A., et al. (2012). IL-7 Functionally Segregates the Pro-B Cell Stage by Regulating Transcription of Recombination Mediators across Cell Cycle. *188*, 6084–6092.

Jones, R.G., Plas, D.R., Kubek, S., Buzzai, M., Mu, J., Xu, Y., Birnbaum, M.J., and Thompson, C.B. (2005). AMP-Activated Protein Kinase Induces a p53-Dependent Metabolic Checkpoint. Mol. Cell *18*, 283–293.

Joshi, I., Yoshida, T., Jena, N., Qi, X., Zhang, J., Van Etten, R.A., and Georgopoulos, K. (2014). Loss of Ikaros DNA-binding function confers integrin-dependent survival on pre-B cells and progression to acute lymphoblastic leukemia. Nat. Immunol. *15*, 294–304.

Kan, O., Baldwin, S.A., and Whetton, A.D. (1994). Apoptosis is regulated by the rate of glucose transport in an interleukin 3 dependent cell line. J. Exp. Med. *180*, 917–923.

Kanei-Ishii, C., MacMillan, E.M., Nomura, T., Sarai, A., Ramsay, R.G., Aimoto, S., Ishii, S., and Gonda, T.J. (1992). Transactivation and transformation by Myb are negatively regulated by a leucine-zipper structure. Proc. Natl. Acad. Sci. *89*, 3088–3092.

Kanei-Ishii, C., Ninomiya-Tsuji, J., Tanikawa, J., Nomura, T., Ishitani, T., Kishida, S., Kokura, K., Kurahashi, T., Ichikawa-Iwata, E., Kim, Y., et al. (2004). Wnt-1 signal induces phosphorylation and degradation of c-Myb protein via TAK1, HIPK2, and NLK. Genes & Dev. *18*, 816–829.

Kastner, P., Dupuis, A., Gaub, M.-P., Herbrecht, R., Lutz, P., and Chan, S. (2013). Function of Ikaros as a tumor suppressor in B cell acute lymphoblastic leukemia. Am. J. Blood Res. *3*, 1–13.

Kawano, Y., Yoshikawa, S., Minegishi, Y., and Karasuyama, H. (2006). Pre-B Cell Receptor Assesses the Quality of IgH Chains and Tunes the Pre-B Cell Repertoire by Delivering Differential Signals. J. Immunol. *177*, 2242–2249.

Kikuchi, K., Lai, A.Y., Hsu, C.-L., and Kondo, M. (2005). IL-7 receptor signaling is necessary for stage transition in adult B cell development through up-regulation of EBF. J. Exp. Med. *201*, 1197–1203.

Kikuchi, K., Kasai, H., Watanabe, A., Lai, A.Y., and Kondo, M. (2008). IL-7 Specifies B Cell Fate at the Common Lymphoid Progenitor to Pre-ProB Transition Stage by Maintaining Early B Cell Factor Expression. J. Immunol. *181*, 383–392.

Klempnauer, K.H., and Bishop, J.M. (1984). Neoplastic transformation by E26 leukemia virus is mediated by a single protein containing domains of gag and myb genes. J. Virol. *50*, 280–283.

Klempnauer, K.H., Gonda, T.J., Cell, J.M.B., and 1982 (1982). Nucleotide sequence of the retroviral leukemia gene v-myb and its cellular progenitor c-myb: the architecture of a transduced oncogene. Elsevier *31*, 453–463.

Klempnauer, K.H., Ramsay, G., Bishop, J.M., Moscovici, M.G., Moscovici, C., McGrath, J.P., and Levinson, A.D. (1983). The product of the retroviral transforming gene v-myb is a truncated version of the protein encoded by the cellular oncogene c-myb. Cell *33*, 345–355.

Kojima, H., Kobayashi, A., Sakurai, D., Kanno, Y., Hase, H., Takahashi, R., Totsuka, Y., Semenza, G.L., Sitkovsky, M. V, and Kobata, T. (2010). Differentiation stage-specific requirement in hypoxia-inducible factor-1alpha-regulated glycolytic pathway during murine B cell development in bone marrow. J. Immunol. *184*, 154–163.

Kondo, M., Weissman, I.L., and Akashi, K. (1997). Identification of clonogenic common lymphoid progenitors in mouse bone marrow. Cell *91*, 661–672.

Kumar, A., Baker, S.J., Lee, C.M., and Reddy, E.P. (2003). Molecular Mechanisms Associated with the Regulation of Apoptosis by the Two Alternatively Spliced Products of c-Myb. Mol. Cell. Biol. *23*, 6631–6645.

Kuo, T.C., and Schlissel, M.S. (2009). Mechanisms controlling expression of the RAG locus during lymphocyte development. Curr. Opin. Immunol. *21*, 173–178.

Labi, V., Erlacher, M., Kiessling, S., Manzl, C., Frenzel, A., O'Reilly, L., Strasser, A., and Villunger, A. (2008). Loss of the BH3-only protein Bmf impairs B cell homeostasis and accelerates gamma irradiation-induced thymic lymphoma development. J. Exp. Med. *205*, 641–655.

Lachaal, M., Spangler, R.A., and Jung, C.Y. (2001). Adenosine and adenosine triphosphate modulate the substrate binding affinity of glucose transporter GLUT1 in vitro. Biochim. Biophys.

Acta - Biomembr. *1511*, 123–133.

Lahortiga, I., De Keersmaecker, K., Van Vlierberghe, P., Graux, C., Cauwelier, B., Lambert, F., Mentens, N., Beverloo, H.B., Pieters, R., Speleman, F., et al. (2007). Duplication of the MYB oncogene in T cell acute lymphoblastic leukemia. Nat. Genet. *39*, 593–595.

Lang, G., White, J.R., Argent-Katwala, M.J.G., Allinson, C.G., and Weston, K. (2005). Myb proteins regulate the expression of diverse target genes. Oncogene *24*, 1375–1384.

Lee, Y.J., Chen, J.C., Amoscato, A.A., Bennouna, J., Spitz, D.R., Suntharalingam, M., and Rhee, J.G. (2001). Protective role of Bcl2 in metabolic oxidative stress-induced cell death. J. Cell Sci. *114*, 677–684.

Leprince, D., Gegonne, A., Coll, J., de Taisne, C., Schneeberger, A., Lagrou, C., and Stehelin, D. (1983). A putative second cell-derived oncogene of the avian leukaemia retrovirus E26. Nat. … *306*, 395–397.

Leverson, J.D., Koskinen, P.J., Orrico, F.C., Rainio, E.M., Jalkanen, K.J., Dash, A.B., Eisenman, R.N., and Ness, S.A. (1998). Pim-1 kinase and p100 cooperate to enhance c-Myb activity. Mol. Cell *2*, 417–425.

Lewis, B.C., Prescott, J.E., Campbell, S.E., Shim, H., Orlowski, R.Z., and Dang, C. V (2000). Tumor induction by the c-Myc target genes rcl and lactate dehydrogenase A. Cancer Res. *60*, 6178–6183.

Li, Y.-S., Wasserman, R., Hayakawa, K., and Hardy, R.R. (1996). Identification of the Earliest B Lineage Stage in Mouse Bone Marrow. Immunity *5*, 527–535.

Li, Z., Schulz, M.H., Look, T., Begemann, M., Zenke, M., and Costa, I.G. (2019). Identification of transcription factor binding sites using ATAC-seq. Genome Biol. *20*, 45.

Liberzon, A., Subramanian, A., Pinchback, R., Thorvaldsdottir, H., Tamayo, P., and Mesirov, J.P. (2011). Molecular signatures database (MSigDB) 3.0. Bioinformatics *27*, 1739–1740.

Liberzon, A., Birger, C., Thorvaldsdottir, H., Ghandi, M., Mesirov, J.P., and Tamayo, P. (2015). The Molecular Signatures Database Hallmark Gene Set Collection. Cell Syst. *1*, 417–425.

Lin, H., and Grosschedl, R. (1995). Failure of B-cell differentiation in mice lacking the transcription factor EBF. Nat. … *376*, 263–268.

Lipsick, J.S., and Wang, D.M. (1999). Transformation by v-Myb. Oncogene *18*, 3047–3055.

Liu, C., Wang, M., Wei, X., Wu, L., Xu, J., Dai, X., Xia, J., Cheng, M., Yuan, Y., Zhang, P., et al. (2019). An ATAC-seq atlas of chromatin accessibility in mouse tissues. Sci. Data *6*, 65.

Liu, W., Shen, S.-M., Zhao, X.-Y., and Chen, G.-Q. (2012). Targeted genes and interacting proteins of hypoxia inducible factor-1. Int. J. Biochem. Mol. Biol. *3*, 165–178.

van Lohuizen, M., Verbeek, S., Scheijen, B., Wientjens, E., van der Gulden, H., and Berns, A. (1991). Identification of cooperating oncogenes in E mu-myc transgenic mice by provirus tagging. Cell *65*, 737–752.

van Loo, P.F., Dingjan, G.M., Maas, A., and Hendriks, R.W. (2007). Surrogate-light-chain silencing is not critical for the limitation of pre-B cell expansion but is for the termination of constitutive signaling. Immunity *27*, 468–480.

Love, M.I., Huber, W., and Anders, S. (2014). Moderated estimation of fold change and dispersion for RNA-seq data with DESeq2. Genome Biol. *15*, 550.

Lovell, J.F., Billen, L.P., Bindner, S., Shamas-Din, A., Fradin, C., Leber, B., and Andrews, D.W. (2008). Membrane Binding by tBid Initiates an Ordered Series of Events Culminating in Membrane Permeabilization by Bax. Cell *135*, 1074–1084.

Lu, J., Guo, S., Ebert, B.L., Zhang, H., Peng, X., Bosco, J., Pretz, J., Schlanger, R., Wang, J.Y., Mak, R.H., et al. (2008). MicroRNA-mediated control of cell fate in megakaryocyte-erythrocyte progenitors. Dev. Cell *14*, 843–853.

Lu, L., Chaudhury, P., and Osmond, D.G. (1999). Regulation of cell survival during B lymphopoiesis: apoptosis and Bcl-2/Bax content of precursor B cells in bone marrow of mice with altered expression of IL-7 and recombinase-activating gene-2. J. Immunol. *162*, 1931–1940.

Lu, R., Medina, K.L., Lancki, D.W., and Singh, H. (2003). IRF-4,8 orchestrate the pre-B-to-B transition in lymphocyte development. Genes & Dev. *17*, 1703–1708.

Lunt, S.Y., and Vander Heiden, M.G. (2011). Aerobic glycolysis: meeting the metabolic requirements of cell proliferation. Annu. Rev. Cell Dev. Biol. *27*, 441–464.

Ma, S., Turetsky, A., Trinh, L., and Lu, R. (2006). IFN regulatory factor 4 and 8 promote Ig light chain kappa locus activation in pre-B cell development. J. Immunol. *177*, 7898–7904.

Ma, S., Pathak, S., Trinh, L., and Lu, R. (2008). Interferon regulatory factors 4 and 8 induce the expression of Ikaros and Aiolos to down-regulate pre-B-cell receptor and promote cell-cycle withdrawal in pre-B-cell development. Blood *111*, 1396–1403.

Ma, S., Pathak, S., Mandal, M., Trinh, L., Clark, M.R., and Lu, R. (2010). Ikaros and Aiolos inhibit pre-B-cell proliferation by directly suppressing c-Myc expression. Mol. Cell. Biol. *30*, 4149–4158.

Macheda, M.L., Rogers, S., and Best, J.D. (2004). Molecular and cellular regulation of glucose transporter (GLUT) proteins in cancer. J. Cell. Physiol. *202*, 654–662.

Maciver, N.J., Jacobs, S.R., Wieman, H.L., Wofford, J.A., Coloff, J.L., and Rathmell, J.C. (2008). Glucose metabolism in lymphocytes is a regulated process with significant effects on immune cell function and survival. J. Leukoc. Biol. *84*, 949–957.

Majewski, N., Nogueira, V., Robey, R.B., and Hay, N. (2003). Akt Inhibits Apoptosis Downstream of BID Cleavage via a Glucose-Dependent Mechanism Involving Mitochondrial Hexokinases. Mol. Cell. Biol. *24*, 730–740.

Majewski, N., Nogueira, V., Bhaskar, P., Coy, P.E., Skeen, J.E., Gottlob, K., Chandel, N.S., Thompson, C.B., Robey, R.B., and Hay, N. (2004). Hexokinase-Mitochondria Interaction Mediated by Akt Is Required to Inhibit Apoptosis in the Presence or Absence of Bax and Bak. Mol. Cell *16*, 819–830.

Malaterre, J., Carpinelli, M., Ernst, M., Alexander, W., Cooke, M., Sutton, S., Dworkin, S., Heath, J.K., Frampton, J., McArthur, G., et al. (2007). c-Myb is required for progenitor cell homeostasis in colonic crypts. Proc. Natl. Acad. Sci. *104*, 3829–3834.

Malaterre, J., Mantamadiotis, T., Dworkin, S., Lightowler, S., Yang, Q., Ransome, M.I., Turnley, A.M., Nichols, N.R., Emambokus, N.R., Frampton, J., et al. (2008). c-Myb Is Required for Neural Progenitor Cell Proliferation and Maintenance of the Neural Stem Cell Niche in Adult Brain. Stem Cells *26*, 173–181.

Malin, S., McManus, S., Cobaleda, C., Novatchkova, M., Delogu, A., Bouillet, P., Strasser, A., and Busslinger, M. (2010). Role of STAT5 in controlling cell survival and immunoglobulin gene recombination during pro-B cell development. Nat. Immunol. *11*, 171–179.

Malumbres, M. (2014). Cyclin-dependent kinases. Genome Biol. *15*, 110–122.

Mandal, M., Powers, S.E., Ochiai, K., Georgopoulos, K., Kee, B.L., Singh, H., and Clark, M.R. (2009). Ras orchestrates exit from the cell cycle and light-chain recombination during early B cell development. Nat. Immunol. *10*, 1110–1117.

Mandal, M., Powers, S.E., Maienschein-Cline, M., Bartom, E.T., Hamel, K.M., Kee, B.L., Dinner,

A.R., and Clark, M.R. (2011). Epigenetic repression of the Igk locus by STAT5-mediated recruitment of the histone methyltransferase Ezh2. Nat. Immunol. *12*, 1212–1220.

Manzotti, G., Mariani, S.A., Corradini, F., Bussolari, R., Cesi, V., Vergalli, J., Ferrari-Amorotti, G., Fragliasso, V., Soliera, A.R., Cattelani, S., et al. (2012). Expression of p89 c-Mybex9b, an alternatively spliced form of c-Myb, is required for proliferation and survival of p210BCR/ABL-expressing cells. Blood Cancer J. *2*, 1–11.

Maraskovsky, E., Peschon, J.J., McKenna, H., Teepe, M., and Strasser, A. (1998). Overexpression of Bcl-2 does not rescue impaired B lymphopoiesis in IL-7 receptor-deficient mice but can enhance survival of mature B cells. Int. Immunol. *10*, 1367–1375.

Marshall, A.J., Fleming, H.E., Wu, G.E., and Paige, C.J. (1998). Modulation of the IL-7 dose-response threshold during pro-B cell differentiation is dependent on pre-B cell receptor expression. J. Immunol. *161*, 6038–6045.

Mason, E.F., and Rathmell, J.C. (2011). Cell metabolism: An essential link between cell growth and apoptosis. Biochim. Biophys. Acta - Mol. Cell Res. *1813*, 645–654.

McBlane, J.F., van Gent, D.C., Ramsden, D.A., Romeo, C., Cuomo, C.A., Gellert, M., and Oettinger, M.A. (1995). Cleavage at a V(D)J Recombination Signal Requires Only RAG1 and RAG2 Proteins and Occurs in Two Steps. 1–9.

McCann, S., Sullivan, J., Guerra, J., Arcinas, M., and Boxer, L.M. (1995). Repression of the c-myb gene by WT1 protein in T and B cell lines. J. Biol. Chem. *270*, 23785–23789.

McClintock, D.S., Santore, M.T., Lee, V.Y., Brunelle, J., Budinger, G.R.S., Zong, W.X., Thompson, C.B., Hay, N., and Chandel, N.S. (2002). Bcl-2 Family Members and Functional Electron Transport Chain Regulate Oxygen Deprivation-Induced Cell Death. *22*, 94–104.

McClinton, D., Stafford, J., Brents, L., Bender, T.P., and Kuehl, W.M. (1990). Differentiation of mouse erythroleukemia cells is blocked by late up-regulation of a c-myb transgene. Mol. Cell. Biol. *10*, 705–710.

McHeyzer-Williams, L.J., and McHeyzer-Williams, M.G. (2005). ANTIGEN-SPECIFIC MEMORY B CELL DEVELOPMENT. Annu. Rev. Immunol. *23*, 487–513.

Medina, K.L., Pongubala, J.M.R., L Reddy, K., Lancki, D.W., DeKoter, R.P., Kieslinger, M., Grosschedl, R., and Singh, H. (2004). Assembling a Gene Regulatory Network for Specification of the B Cell Fate. Dev. Cell *7*, 607–617.

Merino, R., Ding, L., Veis, D.J., Korsmeyer, S.J., and Nunez, G. (1994). Developmental regulation of the Bcl-2 protein and susceptibility to cell death in B lymphocytes. EMBO J. *13*, 683–691.

Miao, R.Y., Drabsch, Y., Cross, R.S., Cheasley, D., Carpinteri, S., Pereira, L., Malaterre, J., Gonda, T.J., Anderson, R.L., and Ramsay, R.G. (2011). MYB is essential for mammary tumorigenesis. Cancer Res. *71*, 7029–7037.

Miglarese, M.R., Richardson, A.F., Aziz, N., and Bender, T.P. (1996). Differential regulation of c-Myb-induced transcription activation by a phosphorylation site in the negative regulatory domain. J. Biol. Chem. *271*, 22697–22705.

Mikkola, I., Heavey, B., Horcher, M., and Busslinger, M. (2002). Reversion of B cell commitment upon loss of Pax5 expression. Science (80-.). *297*, 110–113.

Milutinovic, S., Brown, S.E., Zhuang, Q., and Szyf, M. (2004). DNA Methyltransferase 1 Knock Down Induces Gene Expression by a Mechanism Independent of DNA Methylation and Histone Deacetylation. J. Biol. Chem. *279*, 27915–27927.

Mink, S., Kerber, U., and Klempnauer, K.H. (1996). Interaction of C/EBPbeta and v-Myb is

required for synergistic activation of the mim-1 gene. Mol. Cell. Biol. *16*, 1316–1325.

Mitra, P. (2018). Transcription regulation of MYB: a potential and novel therapeutic target in cancer. Ann. Transl. Med. *6*, 443–443.

Mitra, P., Pereira, L.A., Drabsch, Y., Ramsay, R.G., and Gonda, T.J. (2012). Estrogen receptor-α recruits P-TEFb to overcome transcriptional pausing in intron 1 of the MYB gene. Nucleic Acids Res. *40*, 5988–6000.

Mizoguchi, A., and Bhan, A.K. (2006). A Case for Regulatory B Cells. J. Immunol. *176*, 705–710.

Molnár, A., and Georgopoulos, K. (1994). The Ikaros gene encodes a family of functionally diverse zinc finger DNA-binding proteins. Mol. Cell. Biol. *14*, 8292–8303.

Morgan, D.O. (1995). Principles of CDK regulation. Nat. … *374*, 131–134.

Mucenski, M.L., McLain, K., Kier, A.B., Swerdlow, S.H., Schreiner, C.M., Miller, T.A., Pietryga, D.W., Scott, W.J., and Potter, S.S. (1991). A functional c-myb gene is required for normal murine fetal hepatic hematopoiesis. Cell *65*, 677–689.

Mukai, H.Y., Motohashi, H., Ohneda, O., Suzuki, N., Nagano, M., and Yamamoto, M. (2006). Transgene Insertion in Proximity to thec-myb Gene Disrupts Erythroid-Megakaryocytic Lineage Bifurcation. Mol. Cell. Biol. *26*, 7953–7965.

Mullighan, C.G., Miller, C.B., Radtke, I., Phillips, L.A., Dalton, J., Ma, J., White, D., Hughes, T.P., Le Beau, M.M., Pui, C.-H., et al. (2008). BCR–ABL1 lymphoblastic leukaemia is characterized by the deletion of Ikaros. Nat. … *453*, 110–114.

Muschen, M. (2019). Metabolic gatekeepers to safeguard against autoimmunity and oncogenic B cell transformation. Nat. Publ. Gr. 1–12.

Nakagoshi, H., Kanei-Ishii, C., Sawazaki, T., Mizuguchi, G., and Ishii, S. (1992). Transcriptional activation of the c-myc gene by the c-myb and B-myb gene products. Oncogene *7*, 1233–1240.

Nakayama, J., Yamamoto, M., Hayashi, K., Satoh, H., Bundo, K., Kubo, M., Goitsuka, R., Farrar, M.A., and Kitamura, D. (2009). BLNK suppresses pre-B-cell leukemogenesis through inhibition of JAK3. Blood *113*, 1483–1492.

Navarro, F., Gutman, D., Meire, E., Cáceres, M., Rigoutsos, I., Bentwich, Z., and Lieberman, J. (2009). miR-34a contributes to megakaryocytic differentiation of K562 cells independently of p53. Blood *114*, 2181–2192.

Nemazee, D. (2006). Receptor editing in lymphocyte development and central tolerance. Nat. Rev. Immunol. *6*, 728–740.

Neph, S., Vierstra, J., Stergachis, A.B., Reynolds, A.P., Haugen, E., Vernot, B., Thurman, R.E., John, S., Sandstrom, R., Johnson, A.K., et al. (2012). An expansive human regulatory lexicon encoded in transcription factor footprints. Nat. Publ. Gr. *488*, 83–90.

Ness, S.A., Kowenz-Leutz, E., Casini, T., Graf, T., and Leutz, A. (1993). Myb and NF-M: Combinatorial activators of myeloid genes in heterologous cell types. Genes Dev. *7*, 749–759.

Nishana, M., and Raghavan, S.C. (2012). Role of recombination activating genes in the generation of antigen receptor diversity and beyond. Immunology *137*, 271–281.

Nitta, T., Nasreen, M., Seike, T., Goji, A., Ohigashi, I., Miyazaki, T., Ohta, T., Kanno, M., and Takahama, Y. (2006). IAN Family Critically Regulates Survival and Development of T Lymphocytes. PLoS Biol. *4*, e103-13.

Nomura, T., Sakai, N., Sarai, A., Sudo, T., Kanei-Ishii, C., Ramsay, R.G., Favier, D., Gonda, T.J., and Ishii, S. (1993). Negative autoregulation of c-Myb activity by homodimer formation through

the leucine zipper. J. Biol. Chem. *268*, 21914–21923.

Nomura, T., Tanikawa, J., Akimaru, H., Kanei-Ishii, C., Ichikawa-Iwata, E., Khan, M.M., Ito, H., and Ishii, S. (2004). Oncogenic Activation of c-Myb Correlates with a Loss of Negative Regulation by TIF1β and Ski. J. Biol. Chem. *279*, 16715–16726.

Nutt, S.L., and Kee, B.L. (2007). The transcriptional regulation of B cell lineage commitment. Immunity *26*, 715–725.

Nutt, S.L., Heavey, B., Rolink, A., and Busslinger, M. (1999). Commitment to the B-lymphoid lineage depends on the transcription factor Pax5. Nat. … *401*, 556–562.

O'Neill, L.A.J., Kishton, R.J., and Rathmell, J. (2016). A guide to immunometabolism for immunologists. Nat. Rev. Immunol. *16*, 553–565.

O'Reilly, L.A., Kruse, E.A., Puthalakath, H., Kelly, P.N., Kaufmann, T., Huang, D.C.S., and Strasser, A. (2009). MEK/ERK-mediated phosphorylation of Bim is required to ensure survival of T and B lymphocytes during mitogenic stimulation. J. Immunol. *183*, 261–269.

O'Riordan, M., and Grosschedl, R. (1999). Coordinate regulation of B cell differentiation by the transcription factors EBF and E2A. Immunity *11*, 21–31.

O'Rourke, J.P., and Ness, S.A. (2008). Alternative RNA splicing produces multiple forms of c-Myb with unique transcriptional activities. Mol. Cell. Biol. *28*, 2091–2101.

O'Shea, J.J., and Plenge, R. (2012). JAK and STAT Signaling Molecules in Immunoregulation and Immune-Mediated Disease. Immunity *36*, 542–550.

Ochiai, K., Maienschein-Cline, M., Mandal, M., Triggs, J.R., Bertolino, E., Sciammas, R., Dinner, A.R., Clark, M.R., and Singh, H. (2012). A self-reinforcing regulatory network triggered by limiting IL-7 activates pre-BCR signaling and differentiation. Nat. Immunol. *13*, 300–307.

Oelgeschläger, M., Krieg, J., Lüscher-Firzlaff, J.M., and Luscher, B. (1995). Casein kinase II phosphorylation site mutations in c-Myb affect DNA binding and transcriptional cooperativity with NF-M. Mol. Cell. Biol. *15*, 5966–5974.

Oh, I.H., and Reddy, E.P. (1999). The myb gene family in cell growth, differentiation and apoptosis. Oncogene *18*, 3017–3033.

Ohtsubo, M., Theodoras, A.M., Schumacher, J., Roberts, J.M., and Pagano, M. (1995). Human cyclin E, a nuclear protein essential for the G1-to-S phase transition. Mol. Cell. Biol. *15*, 2612–2624.

Okkenhaug, K., and Vanhaesebroeck, B. (2003). PI3K in lymphocyte development, differentiation and activation. Nat. Rev. Immunol. *3*, 317–330.

Okoshi, R., Ozaki, T., Yamamoto, H., Ando, K., Koida, N., Ono, S., Koda, T., Kamijo, T., Nakagawara, A., and Kizaki, H. (2008). Activation of AMP-activated protein kinase induces p53-dependent apoptotic cell death in response to energetic stress. J. Biol. Chem. *283*, 3979–3987.

Oliver, P.M., Wang, M., Zhu, Y., White, J., Kappler, J., and Marrack, P. (2004). Loss of Bim allows precursor B cell survival but not precursor B cell differentiation in the absence of interleukin 7. J. Exp. Med. *200*, 1179–1187.

Opferman, J.T. (2008). Apoptosis in the development of the immune system. Cell Death Differ. *15*, 234–242.

Opferman, J.T., Letai, A., Beard, C., Sorcinelli, M.D., Ong, C.C., and Korsmeyer, S.J. (2003). Development and maintenance of B and T lymphocytes requires antiapoptotic MCL-1. Nat. … *426*, 671–676.

Osthus, R.C., Shim, H., Kim, S., Li, Q., Reddy, R., Mukherjee, M., Xu, Y., Wonsey, D., Lee, L.A.,

and Dang, C. V (2000). Deregulation of Glucose Transporter 1 and Glycolytic Gene Expression by c-Myc. *275*, 21797–21800.

Ouyang, Y.-B., and Giffard, R.G. (2016). Bcl-x LMaintains Mitochondrial Function in Murine Astrocytes Deprived of Glucose. J. Cereb. Blood Flow & Metab. *23*, 275–279.

Palmada, M., Boehmer, C., Akel, A., Rajamanickam, J., Jeyaraj, S., Keller, K., and Lang, F. (2006). SGK1 kinase upregulates GLUT1 activity and plasma membrane expression. Diabetes *55*, 421–427.

Papavasiliou, F. (1996). Surrogate or conventional light chains are required for membrane immunoglobulin mu to activate the precursor B cell transition [published erratum appears in J Exp Med 1997 Jan 6;185(1):183]. J. Exp. Med. *184*, 2025–2030.

Park, H., Staehling, K., Tsang, M., Appleby, M.W., Brunkow, M.E., Margineantu, D., Hockenbery, D.M., Habib, T., Liggitt, H.D., Carlson, G., et al. (2012). Disruption of Fnip1 Reveals a Metabolic Checkpoint Controlling B Lymphocyte Development. Immunity *36*, 769–781.

Pattabiraman, D.R., and Gonda, T.J. (2013). Role and potential for therapeutic targeting of MYB in leukemia. Leukemia *27*, 269–277.

Pattabiraman, D.R., McGirr, C., Shakhbazov, K., Barbier, V., Krishnan, K., Mukhopadhyay, P., Hawthorne, P., Trezise, A., Ding, J., Grimmond, S.M., et al. (2014). Interaction of c-Myb with p300 is required for the induction of acute myeloid leukemia (AML) by human AML oncogenes. Blood *123*, 2682–2690.

Pear, W. (2001). Transient transfection methods for preparation of high-titer retroviral supernatants. Curr. Protoc. Mol. Biol. *Chapter 9*, Unit9.11.

Pear, W.S., Nolan, G.P., Scott, M.L., and Baltimore, D. (1993). Production of high-titer helper-

free retroviruses by transient transfection. Proc. Natl. Acad. Sci. *90*, 8392–8396.

Pedrazzoli, P., Bains, M.A., Watson, R., Fisher, J., Hoy, T.G., and Jacobs, A. (1989). c-myc and c-myb oncoproteins during induced maturation of myeloid and erythroid human leukemic cell lines. Cancer Res. *49*, 6911–6916.

Pereira, L.A., Hugo, H.J., Malaterre, J., Huiling, X., Sonza, S., Cures, A., Purcell, D.F.J., Ramsland, P.A., Gerondakis, S., Gonda, T.J., et al. (2015). MYB Elongation Is Regulated by the Nucleic Acid Binding of NFκB p50 to the Intronic Stem-Loop Region. PLoS One *10*, e0122919-25.

Persson, M., Andren, Y., Mark, J., Horlings, H.M., Persson, F., and Stenman, G. (2009). Recurrent fusion of MYB and NFIB transcription factor genes in carcinomas of the breast and head and neck. Proc. Natl. Acad. Sci. U. S. A. *106*, 18740–18744.

Peschon, J., Morrissey, P., Grabstein, K., Ramsdell, F., Maraskovsky, E., Gliniak, B., Park, L., Ziegler, S., Williams, D., Ware, C., et al. (1994). Early Lymphocyte Expansion Is Severely Impaired in Interleukin 7 Receptor-deficient Mice. J. Exp. Med. *180*, 1955–1960.

Pfaffl, M.W. (2001). A new mathematical model for relative quantification in real-time RT-PCR. Nucleic Acids Res. *29*, e45.

Pillai, S., and Cariappa, A. (2009). The follicular versus marginal zone B lymphocyte cell fate decision. *9*, 767–777.

Poirier, Y., Kozak, C., and Jolicoeur, P. (1988). Identification of a common helper provirus integration site in Abelson murine leukemia virus-induced lymphoma DNA. J. Virol. *62*, 3985–3992.

Pongubala, J.M.R., Northrup, D.L., Lancki, D.W., Medina, K.L., Treiber, T., Bertolino, E.,

Thomas, M., Grosschedl, R., Allman, D., and Singh, H. (2008). Transcription factor EBF restricts alternative lineage options and promotes B cell fate commitment independently of Pax5. Nat. Immunol. *9*, 203–215.

Powers, S.E., Mandal, M., Matsuda, S., Miletic, A. V, Cato, M.H., Tanaka, A., Rickert, R.C., Koyasu, S., and Clark, M.R. (2012). Subnuclear cyclin D3 compartments and the coordinated regulation of proliferation and immunoglobulin variable gene repression. J. Exp. Med. *209*, 2199–2213.

Quintana, A.M., Liu, F., O'Rourke, J.P., and Ness, S.A. (2011a). Identification and regulation of c-Myb target genes in MCF-7 cells. BMC Cancer *11*, 30.

Quintana, A.M., Zhou, Y.E., Pena, J.J., O'Rourke, J.P., and Ness, S.A. (2011b). Dramatic repositioning of c-Myb to different promoters during the cell cycle observed by combining cell sorting with chromatin immunoprecipitation. PLoS One *6*, e17362.

Ramadani, F., Bolland, D.J., Garcon, F., Emery, J.L., Vanhaesebroeck, B., Corcoran, A.E., and Okkenhaug, K. (2010). The PI3K Isoforms p110a and p110d Are Essential for Pre–B Cell Receptor Signaling and B Cell Development. *3*, 1–11.

Ramaswamy, K., Forbes, L., Minuesa, G., Gindin, T., Brown, F., Kharas, M.G., Krivtsov, A. V., Armstrong, S.A., Still, E., De Stanchina, E., et al. (2018). Peptidomimetic blockade of MYB in acute myeloid leukemia. Nat. Commun. *9*.

Ramsay, R.G., and Gonda, T.J. (2008). MYB function in normal and cancer cells. Nat. Rev. Cancer *8*, 523–534.

Ramsay, R.G., Ikeda, K., Rifkind, R.A., and Marks, P.A. (1986). Changes in gene expression associated with induced differentiation of erythroleukemia: protooncogenes, globin genes, and cell

division. Proc. Natl. Acad. Sci. *83*, 6849–6853.

Ramsay, R.G., Thompson, M.A., Hayman, J.A., Reid, G., Gonda, T.J., and Whitehead, R.H. (1992). Myb expression is higher in malignant human colonic carcinoma and premalignant adenomatous polyps than in normal mucosa. Cell Growth Differ. *3*, 723–730.

Rathmell, J.C., Fox, C.J., Plas, D.R., Hammerman, P.S., Cinalli, R.M., and Thompson, C.B. (2003). Akt-directed glucose metabolism can prevent Bax conformation change and promote growth factor-independent survival. Mol. Cell. Biol. *23*, 7315–7328.

Reth, M., and Nielsen, P. (2014). Signaling circuits in early B-cell development. Adv. Immunol. *122*, 129–175.

Retter, M.W., and Nemazee, D. (1998). Receptor editing occurs frequently during normal B cell development. J. Exp. Med. *188*, 1231–1238.

Reynaud, D., Demarco, I.A., Reddy, K.L., Schjerven, H., Bertolino, E., Chen, Z., Smale, S.T., Winandy, S., and Singh, H. (2008). Regulation of B cell fate commitment and immunoglobulin heavy-chain gene rearrangements by Ikaros. Nat. Immunol. *9*, 927–936.

Ritchie, M.E., Phipson, B., Wu, D., Hu, Y., Law, C.W., Shi, W., and Smyth, G.K. (2015). limma powers differential expression analyses for RNA-sequencing and microarray studies. Nucleic Acids Res. *43*, e47.

Robey, R.B., and Hay, N. (2005). Mitochondrial hexokinases: guardians of the mitochondria. Cell Cycle *4*, 654–658.

Robey, R.B., and Hay, N. (2006). Mitochondrial hexokinases, novel mediators of the antiapoptotic effects of growth factors and Akt. Oncogene *25*, 4683–4696.

Roessler, S., György, I., Imhof, S., Spivakov, M., Williams, R.R., Busslinger, M., Fisher, A.G., and

Grosschedl, R. (2007). Distinct promoters mediate the regulation of Ebf1 gene expression by interleukin-7 and Pax5. Mol. Cell. Biol. *27*, 579–594.

Rolink, A., Grawunder, U., Winkler, T.H., Karasuyama, H., and Melchers, F. (1994). IL-2 receptor alpha chain (CD25, TAC) expression defines a crucial stage in pre-B cell development. Int. Immunol. *6*, 1257–1264.

Rolink, A.G., Winkler, T., Melchers, F., and Andersson, J. (2000). Precursor B cell receptor-dependent B cell proliferation and differentiation does not require the bone marrow or fetal liver environment. J. Exp. Med. *191*, 23–32.

Rosser, E.C., and Mauri, C. (2015). Regulatory B Cells: Origin, Phenotype, and Function. Immunity *42*, 607–612.

Rumfelt, L.L., Zhou, Y., Rowley, B.M., Shinton, S.A., and Hardy, R.R. (2006). Lineage specification and plasticity in CD19- early B cell precursors. J. Exp. Med. *203*, 675–687.

Ruzankina, Y., Pinzon-Guzman, C., Asare, A., Ong, T., Pontano, L., Cotsarelis, G., Zediak, V.P., Velez, M., Bhandoola, A., and Brown, E.J. (2007). Deletion of the Developmentally Essential Gene ATR in Adult Mice Leads to Age-Related Phenotypes and Stem Cell Loss. Cell Stem Cell *1*, 113–126.

Sæther, T., Berge, T., Ledsaak, M., Matre, V., Alm-Kristiansen, A.H., Dahle, O., Aubry, F., and Gabrielsen, O.S. (2007). The chromatin remodeling factor Mi-2alpha acts as a novel co-activator for human c-Myb. J. Biol. Chem. *282*, 13994–14005.

Sakamoto, H., Dai, G., Tsujino, K., Hashimoto, K., Huang, X., Fujimoto, T., Mucenski, M., Frampton, J., and Ogawa, M. (2006). Proper levels of c-Myb are discretely defined at distinct steps of hematopoietic cell development. Blood *108*, 896–903.

Sakura, H., Kanei-Ishii, C., Nagase, T., Nakagoshi, H., Gonda, T.J., and Ishii, S. (1989). Delineation of three functional domains of the transcriptional activator encoded by the c-myb protooncogene. Proc. Natl. Acad. Sci. *86*, 5758–5762.

Sala, A., Nicolaides, N.C., Engelhard, A., Bellon, T., Lawe, D.C., Arnold, A., Graña, X., Giordano, A., and Calabretta, B. (1994). Correlation between E2F-1 requirement in the S phase and E2F-1 transactivation of cell cycle-related genes in human cells. Cancer Res. *54*, 1402–1406.

Sandberg, M.L., Sutton, S.E., Pletcher, M.T., Wiltshire, T., Tarantino, L.M., Hogenesch, J.B., and Cooke, M.P. (2005). c-Myb and p300 Regulate Hematopoietic Stem Cell Proliferation and Differentiation. Dev. Cell *8*, 153–166.

Sandoval, G.J., Graham, D.B., Bhattacharya, D., Sleckman, B.P., Xavier, R.J., and Swat, W. (2013). Cutting edge: cell-autonomous control of IL-7 response revealed in a novel stage of precursor B cells. J. Immunol. *190*, 2485–2489.

Sano, Y., and Ishii, S. (2001). Increased Affinity of c-Myb for CREB-binding Protein (CBP) after CBP-induced Acetylation. J. Biol. Chem. *276*, 3674–3682.

Sarvaiya, P.J., Schwartz, J.R., Hernandez, C.P., Rodriguez, P.C., and Vedeckis, W. V (2012). Role of c-Myb in the survival of pre B-cell acute lymphoblastic leukemia and leukemogenesis. Am. J. Hematol. *87*, 969–976.

Saxton, R.A., and Sabatini, D.M. (2017). mTOR Signaling in Growth, Metabolism, and Disease. Cell *168*, 960–976.

Schaefer, C.F., Anthony, K., Krupa, S., Buchoff, J., Day, M., Hannay, T., and Buetow, K.H. (2009). PID: The pathway interaction database. Nucleic Acids Res. *37*, 674–679.

Schatz, D.G., Oettinger, M.A., and Baltimore, D. (1989). The V(D)J recombination activating

gene, RAG-1. Cell *59*, 1035–1048.

Schwickert, T.A., Tagoh, H., Gültekin, S., Dakic, A., Axelsson, E., Minnich, M., Ebert, A., Werner, B., Roth, M., Cimmino, L., et al. (2014). Stage-specific control of early B cell development by the transcription factor Ikaros. Nat. Immunol. *15*, 283–293.

Seet, C.S., Brumbaugh, R.L., and Kee, B.L. (2004). Early B Cell Factor Promotes B Lymphopoiesis with Reduced Interleukin 7 Responsiveness in the Absence of E2A. J. Exp. Med. *199*, 1689–1700.

Shen-Ong, G.L., Luscher, B., and Eisenman, R.N. (1989). A second c-myb protein is translated from an alternatively spliced mRNA expressed from normal and 5'-disrupted myb loci. Mol. Cell. Biol. *9*, 5456–5463.

Shen-Ong, G.L., Skurla, R.M., Owens, J.D., and Mushinski, J.F. (1990). Alternative splicing of RNAs transcribed from the human c-myb gene. Mol. Cell. Biol. *10*, 2715–2722.

Sherr, C.J. (1994). G1 phase progression: cycling on cue. Cell *79*, 551–555.

Shinkai, Y., Rathbun, G., Lam, K.P., Oltz, E.M., Stewart, V., Mendelsohn, M., Charron, J., Datta, M., Young, F., and Stall, A.M. (1992). RAG-2-deficient mice lack mature lymphocytes owing to inability to initiate V(D)J rearrangement. Cell *68*, 855–867.

Soh, J.-W., and Weinstein, I.B. (2003). Roles of Specific Isoforms of Protein Kinase C in the Transcriptional Control of Cyclin D1 and Related Genes. J. Biol. Chem. *278*, 34709–34716.

Srinivasan, L., Sasaki, Y., Calado, D.P., Zhang, B., Paik, J.-H., DePinho, R.A., Kutok, J.L., Kearney, J.F., Otipoby, K.L., and Rajewsky, K. (2009). PI3 Kinase Signals BCR-Dependent Mature B Cell Survival. *139*, 573–586.

Stadhouders, R., Thongjuea, S., Andrieu-Soler, C., Palstra, R.-J., Bryne, J.C., van den Heuvel, A.,

Stevens, M., de Boer, E., Kockx, C., van der Sloot, A., et al. (2011). Dynamic long-range chromatin interactions control Myb proto-oncogene transcription during erythroid development. EMBO J. *31*, 986–999.

Stein, M., Dütting, S., Mougiakakos, D., Bösl, M., Fritsch, K., Reimer, D., Urbanczyk, S., Steinmetz, T., Schuh, W., Bozec, A., et al. (2017). A defined metabolic state in pre B cells governs B-cell development and is counterbalanced by Swiprosin-2/ EFhd1. Nat. Publ. Gr. *24*, 1–14.

Storch, B., Meixlsperger, S., and Jumaa, H. (2007). The Ig-alpha ITAM is required for efficient differentiation but not proliferation of pre-B cells. Eur. J. Immunol. *37*, 252–260.

Strasser, A. (2005). The role of BH3-only proteins in the immune system. Nat. Publ. Gr. *5*, 189–200.

Strasser, A., Whittingham, S., Vaux, D.L., Bath, M.L., Adams, J.M., Cory, S., and Harris, A.W. (1991). Enforced Bcl2 expression in B-lymphoid cells prolongs antibody responses and elicits autoimmune disease. Proc. Natl. Acad. Sci. *88*, 8661–8665.

Subramanian, A., Tamayo, P., Mootha, V.K., Mukherjee, S., Ebert, B.L., Gillette, M.A., Paulovich, A., Pomeroy, S.L., Golub, T.R., Lander, E.S., et al. (2005). Gene set enrichment analysis: a knowledge-based approach for interpreting genome-wide expression profiles. Proc. Natl. Acad. Sci. *102*, 15545–15550.

Suhasini, M., and Pilz, R.B. (1999). Transcriptional elongation of c-myb is regulated by NF-κB (p50/RelB). Oncogene *18*, 7360–7369.

Sullivan, J., Feeley, B., Guerra, J., and Boxer, L.M. (1997). Identification of the major positive regulators of c-myb expression in hematopoietic cells of different lineages. J. Biol. Chem. *272*, 1943–1949.

Sullivan, W.J., Mullen, P.J., Schmid, E.W., Flores, A., Momcilovic, M., Sharpley, M.S., Jelinek, D., Whiteley, A.E., Maxwell, M.B., Wilde, B.R., et al. (2018). Extracellular Matrix Remodeling Regulates Glucose Metabolism through TXNIP Destabilization. Cell *175*, 117-132.e21.

Sun, L., Liu, A., and Georgopoulos, K. (1996). Zinc finger-mediated protein interactions modulate Ikaros activity, a molecular control of lymphocyte development. EMBO J. *15*, 5358–5369.

Tahirov, T.H., Sato, K., Ichikawa-Iwata, E., Sasaki, M., Inoue-Bungo, T., Shiina, M., Kimura, K., Takata, S., Fujikawa, A., Morii, H., et al. (2002). Mechanism of c-Myb-C/EBPβ cooperation from separated sites on a promoter. Cell *108*, 57–70.

Takeuchi, O., Fisher, J., Suh, H., Harada, H., Malynn, B.A., and Korsmeyer, S.J. (2005). Essential role of BAX,BAK in B cell homeostasis and prevention of autoimmune disease. Proc. Natl. Acad. Sci. *102*, 11272–11277.

Tanikawa, J., Yasukawa, T., Enari, M., Ogata, K., Nishimura, Y., Ishii, S., and Sarai, A. (1993). Recognition of specific DNA sequences by the c-myb protooncogene product: role of three repeat units in the DNA-binding domain. Proc. Natl. Acad. Sci. *90*, 9320–9324.

Tarasov, K. V, Tarasova, Y.S., Tam, W.L., Riordon, D.R., Elliott, S.T., Kania, G., Li, J., Yamanaka, S., Crider, D.G., Testa, G., et al. (2008). B-MYB Is Essential for Normal Cell Cycle Progression and Chromosomal Stability of Embryonic Stem Cells. PLoS One *3*, e2478-16.

Tavner, F.J., Simpson, R., Tashiro, S., Favier, D., Jenkins, N.A., Gilbert, D.J., Copeland, N.G., MacMillan, E.M., Lutwyche, J., Keough, R.A., et al. (1998). Molecular cloning reveals that the p160 Myb-binding protein is a novel, predominantly nucleolar protein which may play a role in transactivation by Myb. Mol. Cell. Biol. *18*, 989–1002.

Thomas, M.D., Kremer, C.S., Ravichandran, K.S., Rajewsky, K., and Bender, T.P. (2005). c-Myb

Is Critical for B Cell Development and Maintenance of Follicular B Cells. Immunity *23*, 275–286.

Tiegs, S.L., Russell, D.M., and Nemazee, D. (1993). Receptor editing in self-reactive bone marrow B cells. J. Exp. Med. *177*, 1009–1020.

Toth, C.R., Hostutler, R.F., Baldwin Jr, A.S., and Bender, T.P. (1995). Members of the Nuclear Factor κB Family Transactivate the Murine c-myb Gene. J. Biol. Chem. *270*, 7661–7671.

Tussiwand, R., Bosco, N., Ceredig, R., and Rolink, A.G. (2009). Tolerance checkpoints in B-cell development: Johnny B good. Eur. J. Immunol. *39*, 2317–2324.

Urbanczyk, S., Stein, M., Schuh, W., Jack, H.-M., Mougiakakos, D., and Mielenz, D. (2018). Regulation of Energy Metabolism during Early B Lymphocyte Development. Int. J. Mol. Sci. *19*, 2116–2192.

Uttarkar, S., Dassé, E., Coulibaly, A., Steinmann, S., Jakobs, A., Schomburg, C., Trentmann, A., Jose, J., Schlenke, P., Berdel, W.E., et al. (2016a). Targeting acute myeloid leukemia with a small molecule inhibitor of the Myb/p300 interaction. Blood *127*, 1173–1182.

Uttarkar, S., Piontek, T., Dukare, S., Schomburg, C., Schlenke, P., Berdel, W.E., Muller-Tidow, C., Schmidt, T.J., and Klempnauer, K.H. (2016b). Small-molecule disruption of the Myb/p300 cooperation targets acute myeloid leukemia cells. Mol. Cancer Ther. *15*, 2905–2915.

Vermeulen, K., Van Bockstaele, D.R., and Berneman, Z.N. (2003). The cell cycle: a review of regulation, deregulation and therapeutic targets in cancer. Cell Prolif. *36*, 131–149.

Vogler, L.B., Crist, W.M., Bockman, D.E., Pearl, E.R., Lawton, A.R., and Cooper, M.D. (1978). Pre-B-cell leukemia. A new phenotype of childhood lymphoblastic leukemia. N. Engl. J. Med. *298*, 872–878.

Waldhart, A.N., Dykstra, H., Peck, A.S., Boguslawski, E.A., Madaj, Z.B., Wen, J., Veldkamp, K.,

Hollowell, M., Zheng, B., Cantley, L.C., et al. (2017). Phosphorylation of TXNIP by AKT Mediates Acute Influx of Glucose in Response to Insulin. CellReports *19*, 2005–2013.

Waldron, T., De Dominici, M., Soliera, A.R., Audia, A., Iacobucci, I., Lonetti, A., Martinelli, G., Zhang, Y., Martinez, R., Hyslop, T., et al. (2012). c-Myb and its target Bmi1 are required for p190BCR/ABL leukemogenesis in mouse and human cells. Leukemia *26*, 644–653.

Wang, H., and Clarke, S.H. (2007). Association of the pre-B cell receptor (BCR) expression level with the quality of pre-BII cell differentiation reveals hierarchical pre-BCR function. Mol. Immunol. *44*, 1765–1774.

Wang, Q.F., Lauring, J., and Schlissel, M.S. (2000). c-Myb binds to a sequence in the proximal region of the RAG-2 promoter and is essential for promoter activity in T-lineage cells. Mol. Cell. Biol. *20*, 9203–9211.

Wang, Y.-H., Stephan, R.P., Scheffold, A., Kunkel, D., Karasuyama, H., Radbruch, A., and Cooper, M.D. (2002). Differential surrogate light chain expression governs B-cell differentiation. Blood *99*, 2459–2467.

Westin, E.H., Gallo, R.C., Arya, S.K., Eva, A., Souza, L.M., Baluda, M.A., Aaronson, S.A., and Wong-Staal, F. (1982). Differential expression of the amv gene in human hematopoietic cells. Proc. Natl. Acad. Sci. *79*, 2194–2198.

Weston, K., and Bishop, J.M. (1989). Transcriptional activation by the v-myb oncogene and its cellular progenitor, c-myb. Cell *58*, 85–93.

Wieman, H.L., Wofford, J.A., and Rathmell, J.C. (2007). Cytokine stimulation promotes glucose uptake via phosphatidylinositol-3 kinase/Akt regulation of Glut1 activity and trafficking. Mol. Biol. Cell *18*, 1437–1446.

Williams, G.H., and Stoeber, K. (2011). The cell cycle and cancer. J. Pathol. *226*, 352–364.

Wilson, J.E. (2003). Isozymes of mammalian hexokinase: structure, subcellular localization and metabolic function. J. Exp. Biol. *206*, 2049–2057.

Winn, L.M., Lei, W., and Ness, S.A. (2003). Pim-1 phosphorylates the DNA binding domain of c-Myb. Cell Cycle *2*, 258–262.

Wofford, J.A., Wieman, H.L., Jacobs, S.R., Zhao, Y., and Rathmell, J.C. (2008). IL-7 promotes Glut1 trafficking and glucose uptake via STAT5-mediated activation of Akt to support T-cell survival. Blood *111*, 2101–2111.

Wu, N., Zheng, B., Shaywitz, A., Dagon, Y., Tower, C., Bellinger, G., Shen, C.-H., Wen, J., Asara, J., McGraw, T.E., et al. (2013). AMPK-Dependent Degradation of TXNIP upon Energy Stress Leads to Enhanced Glucose Uptake via GLUT1. Mol. Cell *49*, 1167–1175.

Xiao, C., Calado, D.P., Galler, Gu., Thai, T.-H., Patterson, H.C., Wang, J., Rajewsky, N., Bender, T.P., and Rajewsky, K. (2007). MiR-150 controls B cell differentiation by targeting the transcription factor c-Myb. Cell *131*, 146–159.

Yamagami, T., ten Boekel, E., Andersson, J., Rolink, A., and Melchers, F. (1999). Frequencies of multiple IgL chain gene rearrangements in single normal or kappaL chain-deficient B lineage cells. Immunity *11*, 317–327.

Yasuda, T., and Kurosaki, T. (2008). Regulation of lymphocyte fate by Ras/ERK signals. Cell Cycle *7*, 3634–3640.

Yoshida, T., Yao-Ming Ng, S., Zúñiga-Pflücker, J.C., and Georgopoulos, K. (2006). Early hematopoietic lineage restrictions directed by Ikaros. Nat. Immunol. *7*, 382–391.

Youle, R.J., and Strasser, A. (2008). The BCL-2 protein family: opposing activities that mediate

cell death. Nat. Rev. Mol. Cell Biol. *9*, 47–59.

Yu, M., Chen, Y., Zeng, H., Zheng, Y., Fu, G., Zhu, W., Broeckel, U., Aggarwal, P., Turner, A., Neale, G., et al. (2017). PLCγ-dependent mTOR signalling controls IL-7-mediated early B cell development. Nat. Commun. *8*, 1457.

Yuan, J., Crittenden, R.B., and Bender, T.P. (2010). c-Myb promotes the survival of CD4+CD8+ double-positive thymocytes through upregulation of Bcl-xL. J. Immunol. *184*, 2793–2804.

Zandi, S., Mansson, R., Tsapogas, P., Zetterblad, J., Bryder, D., and Sigvardsson, M. (2008). EBF1 is essential for B-lineage priming and establishment of a transcription factor network in common lymphoid progenitors. J. Immunol. *181*, 3364–3372.

Zeng, H., and Chi, H. (2014). mTOR signaling and transcriptional regulation in T lymphocytes. Transcription *5*.

Zeng, H., Yu, M., Tan, H., Li, Y., Su, W., Shi, H., Dhungana, Y., Guy, C., Neale, G., Cloer, C., et al. (2018). Discrete roles and bifurcation of PTEN signaling and mTORC1-mediated anabolic metabolism underlie IL-7-driven B lymphopoiesis. Sci. Adv. *4*, eaar5701.

Zhao, H., Kalota, A., Jin, S., and Gewirtz, A.M. (2009). The c-myb proto-oncogene and microRNA-15a comprise an active autoregulatory feedback loop in human hematopoietic cells. Blood *113*, 505–516.

Zhao, H., Jin, S., and Gewirtz, A.M. (2012). The histone acetyltransferase TIP60 interacts with c-Myb and inactivates its transcriptional activity in human leukemia. J. Biol. Chem. *287*, 925–934.

Zhao, L., Glazov, E.A., Pattabiraman, D.R., Al-Owaidi, F., Zhang, P., Brown, M.A., Leo, P.J., and Gonda, T.J. (2011). Integrated genome-wide chromatin occupancy and expression analyses identify key myeloid pro-differentiation transcription factors repressed by Myb. Nucleic Acids

Res. *39*, 4664–4679.

Zhao, Y., Altman, B.J., Coloff, J.L., Herman, C.E., Jacobs, S.R., Wieman, H.L., Wofford, J.A., Dimascio, L.N., Ilkayeva, O., Kelekar, A., et al. (2007). Glycogen Synthase Kinase 3 and 3 Mediate a Glucose-Sensitive Antiapoptotic Signaling Pathway To Stabilize Mcl-1. Mol. Cell. Biol. *27*, 4328–4339.

Zhao, Y., Coloff, J.L., Ferguson, E.C., Jacobs, S.R., Cui, K., and Rathmell, J.C. (2008). Glucose metabolism attenuates p53 and Puma-dependent cell death upon growth factor deprivation. J. Biol. Chem. *283*, 36344–36353.

Zhou, Y., and Ness, S.A. (2011). Myb proteins: angels and demons in normal and transformed cells. Front. Biosci. (Landmark Ed. *16*, 1109–1131.

Zhou, Y.E., O'Rourke, J.P., Edwards, J.S., and Ness, S.A. (2011). Single molecule analysis of c-myb alternative splicing reveals novel classifiers for precursor B-ALL. PLoS One *6*, e22880.

Zor, T., De Guzman, R.N., Dyson, H.J., and Wright, P.E. (2004). Solution Structure of the KIX Domain of CBP Bound to the Transactivation Domain of c-Myb. J. Mol. Biol. *337*, 521–534.